Rethinking Cast in Situ Concrete Structures: A Study of Material Use in Residential Slabs and Walls

Karl Sten & Lukas Wedervang

Avdelningen för Konstruktionsteknik
Lunds Tekniska Högskola
Lunds Universitet, 2026

Rapport TVBK-5322

Abstract

This thesis investigates how material use in cast in situ concrete slabs and walls for multi-storey residential buildings can be reduced by separating the load-bearing concrete from functions that do not have to be solved within the structural member itself. The study is motivated by the high climate impact of concrete construction and by indications that material use in concrete structures has increased over time despite improved materials and more advanced design methods.

The work combines a review of Swedish design practice, regulations and reference structures with parameter-based structural calculations. Two cast in situ residential structures in Lund were used as references: Cykelskrapan from the 1950s and Troja from contemporary practice. Slab alternatives were evaluated using one metre wide slab sections idealised as beam strips, with checks for load-bearing capacity, deflection, crack width and vibration. Wall alternatives were analysed as vertical wall strips under eccentric compression, including reinforced and unreinforced cases with second-order effects.

The results show potential for material reduction in both slabs and walls. For slabs, several analysed alternatives reached larger or comparable spans with a smaller structural concrete thickness than the contemporary reference slab, while still satisfying the adopted structural and serviceability checks. Higher concrete strength alone did not provide a general path to material efficiency. For walls, axial resistance was governed mainly by thickness and effective buckling length, while increased distributed reinforcement had a smaller influence. The wall comparison also showed that many compression dominated wall strips can reach sufficient axial resistance without reinforcement within the adopted limits.

Overall, the study shows that material use in cast in situ concrete structures can be reduced when the role of the load bearing concrete is defined more narrowly. Instead of using the concrete member to solve structural performance, acoustic performance, fire protection and installations at the same time, the results support a design approach where the concrete is used primarily for its load-bearing role. Other building functions should then be handled separately and assessed at system level.

Sammanfattning

Detta examensarbete undersöker hur materialanvändningen i platsgjutna betongbjälklag och betongväggar i flerbostadshus kan minskas genom att separera den bärande betongen från funktioner som inte behöver lösas inom själva den bärande konstruktionsdelen. Studien motiveras av betongbyggandets höga klimatpåverkan och av indikationer på att materialanvändningen i betongkonstruktioner har ökat över tid, trots förbättrade material och mer avancerade dimensioneringsmetoder.

Arbetet kombinerar en genomgång av svensk dimensioneringspraxis, regelverk och referensstrukturer med parameterbaserade konstruktionsberäkningar. Två platsgjutna flerbostadshus i Lund användes som referenser: Cykelskrapan från 1950-talet och Troja från nutida praxis. Bjälklagsalternativen utvärderades med en meter breda bjälklagssnitt idealiserade som balkstrimlor, med kontroller för bärförmåga, nedböjning, sprickbredd och vibration. Väggalternativen analyserades som vertikala väggstrimlor under excentrisk tryckbelastning, där både armerade och oarmerade fall med andra ordningens effekter ingick.

Resultaten visar potential för materialminskning i både bjälklag och väggar. För bjälklag uppnådde flera analyserade alternativ större eller jämförbara spännvidder med en mindre bärande betongtjocklek än det nutida referensbjälklaget, samtidigt som de antagna konstruktionskontrollerna i brottgränstillstånd och bruksgränstillstånd uppfylldes. Högre betongkvalitet gav inte i sig en generell väg till materialeffektivitet. För väggar styrdes bärförmågan främst av tjocklek och effektiv knäcklängd, medan ökad fördelad armering hade mindre påverkan. Jämförelsen av väggar visade även att många tryckdominerade väggstrimlor kan uppnå tillräcklig axiell bärförmåga utan armering inom de antagna begränsningarna.

Sammantaget visar studien att materialanvändningen i platsgjutna betongkonstruktioner kan minskas när den bärande betongens roll definieras mer avgränsat. I stället för att låta betongtvärsnittet lösa bärförmåga, akustik, brandskydd och installationer samtidigt, stödjer resultaten ett dimensioneringssätt där betongen främst används för sin bärande funktion. Övriga byggnadsfunktioner bör då hanteras separat och bedömas på systemnivå.

Acknowledgements

This master's thesis was carried out as the final part of our Master of Science degree in Civil Engineering at Lund University.

We would like to thank our supervisor at Lund University, Miklos Molnar, for valuable guidance, feedback and support throughout the project.

We would also like to express our gratitude to Johan Jönsson at VBK for guidance. His knowledge and experience have been valuable in shaping this thesis and in connecting the work to current structural design practice.

Lastly, we would like to thank everyone who contributed with drawings, information and interviews during the project.

Notations and Symbols

Latin letters

a	depth of the equivalent rectangular concrete stress block
A_c	gross concrete cross-sectional area
$A_{c,ef}$	effective concrete area in tension
A_s	area of tensile reinforcement
$A_{s,\max}$	maximum reinforcement area
$A_{s,\text{mesh}}$	reinforcement area of one welded mesh layer
$A_{s,\text{selected}}$	selected reinforcement area
$A_{s,\text{tot}}$	total reinforcement area
A_{sl}	area of tensile bottom reinforcement
b	width of the cross-section
c	concrete cover
c_{min}	minimum concrete cover
c_{nom}	nominal concrete cover
$C_{Rd,c}$	coefficient for shear resistance according to Eurocode 2
d	effective depth
d'	distance from the compressed edge to the reinforcement layer on the compression side
e_0	initial eccentricity of the axial force
e_{shift}	distance from the centroidal axis to the moment reference level at $y = d$
$E_{c,ef}$	effective modulus of elasticity of concrete
E_{cd}	design value of the modulus of elasticity of concrete
E_{cm}	secant modulus of elasticity of concrete
E_s	modulus of elasticity of reinforcing steel
EI	nominal flexural stiffness
$(EI)_I$	flexural stiffness of the uncracked section
$(EI)_{II}$	flexural stiffness of the cracked section
f_{cd}	design compressive strength of concrete
f_{ck}	characteristic compressive strength of concrete
$f_{ct,ef}$	effective tensile strength of concrete
f_{ctm}	mean axial tensile strength of concrete
f_{min}	minimum fundamental frequency
f_{yd}	design yield strength of reinforcement
G_k	characteristic permanent load
h_0	notional size
$h_{c,ef}$	effective tension area depth
I	second moment of area of the uncracked section
I_c	second moment of area of the concrete section
I_s	second moment of area contribution from reinforcement
k	size factor
K_c	stiffness coefficient for concrete
K_s	stiffness coefficient for reinforcement

k_M	moment coefficient
$k_{M,defl}$	moment coefficient at the section of maximum deflection
$k_{M,field}$	field moment coefficient
$k_{M,sup}$	support moment coefficient
k_t	coefficient depending on load duration
k_V	shear coefficient
k_v	deflection coefficient
L	span length
l_0	effective buckling length
M	bending moment
M_0	first-order bending moment
$M_{0,c}$	first-order bending moment about the centroidal axis
$M_{0,d}$	first-order moment about the reinforcement layer at $y = d$
M_{cr}	cracking moment
M_{defl}	bending moment at the section of maximum deflection
M_{Ed}	design bending moment in the ultimate limit state
$M_{Ed,c}$	amplified design moment about the centroidal axis
$M_{Ed,d}$	design moment about the reinforcement layer at $y = d$
$M_{Ed,SLS}$	bending moment in the serviceability limit state
M_{field}	field moment
M_R	internal moment resistance of the cross-section
M_{shift}	moment contribution from shifting the moment reference point to $y = d$
M_{sup}	support moment
N_B	Euler buckling load based on nominal stiffness
N_{Ed}	design axial force
N_{qp}	quasi-permanent axial force
N_R	internal axial force resultant of the cross-section
N_{Rd}	design axial resistance
q	uniformly distributed load
Q_k	characteristic variable load
q_{SLS}	serviceability load
R_M	moment residual, defined as $M_R - M_{Ed,d}$
R_N	axial force residual, defined as $N_R - N_{Ed}$
RH	relative humidity
s	reinforcement spacing
$s_{r,max}$	maximum crack spacing
t	member thickness or time, depending on context
t_0	concrete age at loading
u	exposed perimeter
v_1	deflection of the uncracked section
v_2	deflection of the cracked section
v_{min}	minimum shear stress resistance
v_{tot}	total deflection
V_{Ed}	design shear force
$V_{Rd,c}$	design shear resistance of a member without shear reinforcement
w_k	crack width
w_{max}	maximum allowable crack width
W	section modulus

x	depth of compression zone or neutral axis depth
y	coordinate measured from the compressed edge of the wall cross-section
y_c	distance from the compressed edge to the concrete compression resultant
z	internal lever arm

Greek letters

α_e	modular ratio between steel and concrete
α_1	strength-dependent creep coefficient
α_2	strength-dependent creep coefficient
α_3	strength-dependent creep coefficient
β	coefficient depending on load duration
$\beta_c(t, t_0)$	factor describing the development of creep with time
$\beta(f_{cm})$	factor depending on mean compressive strength
$\beta(t_0)$	factor depending on concrete age at loading
β_H	coefficient depending on humidity and notional size
γ_c	partial safety factor for concrete
γ_s	partial safety factor for reinforcement
Δc_{dev}	allowance for execution deviation
ε_{cu}	ultimate compressive strain in concrete
ε_s	strain in the reinforcing steel
ε_{sm}	mean strain in the reinforcing steel
ε_{cm}	mean strain in the concrete between cracks
ε_{sy}	yield strain of the reinforcing steel
ζ	distribution factor between uncracked and cracked behaviour
λ	slenderness ratio
λ_{lim}	limiting slenderness ratio
ξ	relative neutral axis depth
ρ	reinforcement ratio
ρ_c	concrete density
ρ_l	longitudinal reinforcement ratio
$\rho_{p,ef}$	effective reinforcement ratio
σ_{cp}	compressive stress in concrete due to axial force
σ_s	stress in the reinforcing steel
ϕ	bar diameter
$\varphi(t, t_0)$	creep coefficient
φ_0	notional creep coefficient
φ_{eff}	effective creep coefficient
φ_{RH}	humidity factor for creep
ω	mechanical reinforcement ratio
ψ_2	quasi-permanent factor for variable load

Contents

1 Introduction

1.1 Background

The construction sector accounts for a significant share of the total carbon emission of society, with the concrete structural frame of multi-storey residential buildings representing one of the largest sources of greenhouse gas emissions. A joint report by Naturvårdsverket and Boverket states that the building and property sector caused approximately 13 million tons of equivalent CO2 in Sweden in 2016, which corresponds to approximately 21% of Sweden's production-based emissions and about 24% of Sweden's territorial emissions [1]. The same report shows that emissions are closely linked to both building activity and supply chains for materials and energy used in construction [1].

Concrete is central in the Swedish context because cement production remains a major domestic emission source. Naturvårdsverket reports that the Swedish cement industry emits about 2.5 million tonnes CO2, corresponding to about 5% of Sweden's greenhouse gas emissions [2]. This is relevant for Swedish housing construction because the large-scale housing programme Miljonprogrammet established production logics that normalised cast in situ concrete structural frames in multi-storey residential buildings [3]. These structures have primarily been optimized for rational and efficient construction processes, resulting in thick slabs and walls that are expected to satisfy several functions simultaneously, including load-bearing capacity, fire resistance, acoustic performance, and space for service installations. Larsson (personal communication, March 23, 2026) noted that, in current residential concrete buildings, acoustic requirements often become a governing factor for the selected thickness [4].

In recent years, this approach has been challenged in Sweden by the development of more climate efficient timber-based structural systems, including cross laminated timber. CLT is supported by comparative life cycle assessment studies that treat timber and concrete frames as separate design options for the same reference building. In an analysis by IVL and Sveriges Byggindustrier of five structural systems for a multi-storey residential reference building, one alternative is a cast in situ concrete frame and another is a massive frame in cross laminated timber, and the reported climate impact for the building stage differs between these systems, for example 290 kg CO2 equivalents per m^2 A_{temp} for the cast in situ concrete system and 223 kg CO2 equivalents per m^2 A_{temp} for the massive CLT system [5]. A key system difference is that timber floor solutions commonly handle building services in adjacent layers rather than inside the load-bearing element. In this way, the structure can focus on the load-bearing capacity of the material while minimizing material use.

For concrete structures, a comparable resource efficient design philosophy is less established. In Swedish multi-storey housing, cast in situ concrete slabs and walls are often detailed to accommodate building services within the structural depth, which

means that the selected thickness is not always governed only by load-bearing capacity and serviceability limit state criteria. When services are integrated in the structural elements, the required cross-section may be governed not only by structural demand but also by practical coordination of installations, building height constraints, and the preference for an established and efficient construction method. Larsson describes embedded services in cast in situ concrete as a common and efficient solution in current residential practice, but also notes that separating the structural frame from the services may improve long-term adaptability and circularity, even if it can increase the total floor build-up [4]. As a result, thinner structural solutions may be possible if building services are instead arranged in separate build-up layers outside the load-bearing slab.

Against this background, there is a clear motivation to reassess the design of concrete structural frames. By adopting principles similar to those used in timber construction, optimizing concrete primarily for load-bearing performance while allowing claddings, additional layers, and freestanding installations to address other functional requirements, it may be possible to reduce material use and, consequently, the climate impact of concrete buildings.

1.2 The Increasing Use of Materials

Empirical evidence indicates that material use in reinforced concrete structures has not decreased over time, despite advancements in analysis tools and material performance. A study within a project funded by Svenska Byggbranschens Utvecklingsfond compares 34 Swedish bridge superstructures built during 1969 to 1977 with bridges from 1997 to 2006 of comparable span lengths. During the time span between the two time periods, significant changes have been made in structural design standards including the change from allowable stress design to partial safety factor design methods. The results indicate that despite the advancements in structural analysis methods and material technology, neither the concrete volume nor the reinforcement content has decreased. Instead, both quantities have increased substantially, by approximately 50% [6].

A recent report by Sweco indicates that the increasing material use in infrastructure projects cannot be explained solely by higher loads or longer service life requirements, but is also linked to regulatory development and project practices. The report states that design standards have gradually become more detailed and require more checks, more documentation, and clearer proof of safety and durability. While these changes aim to ensure reliability and robustness, they may also contribute to systematically larger cross-sections and higher reinforcement ratios in practice. Sweco also points out that complex calculations and verification routines can shift focus from material optimisation to meeting formal requirements. This suggests that the combination of stricter standards and risk-based practice can contribute to higher material quantities even when improved tools could allow more refined designs [7].

In the section on concrete structures (3.3), Sweco highlights that several changes in requirements have contributed to increased material use over time. In particular, stricter durability rules have led to tighter crack width limits, higher minimum reinforcement ratios, and increased concrete cover. Although crack control requirements already existed in older standards, today they are linked to exposure classes and design working life, which often results in more reinforcement than what is required by load-bearing capacity alone. The report also notes that minimum reinforcement rules in Eurocode can give significantly higher reinforcement amounts compared to earlier Swedish rules for similar member thicknesses. In addition, increased cover requirements to protect against corrosion have led to thicker concrete sections. Together, these durability and detailing requirements can drive material quantities upward, even when structural demand has not increased proportionally [7].

1.3 Aim & Scope

The aim of this thesis is to investigate how cast in situ load-bearing walls and slabs in multi-storey residential buildings can be designed more resource efficiently by clearly separating the structural concrete from installations, fire protection and acoustic solutions. The study seeks to quantify the structural material quantities and to discuss the indicative climate implications, rather than performing a complete life cycle assessment of full floor and wall systems.

The study is also relevant in relation to the ongoing shift in Swedish building regulations towards a more performance-based regulatory framework. If compliance is demonstrated through verified performance rather than through prescribed standard solutions, alternative structural concepts may become more relevant in early design stages.

The results are intended to provide a basis for preliminary design decisions by showing how slab thickness, wall thickness, reinforcement amount, concrete strength and support conditions influence the structural capacity and serviceability of cast in situ concrete members. Based on this aim, the thesis addresses the following research questions:

- Can the material use in cast in situ concrete slabs and walls in multi-storey residential buildings be reduced by designing the structural concrete primarily for load-bearing capacity and serviceability, while installations, fire protection and acoustic requirements are handled separately?
- Has the material use in reinforced concrete structures increased over time, and which changes in design standards, verification procedures and practical requirements may explain this development?

To fulfil this aim, the thesis addresses the following objectives. First, to describe and compare a historical and a contemporary cast in situ concrete reference structure in terms of slab thickness, wall thickness, reinforcement and integration of installations.

Second, to investigate the potential reduction in structural slab thickness and reinforcement amount when the slab is governed by load-bearing capacity, deformation and vibration criteria, while acoustic performance and installations are assumed to be handled by additional layers outside the structural concrete. Third, to compare material use between the reference structure and the evaluated structural alternatives. Finally, to discuss how fire requirements, acoustic performance, constructability and cost may affect the feasibility of reducing structural concrete thickness in real projects.

The scope of this thesis is limited to cast in situ load-bearing slabs and walls in multi-storey residential buildings. Prefabricated concrete systems, bridges and other civil engineering structures are not included in the calculation study. Such examples are only used in the literature review to illustrate broader developments in concrete design practice and material use.

2 Method

AI-based tools were used as support during the writing process, mainly for language editing, formulation and structure review. All text developed with such support has been reviewed by the authors. The authors take full responsibility for all content of the thesis.

2.1 Review of historical design context

A review of the historical Swedish regulatory context was carried out to explain how the basis for structural concrete design has changed over time. The review focused on the development from earlier Swedish building regulations, such as BABS and SBN, to the current Eurocode-based design framework. The purpose was to identify how the number of requirements, verification procedures and documentation demands has increased, and how this development may have influenced material use in reinforced concrete structures.

The review was also necessary for the interpretation of the Cykelskrapan reference structure. This structure was designed under a different regulatory framework than the one used in current practice. It was therefore not treated as a structure designed according to present-day Eurocode assumptions, but as an example of a structural solution developed under another design logic, with different calculation methods, material definitions and detailing rules. The historical context was used to avoid interpreting the older slab and wall details only through current design standards.

The historical review was further used to support the discussion of why material use in concrete structures may have increased over time. Previous studies and reports indicate that increased material quantities cannot be explained only by higher loads or longer service life requirements. They may also be related to the development of more detailed design standards, stricter serviceability and durability requirements, increased minimum reinforcement, larger cover requirements and more formalised verification procedures. The review therefore provides a background for comparing the older and contemporary reference structures, and for discussing whether current design practice may contribute to increased material use.

The review also included the recent Swedish reform towards a performance-based regulatory framework. This was used to frame the relevance of alternative design strategies, where structural safety, serviceability and durability must still be verified even if the chosen technical solution differs from established practice.

2.2 Review and interpretation of reference structures

Two existing cast in situ concrete structures were reviewed in order to establish reference cases for the comparison between historical and contemporary design practice. The first reference was Cykelskrapan, a student housing project in Lund from 1956, and the second reference was the Troja student housing project in Lund from 2022. These projects were selected because both include cast in situ concrete floor and wall systems in residential buildings, while representing two different periods of Swedish concrete design.

The purpose of the review was to extract comparable geometric and material parameters for use in the later calculations. The reviewed parameters included slab thickness, total floor depth, wall thickness, concrete strength class, span length, reinforcement layout and interpreted reinforcement area per metre width. The extracted values were then used to define reference cases and to compare how the distribution between load-bearing concrete and non-structural floor build-up differs between the two structures.

The Cykelskrapan reference structure was interpreted from structural drawings. The drawing information was reviewed to identify the load-bearing slab thickness, additional floor layers, wall thickness, concrete class, span length and reinforcement notation. Since the drawings use historical notation and do not always provide a complete reinforcement layout for every structural member, the reinforcement was interpreted from the available section drawings and related details.

The Troja reference structure was reviewed in the same way, based on available structural drawings and project information. The slab and wall dimensions, concrete strength class and reinforcement arrangements were extracted from the drawings. General reinforcement and local supplementary reinforcement were separated where possible, since local reinforcement at wall-slab connections does not represent the general reinforcement level of the slab field. This distinction was necessary in order to avoid treating local detailing reinforcement as uniformly distributed slab reinforcement.

The two reference structures were used as comparative examples. The structures were designed under different regulatory frameworks, with different design assumptions, material definitions and detailing practices. The comparison was therefore used to identify differences in structural thickness, reinforcement level and floor build-up strategy, while the calculation models in the following sections were used to evaluate structural capacity and serviceability in a consistent way.

2A complete historical verification of the Cykelskrapan structure would require the members to be recalculated according to the regulations, material definitions and design assumptions valid at the time of construction. Such a verification was outside the scope of this thesis.

2.3 Expert interviews and professional context

To complement the literature review and the interpretation of the reference structures, expert interviews were conducted with Sven Thelandersson, Robert Larsson and Johan Hellqvist. The purpose of the interviews was to obtain professional context regarding structural design practice, the development of design regulations, and practical factors that influence the design of cast in situ concrete slabs and walls.

The interviews were mainly used as background material and as support for the discussion of the results. They provided insight into how requirements related to acoustics, fire safety, service installations, constructability, design risk and code application may influence material use in practice.

No numerical input values in the slab or wall calculation models were taken directly from the interviews. The calculation results are based on the assumptions, material properties and verification procedures described in the calculation model sections and in Appendices A and B. Statements from the interviews are referenced in the text as personal communication.

2.4 Slab calculation model

The slab calculations were based on the idealised structural systems. The purpose of the model was to evaluate how the allowable span of a cast in situ concrete slab is affected by slab thickness, reinforcement amount, concrete strength and support conditions. The slab was modelled as a one metre wide strip subjected to uniformly distributed load. This model was used to simplify the calculations and to allow a consistent comparison between different slab thicknesses, reinforcement amounts, concrete strength classes and support conditions.

The one metre wide slab strip was treated as a beam strip model and should not be understood as the strip method for plate analysis. The purpose was not to determine a two-way load distribution in a specific floor plan, but to obtain comparable span limits for defined support conditions. This simplification is most representative for one-way slab behaviour, especially for elongated slab fields where the main part of the load is carried in the short direction. For more square slab fields, load transfer in both principal directions may increase the actual capacity compared with the one metre beam strip model. The calculated span limits should therefore be interpreted as conservative for slab geometries with significant two-way action.

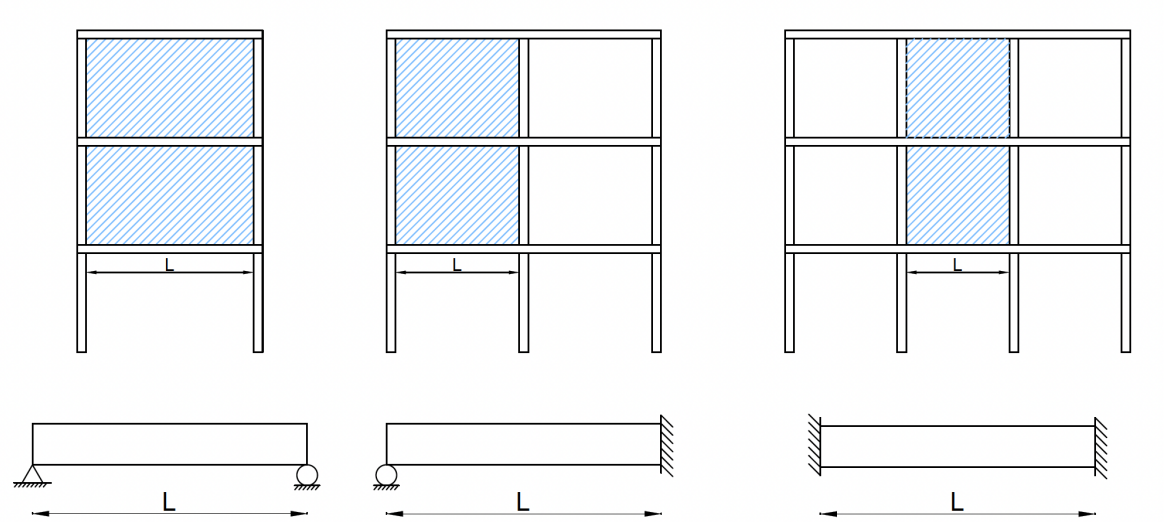

Figure 2.1: Idealisation of the slab systems used in the calculation model.

Three support conditions were considered, as shown in Figure 2.1. The first model represents a single slab bay with simple supports at both ends. This case gives the lowest degree of rotational restraint and was used to represent an edge case where continuity cannot be relied upon. The second model represents a slab bay with one simply supported end and one fixed end. This was used to represent an intermediate case where the slab has continuity on one side but a more flexible or discontinuous boundary on the other side. The third model represents a slab bay with fixed ends at both sides. This was used to represent an internal bay where continuity to adjacent slab fields and supporting walls can provide rotational restraint.

The three structural models were used because the study does not aim to analyse one specific floor plan, but to compare how different support assumptions affect the calculated span limits. This also makes it possible to present span tables that can be applied to different slab situations, rather than only to the two reference structures studied in this thesis. In a real building, the actual support condition depends on the structural layout, adjacent slab fields, reinforcement over supports and cracking behaviour. The three models therefore represent a range of possible boundary conditions, from a simply supported slab bay to an internal bay with rotational restraint at both ends. This approach follows the general principle in EN 1992-1-1 that structural analysis should be based on an idealisation of the geometry and behaviour of the structure that is suitable for the problem being studied [8].

The parameter study was limited to three reinforcement diameters and three concrete strength classes in order to keep the scope of the calculations manageable. The selected reinforcement diameters were $\phi = 6$, 9 and 12 mm. These were chosen to represent both smaller bars, which may be beneficial for crack control, and larger bars, which provide larger reinforcement areas with fewer bars. For each diameter, several reinforcement spacings were analysed in order to obtain a range of reinforcement amounts per metre slab width. Only under-reinforced cross sections were included in the parameter study, while over reinforced cross sections were excluded from the reported results.

The bending resistance was calculated as a singly reinforced cross section in each analysed section, where only the reinforcement on the tensile side was included in the resistance calculation.

The concrete strength classes C12/15, C20/25 and C40/50 were included. These classes were selected to cover a range from low to high concrete strength. This made it possible to study how both strength and stiffness influence the allowable span without expanding the parameter study beyond the scope of the thesis.

This parameter-based approach was used because the study does not aim to design one specific slab, but to identify how different design choices influence the governing span limit. By varying the parameters while applying the same verification procedure, the results show whether the slab is governed by bending resistance, shear resistance, deflection, crack width or vibration for each combination.

For each slab model, the same verification procedure was applied. The ultimate limit state checks included bending resistance and shear resistance without shear reinforcement. The serviceability limit state checks included deflection, crack width and vibration. The detailed calculation procedure and the coefficients used for each structural model are presented in Appendix A.

The concrete density was taken as $\rho_c = 2500$ kg/m^3, the additional permanent floor build-up load as 0.5 kN/m^2, and the imposed residential load as 2.0 kN/m^2. The ultimate limit state load combination was taken as $1.2G_k + 1.5Q_k$, while the serviceability limit state calculations were based on the quasi-permanent combination $G_k + \psi_2 Q_k$, with $\psi_2 = 0.3$.

The nominal concrete cover was taken as $c_{nom} = 20$ mm, based on a minimum cover of 10 mm and an allowance for execution deviation of 10 mm. This was done to keep the comparison consistent and to limit the number of varying input parameters. For $\phi 12$ reinforcement, the bond requirement gives a slightly larger nominal cover of 22 mm. A sensitivity check was therefore carried out for selected span cases. The corrected cover reduced the calculated span capacity by approximately $0.6 - 0.8\%$. The reported $\phi 12$ results therefore slightly overestimate the possible span capacity, but the influence was considered small in relation to the comparative purpose of the parameter study.

The creep coefficient $\varphi(t, t_0)$ was calculated according to EN 1992-1-1, Appendix B. The relative humidity was taken as $RH = 50$ %, the age at loading was taken as $t_0 = 32.5$ days and the considered time was taken as $t = 365$ days. The final creep deformation check for $\varphi_{\infty,t0}$ was not included in the study. This may underestimate long term deflections, but the same assumption was applied consistently in all slab comparisons. Shrinkage curvature was not included in the slab deflection calculation. The crack width verification was carried out according to EN 1992-1-1, Section 7.3.4, with a maximum allowable crack width of $w_{max} = 0.4$ mm for exposure class XC1 [8].

The vibration verification was carried out as a simplified serviceability check. For each slab configuration, the fundamental frequency was estimated from the maximum immediate static deflection of the slab strip using the method presented by MacGregor [9]. The calculation was based on the uncracked gross concrete section and the short

term modulus of elasticity, E_{cm}. The immediate static deflection was calculated using the deflection coefficient corresponding to the considered support condition. The limiting frequency was taken as $f_{min} = 5.2$ Hz, based on the criterion for walking-induced vibrations from Betongelementforeningen [10]. The detailed vibration calculation is presented in Appendix A.

2.5 Wall calculation model

The wall calculations were based on an idealised vertical wall strip with a width of one metre. The purpose of the model was to evaluate how the axial resistance of load-bearing concrete walls is influenced by wall thickness, effective buckling length, concrete strength class and vertical reinforcement amount. The wall was therefore not modelled as part of a complete building system, but as an isolated compression member representative of a vertical load-bearing wall in a multi-storey residential building.

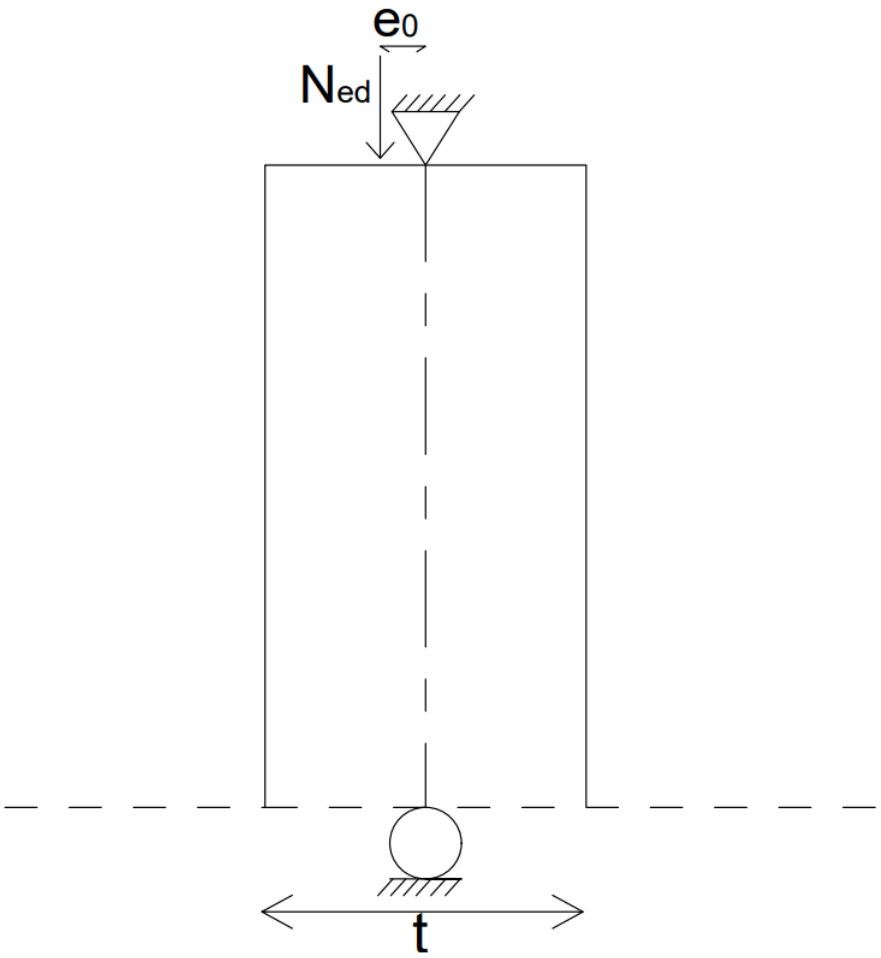

Figure 2.2: Idealised side-view of the wall strip used in the calculation model. The wall has thickness t, effective buckling length l_0 and an axial design load N_{Ed} acting with an initial eccentricity e_0. The wall is idealised as pinned at both ends.

The structural idealisation shown in Figure 2.2 was assumed to be laterally restrained

at the top and bottom while rotations were free. This corresponds to a pinned-pinned column idealisation, where the effective buckling length was taken as equal to the wall height. This assumption was used to obtain a consistent comparison between different wall thicknesses, concrete strength classes and reinforcement amounts. The initial eccentricity of the axial load was included in the calculation model, and the first-order moment was calculated from the axial force and eccentricity.

Both reinforced and unreinforced wall alternatives were analysed. The reinforced wall model was based on strain compatibility and cross-sectional equilibrium under combined axial compression and bending. The section analysis assumed that plane sections remain plane, that concrete in tension is neglected in the ultimate limit state, and that the reinforcement stresses are determined from the calculated strain distribution. Second-order effects were included by amplifying the first-order moment using a nominal stiffness approach. The design axial resistance was then determined numerically as the largest axial force for which both axial force equilibrium and moment equilibrium could be satisfied.

The reinforcement was represented by welded mesh reinforcement placed on both faces of the wall. The mesh designation, for example #5150, refers to a welded mesh with 5 mm bars at 150 mm spacing. The reinforcement area from one mesh layer was therefore doubled in order to obtain the total vertical reinforcement area per metre wall length. The total reinforcement area used in the wall calculations was calculated as

$$A_{s,\mathrm{tot}} = 2A_{s,\mathrm{mesh}} \tag{2.1}$$

where $A_{s,\mathrm{mesh}}$ is the vertical reinforcement area of one mesh layer per metre wall length. The investigated reinforcement meshes are shown in Table 2.1.

Table 2.1: Standard welded reinforcement meshes used to define the investigated wall reinforcement amounts.

Mesh type	**Bar diameter [mm]**	**Spacing [mm]**	$A_{s,\mathrm{mesh}}$ **[mm²/m]**	$A_{s,\mathrm{tot}}$ **[mm²/m]**
#5150	5	150	131	262
#6150	6	150	188	376
#8150	8	150	335	670
#9150	9	150	424	848
#10150	10	150	524	1048

For each wall thickness, the minimum vertical reinforcement requirement was first evaluated, and the smallest standard mesh satisfying this requirement was selected for the main reinforced wall comparison. Additional comparisons were then carried out using constant wall thickness, constant concrete strength class or constant reinforcement amount in order to isolate the influence of individual parameters.

For comparison, an unreinforced wall model was also included. This model was based on the simplified design approach for unreinforced and lightly reinforced concrete walls in EN 1992-1-1, Chapter 12. The unreinforced wall results were only considered applicable when the assumed validity conditions of the simplified model were satisfied,

including the adopted slenderness limitation and the eccentricity assumptions used in the calculation.

The parameter study included wall thicknesses from 120 mm to 220 mm, effective buckling lengths from 2.0 m to 4.0 m and the concrete strength classes C12/15, C20/25 and C30/37. The eccentricity was taken as $e_0 = l_0/400$ in both the reinforced and unreinforced wall comparisons. The parameter range used in the wall study is summarised in Table 2.2.

Table 2.2: Parameter range used in the wall study.

Parameter	**Investigated values**
Wall strip width [m]	1.0
Wall thickness t [mm]	120, 140, 150, 160, 180, 200, 220
Effective buckling length l_0 [m]	2.0–4.0
Concrete strength class	C12/15, C20/25, C30/37
Reinforcement amount $A_{s,\mathrm{tot}}$ [mm^2/m]	262, 376, 670, 848, 1048
Eccentricity assumption	$e_0 = l_0/400$
Output quantity N_{Rd} [kN/m]	Design axial resistance

The detailed calculation procedure, including material properties, creep coefficient, nominal stiffness, second-order moment amplification, strain distribution, equilibrium equations and the unreinforced wall comparison model, is presented in Appendix B.

3 Literature review

3.1 Design Principles in the 20th Century

BABS

In Sweden during the 1950s, building projects were primarily governed by the 1947 Building Ordinance (Byggnadsstadgan) together with technical guidance issued by the National Board of Public Building (Byggnadsstyrelsen) as "Anvisningar till byggnadsstadgan" (BABS). Boverket's historical overview explains that the first guidance connected to the 1947 ordinance was BABS 1946, which remained valid until BABS 1950 entered into force on 1 April 1950 [11].

For structural design, BABS 1950 includes a dedicated part on actions and loading assumptions ("Avdelning I – Påkänningar på byggnads bärande delar"). It specifies which load assumptions should be used when calculating actions on load-bearing structural elements. The document also distinguishes between normal loading conditions, such as permanent and variable loads, and exceptional actions, and describes how these loads should be combined into load cases [12].

Concrete Design Provisions in the 1950s

While BABS provided the overall building-technical framework (including loads), detailed rules for concrete materials and execution were developed in separate documents. In the late 1940s, the Swedish state produced proposals for "Statliga betongbestämmelser". The 1949 material part states that the provisions were intended primarily for common building, bridge and hydraulic structures in concrete and reinforced concrete, and that the responsible authority could, in special cases, specify different requirements and permit different permissible stress levels than those stated [13].

By the late 1950s, concrete design guidance for state-controlled works was formalized further through supplements to earlier state cement/concrete provisions. A 1957 publication described as "Statliga betongbestämmelser D. 2a" (covering design rules for solid concrete slabs and acting as a supplement to parts of the 1934 state cement and concrete provisions) was approved to apply from 10 July 1957 for concrete works executed by several Swedish state agencies [14].

SBN

After BABS, Swedish building rules were updated through Svensk Byggnorm (SBN). Boverket states that SBN 67 entered into force on 1 January 1968 and replaced the earlier guidance linked to the Building Ordinance. In practice, this meant that the national rules were gathered into a more structured and consistent code than the BABS guidance documents [15].

Boverket also describes how SBN was revised in later editions, including SBN 75 and SBN 80, with additional supplements during the period. These revisions increased the level of detail and made the organisation of the requirements clearer across different technical areas. For structural design, the SBN period can therefore be described as a step towards more standardised rules and a clearer basis for verification, where requirements on loads and safety were presented in a more uniform way than before. The overall development during the SBN era reflects a move from earlier guidance style documents towards a national code with clearer structure and more consistent application across projects [15].

An important change during the final part of the SBN period was the introduction of the partial coefficient method for structural design. Earlier Swedish design rules were largely based on permissible stresses, while the newer format separated the safety treatment into partial coefficients for actions, material properties and resistance. The method was introduced through separate provisions for load-bearing structures, SBN avd. 2A and later became the established format in Swedish structural regulations through NR and BKR.

This transition was therefore not a single abrupt change, but a gradual movement from older permissible-stress based design towards limit state design with partial coefficients.

NR

After SBN 80, the regulatory system was restructured through the introduction of Nybyggnadsreglerna (NR). According to Boverket, NR entered into force in 1989 and replaced the previous system under Svensk Byggnorm. For structural design, NR continued the development in which the partial coefficient method and separate provisions for load-bearing structures had already been introduced through SBN avd. 2A. With NR, the regulations shifted more clearly towards functional requirements rather than detailed technical prescriptions, essentially meaning that they specified the required performance rather than prescribing how the structure should be designed in detail [15].

Compared to SBN, NR reduced the level of detailed instructions and instead focused on stating what should be achieved. This meant that designers were given greater responsibility for demonstrating that the requirements were fulfilled. The shift during the NR period can therefore be described as a transition from a more prescriptive code to a system where verification and interpretation played a larger role. This

development laid the foundation for the later introduction of Boverkets byggregler, where the separation between functional building requirements and structural design rules became more explicit [15].

BBR & BKR

After NR, Boverkets byggregler (BBR) was introduced. Boverket states that BBR 1, BFS 1993:57, entered into force on 1 January 1994, and that the NR rules ceased to apply at the same time. In the same reform, Boverkets konstruktionsregler (BKR 1, BFS 1993:58) was introduced as a separate set of rules for structural design [15]. In BKR, the partial coefficient method became the central format for structural verification in Swedish building design. Safety was treated using partial coefficients for actions and resistance, together with safety classes for structural members.

Boverket describes BBR as functional requirements, meaning that the regulations specify the required function of the building, while the way of fulfilling these requirements may vary. In contrast, BKR contained the technical rules for verification of structural safety. This separation meant that BBR regulated overall building performance, while BKR governed the design and calculation of load-bearing structures. The system remained in place, with revisions over time, until BKR was replaced by the Eurocodes through EKS in 2011, while BBR continued as the main set of building regulations [15].

The BKR system remained in force until 2011, when the Eurocodes were introduced as the main basis for structural design in Sweden through Europeiska konstruktionsstandarder (EKS). This marked the transition from a national set of structural rules to a harmonised European design framework. The current system based on Eurocode 2 is described in Section 3.2.1.

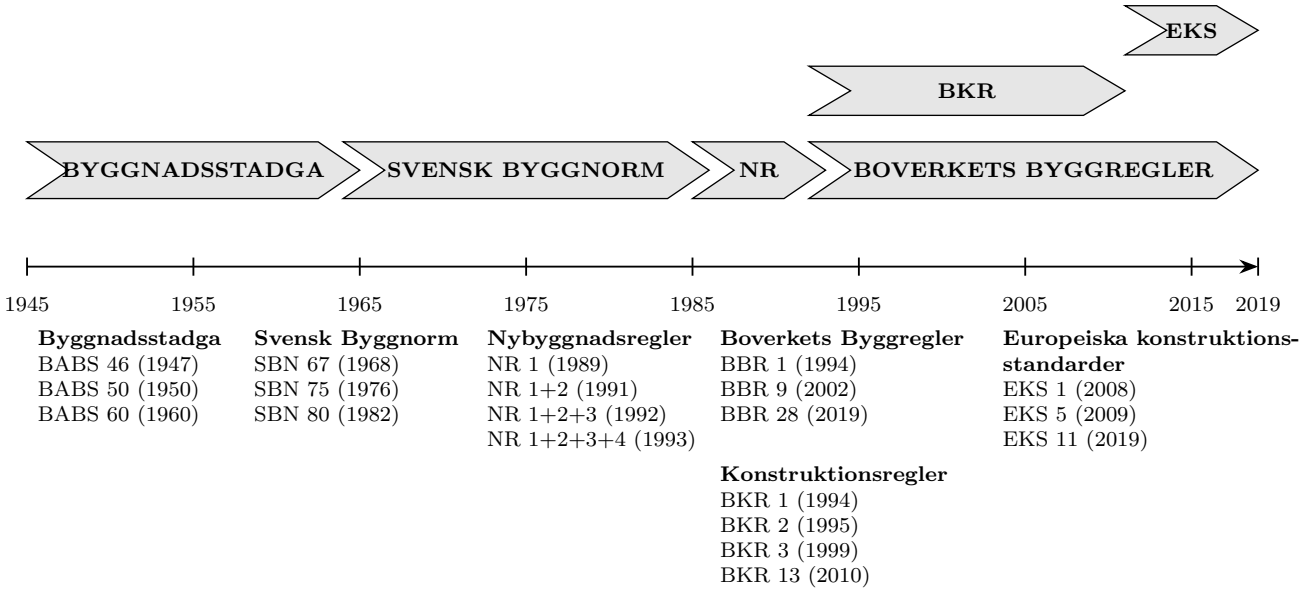

Figure 3.1: Development of Swedish building regulations relevant to structural design. The timeline shows the main regulatory transitions, while only selected representative editions of each regulation are listed for clarity. Based on *Boverkets Byggregler – en historisk överblick* [15].

3.1.1 Cast in situ concrete structure from 1950s, Cykelskrapan

To illustrate how cast in situ concrete floor systems were designed in Swedish residential buildings during the 1950s, a section drawing from Cykelskrapan, a student housing project in Lund from 1956, is analysed. The example provides a concrete reference for how slab thickness, wall thickness and reinforcement were arranged in practice before the introduction of modern design standards. It also serves as a basis for comparison with current floor systems discussed later in the thesis, see Chapter 3.3. The below drawing originates from a structural design prepared for Akademiska Föreningen.

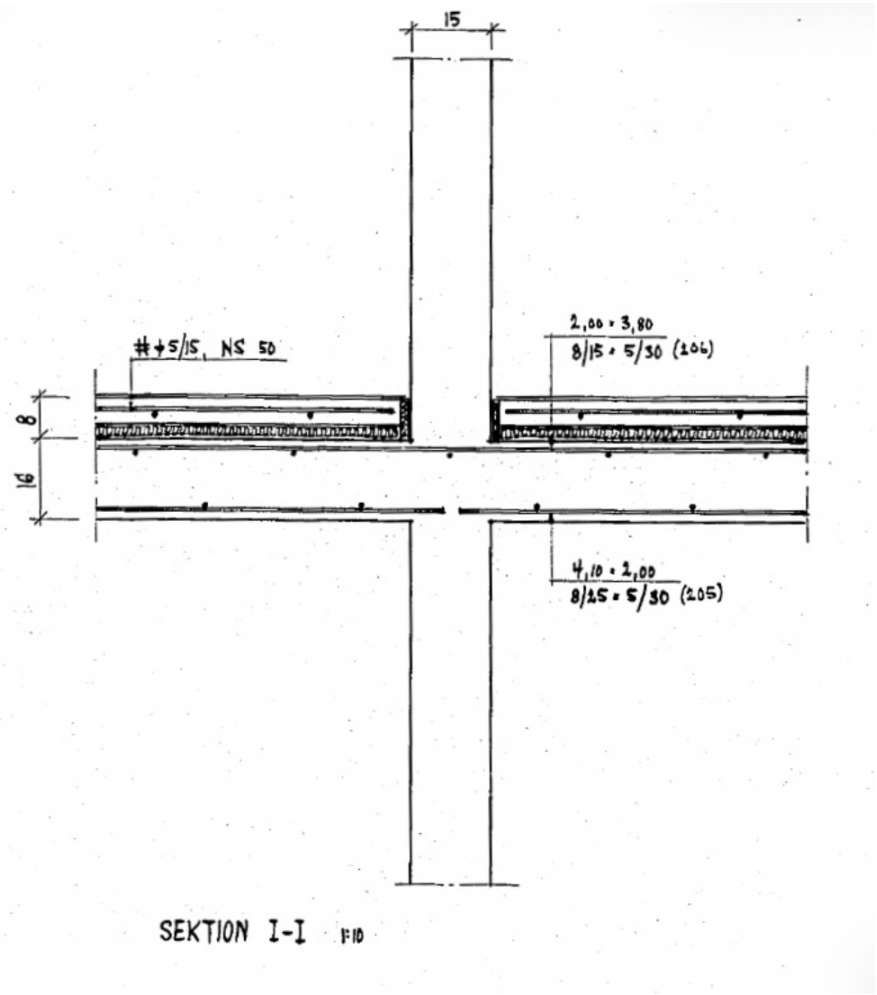

Figure 3.2: Section drawing of a cast in situ concrete floor and load-bearing wall in Cykelskrapan, Lund, dated 1956.

The section shown in Figure 3.2 corresponds to section I–I in the original structural drawings and illustrates the connection between the floor slab and a load-bearing concrete wall. The wall has a thickness of 150 mm and supports a cast in situ reinforced concrete floor slab. The structural drawings further specify the concrete as "Betong II STD, K200" for slabs and walls. This has been interpreted as a cube compressive strength of approximately 20 MPa, which is closest to the modern concrete strength class C16/20. The conversion is approximate, since the historical material designation and the modern Eurocode strength class system are not directly equivalent. According to the section, the structural slab thickness is 160 mm, with an additional 80 mm layer above. This upper layer is interpreted as a non-structural topping or floor build-up, whereas the lower 160 mm constitutes the load-bearing part of the slab. The span of the slab is 3.69 m.

The reinforcement is indicated using Swedish drawing notation typical of the 1950s. The designation "# +5/15, NS 50" is interpreted as a welded reinforcement mesh consisting of Ø5 mm bars at 150 mm spacing in two orthogonal directions. The plus sign indicates reinforcement in both directions, while "NS 50" denotes the steel grade of the welded mesh.

Additional reinforcement is specified over certain parts of the slab using notations such as “2,00–3,80 / 8/15 + 5/30 (206)” and “4,10–2,00 / 8/25 + 5/30 (205)”. These notations are interpreted as local reinforcement arrangements extending over specified lengths of the slab, measured from a reference point shown elsewhere in the drawings. The reinforcement expressions follow the format diameter/spacing, meaning that “8/15” denotes Ø8 mm bars at 150 mm spacing, “8/25” denotes Ø8 mm bars at 250 mm spacing, and “5/30” denotes Ø5 mm bars at 300 mm spacing.

To enable comparison with the Troja slab and the calculation model, the interpreted reinforcement was converted into reinforcement area per metre slab width. By summing the relevant bar arrangements, the reinforcement in the analysed section corresponds to approximately 400 mm^2/m for the top reinforcement and 266 mm^2/m for the bottom reinforcement.

The section therefore indicates that the reinforcement varies along the slab depending on structural demand. In the interpreted section, the local reinforcement ranges from about 266 mm^2/m to 400 mm^2/m. The denser reinforcement is located near the support, which is consistent with higher bending moments in these regions. The numbers in parentheses, such as “(205)” and “(206)”, are interpreted as reinforcement position numbers referring to a reinforcement schedule or bar list in the original drawings.

Overall, the section illustrates a typical Swedish mid-20th-century cast in situ floor system, consisting of a relatively slender load-bearing wall, a 160 mm structural concrete slab, an additional non-structural topping layer, and reinforcement made up of a standardised welded mesh supplemented by local bar reinforcement near supports.

3.2 Design Principles in Current Practice

3.2.1 Eurocode

Current structural design practice in Sweden is based on the European structural design standards known as the EN Eurocodes, which are a series of ten European Standards from EN 1990 to EN 1999 that provide a common approach for the design of buildings and other civil engineering works. The Eurocodes define the overall basis of structural design, actions on structures, and material specific design rules, including concrete design in EN 1992, and they are used together with National Annexes that specify national choices within the common framework. Together, these documents provide the framework for verifying structural safety, serviceability, and durability in current design practice [16].

3.2.2 Ultimate Limit State (ULS)

At the ultimate limit state, the structure is verified against collapse or loss of load-bearing capacity by checking that design effects of actions do not exceed the design resistances of the member. For slabs and walls this is typically done by first determining design internal forces from structural analysis, then verifying cross-section resistance in bending and, where relevant, axial force.

Longitudinal reinforcement is determined by identifying the governing ULS verification for the member and adopting the reinforcement required to satisfy all relevant resistance checks. For many slabs and walls, the required longitudinal reinforcement is obtained from cross-section resistance in bending with or without axial force, where internal compression in concrete and tension in reinforcement are balanced and the design moment is resisted by these resultants acting with an internal lever arm z. In addition to flexural resistance, slabs must be checked for shear and, for flat slabs or around concentrated supports, punching shear, which is treated as a specific ULS verification for slabs. For walls, ULS verification includes combined axial force and bending, and where slenderness effects are significant, second-order moments are included in the design moments used for resistance checks [8] [17].

3.2.3 Serviceability Limit State (SLS)

At the serviceability limit state, the structure is verified to ensure satisfactory performance under normal use. According to EN 1990 Section 1.5.2.14, serviceability limit states are reached when the structure remains safe against collapse but no longer fulfils the functional requirements for normal use, for example due to excessive deflection, cracking, vibration, or stress levels [18]. In Eurocode 2, the SLS framework for reinforced concrete members is addressed in Chapter 7, where the checks are organised around limitation of stresses, crack width, and deflection, and the verifications are performed under relevant service load combinations using either calculation methods or simplified rules [8].

3.2.4 Nonstructural Design Aspects

Eurocode 2 is primarily a structural design standard, and it explicitly states that other requirements such as thermal or acoustic insulation are not considered [8]. In projects where the structure is intentionally made thinner and reinforcement is minimized, several other requirements typically become decisive because they are strongly linked to stiffness, mass, cover margins, and the way the slab interacts with non-structural layers and execution stages.

Acoustic performance

Acoustic performance is a key requirement for floors because it directly affects occupant comfort. Two main mechanisms are relevant: airborne sound, such as speech or music transmitted through the floor, and impact sound, such as footsteps or dropped objects transmitted as vibration through the structure [19]. A concrete slab generally performs well for airborne sound because its mass helps reduce sound transmission. Impact sound is often more demanding, since vibrations can be transmitted through the structural floor and into adjacent rooms.

This is important for the design philosophy studied in this thesis. If the structural slab is made thinner, the mass of the primary concrete element is reduced. The floor system may therefore have smaller acoustic margins and become more dependent on additional non-structural layers to satisfy the required sound class. Larsson also noted that acoustic requirements are often one of the main practical drivers of slab thickness in residential buildings [4]. This suggests that the selected slab thickness in current practice is not always governed primarily by load-bearing demand, but also by the need to satisfy acoustic performance requirements.

Vibrations

Vibration serviceability in buildings is primarily associated with floor structures subjected to human-induced loading. Vertical structural elements such as walls are not typically governing from a vibration comfort perspective in ordinary buildings. Even small structural vibrations can be perceived as uncomfortable by occupants. Guidance used in European practice therefore treats vibration as a comfort and usability requirement and evaluates floors based on dynamic response measures such as natural frequency, damping and vibration level under walking-type excitation [20].

Making a concrete slab thinner generally makes vibration requirements more difficult to satisfy because floor vibration depends mainly on stiffness, mass, and damping. A reduction in thickness lowers bending stiffness significantly and often reduces mass, which can decrease natural frequency and increase vibration response under walking loads [20]. Reducing reinforcement does not normally offset this effect and may further reduce effective stiffness in service due to cracking [20] [21].

Floor vibrations were treated as a serviceability issue because reduced slab thickness affects both stiffness and natural frequency. SS-EN 1990 states that vibration behaviour in the serviceability limit state should be assessed with regard to user comfort and the function of the structure or its components. It also states that the natural frequency of the structure or structural member should be kept above suitable values depending on the building function and the vibration source, and that a more refined dynamic analysis may be required when the natural frequency is lower than the relevant value [22].

For further guidance, SS-EN 1990 refers to ISO 10137, which gives recommendations for evaluating the serviceability of buildings and walkways against vibrations. In this thesis, vibration was therefore included as a simplified serviceability check for the slab models. The calculation method used in the parameter study is described in Appendix A.

Fire

Fire requirements exist because a building must maintain life safety in the case of a fire, by limiting fire spread and by ensuring that key structural elements do not lose their load-bearing capacity prematurely. Structural fire design for concrete is handled in EN 1992-1-2 [23]. The standard provides temperature dependent material models for both concrete and reinforcing steel, including reduction factors for the strength of reinforcement as a function of steel temperature in table 3.2 of EN 1992-1-2 [23]. As temperature increases during fire exposure, the strength of reinforcement decreases accordingly.

EN 1992-1-2 also includes simplified tabulated methods for walls and slabs, where the required fire resistance time is linked to minimum member thicknesses and minimum distances from the exposed surface to the centre of the reinforcement [23]. These requirements ensure that the reinforcement remains sufficiently protected by concrete so that its temperature and therefore its strength reduction remains within acceptable limits during the fire duration. Consequently, reducing slab or wall thickness reduces the available thermal protection for the reinforcement and decreases the geometric margin for cover and construction tolerances [23].

Service Installations in the Structural Frame

In cast in situ residential concrete construction, service installations are often embedded within the slab depth as part of an established and efficient construction method. According to Larsson, this approach is attractive because it helps keep the total floor depth low, which can be important in projects where building height is constrained, while still providing sufficient space for the required service installations. At the same time, he pointed out that longer horizontal service runs in more open floor plans may require sufficient slope, which can in some cases contribute to thicker slabs when installations are cast into the slab. Embedded installations also reduce flexibility, since later changes to pipe routing become more difficult without interventions in the concrete, and incorrect placement may require the slab to be opened after casting [4]. Separating the installations from the load-bearing structure could instead improve long-term adaptability and circularity, although such a solution may increase the total build-up thickness.

3.2.5 Additional Floor Build-Up Layers

To reduce the thickness of the load-bearing concrete, functional requirements, which was discussed in 3.2.4, may need to be addressed by additional layers outside the structural element. Such layers can be used to improve acoustic performance, increase fire resistance, and create space for installations. This section therefore presents examples of non-structural build-up solutions that can support a more material efficient structural design.

Acoustics

One way to improve acoustic performance without relying only on the mass of the structural slab is to add separate floor or ceiling layers. Practical guidance for concrete floors commonly recommends a floating floor build-up, for example a floated plywood floor or similar decoupled layer, to reduce impact vibrations reaching the slab and the room below [19]. Research literature supports the same principle: a floating floor is normally described as an upper layer, such as a panel or screed, placed on a resilient layer on top of the structural concrete slab, and this construction is used specifically to improve impact sound insulation of concrete floors [24].

Suspended ceilings can also contribute to improved acoustic performance by adding a decoupled layer below the slab and by introducing damping and sound absorption in the cavity. Experimental work on floors shows that adding floating floors and suspended ceilings can improve impact sound insulation, and that the ceiling solution can be particularly effective in some configurations [25]. More detailed studies of ceiling systems also show that the improvement depends on the type of hangers and the mechanical coupling, meaning that the detailing of the ceiling suspension is important, not only the presence of a ceiling [26].

Fire

Fire resistance can also be improved by measures outside the load-bearing concrete section. A test based overview of external fire protection systems for concrete lists these main types: spray mortar, coating, precast mortar placed in the formwork before casting, post-fixed board, pre-fixed board placed in the formwork before casting, and combined systems where the lining also provides other functions such as acoustic lining [27] (Section 4.3).

One example of such an external fire protection system is PAROC Figra 170, a stone wool lamella insulation system intended for fire protection of load-bearing concrete slabs and beams. The product is installed on the fire-exposed surface and forms part of a tested fire protection system used to increase the fire resistance of concrete members. Supplier documentation for the stone wool presents the concept of equivalent thickness of concrete, where a given thickness of fire protection is expressed as an equivalent concrete layer based on temperature response during fire exposure. The equivalent thickness is determined according to EN 13381-3 Annex C by comparing temperature

data from a fire test on a fire-protected concrete member with temperature data for an unprotected concrete member, meaning that the method translates the protective effect of the insulation into millimetres of concrete [28].

For the reference case, basic temperature data for an unprotected concrete slab with a thickness of 200 mm were derived from EN 1992-1-2 Figure A.2, and corresponding reference data for an unprotected concrete beam with a section of 300 mm by 600 mm were derived from EN 1992-1-2 Figure A.7 and Figure A.8. The resulting table links insulation thickness to an equivalent concrete thickness for different exposure times according to EN 1361-1, and PAROC states that, in practice, 30 minutes of fire exposure corresponds to 49 mm of concrete being equal to 20 mm of fire protection for a concrete slab, see Table 3.1 [28].

Table 3.1: Equivalent thickness of concrete for PAROC Figra 170 for concrete slabs and beams for different fire exposure durations. Data from PAROC, based on classification report PK2–16–16–001–E–1 [28].

		Equivalent thickness of concrete (mm)					
Element	Figra thickness	30 min	60 min	90 min	120 min	180 min	240 min
Concrete slab	20 mm	49	62	71	74	75	72
Concrete slab	60 mm	87	95	107	116	131	140
Concrete beam	20 mm	36	52	55	54	47	34
Concrete beam	60 mm	65	77	91	102	112	116

This shows that fire resistance can be supplemented by an external protection layer, which may reduce the need to govern slab thickness by fire requirements alone.

3.2.6 Cast in situ concrete structure from 2022, Troja

Troja, developed by AF Bostäder, is a recent student housing project in Kämnärsrätten in northern Lund and can be regarded as part of the latest phase of large-scale student housing development in the area. Troja is planned to be completed in 2026, with move in for the first stage on 15 September 2026 and the second stage in January 2027. The project comprises about 12,000 m^2 of housing, seven buildings of 3 to 7 storeys and accommodation for around 500 students. AF Bostäder presents Troja as a project with a strong sustainability focus, including reduced energy demand, solar panels, limited hardscaping and measures intended to support biodiversity and stormwater management. Because the project represents current practice in student housing construction in Lund, it is relevant as a reference case when comparing present structural solutions for cast in situ concrete walls and slabs with more resource efficient alternatives [29].

For the floor slab, the available drawings indicate a slab thickness of 250 mm on the typical floor, with an additional 15 mm floor build-up above the structural concrete. The material specifications indicate concrete class C40/50 for slabs and a nominal concrete cover of 20 mm.

The bottom reinforcement is specified as ϕ8 c200, corresponding to approximately 252 mm^2/m. The drawings also indicate local supplementary bottom reinforcement at the wall-slab connection, ϕ10 c200 A1500, corresponding to approximately 393 mm^2/m. Where this reinforcement is present, the total bottom reinforcement is therefore approximately 645 mm^2/m. Since this reinforcement is local, it was not treated as the general bottom reinforcement for the entire slab field. The slab top reinforcement could also be identified from the drawings, but it varies depending on the location in the slab. Therefore, instead of defining one general value, selected top reinforcement layouts were used for the comparison cases representing two-span and three-span slab behaviour. The two-span case had a span of 5.5 m and top reinforcement was identified as Ø12 c200, corresponding to approximately 565 mm^2/m. The three-span case had a span of 4.0 m and top reinforcement was identified as Ø12 c300, corresponding to approximately 377 mm^2/m. The selected reinforcement layouts are shown in Appendix D.

For the walls, detail B indicates a wall thickness of 180 mm. The material specifications indicate concrete class C30/37 for inner and outer walls and a nominal concrete cover of 20 mm. The wall reinforcement is 1+1 Ø9 c300, corresponding to approximately 212 mm^2/m per face. The wall detail also indicates local supplementary reinforcement Ø10 c600 C1200×300×1200 at the wall-slab connection, see Figure 3.3.

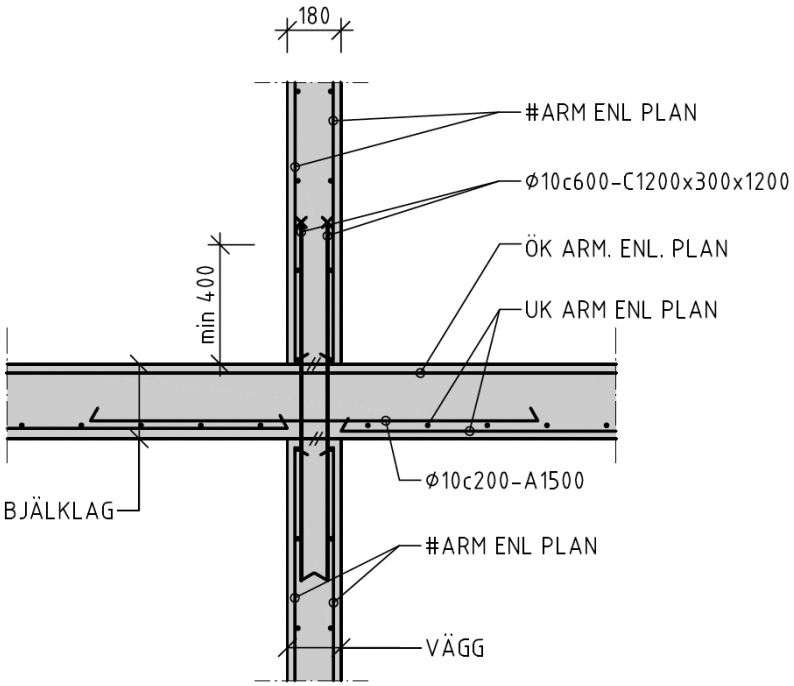

Figure 3.3: Principle detail B showing the wall-slab connection in the Troja project, including slab thickness, wall thickness and indicated reinforcement [30].

3.3 Comparison of two concrete frames

The two reference cases represent two examples of cast in situ concrete floor structures in student housing. The first case is based on Cykelskrapan, a student housing project in Lund from 1956, while the second case is based on the Troja project in Lund from 2022. The comparison is based on the slab and wall dimensions, concrete strength classes, reinforcement layouts and the relation between the load-bearing concrete and the additional floor build-up. The main quantified differences are summarised in Table 3.2.

The comparison must first be interpreted in relation to the span lengths of the two reference cases. The analysed Cykelskrapan slab has a span of 3.69 m. In the Troja project, the identified span is 5.5 m for the two-span case and 4.0 m for the three-span case. The comparison of slab thickness and reinforcement should therefore be read together with the span and support conditions, since the structural demand is not governed by thickness alone.

The Cykelskrapan floor structure consists of a 160 mm load-bearing concrete slab with an additional 80 mm layer above the structural slab. The total floor depth shown in the section is therefore approximately 240 mm, but only 160 mm is interpreted as load-bearing concrete. In the Troja project, the typical floor slab consists of a 250 mm load-bearing concrete slab with an additional 15 mm floor build-up. The total floor depth is therefore approximately 265 mm. This means that the total floor depth is only approximately 10 % larger in the Troja case, while the load-bearing concrete slab is approximately 56 % thicker.

The concrete strength also differs between the two cases. In Cykelskrapan, the concrete is specified as *Betong II STD, K200*. This has been interpreted as a cube compressive strength of approximately 20 MPa, which is closest to the modern concrete strength class C16/20. In the Troja project, the slab concrete is specified as C40/50. Based on the characteristic cylinder strength f_{ck}, this corresponds to an increase from approximately 16 MPa to 40 MPa.

The higher concrete strength class in the contemporary reference structure may also reflect changed production conditions. In older construction, site time was not the same driving factor as it is today. In current construction, labour time, drying time and the pace of following work stages have a larger influence on design choices. Higher concrete classes can therefore be used to obtain faster strength development and a more predictable drying process. The increase in concrete class should therefore not only be interpreted as a structural requirement, but also as a response to modern demands for faster and more predictable production [31].

The reinforcement layout shows both similarities and differences. In the Cykelskrapan slab, the reinforcement is based on welded mesh with local supplementary reinforcement. The interpreted reinforcement amounts in the studied section are approximately 266 mm^2/m for the bottom reinforcement and 400 mm^2/m for the top reinforcement. Since the available Cykelskrapan drawings are interpreted as representing a three-span case, the reinforcement comparison in Table 3.2 is based on the corresponding three-span reinforcement layout in the Troja slab. In the Troja slab, the general bottom

reinforcement is specified as $\phi 8$ $c200$, corresponding to approximately 252 mm^2/m. This is approximately 5 % lower than the interpreted bottom reinforcement in the Cykelskrapan slab. The selected Troja top reinforcement for the three-span case is $\phi 12$ $c300$, corresponding to approximately 377 mm^2/m, which is approximately 6 % lower than the interpreted top reinforcement in the Cykelskrapan slab.

Local supplementary bottom reinforcement $\phi 10$ $c200$ $A1500$, corresponding to 393 mm^2/m, is also indicated at the wall-slab connection in the Troja slab. Where this reinforcement is present, the total bottom reinforcement is approximately 645 mm^2/m. This corresponds to approximately 143 % more reinforcement than the interpreted bottom reinforcement in the Cykelskrapan slab. However, since this reinforcement is local, it is not treated as the general bottom reinforcement for the slab field.

The wall thickness has also increased between the two reference cases. In the Cykelskrapan case, the analysed section identifies a 150 mm load-bearing wall. In the Troja project, the corresponding wall thickness is 180 mm, which corresponds to an increase of approximately 20 %. This difference should be interpreted together with the floor systems, since the Troja wall supports a thicker load-bearing concrete slab and therefore a higher permanent load from the floor structure.

For the Cykelskrapan wall, the analysed section identifies a 150 mm load-bearing concrete wall. However, no complete general reinforcement layout for this wall has been identified in the available section drawing. The Cykelskrapan wall is therefore used only as a reference for wall thickness and structural arrangement, not as a reference for wall reinforcement amount.

The Troja wall is reinforced with $1 + 1$ $\phi 9$ $c300$, corresponding to approximately 212 mm^2/m per face, or 424 mm^2/m in total. The wall detail also includes local supplementary reinforcement at the wall-slab connection.

Table 3.2: Comparison between the Cykelskrapan and Troja floor wall structures. The local bottom reinforcement refers to the wall-slab connection in the Troja slab. No general wall reinforcement amount was identified for the Cykelskrapan wall in the analysed section drawing.

Parameter	**Cykelskrapan**	**Troja**	**Difference**
Slab span (three-span case)	3.69 m	4.0 m	+8 %
Slab span (two-span case)	–	5.5 m	–
Structural slab thickness	160 mm	250 mm	+56 %
Total floor depth	240 mm	265 mm	+10 %
Wall thickness	150 mm	180 mm	+20 %
Concrete strength class, slab	C16/20	C40/50	
Bottom reinforcement	266 mm^2/m	252 mm^2/m	−5 %
Top reinforcement, three-span case	400 mm^2/m	377 mm^2/m	−6 %
Bottom reinforcement including local supplement	266 mm^2/m	645 mm^2/m	+143 %
Wall reinforcement	Not identified	424 mm^2/m	–

Overall, the comparison shows that the modern Troja reference case uses a thicker load-bearing concrete slab and wall than the Cykelskrapan reference case, as shown in Table 3.2. The increase is most evident when only the structural concrete thickness is considered, since the slab thickness increases from 160 mm to 250 mm, corresponding to approximately 56 %. However, when the additional floor layers are included, the total floor depth only increases by approximately 10 %. This indicates that the main difference is not only the total floor depth, but how much of that depth is assigned to the load-bearing concrete structure. The Cykelskrapan case includes a larger non-structural layer above the slab, whereas the Troja case places a larger part of the floor depth within the structural concrete slab. For the walls, the comparison is limited to wall thickness and the reinforcement identified in the Troja reference detail. Since no general reinforcement amount was identified for the Cykelskrapan wall in the analysed section drawing, the Cykelskrapan wall is not used as a reinforcement reference in the comparison.

3.4 Limitations and Opportunities in Eurocode

Eurocode 2 provides a framework for the design of reinforced concrete structures. Within this framework, several alternative analysis and verification approaches are permitted. These choices can influence the required reinforcement, cross-sectional dimensions, and therefore the overall material use.

This can be seen in several parts of the code. For example, in Chapter 7 *Serviceability Limit States*, deflection in the serviceability limit state may be verified either by simplified span to depth rules or by explicit calculation of deformations. In Chapter 5 *Structural Analysis*, several analysis approaches are allowed, including linear elastic analysis, linear analysis with limited redistribution, and non-linear analysis [8]. Since different analysis and verification methods may lead to different internal forces and deformation demands, it is relevant to investigate more than one permitted method and evaluate which approach results in the lowest reinforcement or cross-sectional dimensions while still satisfying the Eurocode requirements.

3.4.1 Slabs

For slabs in residential buildings, Eurocode 2 offers several places where material use can be tightened by choosing a design option that still fulfils the code requirements, rather than using a single conservative default. However, when exploring the possibility of reducing slab thickness in concrete floor systems, serviceability limit state requirements often become critical. Even if the ultimate load-bearing capacity can be satisfied, its behaviour in service can become more difficult to control. Serviceability requirements therefore play an important role when evaluating more material-efficient slab designs.

The first limitation listed in EC2-1-1 is limitation of stresses (Chapter 7.2) [8]. A thinner slab has a smaller effective depth and lower bending stiffness. For the same load effects, this generally leads to higher stresses in both the concrete and the rein-

forcement, as well as larger strains and deflections. Higher compressive stress levels may also increase creep related effects, which would make it more difficult to satisfy the serviceability requirements [8].

The second limitation is limitation of crack width (Chapter 7.3) [8]. A thinner slab usually means a smaller effective depth d. For the same bending moment, that typically results in higher reinforcement stress, σ_s, which means higher steel strain. Since crack width is strongly linked to steel strain, this means a thinner slab directly leads to larger crack widths, so meeting the crack limit $w_k \leq w_{max}$ becomes more difficult often requiring more reinforcement and/or smaller bar spacing/diameters [8].

The third and last limitation listed in Chapter 7.4 in EC2-1-1 is limitation of deflection [8]. Deflection is governed by bending stiffness EI. For a slab, the second moment of area scales roughly as $I \propto h^3$. So, making the slab thinner will reduce stiffness quickly and deflections increase substantially, especially long-term deflection due to creep [8].

While serviceability requirements often govern slab thickness, Eurocode 2 also contains several provisions within the ultimate limit state that may influence the required reinforcement and therefore the overall material use.

In Chapter 5.6, the code allows the use of plastic analysis for beams, frames, and slabs in the ultimate limit state, provided that sufficient rotation capacity and ductility are ensured. In continuous slabs, elastic analysis often results in high negative bending moments over supports, which in turn governs the required top reinforcement. By using plastic analysis, a redistribution of moments may be assumed, allowing part of the peak support moment to be transferred to adjacent spans. This reduces the maximum design moment in critical sections and can therefore reduce the required reinforcement [8].

Chapter 6 *Ultimate Limit States*, governs the ultimate limit state verification of shear. According to Section 6.2.2, members that do not require calculated shear reinforcement may be designed without shear reinforcement if the design shear force does not exceed the concrete shear resistance without shear reinforcement, $V_{Rd,c}$. In such cases, the concrete alone is assumed to carry the shear force, and no minimum shear reinforcement needs to be provided for ULS [8].

In Chapter 9, Section 9.3 *Solid slabs*, the code specifies how much reinforcement must be continued and anchored at supports, and it gives explicit minimum provisions for cases where partial fixity (delvis inspänt) exists but is not included in the analysis. For example, the rules require some top reinforcement to remain beyond the section with the highest moment. At least 25% of the reinforcement needed for the maximum span moment must be continued over a specified length. The same section also states that reinforcement provided for other purposes may normally be counted as free edge reinforcement. This means that the same reinforcement can fulfil several detailing requirements instead of adding separate bars. For shear detailing, Section 9.3.2 states that slabs with shear reinforcement should have a minimum thickness of 200 mm. The section also refers to the definition of minimum shear reinforcement in Section 9.2.2, where the reinforcement ratio w_{min} shall not be lower than the value given by expression (9.5N) [8].

In addition to these detailing provisions, Eurocode 2 also leaves some room for interpretation in how crack control is understood in relation to the intended use of the slab. According to SS-EN 1992-1-1, cracking shall be limited so that it does not impair the proper functioning or durability of the structure, nor cause its appearance to be unacceptable. The code therefore recognises both durability and visual considerations as relevant design criteria [8].

However, in multi-storey residential buildings the floor slabs could be concealed by suspended ceilings, service installations or additional build-up layers. In these situations, visual requirements related to cracking can be largely irrelevant. When the structural surface is not intended to remain visible, crack width limitation may primarily be governed by concrete cover and corrosion risk rather than architectural appearance.

This distinction is relevant for the studied design strategy, where the structural concrete is separated from architectural finish layers and other functional layers. If the relevant exposure class is satisfied and reinforcement corrosion is prevented, cracking that remains within durability controlled limits may be acceptable in a concealed slab system. Other serviceability criteria, such as deflection and vibration, must still be fulfilled. Concealed slab systems may therefore allow a different interpretation of crack control than exposed concrete surfaces, which can create opportunities for material optimisation.

3.4.2 Walls

For load-bearing walls in multi-storey residential buildings, Eurocode 2 allows reduced reinforcement when the wall behaviour is governed mainly by compression. SS-EN 1992-1-1, Chapter 12 *Plain and lightly reinforced concrete structures* gives an alternative design approach for members that are predominantly subjected to axial compression and where tensile stresses are avoided or kept within defined limits. The chapter can be applied to load-bearing walls where the structural response is primarily governed by normal force rather than bending [8].

If a wall fulfils the applicability conditions of Chapter 12, the ultimate limit state and serviceability limit state verifications are carried out according to the specific rules given in this chapter. The wall is then primarily checked for axial compression resistance, stability and the effects of eccentricity. The design compressive strength of concrete and the effective cross-sectional area govern the resistance. second-order effects and initial eccentricities must be included in the verification [8].

However, purely centric compression is generally not allowed to be assumed. Eurocode requires consideration of minimum eccentricities, which introduce bending moments in the wall. If the resulting tensile stresses exceed the limits defined in Chapter 12, the simplified compression based design is no longer valid [8].

If these conditions are satisfied, the wall can be treated as a lightly reinforced or unreinforced member rather than as a conventionally bending designed reinforced concrete wall. This means that some reinforcement that would otherwise be required to resist bending tension or to satisfy minimum reinforcement rules for reinforced walls may

be reduced or, in some cases, excluded. Reinforcement may still be required locally for detailing and execution, for example around openings, at wall-slab connections and for anchorage, but the global wall design can be based on compression-dominated behaviour rather than flexural capacity.

In practice, Chapter 12 can therefore be used for non-slender, centrally loaded walls where vertical load transfer dominates and horizontal actions are limited. Slender walls, stabilising walls subjected to wind loads, or walls with significant bending demand will normally require conventional reinforced concrete design [8].

Furthermore, Section 9.6 can be used as a framework for limiting reinforcement in load-bearing walls by clearly defining minimum levels and detailing requirements, rather than relying on project-specific conservative practice [8].

The section applies to walls where reinforcement contributes to the load-bearing capacity and where the ratio between length and thickness is at least 4. Walls mainly subjected to transverse loading are instead designed according to the slab provisions in Section 9.3. This distinction allows the designer to separate compression-dominated walls from bending-dominated walls, reducing the risk of applying slab reinforcement levels to walls that primarily carry axial load [8].

For walls designed according to Section 9.6, a recommended range for vertical reinforcement is given. The vertical reinforcement should be at least 0.002 A_c and not more than 0.04 A_c outside lap zones. When minimum reinforcement governs, it should be distributed equally between the two faces of the wall. In practice, this means that the reinforcement can often be kept close to the minimum requirement when higher ratios are not needed for axial force, bending resistance, or crack control, which reduces the total amount of steel [8].

Horizontal reinforcement must be provided on both faces. A recommended minimum amount is 25% of the vertical reinforcement area, but not less than $A_{s,hmin}$ (which cannot be less than 0.001 A_c). Since the horizontal reinforcement is linked to the vertical reinforcement, limiting the vertical reinforcement to what is structurally required also limits the total horizontal reinforcement [8].

3.5 Factors Contributing to Increased Material Use

3.5.1 Challenges in Eurocode 2

The current Eurocode framework has developed into an extensive and highly complex system of detailed provisions, which in practice can be difficult to navigate and critically apply. As documented in *Resursslöseri i anläggningsbyggandet?*, the volume of regulations governing structural design has increased dramatically over time. Whereas earlier bridge standards comprised only a few dozen pages, the introduction of Eurocode resulted in a system including several thousand pages, together with national annexes and application documents, see Figure 3.4 [7]. Although the figure refers to bridge design, a similar broader regulatory development can also be observed in building construction, where Eurocode-based design has introduced a larger body of rules, national annexes and complementary guidance documents.

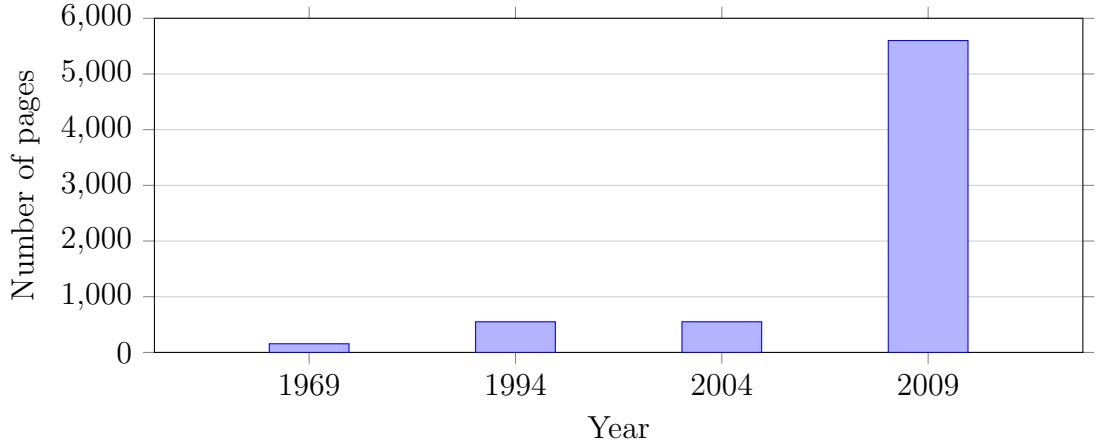

Figure 3.4: Change over time in the number of pages of design rules relevant for road bridge design. Based on *Resursslöseri i anläggningsbyggandet?* [7].

Section 4.2 in the same report highlights how this growing level of detail and formalization has shifted focus from engineering judgement towards rule interpretation. This development was further reinforced by one of the authors, Sven Thelandersson, in an interview, where he described how designers today must first relate to the extensive Eurocode documents and then to national adaptations such as EKS, resulting in a layered and demanding regulatory structure.

One consequence of this development is that the design process can become increasingly checklist-oriented, where the main objective is to satisfy each individual verification rather than to assess which mechanisms are actually governing in the specific case. When many provisions are applied in parallel, the design may become governed by the single most demanding check, even when the underlying effect is uncertain or not decisive for the real structural behaviour. Thelandersson further notes that this tendency is reinforced by a professional culture in which engineers seek to avoid mistakes and objections in reviews and approvals, and therefore tend to choose the safest and most restrictive interpretation. The report also points out that for several durability-related rules, the designer may not be able to judge whether the assumed

problem is actually present, and therefore applies the rules anyway, which can increase reinforcement quantities [7].

This issue becomes particularly important in serviceability limit state design, where the structural behaviour itself is associated with significant uncertainty. Long-term effects such as creep, shrinkage, cracking and tension stiffening are represented in the code through simplified mechanical models that approximate complex physical processes. In practical applications, the accuracy of serviceability predictions is further limited by uncertain load history and highly variable material properties. The resulting deformation or crack width is therefore not an exact value, but a calculated estimate based on assumed parameters and modelling choices [32].

Crack control provides a clear example of this problem. Research indicates that it is difficult to justify a universal surface crack width requirement solely on durability grounds. The relationship between visible cracks and long-term corrosion processes is not fully understood, and predictive models remain approximate. As a pragmatic alternative, it has been suggested that controlling reinforcement stress in the cracked section may in some cases provide a more rational basis than enforcing strict surface crack width limits. If crack width limitations are instead motivated by aesthetic considerations, they should logically depend on factors such as viewing distance, exposure conditions and the intended architectural quality of the element [32].

Taken together, this illustrates how the increasing scope and complexity of the Eurocode framework may influence design practice and contribute to higher material use. In particular, when serviceability requirements are treated as absolute and uniform numerical limits, independent of context, they may lead to conservative reinforcement layouts and increased material quantities rather than engineering optimisation.

A concrete example of this is presented in Section 2.3.5, *Transport culverts at Malmö General Hospital*, where a culvert built in 1960 is compared with two newer culverts constructed around 2020 for the same hospital, with essentially the same function and comparable geometry. The reinforcement amount increased from 156 kg per meter in the 1960 structure to 550 kg per meter and 760 kg per meter in the newer designs. According to the report, the main reason for this increase was changes in the rules for minimum or nominal reinforcement, which have been tightened over time [7].

In the interview, Thelandersson further emphasized that this example is also relevant to cast in situ basement walls in buildings, where minimum reinforcement rules can lead to substantial reinforcement quantities when applied mechanically. In such cases, designers may adopt the most severe interpretation of the provisions, which can significantly increase the required steel content [7].

3.5.2 Effects of Computer-Aided Design

Computer-aided design is often presented as a way to improve accuracy and enable more material-efficient structures, but the report *Resursslöseri i anläggningsbyggandet?* argues that the practical effect can be the opposite. It highlights that the shift from simpler 2D models to detailed 3D FEM analyses increases the time spent on building, verifying, and evaluating calculation models, and that modelling choices and insufficient quality control can lead to increased resource use, primarily through higher reinforcement quantities. The report therefore frames advanced FEM analyses as a separate driver of increased material consumption, especially when optimisation requires extensive post-processing and specialist competence that is difficult to apply under typical project constraints [7].

Thelandersson et al. further argues that modern calculation software can lead to designs where results are followed without enough judgement. Loads and simplified assumptions are entered into complex models, and the output can show local stress peaks or effects that mainly come from the modelling rather than from real structural behaviour. If these peaks are then used directly for design without any processing, the result can be unnecessary reinforcement and higher material use, instead of a solution based on engineering assessment of what is actually governing [7].

The report also demonstrates this through a detailed case study of a portal frame bridge, where the same structure was analysed using different modelling strategies. A simple 2D analysis resulted in almost the same reinforcement amount as the bridge that was actually constructed, while a 3D analysis without careful post-processing led to an 81% increase in reinforcement. Only when the 3D model was extensively post processed and optimised did it yield a lower reinforcement quantity than the reinforcement provided in the constructed bridge, but this required significant time, expertise, and was not production adapted. The study therefore concludes that advanced FEM analyses do not automatically lead to more efficient structures, and in practical design situations they may instead increase material consumption if not handled with great care [7].

3.6 The Shift Towards Performance-Based Building Regulations in Sweden

The recent Swedish regulatory reform known as *Möjligheternas byggregler*, led by Boverket, introduced new building regulations that entered into force on July 1, 2025. The reform restructures the regulatory framework and shifts from detailed prescriptive requirements towards a more clearly performance-based system.

Within this new structure, structural safety is regulated through Boverket's new regulations on load-bearing capacity, stability and durability, formally designated BFS 2024:6. Instead of prescribing specific technical solutions, the regulations define the functional requirements that buildings must fulfil in accordance with the Planning and Building Act (*Plan- och bygglagen*) and the Planning and Building Ordinance

(*Plan- och byggförordningen*). The intention is to promote innovation and allow greater flexibility in design, materials and construction methods, while placing increased responsibility on designers and developers to verify through calculation, analysis and documentation that the essential technical requirements are satisfied.

BFS 2024:6 represents a clear change in how structural requirements are formulated in the Swedish building regulatory system. Compared to the previous framework, where BBR, EKS and the Eurocodes were closely connected, the new regulation moves more explicitly towards a performance-based structure. The focus is now placed on whether the chosen design fulfils the required performance in terms of load-bearing capacity, stability and durability.

Under the earlier system, as discussed in Section 3.2.1, compliance was met in practice by following detailed general recommendations and applying the Eurocodes together with the Swedish national annexes. Although the general recommendations were formally non-mandatory, they are frequently treated as such in practice. According to Boverket, this gradually led to a system that became increasingly standardised and, to some extent, restrictive in terms of alternative technical solutions. In BFS 2024:6, the Eurocodes are still presented as a recognised and reliable method for structural design, but they are no longer framed as the only accepted route to compliance. Alternative methods may be used, provided that the required level of safety and reliability is achieved. The regulation refers explicitly to safety classes and associated reliability requirements, which shifts the emphasis from strictly following a given calculation method to demonstrating that an adequate safety level has been reached.

The intention behind this change is to create better conditions for innovation and technical development within the construction sector. At the same time, the actual impact of the reform will depend on how the industry responds. Designers, contractors and developers now have greater responsibility to justify their technical choices. Whether this will result in new structural solutions or mainly continued use of established design practices remains to be seen.

Boverket has also stated that the new regulatory structure aims to simplify the system and make it easier to apply. However, a more performance-oriented framework may also make compliance assessment more demanding, particularly for building inspectors and supervisory authorities. When fewer predefined solutions are referenced, the evaluation must instead focus on whether the chosen solution demonstrably satisfies the functional requirements.

For structural elements such as cast in situ slabs and load-bearing walls, this shift is particularly relevant. Since BFS 2024:6 formulates the requirements in functional terms rather than prescribing specific numerical criteria, the actual material demand depends on how compliance is demonstrated. In practice, this means that the extent to which slab thickness, wall thickness and reinforcement can be reduced is closely linked to the chosen verification approach and to how structural and serviceability performance are defined.

For this thesis, the reform is relevant because it highlights the difference between satisfying a prescribed design route and demonstrating that a chosen structural concept

fulfils the required performance. The alternative slab and wall solutions studied in this work should therefore be understood as examples of structural concepts that may become relevant in a more performance-based design context, provided that all relevant requirements are verified.

Overall, BFS 2024:6 can be seen as part of a shift from a method-driven system towards a framework that emphasises performance, verification and responsibility.

4 Results

This chapter presents the results from the slab and wall calculations. The chapter is divided into two parts. Section 4.1 presents the slab results, and Section 4.2 presents the wall results. The complete parameter studies are presented in Appendix C, while this chapter focuses on the results most relevant for the comparison between the reference structures and the material efficient alternatives.

4.1 Slabs

The slab results are presented as the maximum allowable span obtained from the governing verification. For each combination of slab thickness, reinforcement amount, concrete strength class and support condition, the limiting span was determined from bending resistance, shear resistance, deflection, crack width and vibration.

4.1.1 Reference case based on the Cykelskrapan slab

The first reference case was selected to represent a slab configuration comparable to the Cykelskrapan reference slab. The case is based on C16/20 concrete, $\phi 9$ reinforcement and the three span support model. As shown schematically in Figure 4.1, top reinforcement was considered over the support regions, while bottom reinforcement was considered in the span regions. The bending resistance was evaluated separately for the support and field sections, using the reinforcement located on the tensile side of the section. The results are presented as maximum allowable span for different slab thicknesses and reinforcement areas.

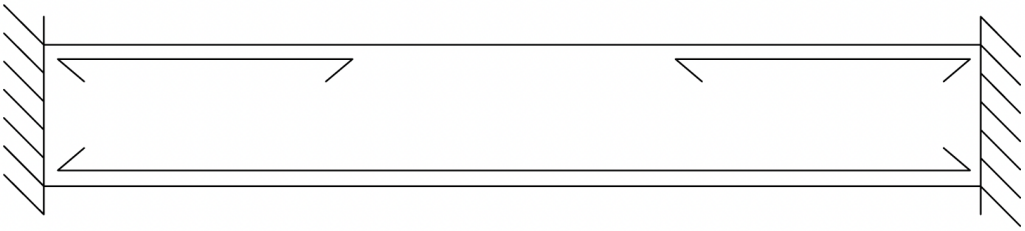

Figure 4.1: Schematic illustration of the slab model used for the Cykelskrapan reference case, showing the assumed support condition and the reinforcement considered in the support and field sections.

Figure 4.2 shows that the allowable span increases with both slab thickness and reinforcement area. However, the increase is not linear for all thicknesses. For lower reinforcement areas, the span capacity increases clearly as more reinforcement is added. At higher reinforcement areas, the curves become flatter, especially for the thinner slabs. This indicates that additional reinforcement becomes less effective once deflection starts to govern the allowable span.

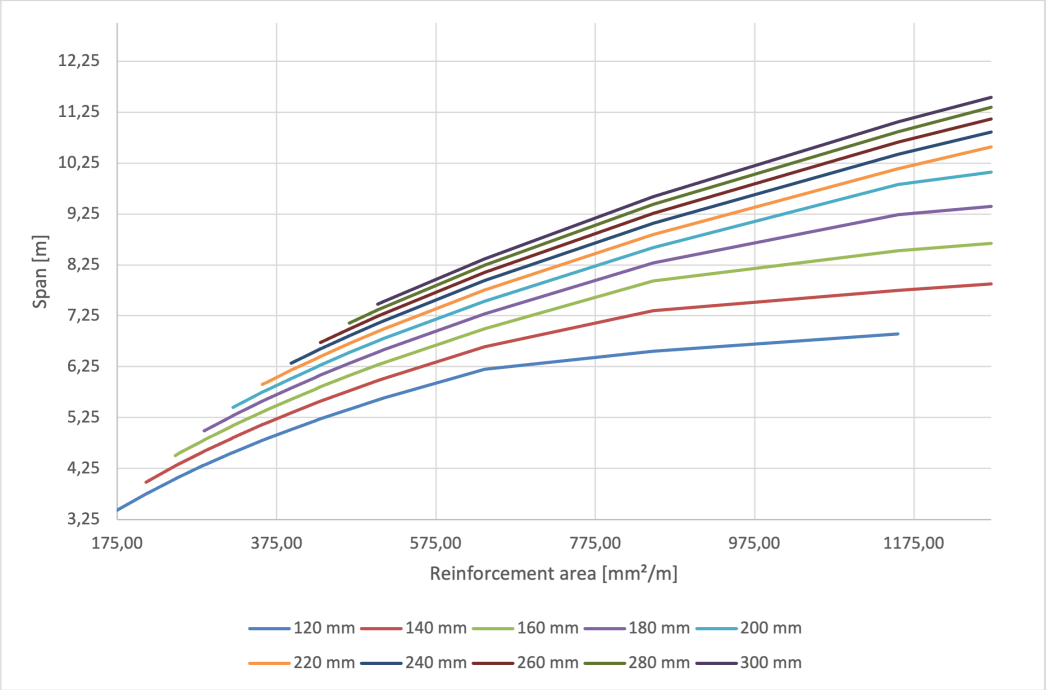

Figure 4.2: Maximum allowable span as a function of reinforcement area for slabs with C16/20 concrete, $\phi 9$ reinforcement and the three-span support model. Each line represents a slab thickness between 120 mm and 300 mm. The allowable span is governed by the limiting verification among bending resistance, shear resistance, deflection, crack width and vibration.

Table 4.1 shows the same results together with the governing verification. The reinforcement areas in the table refer to the tensile reinforcement used in the support section, since support bending governs most combinations in the three span model. The corresponding field section was also checked using tensile reinforcement in the span region, although it did not govern any of the combinations presented. For most combinations, the allowable span is governed by bending resistance. For the highest reinforcement areas in the thinner slabs, the governing criterion changes to deflection. This means that the limiting factor shifts from resistance to stiffness when the reinforcement amount is increased.

Table 4.1: Maximum allowable span for the slab using C16/20, $\phi 9$ and the three span support model. The columns marked "min" include the minimum reinforcement required for the corresponding slab thickness. The column marked "max" indicates the largest reinforcement level before over reinforced behaviour for the corresponding slab thickness. Orange cells are governed by bending resistance, while green cells are governed by deflection.

A_s [mm^2/m]	min 120	min 140	min 160	$s250$	$s225$	min 180	$s200$	min 200	min 220	$s175$	min 240	$s150$	min 260	min 280	min 300	$s125$	$s100$	$s75$	max 120	$s50$
t [mm]	175	211	248	254	283	284	318	320	357	364	393	424	430	466	502	509	636	848	1155	1272
120	3.43	3.75	4.05	4.10	4.31	4.32	4.55	4.57	4.80	4.84	5.02	5.19	5.22	5.42	5.60	5.63	6.20	6.56	6.89	
140		3.98	4.30	4.35	4.58	4.59	4.84	4.86	5.11	5.16	5.34	5.53	5.57	5.78	5.98	6.01	6.64	7.35	7.75	7.87
160			4.51	4.56	4.80	4.81	5.08	5.09	5.36	5.41	5.61	5.81	5.85	6.07	6.29	6.33	7.00	7.94	8.53	8.67
180						4.99	5.27	5.29	5.57	5.62	5.83	6.04	6.08	6.32	6.54	6.58	7.29	8.29	9.24	9.40
200								5.45	5.75	5.80	6.02	6.24	6.28	6.52	6.76	6.80	7.54	8.59	9.83	10.08
220									5.90	5.96	6.18	6.41	6.45	6.70	6.94	6.99	7.76	8.85	10.14	10.57
240											6.32	6.55	6.60	6.86	7.10	7.15	7.94	9.07	10.42	10.86
260													6.73	6.99	7.24	7.29	8.10	9.27	10.66	11.12
280														7.11	7.37	7.42	8.25	9.44	10.87	11.35
300															7.48	7.53	8.37	9.59	11.06	11.55

Note. Empty cells indicate reinforcement amounts below the minimum reinforcement requirement or over reinforced cross sections excluded from the results.

For the 160 mm slab, which is comparable to the structural thickness of the Cykelskrapan reference slab, the span identified from the structural drawings is 3.69 m. Two comparisons were made, as shown in Table 4.2. The first comparison relates the reference span to the calculated allowable span for a 160 mm slab with minimum reinforcement, $A_{s,\min} = 248$ mm^2/m. The second comparison relates the reference span to the calculated allowable span for a 160 mm slab with the reinforcement level closest to the interpreted support reinforcement in the Cykelskrapan slab. This gives utilisation ratios of $L_{\text{ref}}/L_{\text{allow}} = 0.82$ and 0.66, respectively.

Table 4.2: Comparison between the Cykelskrapan slab span and calculated allowable spans for the three-span support model. The comparison is based on a 160 mm slab with C16/20 concrete.

Comparison basis	A_s [mm^2/m]	L_{ref} [m]	L_{allow} [m]	$L_{\text{ref}}/L_{\text{allow}}$
Minimum reinforcement for 160 mm slab	248	3.69	4.51	0.82
Closest level to interpreted support reinforcement	393	3.69	5.61	0.66

Across the studied reinforcement range, the calculated allowable span for the 160 mm slab increases from 4.51 m at the minimum reinforcement level to 8.67 m at the highest reinforcement level included in the study. The results show that the span capacity of a thin cast in situ slab is strongly dependent on the amount of reinforcement, but that serviceability limits become increasingly important at higher reinforcement levels.

4.1.2 Reference case based on the Troja slab

The Troja slab was compared with the calculation model using the actual spans identified from the drawings. The two-span case has a span of 5.50 m, while the three-span case has a span of 4.00 m. Both comparison cases were governed by support bending in the calculation model. The results are presented in Table 4.3.

For the two-span case, the drawing based top reinforcement was identified as ϕ12 c200, corresponding to approximately 565 mm^2/m. Since the governing verification is support bending, this reinforcement level was used in the comparison with the 5.50 m Troja span. This gives a calculated allowable span of 6.30 m, which is larger than the span identified in the Troja drawings.

The simplified support condition used for the two span comparison is shown in Figure 4.3. The support reinforcement was evaluated over the fixed end, while the field reinforcement was evaluated in the span region.

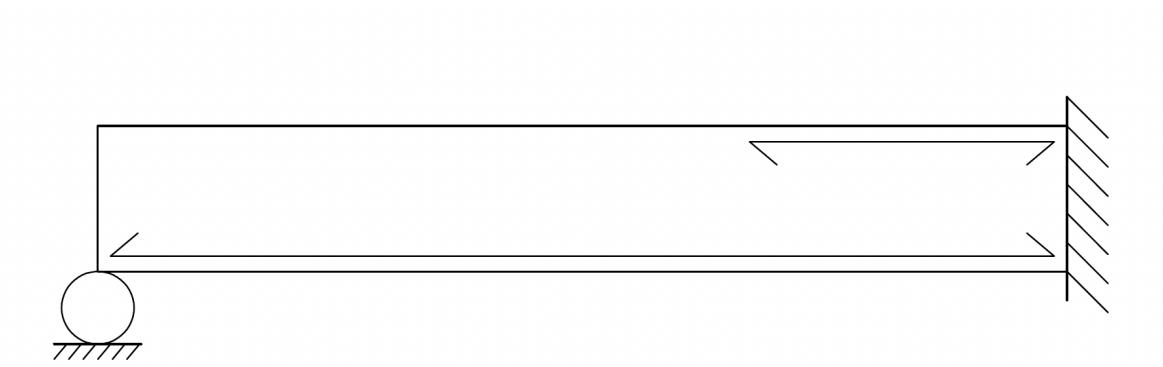

Figure 4.3: Schematic illustration of the slab model used for the Troja two span comparison, showing the assumed support condition and the reinforcement considered in the support and field sections.

For the three-span case, the drawing based top reinforcement was identified as ϕ12 c300, corresponding to approximately 377 mm^2/m. Since this is lower than the minimum reinforcement level used in the calculation model for a 250 mm slab, the comparison was based on $A_s = 408$ mm^2/m. This gives a calculated allowable span of 6.55 m, which is larger than the 4.00 m span identified in the Troja drawings.

For the three span comparison, the corresponding three span support model was used, as seen in Figure 4.1, with support reinforcement evaluated over the internal support region.

Table 4.3: Comparison between the Troja slab spans and the calculated maximum allowable span for the two-span and three-span support models. The comparison is based on a 250 mm slab with C40/50 concrete.

Support model	L_{Troja} [m]	A_s [mm^2/m]	L_{allow} [m]	$L_{\text{Troja}}/L_{\text{allow}}$	Governing verification
two-span	5.50	565	6.30	0.87	Support bending
three-span	4.00	408	6.55	0.61	Support bending

Both comparison cases are below the calculated allowable span limits in the simplified strip model. The utilisation ratio is 0.87 for the two-span case and 0.61 for the three-span case.

4.1.3 Influence of concrete strength class

The influence of concrete strength class was studied for the three-span support model, using ϕ9 reinforcement and three slab thicknesses: 120 mm, 200 mm and 300 mm. The results are shown in Figure 4.4.

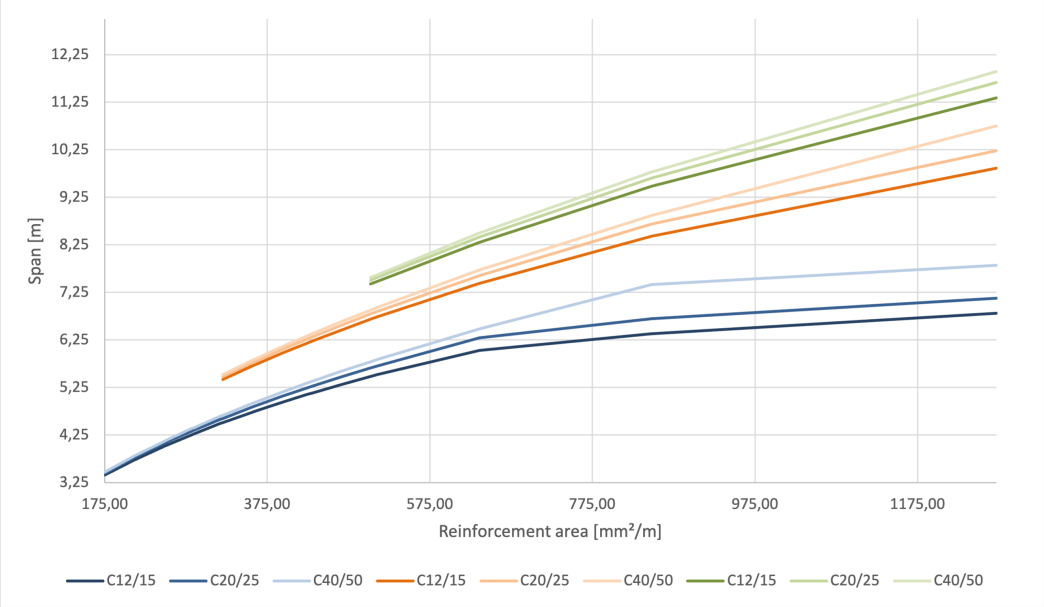

Figure 4.4: Influence of concrete strength class on the maximum allowable span for slabs with ϕ9 reinforcement and the three-span support model. The results are shown for slab thicknesses of 120 mm, 200 mm and 300 mm. Blue lines represent 120 mm slabs, orange lines represent 200 mm slabs and green lines represent 300 mm slabs. Within each colour group, the darker line represents C12/15, the middle line represents C20/25 and the lighter line represents C40/50.

For the minimum reinforcement level corresponding to each slab thickness, the concrete strength class has almost no influence on the maximum allowable span. This can be seen for all three studied thicknesses, where the curves for C12/15, C20/25 and C40/50 are close to each other at the lowest reinforcement levels. This indicates that when

the slab is reinforced only according to the minimum reinforcement requirement, the allowable span is mainly controlled by the reinforcement amount and slab thickness rather than by the concrete strength class.

The influence of concrete strength class becomes more visible at higher reinforcement levels. The difference is largest for the 120 mm slab, where the C40/50 curve separates from the C12/15 and C20/25 curves at high reinforcement areas. In this range, the governing verification changes from bending resistance to deflection. The larger difference can therefore be explained by the way concrete strength affects the deflection calculation. A higher concrete strength class gives a higher modulus of elasticity, E, and a higher tensile strength, f_{ctm}. This raises the cracking moment and affects the transition between uncracked and cracked stiffness in the deflection calculation. Since the 120 mm slab has a low second moment of area, the calculated deflection is especially sensitive to changes in stiffness and cracking behaviour.

For the thicker slabs, the same tendency can be seen, but the difference between concrete strength classes remains smaller. This shows that increasing the concrete strength class gives a limited improvement compared with increasing the slab thickness or reinforcement area. The result therefore suggests that concrete strength class is not the main parameter controlling the allowable span in the studied slab cases, except when deflection governs in thin slabs with high reinforcement levels.

The same comparison was also carried out for the one-span and two-span support models. These results showed the same general tendency, namely that the concrete strength class has a limited influence at low reinforcement levels, while the effect becomes more visible when deflection governs at higher reinforcement levels. The corresponding results for the one-span and two-span support models are presented in Appendix C.1.4.

4.1.4 Influence of support conditions

The influence of support conditions was studied by comparing the one-span, two-span and three-span support models for a 200 mm slab with C20/25 concrete and $\phi 9$ reinforcement. The results are shown in Figure 4.5.

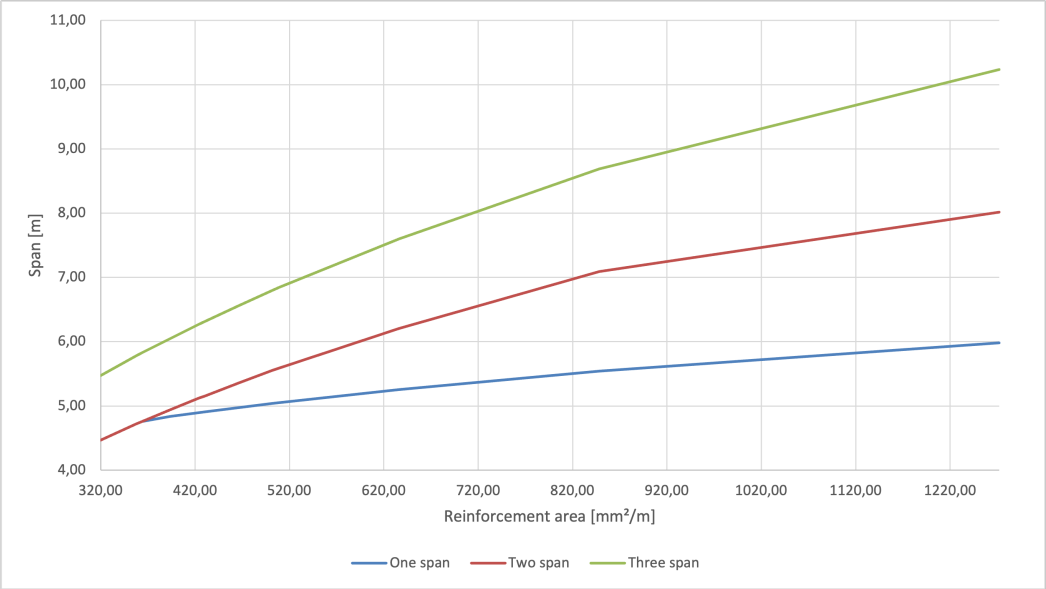

Figure 4.5: Influence of support condition on the maximum allowable span for a 200 mm slab with C20/25 concrete and $\phi 9$ reinforcement. The one-span, two-span and three-span support models are compared for increasing reinforcement area. The results show that the allowable span increases with increasing continuity in the slab system.

The support condition has a clear influence on the maximum allowable span. The one-span model gives the lowest allowable spans, while the three-span model gives the highest allowable spans. This is expected, since increased continuity reduces the governing bending moments and deflections.

For the 200 mm slab at the minimum reinforcement level, the one-span and two-span models both give an allowable span of 4.47 m, while the three-span model gives 5.48 m. The one-span and two-span models give the same result because bending resistance governs in both cases. Although the governing moment occurs at different locations, at midspan in the one-span model and at the support in the two-span model, the same moment coefficient is used in the calculation model. This explains why the curves follow each other when bending resistance governs.

As the reinforcement area increases, the governing verification for the one-span model changes from bending resistance to deflection. From this point, the one-span curve no longer follows the two-span curve. At the highest reinforcement level, the corresponding spans are 5.98 m, 8.02 m and 10.23 m. This shows that the effect of support condition becomes more significant as the reinforcement amount increases, where the effect of stiffness and continuity becomes more important.

4.1.5 Summary

Overall, the slab results show that slab thickness and support condition have the largest influence on the maximum allowable span. Increasing the reinforcement area increases the allowable span when bending resistance governs, but the effect becomes smaller when deflection becomes governing. This shows that additional reinforcement is not always an efficient way of increasing the span, especially for thinner slabs where stiffness becomes decisive.

For the Cykelskrapan reference case, the identified span of 3.69 m is below the calculated allowable span for the corresponding 160 mm slab. At the minimum reinforcement level, the calculated allowable span is 4.53 m. For the reinforcement level closest to the interpreted support reinforcement in the reference slab, the calculated allowable span is 5.65 m. This indicates that the analysed Cykelskrapan slab is below the calculated span limit within the simplified three-span model.

For the Troja reference case, both selected comparison spans are also below the calculated allowable span limits. The two-span case has a utilisation ratio of 0.87, while the three-span case has a utilisation ratio of 0.61. Both cases are governed by support bending in the calculation model.

The influence of concrete strength class is limited for the studied cases, especially at minimum reinforcement levels. A higher concrete strength class gives a larger effect mainly when deflection governs, since the stiffness and cracking resistance of the concrete then affect the result more directly. The results therefore indicate that the allowable span is primarily governed by structural thickness, reinforcement amount and support condition, rather than by concrete strength class alone.

4.2 Walls

The wall results are presented as design axial resistance, N_{Rd}, in kN/m. For each combination of wall thickness, effective buckling length, concrete strength class and vertical reinforcement amount, the axial resistance was calculated using the wall model described in Section 2.5. The full calculation procedure is presented in Appendix B.

In all wall calculations, the initial eccentricity of the axial load was taken as

$$e_0 = \frac{l_0}{400}$$

where l_0 is the effective buckling length. The same eccentricity assumption was used for both the reinforced and unreinforced wall comparisons.

The reinforced wall results are first presented for the smallest valid standard welded mesh satisfying the adopted minimum vertical reinforcement requirement for each wall thickness. Additional comparisons are then used to isolate the influence of wall thickness, concrete strength class and reinforcement amount. Finally, the corresponding unreinforced wall results are presented for the combinations satisfying the adopted validity requirements.

The wall thicknesses identified in the reference structures, 150 mm for Cykelskrapan and 180 mm for Troja, are included in the investigated parameter range. However, since no general reinforcement amount was identified for the Cykelskrapan wall in the analysed section drawing, the wall results are treated as a parameter study rather than as a direct verification of the existing wall.

4.2.1 Reinforced wall results

The reinforced wall results were first evaluated by identifying the smallest standard welded mesh satisfying the adopted minimum vertical reinforcement requirement for each wall thickness. The minimum reinforcement requirement was calculated for a one metre wide wall strip, and the smallest valid standard mesh was then selected from the investigated mesh alternatives. The resulting minimum reinforcement selection is shown in Table 4.4.

Table 4.4: Minimum vertical reinforcement requirement and smallest standard mesh satisfying the requirement for each wall thickness.

Wall thickness [mm]	$A_{s,\min}$ **[mm²/m]**	**Smallest valid mesh**	$A_{s,\text{tot}}$ **[mm²/m]**
120	240	#5150	262
140	280	#6150	376
150	300	#6150	376
160	320	#6150	376
180	360	#6150	376
200	400	#8150	670
220	440	#8150	670

Figure 4.6 shows the design axial resistance of reinforced wall strips for concrete class C20/25 when the smallest valid standard mesh is used for each wall thickness. The figure therefore represents the lowest-reinforcement valid solution within the investigated set of standard meshes for each wall thickness. Since the selected reinforcement amount changes between the wall thicknesses, the curves show the combined effect of wall thickness and reinforcement selection.

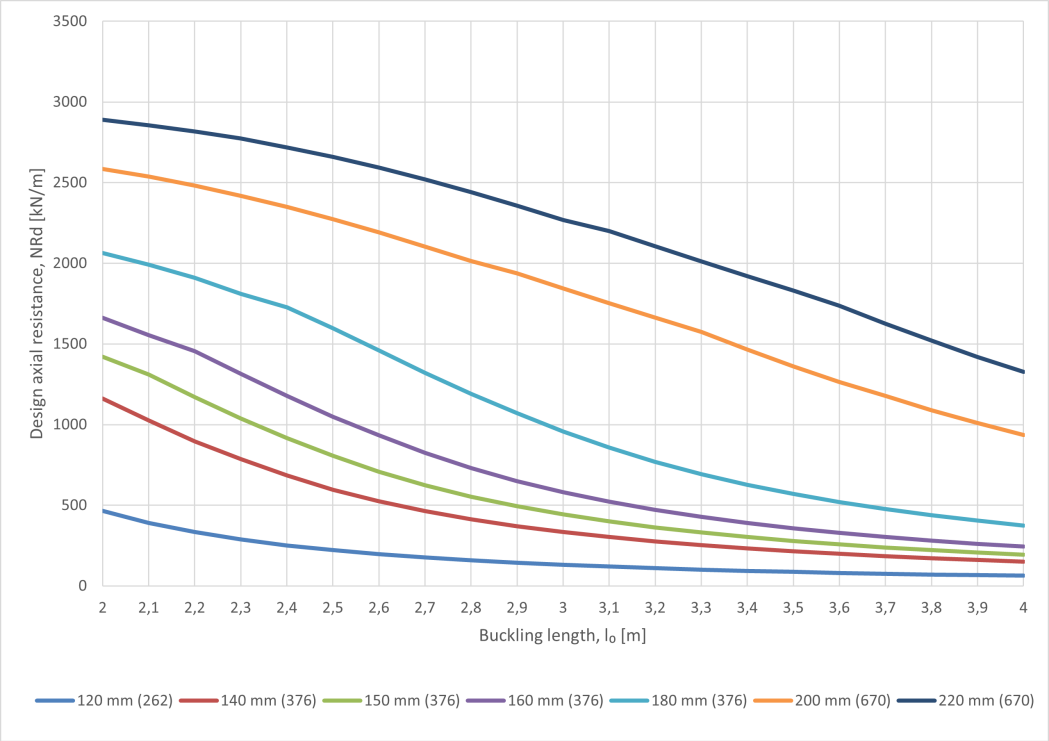

Figure 4.6: Design axial resistance N_{Rd} as a function of effective buckling length for reinforced wall strips with concrete class C20/25 and the smallest standard mesh satisfying the adopted minimum reinforcement requirement for each wall thickness. The value in parentheses in the legend denotes $A_{s,\mathrm{tot}}$ in mm^2/m.

The results show that the design axial resistance decreases with increasing effective buckling length and increases with wall thickness. The reduction with increasing buckling length reflects the increasing influence of slenderness and second-order effects. The increase between neighbouring wall thicknesses is not only caused by the larger concrete cross-section, but also by the change in selected reinforcement amount. This is especially relevant when the selected mesh changes from #5150 to #6150 or from #6150 to #8150.

To isolate the influence of wall thickness more clearly, the same comparison was also performed using a constant reinforcement amount of $A_{s,\mathrm{tot}} = 670$ mm^2/m for all wall thicknesses. This corresponds to mesh #8150 on both wall faces. The results are shown in Figure 4.7.

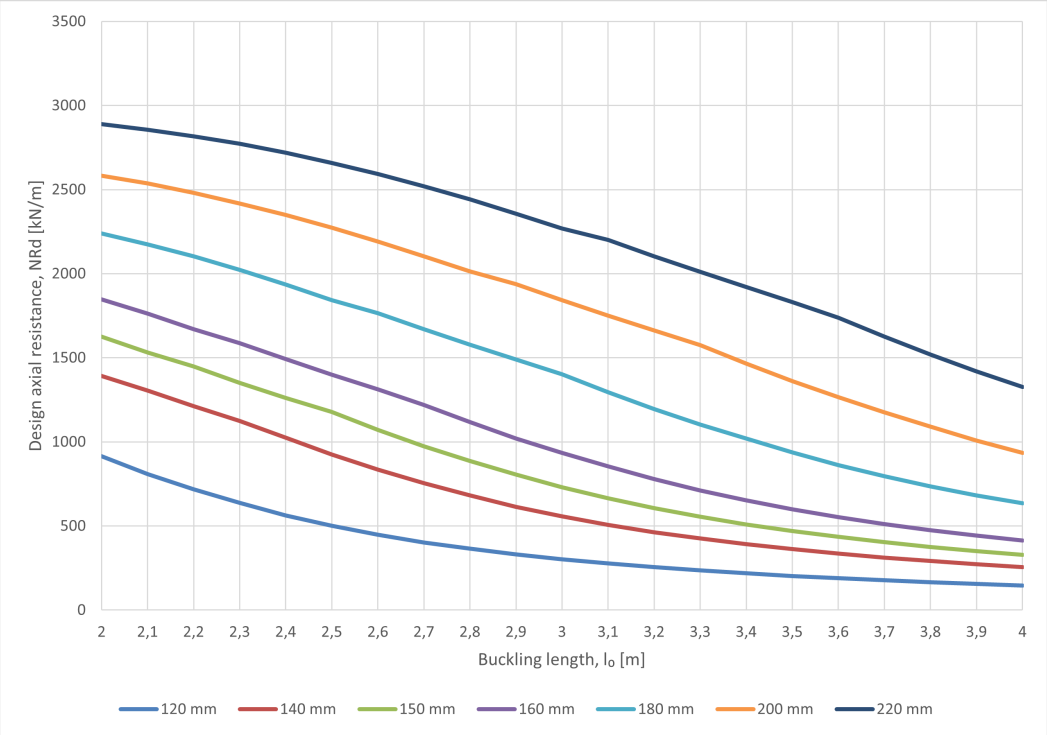

Figure 4.7: Influence of wall thickness on the design axial resistance of reinforced wall strips with concrete class C20/25 and constant reinforcement amount $A_{s,\mathrm{tot}} = 670$ mm^2/m.

Figure 4.7 shows that increasing the wall thickness increases the design axial resistance for all investigated buckling lengths when the reinforcement amount is kept constant. Compared with Figure 4.6, this figure separates the effect of wall thickness from the effect of changing reinforcement mesh. The resistance still decreases significantly with increasing buckling length, which shows that slenderness has a strong influence on the calculated axial resistance.

To isolate the influence of concrete strength, a 180 mm reinforced wall strip was evaluated for the three investigated concrete strength classes using the same reinforcement amount, $A_{s,\mathrm{tot}} = 376$ mm^2/m. This corresponds to mesh #6150, which is the smallest standard mesh satisfying the adopted minimum reinforcement requirement for the 180 mm wall. The results are shown in Figure 4.8.

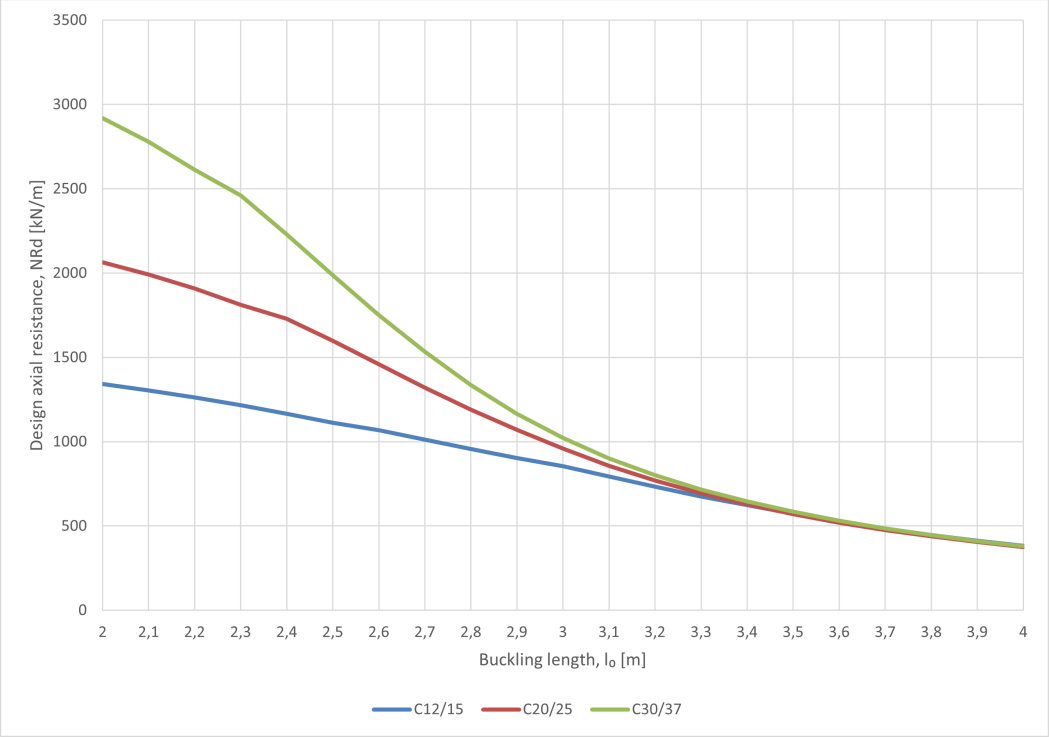

Figure 4.8: Influence of concrete strength class on the design axial resistance of a 180 mm reinforced wall strip with $A_{s,\mathrm{tot}} = 376$ mm^2/m.

Figure 4.8 shows that increasing the concrete strength class gives a higher design axial resistance, especially for shorter buckling lengths. As the buckling length increases, the curves become closer. This indicates that the resistance of longer and more slender walls is increasingly governed by stability and second-order effects rather than by concrete compressive strength alone.

To evaluate the influence of reinforcement amount, a 180 mm wall strip with concrete class C20/25 was analysed using different valid reinforcement amounts. The wall thickness and concrete strength class were kept constant in order to isolate the effect of the vertical reinforcement area. The results are shown in Figure 4.9.

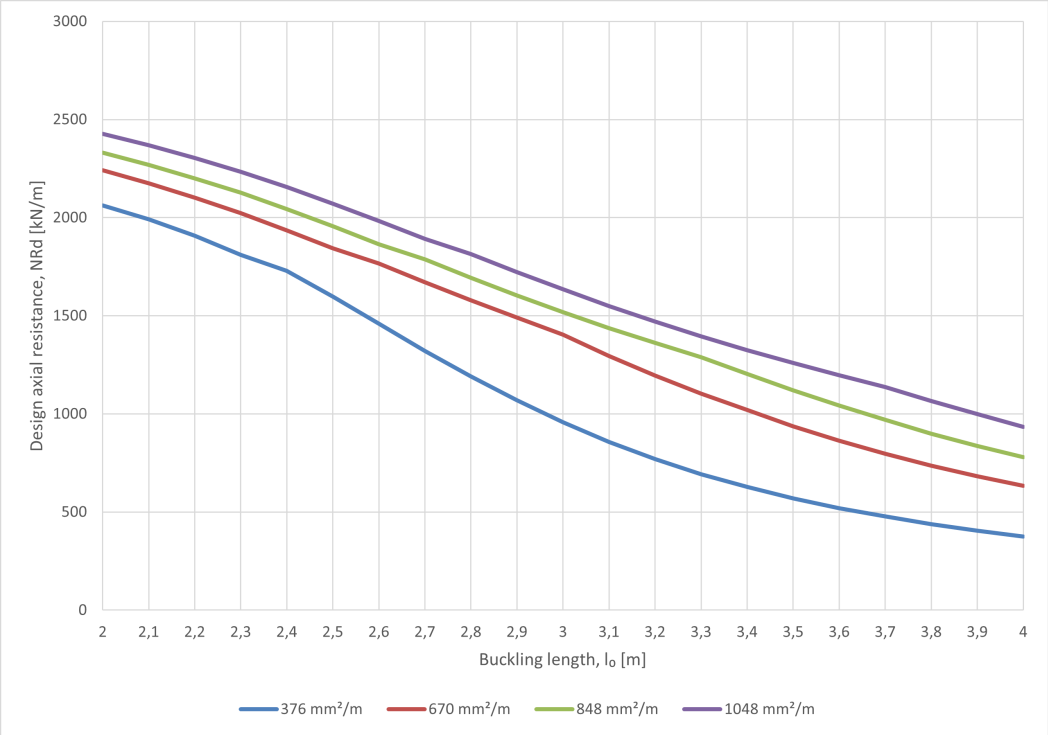

Figure 4.9: Influence of vertical reinforcement amount on the design axial resistance of a 180 mm reinforced wall strip with concrete class C20/25.

Figure 4.9 shows that increasing the vertical reinforcement amount increases the design axial resistance of the 180 mm wall strip for all investigated buckling lengths. The increase is caused not only by the direct axial contribution from the reinforcement, but also by the increased moment resistance of the cross-section, which allows a larger concrete compression zone to be mobilised.

However, the increase in resistance is not proportional to the increase in reinforcement area. For example, at $l_0 = 2.4$ m, increasing the reinforcement from $A_{s,\text{tot}} = 376$ mm^2/m to $A_{s,\text{tot}} = 1048$ mm^2/m corresponds to a factor of 2.79 increase in vertical reinforcement. The calculated design axial resistance increases from 1728 kN/m to 2156 kN/m, corresponding to an increase of approximately 25%. This shows that additional reinforcement increases the resistance, but with a clear diminishing return for this wall configuration.

As an additional project related reference point, a reinforced wall case based on the Troja wall parameters was evaluated. The case was based on a 180 mm wall, concrete class C30/37 and a total vertical reinforcement area of $A_{s,\text{tot}} = 424$ mm^2/m, corresponding to the interpreted $1 + 1$ $\phi 9$ $c300$ wall reinforcement. The effective buckling length was taken as $l_0 = 2.765$ m, based on the storey-height identified in the Troja section drawing.

For this reference case, the calculated design axial resistance was

$$N_{Rd} = 1487 \text{ kN/m}.$$

This value is included as a project related reference point for the reinforced wall model and should not be interpreted as a complete verification of the Troja wall system.

4.2.2 Unreinforced wall results

The unreinforced wall results were evaluated in order to identify the wall geometries for which the unreinforced wall model is applicable. Only combinations satisfying the adopted validity requirements, including the slenderness limitation and the eccentricity assumption used in the calculation model, are included in the comparison. Combinations outside the valid range are excluded from the diagrams.

To make the applicability of the unreinforced wall alternative clearer, the adopted slenderness limitation was translated into an approximate maximum effective buckling length for each wall thickness. According to EN 1992-1-1, the slenderness ratio is defined as

$$\lambda = \frac{l_0}{i}$$

where l_0 is the effective buckling length and (i) is the radius of gyration of the cross-section. For cast in situ unreinforced concrete walls, the adopted slenderness limit is $\lambda \leq 86$ [8]. For the rectangular wall strip used in this study, the radius of gyration in the weak direction was taken as

$$i = \frac{t}{\sqrt{12}}$$

where t is the wall thickness. The maximum effective buckling length was therefore calculated as

$$l_{0,\max} = 86 \cdot \frac{t}{\sqrt{12}}$$

The result is shown in Table 4.5.

Table 4.5: Approximate maximum effective buckling length satisfying the adopted slenderness limit for the unreinforced wall comparison. The values only indicate applicability of the simplified model and do not by themselves verify sufficient axial resistance for a specific building load.

t [mm]	$l_{0,\max}$ [m]	Valid range within study [m]
120	2.98	2.0–2.9
140	3.48	2.0–3.4
150	3.72	2.0–3.7
160	3.97	2.0–3.9
180	4.47	2.0–4.0
200	4.97	2.0–4.0
220	5.46	2.0–4.0

The table shows that the thinner wall sections are only applicable for shorter buckling lengths, while wall thicknesses of 180 mm and above are within the adopted slenderness range for the full investigated interval. The table should not be interpreted as a capacity verification for a specific building. It only identifies combinations where the simplified unreinforced wall model may be applied. A separate comparison with the design axial load would still be required in a real project.

Figures 4.10–4.12 show the design axial resistance of unreinforced wall strips for the investigated concrete strength classes C12/15, C20/25 and C30/37. For all three concrete strength classes, the axial resistance decreases with increasing buckling length, which reflects the increasing influence of slenderness and eccentricity. The results also show that wall thickness has a strong influence on the resistance, with thicker walls providing higher design axial resistance.

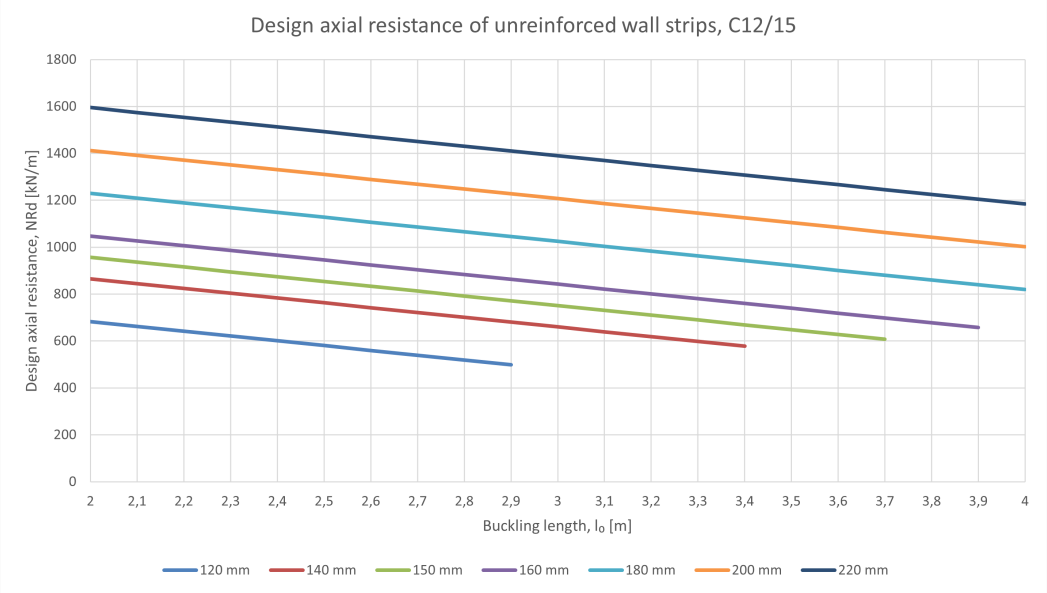

Figure 4.10: Design axial resistance of unreinforced wall strips for concrete class C12/15 as a function of effective buckling length and wall thickness. Only combinations satisfying the adopted validity requirements are included.

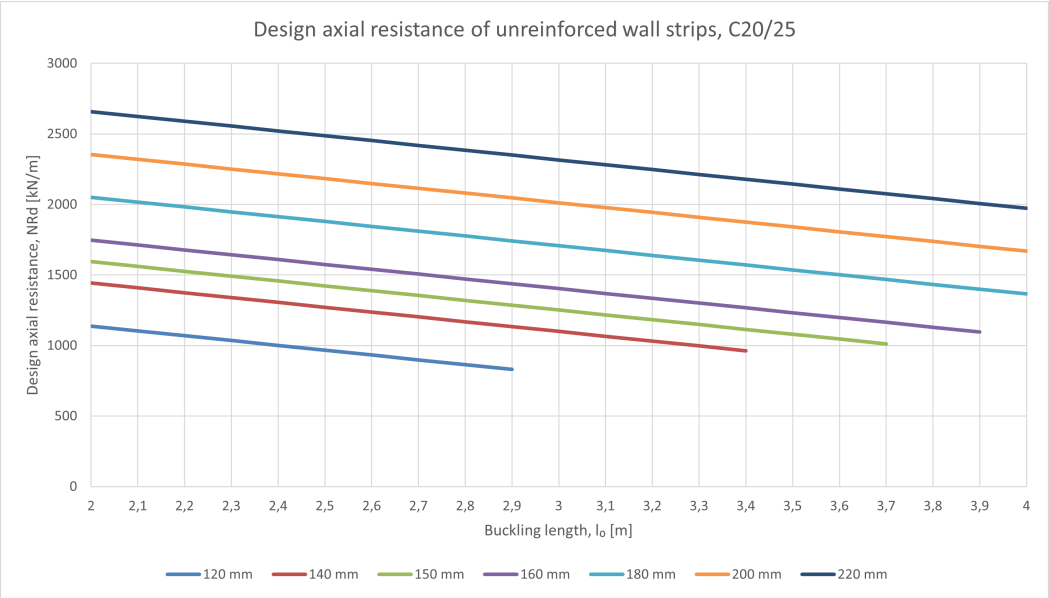

Figure 4.11: Design axial resistance of unreinforced wall strips for concrete class C20/25 as a function of effective buckling length and wall thickness. Only combinations satisfying the adopted validity requirements are included.

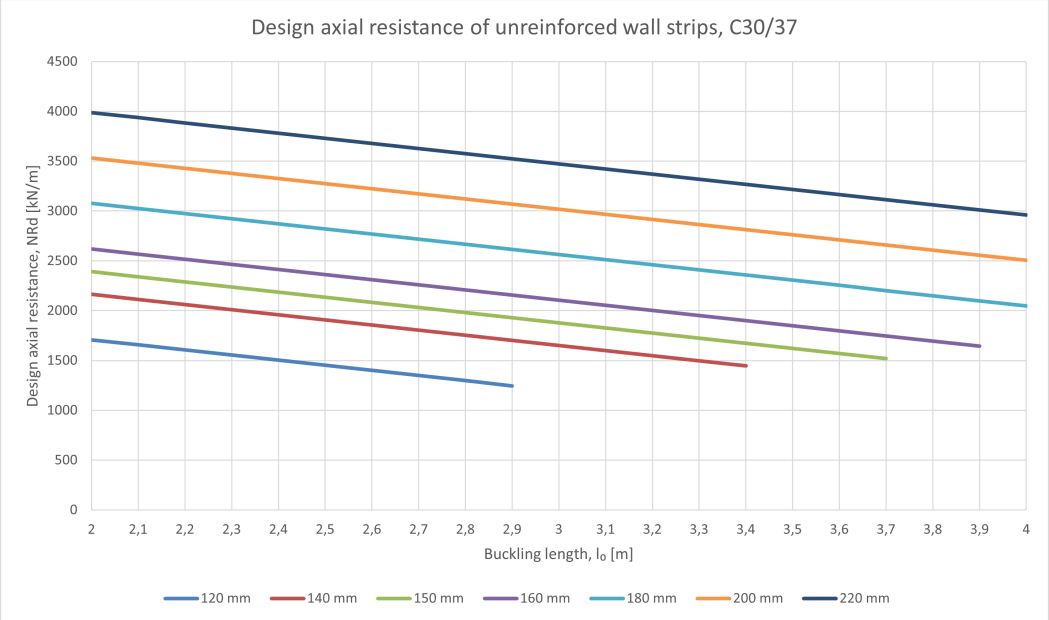

Figure 4.12: Design axial resistance of unreinforced wall strips for concrete class C30/37 as a function of effective buckling length and wall thickness. Only combinations satisfying the adopted validity requirements are included.

The comparison between the three concrete strength classes shows that concrete strength has a large influence on the calculated axial resistance in the unreinforced wall model. For example, for a 180 mm wall with $l_0 = 2.4$ m, the design axial resistance increases from 1148 kN/m for C12/15 to 1914 kN/m for C20/25 and 2870 kN/m for C30/37. This corresponds to an increase of approximately 67% from C12/15 to C20/25, and approximately 150% from C12/15 to C30/37.

This shows that the selected concrete strength class strongly affects the resistance level of an unreinforced wall. However, it does not change the adopted validity range of the simplified model, which is controlled by wall thickness and effective buckling length. The unreinforced wall results therefore show that compression-dominated wall solutions may be possible for certain combinations of wall thickness, buckling length and concrete strength class.

4.2.3 Comparison between reinforced and unreinforced wall design models

This section compares the calculated axial resistance obtained from two different Eurocode-based wall design models. The reinforced wall results are based on the reinforced concrete wall model described in Appendix B, where the resistance is calculated from strain compatibility and cross-sectional equilibrium, with second-order effects included through the nominal stiffness approach. The unreinforced wall results are based on the simplified design model for plain and lightly reinforced concrete members in Chapter 12 of EN 1992-1-1.

The purpose of the comparison is therefore not to isolate the physical effect of removing reinforcement from an otherwise identical wall. Instead, the comparison illustrates how the calculated axial resistance differs when a compression-dominated wall is evaluated using the reinforced wall model and the simplified unreinforced wall model. The results should consequently be interpreted as a comparison between design models, with different assumptions and validity conditions.

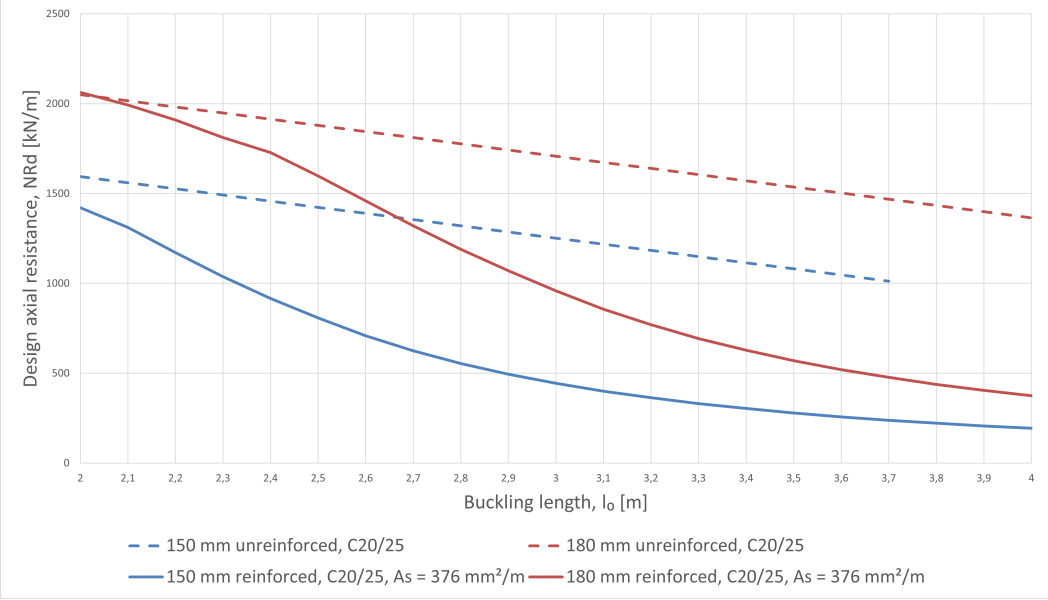

Figure 4.13: Comparison of calculated axial resistance from the reinforced and unreinforced wall models for selected wall thicknesses in concrete class C20/25. The reinforced alternatives use $A_{s,\mathrm{tot}} = 376$ mm^2/m, while the unreinforced alternatives are only shown within the adopted validity range. The figure compares model outputs and should not be interpreted as a direct physical comparison of the same wall with and without reinforcement.

The comparison shows that the simplified Chapter 12 model gives higher calculated axial resistance than the reinforced wall model for several of the valid compression-dominated cases. This should not be interpreted as a general conclusion that an unreinforced wall has higher real load-bearing capacity than a reinforced wall. The difference is partly a consequence of the fact that the two alternatives are evaluated with different design models. The reinforced wall model treats the member as a reinforced concrete section under combined axial force and bending, while the Chapter 12 model is specifically formulated for plain or lightly reinforced members where the behaviour is dominated by compression and the validity requirements are satisfied.

The result therefore suggests that the reinforced wall model used in this study may be conservative for cases where compression dominates and tensile stresses are limited. For such cases, the Chapter 12 model can provide a relevant alternative design route, provided that the slenderness, eccentricity and other applicability requirements are fulfilled. The material implication is not that reinforcement reduces the physical capacity, but that distributed wall reinforcement may be unnecessary in some compression-dominated walls when the wall can be verified using the simplified unreinforced wall model.

The potential material implication of using the Chapter 12 design route is mainly related to the possible reduction of distributed reinforcement in compression-dominated wall fields. To quantify this effect, the smallest valid reinforced wall alternatives from Table 4.4 were converted into an indicative climate impact of the vertical reinforcement, normalised per cubic metre of wall concrete. The result is shown in Table 4.6.

Table 4.6: Indicative climate impact of the vertical reinforcement in the smallest valid reinforced wall alternatives, normalised per cubic metre of wall concrete. The values only include the vertical reinforcement used in the axial wall model.

t [mm]	Mesh	$A_{s,\mathrm{tot}}$ [mm^2/m]	kgCO_2e/m^3 wall concrete
120	#5150	262	10.2
140	#6150	376	12.6
150	#6150	376	11.7
160	#6150	376	11.0
180	#6150	376	9.8
200	#8150	670	15.7
220	#8150	670	14.2

The values were calculated using an indicative climate factor of 0.596 kgCO_2e/kg for reinforcement steel, based on the value reported by Klimatguiden for reinforcement steel according to Boverket [33]. The reinforcement impact was then divided by the concrete volume of the corresponding wall strip. The values should therefore be interpreted as indicative rather than product-specific.

Table 4.6 shows that the vertical reinforcement in the smallest valid reinforced wall alternatives corresponds to approximately 9.8–15.7 kgCO_2e/m^3 of wall concrete. If an unreinforced wall alternative is permitted, this represents the direct saving associated with the distributed vertical reinforcement used in the wall model.

In practice, a welded reinforcement mesh also contains horizontal reinforcement. If the same mesh is used in both directions, the climate impact of the distributed mesh would be approximately twice the values shown in Table 4.6. For example, the 180 mm wall with #6150 mesh corresponds to approximately 9.8 $kgCO_2e/m^3$ for the vertical reinforcement only, or approximately 19.6 $kgCO_2e/m^3$ if the horizontal reinforcement in the mesh is also included.

The actual saving in a complete wall would still depend on the final reinforcement layout. Local reinforcement may be required even if the main wall field is designed as unreinforced or lightly reinforced.

4.2.4 Summary

Overall, the wall results show that wall thickness and effective buckling length have a strong influence on the design axial resistance. Increasing the wall thickness increases the resistance, while increasing the buckling length reduces the resistance because slenderness and second-order effects become more important. Concrete strength class has a clear influence, especially for shorter and less slender walls, while its effect becomes smaller when stability effects become more dominant.

The reinforcement amount also affects the calculated resistance, but the increase is not proportional to the increase in reinforcement area. For the 180 mm wall with C20/25 concrete, increasing the vertical reinforcement from $A_{s,\mathrm{tot}} = 376$ mm^2/m to $A_{s,\mathrm{tot}} = 1048$ mm^2/m increased the calculated resistance by approximately 25% at $l_0 = 2.4$ m. This shows that additional distributed reinforcement can improve the resistance, but with diminishing return for the studied wall configuration.

The Troja related reinforced wall reference case, based on a 180 mm wall with C30/37 concrete, $A_{s,\mathrm{tot}} = 424$ mm^2/m and $l_0 = 2.765$ m, gave a calculated design axial resistance of 1487 kN/m. This value was included only as a project-related reference point and not as a complete verification of the Troja wall system.

The unreinforced wall comparison shows that compression-dominated wall solutions may be possible for certain combinations of wall thickness, buckling length and concrete strength class, provided that the adopted validity requirements are satisfied. Concrete strength has a large influence on the resistance level in the unreinforced model, but it does not remove the limitations caused by slenderness and eccentricity.

The material comparison shows that avoiding distributed vertical reinforcement can give a direct indicative saving of approximately 9.8–15.7 $kgCO_2e/m^3$ of wall concrete for the smallest valid reinforced wall alternatives. If the horizontal reinforcement in a standard welded mesh is also avoided, the saving associated with the distributed mesh may be approximately twice as large. This does not mean that all reinforcement can be omitted in a real wall, since local reinforcement may still be required even when the main wall field is designed as unreinforced or lightly reinforced.

5 Discussion

5.1 Interpretation of the reference structures

The two reference structures should be interpreted as comparative examples rather than as direct evidence of general design practice. Cykelskrapan and Troja were selected because both are cast in situ concrete structures in residential buildings and because sufficient drawing information was available to extract slab thickness, wall thickness, span lengths and reinforcement amounts. The purpose of the comparison is therefore to discuss differences between two documented structures from different periods, not to establish a statistical trend for Swedish residential concrete buildings. A larger survey of buildings would be required to determine whether the observed differences are representative of Swedish practice more generally.

Cykelskrapan also has to be interpreted in relation to the design practice and regulatory framework of its time. The building was designed in 1956 and was therefore not designed according to present-day Eurocode assumptions. The available drawings also do not provide the same level of information as modern structural documentation. This introduces uncertainty, especially for reinforcement that may vary along the slab or be specified in other drawings not included in the analysed material. For this reason, Cykelskrapan is mainly used to illustrate a structural arrangement from another design period, not as a complete verification of the structural efficiency of the building.

The Troja project should also be interpreted with caution. When the drawings for the project were provided, it was stated that Troja generally uses relatively small reinforcement amounts compared with common contemporary practice. This means that Troja may represent a relatively material efficient modern example rather than an average current residential concrete structure. As a result, the comparison may underestimate the difference between Cykelskrapan and more typical modern projects. This further supports that more reference buildings would be needed to describe present-day practice more generally.

Another limitation is that the selected spans in both Cykelskrapan and Troja cannot be confirmed as the governing spans for the slab thicknesses and reinforcement amounts used in the projects. In a real building, the slab thickness and the reinforcement amounts may be governed by another part of the floor system, a larger span, local openings, detailing requirements, acoustic requirements, fire requirements or installation zones. This applies especially when only selected drawings or sections are used as the basis for the comparison. The analysed spans should therefore be understood as representative cases taken from the available drawings, not as confirmed governing design cases for the whole floor system.

The comparison between the Troja reinforcement and the calculation model must also be made carefully. In the selected three-span case, the identified top reinforcement is ϕ12 c300, corresponding to approximately 377 mm^2/m. This is slightly lower than the minimum reinforcement level used in the calculation model for a 250 mm slab. This does not mean that the Troja slab does not satisfy the design requirements. The real project may include local reinforcement, moment redistribution, different assumptions, additional reinforcement in other directions or detailing effects that are not captured by the simplified one metre strip model used in this thesis. For consistency, the calculated comparison was therefore based on the minimum reinforcement level required by the model, rather than on a direct redesign of the Troja slab.

Overall, the reference structures are useful for showing project-specific differences in structural thickness, reinforcement layout and floor build-up strategy between two periods. The comparison shows that the Troja slab has a larger structural concrete thickness than the Cykelskrapan slab, while the total floor depth differs much less. The reference structures are therefore used as a basis for discussing possible changes in design practice and in the distribution between structural and non-structural functions.

5.2 Potential for reducing material use in slabs

The slab results indicate that there is potential to reduce the amount of load-bearing concrete in cast in situ slabs when the slab is designed primarily for load-bearing capacity and serviceability. This is most clearly seen in the comparison with the Troja slab. The selected Troja slab has a structural thickness of 250 mm, but the simplified strip model showed that both analysed Troja spans were below the calculated allowable span limits. The two-span case had a utilisation ratio of 0.87, while the three-span case had a utilisation ratio of 0.61. Within the assumptions of the model, this suggests that the selected Troja slab contains structural reserve for the analysed spans.

The comparison with Cykelskrapan supports the same general interpretation. The Cykelskrapan slab has a structural thickness of 160 mm and an identified span of 3.69 m. In the calculation model, the corresponding 160 mm slab reached a calculated allowable span of 4.53 m at the minimum reinforcement level and 5.65 m at the reinforcement level closest to the interpreted support reinforcement in the drawing. This shows that a relatively thin cast in situ slab can satisfy the applied load-bearing and serviceability checks for moderate residential spans, provided that the support conditions and reinforcement layout are suitable.

However, the results should not be interpreted as complete optimised slab designs. The calculated span limits are based on simplified strip models with fixed support assumptions and should therefore be understood as indicators of structural potential rather than final design recommendations. More detailed project-specific design could adapt reinforcement layout, moment redistribution and local detailing more directly to the actual floor system.

The slab analysis in this thesis is limited to solid slabs with uniform thickness. Other cast in situ floor types, such as ribbed slabs or T-beam floor systems, may achieve

higher structural efficiency by placing more concrete where it contributes most to bending stiffness and resistance. Similar parameter-based analyses could therefore be carried out for such floor systems. However, these alternatives were outside the scope of this study, since the comparison was focused on the solid slab systems identified in the two reference structures.

Moment redistribution was not included in the calculation model. A design using moment redistribution could potentially reduce the peak support moments in continuous slab systems, but this would also require verification of the increased field moments and rotation capacity. The calculated span limits may therefore be conservative compared with a separately verified redistribution based design, but this was not investigated further.

The support condition had a major influence on the calculated allowable span. The three-span model gave larger allowable spans than the one-span and two-span models because continuity reduces the governing bending moments and increases the structural efficiency of the slab. This shows that the boundary condition is one of the main factors controlling whether a thinner slab can be used. Material savings are therefore more realistic in internal slab fields where continuity can be relied upon, while edge bays, discontinuous slab fields and areas with uncertain restraint have a smaller potential for reducing thickness.

The results also show that increasing reinforcement is not always an efficient way to increase the allowable span. When bending resistance governs, additional reinforcement increases the calculated span capacity. When deflection starts to govern, the effect of additional reinforcement becomes smaller because the limiting parameter shifts from resistance to stiffness. This is important for material-efficient slab design, since adding reinforcement to compensate for a thinner slab may not always give a proportional structural benefit.

Concrete strength class had a more limited influence than slab thickness and support condition. At minimum reinforcement levels, the calculated allowable spans were almost unaffected by concrete strength class. The effect became more visible when deflection governed, especially for thinner slabs with higher reinforcement levels. This indicates that increasing concrete strength is not the main route to reducing slab material use; thickness, reinforcement amount and boundary conditions were more decisive.

Crack width did not govern any of the analysed slab cases. This is notable because crack width limitations and minimum reinforcement requirements are often discussed as factors that increase reinforcement amounts in current practice. In this study, the slabs were assessed for indoor exposure class XC1 and were assumed to be concealed by additional floor or ceiling layers. For this type of floor concept, crack width should be assessed with regard to durability and structural function rather than visual appearance. Additional reinforcement provided only to satisfy an appearance-related crack width limit would therefore increase material use without improving the load-bearing capacity of the slab.

Overall, the slab results indicate that cast in situ slabs can be designed with less load-

bearing concrete than in the analysed modern reference slab. The largest potential appears to be in continuous slab fields with moderate spans, where serviceability requirements can still be satisfied. However, this conclusion only concerns the structural concrete. Whether the complete floor system becomes more material efficient depends on how acoustic performance, fire protection and service installations are solved outside the load-bearing slab.

5.3 Potential for reducing material use in walls

The wall results show that the potential for reducing material use in load-bearing walls is mainly governed by the relation between wall thickness, effective buckling length and axial load level. Increasing the wall thickness increases the design axial resistance, while increasing the effective buckling length reduces the resistance because slenderness and second-order effects become more important. Wall optimisation should therefore not be based only on concrete strength or reinforcement amount. The relation between storey height and wall thickness is one of the main parameters controlling whether a thinner or less reinforced wall can be used.

The effect of concrete strength class depends strongly on slenderness. For shorter and less slender walls, the resistance is more directly governed by the material resistance of the concrete cross-section, and increasing the concrete strength class can therefore increase the axial resistance. For longer and more slender walls, the resistance curves for different concrete classes become closer, which shows that stability effects become more important than compressive strength alone. Wall thickness is therefore often a more effective parameter, since it increases both the concrete area and the flexural stiffness of the wall.

Wall thickness is particularly influential because it increases both the concrete area and the flexural stiffness of the wall. The increase in stiffness is important for slender walls, since it reduces the sensitivity to second-order effects.

The reinforcement amount also affects the calculated axial resistance, but the effect is not proportional to the increase in reinforcement area. For the 180 mm wall with C20/25 concrete and $l_0 = 2.4$ m, increasing the vertical reinforcement from $A_{s,\mathrm{tot}} = 376$ mm^2/m to $A_{s,\mathrm{tot}} = 1048$ mm^2/m corresponds to almost 2.8 times more reinforcement, while the calculated design axial resistance increases by approximately 25%. This shows a clear diminishing return for added distributed reinforcement in this wall configuration.

For compression-dominated walls, distributed reinforcement should therefore not automatically be treated as the main way to increase axial resistance once the minimum reinforcement requirement is satisfied. Wall thickness, slenderness and reinforcement level have to be considered together.

For comparison between wall thicknesses, the climate impact of the vertical reinforcement was divided by the corresponding concrete wall volume. Expressed in this way, the smallest valid reinforced wall alternatives give approximately 9.8–15.7 kg CO_2e

from vertical reinforcement per m^3 of wall. If the horizontal bars in a standard welded mesh are also included, the climate impact of the distributed mesh reinforcement is approximately twice as large. This indicates that reducing distributed mesh reinforcement can be a relevant material-saving measure in wall fields where a reduced-reinforcement or unreinforced design route is structurally permitted.

A limitation of unreinforced wall solutions is that cracking, if it occurs, may become more concentrated than in a reinforced wall. Since this was not evaluated in the axial resistance comparison, crack behaviour should be checked separately before unreinforced wall solutions are used in practice.

The unreinforced wall results show that compression-dominated wall alternatives may be possible for certain combinations of wall thickness, effective buckling length and concrete strength class. This is mainly relevant for walls where vertical load dominates and where bending from horizontal actions, eccentric load transfer and local detailing is limited. The results do not mean that unreinforced walls can replace reinforced concrete walls in all situations. They indicate wall geometries where a reduced-reinforcement or unreinforced design route may be worth investigating further, provided that the wall remains within the validity range of the simplified model and that local reinforcement is provided where required.

The Troja-related wall result illustrates how repeated wall dimensions in a multi-storey building can lead to large differences in utilisation between storeys. A wall near the base carries vertical load from several storeys above, while the same wall near the top carries much less accumulated load. Using the simplified tributary load estimate, the calculated resistance of the Troja-related wall case corresponds to the design vertical load from approximately 16 typical storeys. This does not verify the complete Troja wall system, but it shows that axial load resistance alone is not necessarily the governing reason for using the same wall thickness and reinforcement layout throughout a building. Other requirements, such as standardisation, constructability, robustness, openings, connections and horizontal actions, may instead control the final wall design.

The results support a wall design strategy where wall thickness and reinforcement are differentiated according to structural demand instead of being repeated unchanged throughout the building. The strongest potential is found in repeated internal load bearing walls where vertical compression dominates, openings are limited and horizontal stability is provided by other parts of the structural system. In these cases, minimum reinforcement, reduced reinforcement or an unreinforced wall design can provide a more material efficient alternative to a conventional distributed mesh layout.

5.4 Development of material use over time

The discussion of material use over time is based on two parts: the comparison between the two reference structures and the reviewed literature on changes in concrete design practice and design standards. The two reference structures, Cykelskrapan and Troja, should not be interpreted as a statistical basis for proving a general development over time. They are used as illustrative examples of cast in situ residential concrete structures from two different periods. Broader conclusions about changes in material use must therefore be supported by the literature review and by changes in design standards, rather than by the two project examples alone.

With this limitation in mind, the comparison between Cykelskrapan and Troja indicates that the amount of load-bearing concrete is larger in the contemporary reference structure. The structural slab thickness increases from 160 mm in Cykelskrapan to 250 mm in Troja, corresponding to an increase of approximately 56 %. The wall thickness also increases from 150 mm to 180 mm, corresponding to an increase of approximately 20 %. However, the total floor depth only increases from approximately 240 mm to 265 mm, corresponding to approximately 10 %. In these two reference structures, the main difference is therefore not only the total floor depth, but how the depth is distributed between load-bearing concrete and non-structural layers.

This difference is important when the two reference structures are used to discuss possible changes in floor system strategy. In the Cykelskrapan case, a larger part of the total floor depth is located in the non-structural build-up above the slab, while the structural concrete slab itself is thinner. In the Troja case, a larger part of the total floor depth is assigned to the load-bearing concrete. The comparison therefore suggests a shift in floor system strategy, where the modern solution integrates more functions into the structural concrete slab. This is consistent with current cast in situ practice, where the slab is often expected to contribute not only to load-bearing capacity, but also to acoustic performance, fire separation, installation coordination and production efficiency.

The reinforcement comparison gives a more mixed result. The general bottom reinforcement and the selected top reinforcement in the Troja three-span case are slightly lower than the interpreted reinforcement amounts in the Cykelskrapan slab. This was somewhat unexpected, since one initial assumption of the study was that the modern reference structure would contain more reinforcement. One possible explanation is that Troja was described, when the drawings were provided, as a project with relatively small reinforcement amounts compared with common contemporary practice.

The clearest increase in the two reference structures is therefore found in the structural concrete cross-sections rather than in the distributed slab reinforcement. For walls, the comparison is even more limited, since no complete general reinforcement layout was identified for the Cykelskrapan wall. The development observed in the two reference structures should therefore mainly be interpreted as an increase in load-bearing concrete thickness and a changed distribution between structural and non-structural floor depth, not as clear evidence of increased distributed reinforcement.

The project based comparison should be interpreted together with the literature review. While Cykelskrapan and Troja only provide two examples, previous studies on Swedish concrete structures indicate that both concrete volume and reinforcement content have increased in comparable structures over time. The reviewed literature also indicates that this development cannot be explained only by higher loads or longer service life requirements. More detailed design standards, stricter serviceability and durability requirements, increased minimum reinforcement, larger cover requirements and more formalised verification procedures have also been identified as contributing factors.

The slab results also show how material use can be influenced by serviceability and minimum reinforcement requirements. In several cases, deflection rather than ultimate load-bearing capacity governed the allowable span. Crack width did not govern the analysed cases, but crack-control minimum reinforcement may still increase the lowest permitted reinforcement amount. This illustrates how formal serviceability and detailing requirements can increase material use even when the member has sufficient load-bearing resistance.

The wall results also show how material use can be influenced by minimum reinforcement and detailing requirements. Even when the axial resistance of a compression-dominated wall is sufficient, conventional reinforced wall design may still require distributed vertical and horizontal reinforcement, as well as local reinforcement around openings, wall ends and wall-slab connections. This means that material use in walls may be governed not only by axial load capacity, but also by detailing practice, robustness requirements and the chosen design solution.

The development of design standards may also influence engineering practice. As the regulatory framework becomes more detailed, designers may be encouraged to satisfy each individual check conservatively rather than to evaluate which mechanisms are actually governing for the specific structure. This can increase material use, especially when serviceability and durability requirements are applied uniformly without considering whether the practical risk is relevant for the actual exposure class, surface use or structural function.

Advanced structural modelling is another factor that can influence material use. More detailed calculation models can in principle reproduce the structural behaviour more accurate, but they do not automatically lead to lower material quantities. As discussed in Section 3.5.2, detailed finite-element models can produce local force peaks that partly depend on modelling choices. If such results are used directly for reinforcement design without sufficient engineering assessment and post-processing, the reinforcement amount can increase even when the global structural behaviour does not require it. This supports the interpretation that material use is influenced not only by formal code requirements, but also by how calculation results are interpreted and translated into reinforcement layouts in practice.

At the same time, the comparison with Troja also shows that material development is not one sided. The Troja slab uses a higher concrete strength class than Cykelskrapan, but the project-specific concrete has a lower declared climate impact per cubic metre than the generic value used for the interpreted Cykelskrapan concrete. This means

that an increase in concrete volume does not necessarily lead to the same proportional increase in climate impact. However, from a resource efficiency perspective, reducing the amount of concrete remains relevant, since climate improved concrete reduces the impact per cubic metre but does not remove the environmental importance of material quantity.

Overall, the study supports the conclusion that the load-bearing concrete thickness is larger in the contemporary reference structure than in the historical reference structure, while the reinforcement comparison is less clear. The observed difference between the two reference structures is mainly a shift in structural concrete volume and in how structural concrete is used within the building system, rather than proof of a general increase in all material quantities over time.

5.5 Separation of structural and non-structural functions

A central idea in this thesis is that the load-bearing concrete does not necessarily have to solve all building functions at the same time. In current cast in situ residential construction, the slab often functions as a structural member, an acoustic mass, a fire-separating element and a zone for service installations. This can be efficient from a production perspective, but it also means that the selected slab thickness may be governed by requirements that are not directly related to the structural capacity or serviceability of the concrete member.

The slab results support the idea that thinner structural slabs may be possible when the concrete is assessed primarily as a load-bearing element. If non-structural functions are handled separately, the structural concrete thickness can be linked more directly to bending resistance, shear resistance, deflection and vibration. For walls, the same principle means that wall thickness and distributed reinforcement can be related more directly to axial load resistance, slenderness and stability requirements, while other performance requirements are verified as part of the complete wall system.

Separating services and functional layers from the load-bearing concrete may also improve long-term adaptability. If pipe routes, ducts and technical systems are placed in accessible layers, future maintenance and replacement can be carried out with less intervention in the structural frame. This may reduce refurbishment complexity and support circularity, since installations and finishes usually have shorter service lives than the concrete structure.

However, separating functions does not automatically make the complete building system more material efficient. One reason why cast in situ concrete remains attractive is that one integrated member can satisfy several structural and functional requirements at the same time. If these functions are moved to separate layers, the total floor system may require additional materials in the form of floating floors, suspended ceilings, fire protection boards, acoustic layers or service zones. The relevant comparison is therefore not between structural slab thicknesses alone, but between complete floor and

wall systems that fulfil the same structural and functional requirements. The concept is only beneficial if the reduction in structural concrete is not outweighed by added layers, increased complexity or transferred material use elsewhere in the building.

This design philosophy is consistent with a performance-based regulatory framework. Such a framework does not require the structural concrete itself to solve every building function, but it does require that the complete building system fulfils the required performance. The approach investigated in this thesis should therefore be understood as a system-level design strategy rather than as a simple reduction of concrete thickness.

5.6 Practical limitations

Even if a thinner structural slab is possible in the calculation model, practical implementation is controlled by acoustic performance, fire resistance, service installations, total floor depth, buildability, construction sequence and cost.

Acoustic performance is one of the practical limitations. A thinner concrete slab has lower mass and stiffness, which may make it more dependent on additional acoustic measures such as floating floors, resilient layers or suspended ceilings. If these layers are required to satisfy impact sound or airborne sound requirements, part of the material saving in the structural slab may be transferred to the non-structural build-up. The structural results cannot be evaluated separately from the acoustic solution.

Fire safety is another limitation. Reducing the concrete thickness reduces the available thermal protection for the reinforcement and reduces the margin for cover and execution tolerances. External fire protection may be used to compensate for a thinner load-bearing section, but this introduces additional materials, work operations and interfaces between trades. A thinner slab may therefore be structurally possible at normal temperature while still requiring additional measures to satisfy fire resistance requirements.

Service installations are also important. In current cast in situ residential construction, installations are often embedded in or coordinated with the structural slab because this can be efficient in production and can help limit the total floor depth. Moving installations outside the structural concrete may improve flexibility and make future changes easier, but it may also require suspended ceilings, service zones or raised floor build-ups. This can increase the total floor depth and may affect floor to ceiling height, building height limits or the number of possible storeys. The current practice of integrating several functions into the concrete slab is therefore not unreasonable from a production and coordination perspective.

The separation of functions also changes the design process. Instead of solving several requirements through a thick concrete slab, the structural engineer, acoustic consultant, fire consultant and installation designer must coordinate a layered floor system. This can create opportunities for more targeted material use, but it also requires earlier coordination and clearer responsibility between disciplines. If the additional layers are designed late in the project, the theoretical saving in structural concrete may be

difficult to realise in practice.

The total floor depth is therefore a key practical constraint. The comparison between Cykelskrapan and Troja showed that the difference in total floor depth is much smaller than the difference in structural concrete thickness. This indicates that reducing the load-bearing slab thickness does not automatically reduce the total floor system depth. If the removed concrete thickness is replaced by acoustic layers, fire protection or installation zones, the complete floor system may become similar in height to the conventional solution, or in some cases thicker.

Buildability must also be considered. A thinner slab has smaller tolerances for reinforcement placement, cover, openings and embedded details. It may also be more sensitive to construction stage loads, temporary supports and deviations during casting. If additional layers are used to solve acoustic, fire and installation requirements, the construction sequence becomes more dependent on coordination between several disciplines. This may reduce the simplicity that is one of the advantages of conventional cast in situ concrete floors.

Walls have a different set of practical limitations. Reduced reinforcement or unreinforced wall design is mainly relevant where vertical compression dominates. In real buildings, walls may also be controlled by openings, wall ends, wall-slab connections, robustness requirements and the global stability system. These effects must be verified before the isolated wall-strip results can be used in a project-specific design.

The influence of concrete strength class should also be interpreted from a practical perspective. In the structural slab results, increasing the concrete strength class had a limited influence on the allowable span compared with slab thickness, reinforcement amount and support condition. However, concrete strength class may still be important for production and economy. A higher strength class can affect drying time, formwork removal and construction speed, which may influence the total project economy more than the structural resistance itself. The choice of concrete class should therefore not only be discussed as a structural parameter, but also as a production related decision.

Cost is another limitation. A thinner structural slab may reduce concrete volume, but the total cost depends on the complete floor system and construction process. A solution with less concrete is therefore not automatically cheaper. The economic benefit depends on whether the reduction in concrete volume is large enough to compensate for the additional materials and work required in the complete floor build-up.

Although the new regulatory framework may allow greater freedom in principle, practical implementation depends on whether designers, contractors, clients and reviewing authorities are willing to accept alternative verification routes. Established Eurocode-based solutions may still be preferred because they are familiar, easier to review and associated with lower perceived project risk. The possibility of using alternative design concepts therefore does not remove the need for robust documentation, quality control and clear verification of the complete building performance.

Overall, the practical limitations show that reducing the structural concrete thickness is only feasible if the complete floor or wall system still satisfies acoustic, fire, installation, production and cost requirements. The challenge is therefore to reduce load-bearing concrete without creating a solution that becomes larger, more material intensive or more complicated to build.

5.7 Limitations of the study

The structural analyses in this thesis were limited to solid cast in situ slabs and wall strips with uniform thickness. The slab study only considered solid slabs idealised as one metre wide beam strips. More structurally efficient floor systems, such as ribbed slabs, T-beam floor systems or hollow-core slabs, were outside the scope of the analysis. Although the thesis focuses on cast in situ concrete, it is also possible to cast floor systems with non-uniform cross-sections, such as ribbed or T-beam systems. Similar parameter-based analyses could therefore be carried out for such alternatives, but they were not included because the reference structures considered in this study were based on solid slab systems.

The reference comparison is limited by the small number of analysed projects and by the available drawing information. Cykelskrapan and Troja provide two documented examples from different periods, but they cannot represent Swedish residential concrete construction as a whole. The selected spans and reinforcement layouts should therefore be understood as drawing-based comparison cases rather than complete design reconstructions.

The slab model is another limitation. The floor slabs were modelled as one metre wide strips subjected to uniformly distributed load. This made it possible to compare thickness, reinforcement amount, concrete strength class and support condition in a consistent way, but it does not capture the full behaviour of a real floor system. Transverse load distribution, openings, local reinforcement, construction joints, varying boundary conditions and interaction with surrounding walls were not included. The calculated allowable spans should therefore be interpreted as simplified structural indicators rather than final design values.

The reinforcement layout was not optimised, as discussed in Section 5.2. The parameter study varied reinforcement amount, but not the detailed placement of reinforcement in relation to the moment distribution. Plastic moment redistribution was also not included. The calculated span limits may therefore be conservative for continuous slab systems where sufficient rotation capacity and detailing would allow redistribution.

The treatment of minimum reinforcement is also a limitation. The slab parameter study used the minimum reinforcement requirements for detailing in EN 1992-1-1, Section 9. The separate minimum reinforcement requirement for crack width control in Section 7.3.2 was not evaluated independently. This distinction is relevant because Boverket distinguishes between minimum reinforcement for crack width limitation and minimum reinforcement for detailing, brittle failure and avoidance of larger excessive cracking [34]. As discussed in Section 5.4, crack control minimum reinforcement may

increase the lowest permitted reinforcement amount even when the calculated crack width itself is not governing.

If the Section 7.3.2 requirement had resulted in a higher minimum reinforcement amount than the Section 9 detailing requirement, some of the lowest reinforcement levels used in the parameter study would have needed to be increased. This affects the certainty of the reported minimum reinforcement levels and material quantities, but it does not necessarily mean that crack width would have been functionally governing for the concealed XC1 slab concept studied in this thesis.

The wall model was also simplified. The walls were analysed as isolated one metre wide vertical strips with an assumed effective buckling length and simplified eccentricity. The model only evaluates vertical axial resistance under the adopted buckling assumptions and does not include complete building stability, wind actions, in-plane shear resistance, load redistribution between walls, floor-wall interaction, openings, wall ends or local force transfer at wall-slab connections. These effects may introduce bending moments and transverse forces that are not included in the isolated strip model. This is particularly important for the unreinforced wall alternatives, since these are only relevant when the wall behaviour remains compression-dominated. The results should therefore be interpreted as identifying potentially favourable wall geometries rather than complete wall designs.

The study does not include a full design of the non-structural build-up. Acoustic performance, fire resistance and service installations were discussed as important design aspects, but complete solutions were not dimensioned and compared in detail. The study can therefore show the structural potential for reducing load-bearing concrete, but not determine whether the complete floor system would have lower material use, climate impact or cost after all additional layers are included.

The climate comparison is limited by the available data. For Troja, project-specific climate data were available for the concrete, while the Cykelskrapan comparison had to rely on generic modern climate data for an interpreted concrete class. The original concrete mix, cement content and production conditions for Cykelskrapan are not known. The climate comparison should therefore be interpreted as indicative rather than as a direct historical life cycle comparison.

Finally, cost and production consequences were not quantified. Factors such as drying time, formwork cycle, labour, construction sequence, coordination of installations, building height and acoustic or fire protection systems may have a large influence on whether a thinner structural slab is feasible in practice. These aspects were discussed qualitatively, but a complete economic evaluation was outside the scope of the study.

5.8 Future research

This thesis has focused on the structural potential for reducing the amount of load-bearing concrete in cast in situ slabs and walls. A natural continuation would be to study the complete floor system in more detail. In this work, additional build-up layers for acoustics, fire protection and service installations have mainly been discussed at a conceptual level. A future study could therefore develop and compare complete floor build-up solutions where the structural slab is made thinner and the remaining functions are handled outside the load-bearing concrete.

Further research is also needed for load-bearing walls. The wall study in this thesis was based on isolated one metre wall strips, while real walls act as part of a complete building system. Future studies could therefore apply the reduced-reinforcement and unreinforced wall concepts to complete wall layouts, where the interaction between vertical load transfer, stability requirements and local detailing can be studied more realistically. This would make it possible to identify where compression-dominated wall solutions can be used in a real building, and how wall thickness and reinforcement can be varied between storeys without compromising stability, robustness or practical detailing.

5.9 Implications for preliminary design

The results from the parameter studies are most useful in the early stages of design, where the main structural dimensions and system principles are still possible to influence. At this stage, the purpose is not to produce a complete member design, but to identify which parameters are likely to govern the material use and where further optimisation may be worthwhile.

For slabs, the diagrams and tables can be used as preliminary design maps showing how the allowable span is affected by slab thickness, reinforcement amount, concrete strength class and support condition. They make it possible to identify whether a given slab concept is mainly limited by bending resistance, deflection, crack width or vibration. This is useful because different governing criteria require different design responses. If bending resistance governs, additional reinforcement or improved continuity may be effective. If deflection or vibration governs, increasing reinforcement alone may give limited benefit, slab thickness, support conditions or floor build-up strategy may be more important.

For walls, the results can be used in early design to identify how axial resistance is affected by wall thickness, effective buckling length, concrete strength class and vertical reinforcement amount. The wall diagrams can help identify when a wall is primarily governed by cross-sectional resistance and when slenderness and second-order effects become more important. They also indicate which wall geometries may be worth investigating further as lightly reinforced or unreinforced compression-dominated alternatives. In this way, the wall results can support early decisions about whether repeated wall dimensions are appropriate, or whether wall thickness and reinforce-

ment should be varied according to load level and slenderness.

The appendix tables and diagrams should therefore be interpreted as preliminary screening tools rather than final design tables. They can be used to compare alternatives, identify governing parameters and decide which slab or wall concepts are worth developing further. However, a complete project-specific design must still verify the full structural system, including load redistribution, detailing, stability and relevant non-structural requirements.

The main implication for preliminary design is that material-efficient concrete structures should be evaluated as systems rather than by increasing individual parameters in isolation. For slabs, support condition and serviceability behaviour should be considered before simply increasing reinforcement or concrete strength. For walls, thickness, buckling length and actual axial load level should be considered before adopting the same reinforced wall solution throughout the building. Used in this way, the parameter studies provide a basis for asking more targeted design questions at an early stage and for avoiding unnecessarily conservative structural dimensions.

6 Conclusion

The literature review indicates that material use in reinforced concrete structures has increased over time, despite improved materials and more advanced design methods. This development appears to be related to more detailed design standards, stricter serviceability and durability requirements, increased verification demands and current design practice.

The calculation results indicate that the structural concrete thickness in cast in situ residential slabs and walls can be reduced under the adopted assumptions, when the concrete member is assessed primarily for structural performance. The results should therefore be understood as showing where structural concrete could be reduced, not as a full comparison of complete floor and wall systems.

For slabs, several analysed alternatives satisfied the adopted checks for load-bearing capacity, deflection, crack width and vibration with a smaller structural concrete thickness than the contemporary reference slab. This shows that thinner cast in situ slabs can be structurally realistic for moderate residential spans when they are verified for the relevant load-bearing and serviceability checks. The results also show that higher concrete strength is not a general route to material efficiency. Slab thickness, reinforcement amount and support condition had a clearer influence on the calculated span capacity.

For walls, the results show that axial resistance is governed mainly by wall thickness and effective buckling length. Increasing the amount of distributed vertical reinforcement gave a smaller effect than changing the wall geometry. The unreinforced wall comparison showed that many compression-dominated wall strips can reach sufficient axial resistance without reinforcement within the adopted limits. Unreinforced or reduced-reinforcement wall solutions should therefore be considered more actively for internal load-bearing walls where vertical compression dominates and where stability, openings, connections and local force transfer can be verified separately.

The comparison between Cykelskrapan and Troja supports the tendency identified in the literature review, but cannot prove the development on its own. The contemporary reference structure assigns a larger part of the floor depth to load bearing concrete. The structural slab thickness increases from 160 mm to 250 mm, while the total floor depth increases only slightly. The wall thickness also increases from 150 mm to 180 mm. This indicates that the difference between the two reference structures is not only related to total floor depth, but also to how much of that depth is assigned to the structural concrete.

The results can be used as preliminary design guidance for identifying where slimmer cast in situ concrete solutions are structurally realistic. For slabs, early design should distinguish between the thickness required for structural performance and the thickness required for other floor functions. For walls, early design should focus on wall thickness, effective buckling length and axial load level before adopting the same reinforced wall solution throughout the building. A complete project design must still verify acoustics, fire resistance, installations, robustness, local detailing and production. These requirements should be verified at system level rather than translated directly into more load-bearing concrete or reinforcement.

Bibliography

[1] Naturvårdsverket and Boverket. *Klimatscenarier för bygg- och fastighetssektorn: Förslag på metod för bättre beslutsunderlag*. Naturvårdsverket and Boverket, Sept. 20, 2019. URL: https://www.naturvardsverket.se/contentassets/8897c1c6a8a44c6e8461443625909c86/klimatscenarier-for-bygg-och-fastighetssektorn.pdf (visited on 02/11/2026).

[2] Naturvårdsverket. *Klimatneutral betong genom kravställning*. 6967. Naturvårdsverket, 2021. URL: https://www.naturvardsverket.se/globalassets/media/publikationer-pdf/6900/978-91-620-6967-4.pdf (visited on 02/11/2026).

[3] Boverket. *Miljonprogrammet*. Boverket. n.d. URL: https://www.boverket.se/sv/samhallsplanering/stadsutveckling/miljonprogrammet/ (visited on 02/11/2026).

[4] Robert Larsson. *Interview on cast in situ concrete construction in residential buildings*. Personal communication, interview by the authors, 23 March 2026. 2026.

[5] Tove Malmqvist, Martin Erlandsson, Nicolas Francart, Johnny Kellner, and Pär Åhman. *Minskad klimatpåverkan från flerbostadshus: LCA av fem byggsystem (kortrapport)*. Reviderad 2018-09-10. Sveriges Byggindustrier, 2018. URL: https://kunskap.ivl.se/download/18.5236a218179c58aa6141768/1623851544301/Kortrapport_LCA%20av%20fem%20byggsystem.pdf (visited on 02/11/2026).

[6] Thomas Olofsson. *Delrapport: BRO*. Version 2010-11-04. Bilaga C till SBUF-projekt 12180. Bygginnovationen (VINNOVA-finansierat forsknings- och utvecklingsprogram), Nov. 2010. URL: https://vpp.sbuf.se/Public/Documents/ProjectDocuments/B54E9551-2CDB-4351-9D02-65966F87BE09/FinalReport/SBUF%2012180%20Bilaga%20C-Bro.pdf (visited on 02/17/2026).

[7] Ivar Björnsson, Thomas Kamrad, Karl Lundstedt, Sven Thelandersson, Anders Lövquist, and Stefan Gustafsson. *Resursslöseri i anläggningsbyggandet? Vad kan vi lära av 50 års utveckling?* TVBK-3080. Lunds universitet, Lunds Tekniska Högskola (LTH), Avdelning för Konstruktionsteknik, 2025. URL: https://www.sweco.se/wp-content/uploads/sites/3/2025/04/Rapport-resurssloseri-inom-anlaggning.pdf (visited on 02/17/2026).

[8] *SS-EN 1992-1-1:2005 Eurocode 2: Design of concrete structures Part 1-1: General rules and rules for buildings*. European Standard. Swedish adoption of EN 1992-1-1:2004. Svenska Institutet för Standarder (SIS) and European Committee for Standardization (CEN), 2005.

[9] James G. MacGregor. *Reinforced Concrete: Mechanics and Design*. 3rd ed. Upper Saddle River, New Jersey: Prentice Hall, 2007.

[10] Betongelementforeningen. *Svingninger av betongelementer*. Updated version of earlier publication (2002). Betongelementforeningen, Jan. 2005.

[11] Boverket. *BABS från 1947 till 1968*. Granskad: 12 augusti 2024. 2024. URL: https://www.boverket.se/sv/lag--ratt/aldre-lagar-regler--handbocker/aldre-regler-om-byggande/babs-fran-1947-till-1968/ (visited on 02/10/2026).

[12] Boverket. *Byggnadsstadga med byggnadsbestämmelser (BABS 1950)*. Boverket. 1950. URL: https://www.boverket.se/contentassets/4e14d56168e14bbba074de978b141591/babs-1950.pdf (visited on 02/10/2026).

[13] Statens offentliga utredningar. *Betänkande angående byggnadsbestämmelser*. SOU 1949:64. Byggnadsstadgeutredningen, 1949. URL: https://filedn.com/ljdBas5OJsrLJOq6KhtBYC4/forarbeten/sou/1949/sou-1949-64.pdf (visited on 02/10/2026).

[14] *Byggnadsstadgan den 30 juni 1947*. SFS 1947:385. Stockholm: Kungl. Maj:ts kansli, 1947. URL: https://libris.kb.se/bib/619278 (visited on 02/10/2026).

[15] Boverket. *Byggregler: En historisk översikt*. Boverket, 2022. URL: https://www.boverket.se/contentassets/ba75fc25915f4a79bad02ff6e9a5eb02/byggregler-en-historisk-oversikt-2022.pdf (visited on 02/17/2026).

[16] European Commission, Joint Research Centre. *About EN Eurocodes*. European Commission. n.d. URL: https://eurocodes.jrc.ec.europa.eu/en-eurocodes/about-en-eurocodes (visited on 02/10/2026).

[17] Tord Isaksson and Annika Mårtensson. *Byggkonstruktion: Regel- och formelsamling*. 3rd ed. Lund: Studentlitteratur, 2020. ISBN: 978-91-44-13856-5.

[18] *EN 1990:2002 Eurocode: Basis of Structural Design*. European Standard. European Committee for Standardization (CEN), 2002. URL: https://www.phd.eng.br/wp-content/uploads/2015/12/en.1990.2002.pdf (visited on 02/10/2026).

[19] The Soundproofing Company. *Flooring: Protecting a Concrete Slab*. The Soundproofing Company. n.d. URL: https://www.soundproofingcompany.com/soundproofing_101/flooring-protecting-a-concrete-slab (visited on 02/10/2026).

[20] M. Feldmann, Ch. Heinemeyer, Chr. Butz, E. Caetano, A. Cunha, F. Galanti, A. Goldack, O. Hechler, S. Hicks, A. Keil, M. Lukic, R. Obiala, M. Schlaich, G. Sedlacek, A. Smith, and P. Waarts. *Design of Floor Structures for Human Induced Vibrations*. EUR 24084 EN. Luxembourg: European Commission, Joint Research Centre, 2009. DOI: 10.2788/4640.

[21] M. Feldmann, Ch. Heinemeyer, E. Caetano, A. Cunha, F. Galanti, A. Goldack, O. Hechler, S. Hicks, A. Keil, M. Lukic, R. Obiala, M. Schlaich, A. Smith, and P. Waarts. *Human Induced Vibrations of Steel Structures (HIVOSS): Design Guideline for Floors*. RWTH Aachen University, Research Fund for Coal, and Steel (RFCS), 2007. URL: https://www.stahlbau.stb.rwth-aachen.de/projekte/2007/HIVOSS/docs/Guideline_Floors_EN02.pdf (visited on 02/10/2026).

[22] *SS-EN 1990 Eurokod: Grundläggande dimensioneringsregler för bärverk*. Swedish adoption of EN 1990:2002. Approved 2002-06-28. Published 2010-12-21. Corrected version, December 2014. Svenska Institutet för Standarder (SIS), 2010.

[23] *EN 1992-1-2:2004 Eurocode 2: Design of concrete structures Part 1-2: General rules Structural fire design*. European Standard. European Committee for Standardization (CEN), 2004. URL: https://www.phd.eng.br/wp-content/uploads/2015/12/en.1992.1.2.2004.pdf (visited on 02/10/2026).

[24] Jorge P. Arenas and Luis F. Sepúlveda. "Impact sound insulation of a lightweight laminate floor resting on a thin underlayment material above a concrete slab". In: *Journal of Building Engineering* 45 (2022), p. 103537. DOI: 10.1016/j.jobe.2021.103537. URL: https://www.sciencedirect.com/science/article/pii/S2352710221013954 (visited on 02/16/2026).

[25] Xiaoyu Zhang, Xiamin Hu, Hongwei Gong, Jing Zhang, Zhicheng Lv, and Wan Hong. "Experimental study on the impact sound insulation of cross laminated timber and timber-concrete composite floors". In: *Applied Acoustics* 161 (2020), p. 107173. DOI: 10.1016/j.apacoust.2019.107173. URL: https://www.sciencedirect.com/science/article/pii/S0003682X19309545 (visited on 02/16/2026).

[26] Jesse Lietzén, Ville Kovalainen, Lauri Talus, Mikko Kylliäinen, Aitor Lopetegi, and Ander Aldalur. "Sound Insulation of Suspended Ceilings: A FEM-based Comparison of Suspension Systems". In: *Proceedings of Forum Acusticum 2023 (10th Convention of the European Acoustics Association)*. Turin, Italy, Sept. 2023. DOI: 10.61782/fa.2023.1014. URL: https://dael.euracoustics.org/confs/fa2023/data/articles/001014.pdf (visited on 02/16/2026).

[27] Rijkswaterstaat and Efectis Nederland BV. *Fire testing procedure for concrete tunnel linings and other tunnel components*. Efectis-R0695:2020. Date of issue: September 2020. This document supersedes 2008-Efectis-R0695. Efectis Nederland BV and Rijkswaterstaat, Sept. 2020. URL: https://efectis.com/app/uploads/2016/07/Efectis_R0695_2020_Fire_Testing_procedure_concrete_tunnel_linings.pdf (visited on 02/16/2026).

[28] Paroc Group Oy. *Fire Protection Guide Concrete: Loadbearing Concrete Slabs, Hollow-Core Slabs and Beams*. Technical guide, December 2024. Paroc. Dec. 2024. URL: https://www.paroc.com/en/documents/uploads/paroc-fire-protection-guide-concrete.

[29] AF Bostäder. *Troja*. AF Bostäder. n.d. URL: https://www.afbostader.se/projekt/troja/ (visited on 03/27/2026).

[30] DANEWIDS INGENJÖRSBYRÅ AB. *Structural drawings for the Troja project*. Unpublished structural drawings provided through email correspondence. See Appendix D. 2026.

[31] Niklas Johansson. "Uttorkning av betong: Inverkan av cementtyp, betongkvalitet och omgivande fuktförhållanden". ISRN: LUTVDG/TVBM-05/3124-SE. Licentiate thesis. Lund, Sweden: Avdelningen för Byggnadsmaterial, Lunds tekniska högskola, Lunds universitet, 2005. URL: https://lucris.lub.lu.se/ws/portalfiles/portal/4528695/641570.pdf (visited on 05/22/2026).

[32] Mikael Basteskår, Morten Engen, Terje Kanstad, and Kjell Tore Fosså. "A Review of Literature and Code Requirements for the Crack Width Limitations for Design of Concrete Structures in Serviceability Limit States". In: (2019). URL: https://nva.sikt.no/registration/0198cc87037e-24cb76ac-15fa-4e89-8169-885a2aec4608 (visited on 03/09/2026).

[33] Svenska Betongföreningen. *Beräkning – Klimatguiden*. n.d. URL: https://klimatguiden.betongforeningen.se/faktablock/berakning/ (visited on 05/13/2026).

[34] Boverket. *Sprickarmering*. Boverket. n.d. URL: https://www.boverket.se/sv/PBL-kunskapsbanken/regler-om-byggande/boverkets-konstruktionsregler/dimensionering-av-betongkonstruktioner/sprickarmering/ (visited on 03/27/2026).

Appendix A

Slab calculations

A.1 General calculation assumptions

This appendix presents the detailed calculation procedure used for the slab strip models described in Section 2.4. The same verification procedure was applied to all three structural models, while the moment, shear and deflection coefficients were changed according to the assumed support condition.

A.2 Reinforcement limits

Although the slab was analysed as a one metre wide beam strip, the structural member is a solid slab. The reinforcement limits were therefore checked according to SS-EN 1992-1-1:2005, Section 9.3.1.1. This section refers to the reinforcement limits in Section 9.2.1.1, including the recommended maximum reinforcement area [8]

$$A_{s,\max} = 0.04 A_c$$

For the one metre slab strip used in this study, the concrete cross-sectional area is

$$A_c = bh = 1000h$$

where h is the slab thickness in mm. The maximum reinforcement area can therefore be written as

$$A_{s,\max} = 0.04 \cdot 1000h = 40h$$

The resulting maximum reinforcement areas for the studied slab thicknesses are shown in Table A.1.

Table A.1: Maximum reinforcement area for the studied slab thicknesses according to $A_{s,\max} = 0.04A_c$.

Slab thickness h [mm]	$A_{s,\max}$ [mm^2/m]
120	4800
140	5600
160	6400
180	7200
200	8000
220	8800
240	9600
260	10400
280	11200
300	12000

The maximum reinforcement areas are considerably higher than the reinforcement range used in the slab calculations. The maximum reinforcement requirement therefore did not govern any of the studied slab cases.

In addition to the maximum reinforcement area, the bending resistance calculation was limited to normally reinforced cross sections. In this study, a cross section was treated as normally reinforced when the tensile reinforcement reached the design yield strain in the bending resistance calculation, expressed as $\varepsilon_s \geq \varepsilon_{sy}$. Reinforcement combinations where this condition was not satisfied were excluded from the reported span results.

A.3 Structural models and coefficients

The structural models were represented by standard beam coefficients for uniformly distributed load. The coefficients used for bending moment, shear force and deflection are given in Table A.2. The bending moments, shear forces and deflections were calculated as

$$M_{\text{sup}} = k_{M,\text{sup}} q L^2, \tag{A.1}$$

$$M_{\text{field}} = k_{M,\text{field}} q L^2, \tag{A.2}$$

$$V_{Ed} = k_V q L, \tag{A.3}$$

$$v = k_v \frac{qL^4}{EI}. \tag{A.4}$$

Support moments are negative in the structural analysis, but only their absolute values are used in the span calculations. The coefficients in Table A.2 therefore represent moment magnitudes. The coefficient $k_{M,\mathrm{defl}}$ was used only in the deflection verification, where the cracking assessment was evaluated at the section where the maximum immediate deflection occurs.

Table A.2: Coefficients used for the slab strip models.

Structural model	**Support condition**	$k_{M,\mathrm{sup}}$	$k_{M,\mathrm{field}}$	$k_{M,\mathrm{defl}}$	k_V	k_v
Single-span	Simply supported at both ends	n.a.	1/8	1/8	1/2	5/384
two-span equivalent	Fixed at one end and simply supported at one end	1/8	9/128	$\frac{5\sqrt{33}-11}{256}$	5/8	1/185
three-span equivalent	Fixed at both ends	1/12	1/24	1/24	1/2	1/384

A.4 Bending resistance verification

The bending resistance was calculated in accordance with the method presented in *Byggkonstruktion: Regel och formelsamling* by Isaksson and Mårtensson.

The nominal concrete cover was calculated as

$$c_{nom} = c_{min} + \Delta c_{dev} \tag{A.5}$$

where c_{min} is the minimum concrete cover and Δc_{dev} is the allowance for execution deviation. In this study, $\Delta c_{dev} = 10$ mm was used.

The effective depth was then calculated as

$$d = t - c_{\mathrm{nom}} - \frac{\phi}{2} \tag{A.6}$$

where t is the slab thickness and ϕ is the reinforcement diameter.

The tensile reinforcement area was taken as

$$A_s = A_{s,\mathrm{selected}} \tag{A.7}$$

For support sections, A_s denotes the tensile top reinforcement. For field sections, A_s denotes the tensile bottom reinforcement.

Reinforcement on the opposite side of the slab was not included in the bending resistance calculation. The calculated bending resistance should therefore be interpreted as a conservative sectional resistance for slabs where reinforcement is present on both faces.

The reinforcement stress was first taken as the design yield strength,

$$\sigma_s = f_{yd}. \tag{A.8}$$

The depth of the compression zone was then calculated as

$$x = \frac{A_s \sigma_s}{0.8 b f_{cd}}. \tag{A.9}$$

The steel strain was determined as

$$\varepsilon_s = \varepsilon_{cu} \frac{d - x}{x}. \tag{A.10}$$

The steel yield strain was calculated as

$$\varepsilon_{sy} = \frac{f_{yd}}{E_s}. \tag{A.11}$$

The yield assumption was verified by checking that

$$\varepsilon_s \geq \varepsilon_{sy}. \tag{A.12}$$

If the yield strain was not reached, the reinforcement stress was instead calculated using

$$\sigma_s = E_s \varepsilon_s, \tag{A.13}$$

and the compression zone depth was recalculated from equilibrium using Equation A.9.

The moment resistance was then calculated as

$$M_R = f_{cd} \cdot 0.8 x b (d - 0.4x). \tag{A.14}$$

The allowable span was calculated by combining the moment resistance with the relevant moment coefficient from Table A.2. For each support case, both support moment and field moment were checked where applicable. The span corresponding to each bending moment criterion was obtained as

$$L = \sqrt{\frac{M_R}{k_M q}}, \tag{A.15}$$

where M_R is the calculated moment resistance and k_M is the relevant moment coefficient. For the single-span model only the field moment criterion was used, while both support and field moment criteria were considered for the two-span and three-span equivalent models.

A.5 Shear verification

The shear resistance was calculated based on the longitudinal reinforcement ratio

$$\rho_l = \frac{A_{sl}}{bd} \leq 0.02 \tag{A.16}$$

where A_{sl} is the area of the tensile bottom reinforcement.

The size factor was calculated as

$$k = 1 + \sqrt{\frac{200}{d}} \leq 2.0 \tag{A.17}$$

where d is given in mm.

The minimum shear stress resistance was then calculated as

$$v_{\min} = 0.035 \sqrt{k^3 f_{ck}} \tag{A.18}$$

Since no axial force was considered, the compressive stress was taken as

$$\sigma_{cp} = 0 \tag{A.19}$$

The coefficient $C_{Rd,c}$ was taken as

$$C_{Rd,c} = \frac{0.18}{\gamma_c} \tag{A.20}$$

The shear resistance was then determined as

$$V_{Rd,c} = (C_{Rd,c}\, k \sqrt[3]{100 \rho_l f_{ck}} + k_1 \sigma_{cp}) bd \tag{A.21}$$

The calculated shear resistance was then compared with the minimum allowable shear resistance, which had to satisfy

$$V_{Rd,c} \geq (v_{\min} + k_1 \sigma_{cp})\, bd \tag{A.22}$$

The applied shear force was calculated using the relevant shear coefficient from Table A.2,

$$V_{Ed} = k_V q L. \tag{A.23}$$

The allowable span governed by shear was then obtained as

$$L = \frac{V_{Rd,c}}{k_V q}, \tag{A.24}$$

where k_V is the shear coefficient for the considered support condition.

A.6 Deflection verification

The deflection verification was based on the method presented in *Byggkonstruktion: Regel och formelsamling* by Isaksson and Mårtensson. The verification was performed iteratively in Excel. A trial value of the span was first assumed, and the span was then determined using Goal Seek such that the deflection limit was fulfilled. In some cases, no exact solution could be obtained for the deflection limit because the calculated deflection increased discontinuously when the section changed from uncracked to cracked behaviour. In these cases, the allowable span was taken as the largest span immediately before this transition. The reported span therefore corresponds to the maximum span for which the calculated deflection remained below the limiting value before cracking caused a sudden increase in deflection.

For the deflection verification, the cracking assessment was evaluated at the section where the maximum immediate deflection occurs. For the simply supported model and the fixed ended model, this section is located at midspan. For the model with one fixed end and one simply supported end, the maximum deflection occurs at approximately $0.42L$ from the simply supported end. The corresponding service moment at this section was used when calculating the distribution factor ζ. The service moment was calculated as

$$M_{\text{defl}} = k_{M,\text{defl}} q_{SLS} L^2, \tag{A.25}$$

where $k_{M,\text{defl}}$ is the moment coefficient corresponding to the section where the maximum immediate deflection occurs.

The section modulus was calculated as

$$W = \frac{bh^2}{6}. \tag{A.26}$$

The cracking moment was then determined as

$$M_{cr} = f_{ctm} W. \tag{A.27}$$

A distribution factor between uncracked and cracked behaviour was calculated as

$$\zeta = 1 - \beta \left(\frac{M_{cr}}{M_{\text{defl}}} \right)^2, \tag{A.28}$$

where β is a coefficient depending on the load duration. For long-term loading, $\beta = 0.5$ was used. If M_{defl} was lower than the cracking moment, the section was treated as uncracked.

The second moment of area of the uncracked section was taken as

$$I = \frac{bh^3}{12}. \tag{A.29}$$

To account for creep, the effective modulus of elasticity was calculated as

$$E_{c,ef} = \frac{E_{cm}}{1 + \varphi(t, t_0)}, \tag{A.30}$$

where the creep coefficient $\varphi(t, t_0)$ was determined according to the procedure described in Section A.7.

The flexural stiffness of the uncracked section was taken as

$$(EI)_I = E_{c,ef} I. \tag{A.31}$$

For the cracked section, the modular ratio was first calculated as

$$\alpha_e = \frac{E_s}{E_{c,ef}}. \tag{A.32}$$

The reinforcement ratio was calculated as

$$\rho = \frac{A_s}{bd}. \tag{A.33}$$

For the deflection calculation, A_s was taken as the tensile reinforcement in the field section.

The relative neutral axis depth was then determined as

$$\xi = \alpha_e \rho \left(\sqrt{1 + \frac{2}{\alpha_e \rho}} - 1 \right). \tag{A.34}$$

The flexural stiffness of the cracked section was calculated as

$$(EI)_{II} = 0.5 b d^3 \xi^2 E_{c,ef} \left(1 - \frac{\xi}{3} \right). \tag{A.35}$$

The deflection of the uncracked section was calculated as

$$v_1 = k_v \frac{q_{SLS} L^4}{(EI)_I}. \tag{A.36}$$

The deflection of the cracked section was calculated as

$$v_2 = k_v \frac{q_{SLS} L^4}{(EI)_{II}}. \tag{A.37}$$

The total deflection was then obtained by interpolation between cracked and uncracked behaviour,

$$v_{tot} = \zeta v_2 + (1 - \zeta) v_1. \tag{A.38}$$

The deflection requirement was taken as

$$v_{tot} \leq \frac{L}{250}. \tag{A.39}$$

A.7 Creep coefficient

The creep coefficient $\varphi(t, t_0)$ was calculated according to EN 1992-1-1, Appendix B.

The concrete area was calculated as

$$A_c = bh \tag{A.40}$$

The exposed perimeter was taken as

$$u = 2b \tag{A.41}$$

The notional size was then calculated as

$$h_0 = \frac{2A_c}{u} \tag{A.42}$$

The strength dependent factors were calculated as

$$\alpha_1 = \left(\frac{35}{f_{cm}} \right)^{0.7} \tag{A.43}$$

$$\alpha_2 = \left(\frac{35}{f_{cm}} \right)^{0.2} \tag{A.44}$$

$$\alpha_3 = \left(\frac{35}{f_{cm}} \right)^{0.5} \tag{A.45}$$

The humidity factor was calculated as

$$\varphi_{RH} = 1 + \frac{1 - RH/100}{0.1 \sqrt[3]{h_0}} \tag{A.46}$$

for $f_{cm} \leq 35$ MPa, and as

$$\varphi_{RH} = \left(1 + \frac{1 - RH/100}{0.1\sqrt[3]{h_0}}\alpha_1\right)\alpha_2 \tag{A.47}$$

for $f_{cm} > 35$ MPa.

The remaining creep factors were calculated as

$$\beta(f_{cm}) = \frac{16.8}{\sqrt{f_{cm}}} \tag{A.48}$$

$$\beta(t_0) = \frac{1}{0.1 + t_0^{0.2}} \tag{A.49}$$

$$\varphi_0 = \varphi_{RH} \cdot \beta(f_{cm}) \cdot \beta(t_0) \tag{A.50}$$

The factor β_H was calculated as

$$\beta_H = 1.5\left[1 + (0.012RH)^{18}\right]h_0 + 250 \leq \ 1500 \tag{A.51}$$

for $f_{cm} \leq 35$ MPa, and as

$$\beta_H = 1.5\left[1 + (0.012RH)^{18}\right]h_0 + 250\alpha_3 \leq \ 1500\alpha_3 \tag{A.52}$$

for $f_{cm} > 35$ MPa.

The time development factor was then calculated as

$$\beta_c(t, t_0) = \left(\frac{t - t_0}{\beta_H + t - t_0}\right)^{0.3} \tag{A.53}$$

The creep coefficient was finally determined as

$$\varphi(t, t_0) = \varphi_0\beta_c(t, t_0) \tag{A.54}$$

A.8 Crack width verification

The crack width verification was carried out according to EN 1992 part 1 1, Section 7.3.4. The verification was performed iteratively in Excel. A trial value of the span was first assumed, and Excel Goal Seek was then used to determine the span for which the crack width criterion was satisfied.

The crack width was checked using the relevant bending moment coefficient from Table A.2. For the single-span model, only the field moment was checked. For the two-span and three-span equivalent models, both the support moment and the field moment were checked where applicable.

The design service moment was calculated as

$$M_{Ed,SLS} = k_M q_{SLS} L^2, \tag{A.55}$$

where k_M is either $k_{M,\text{sup}}$ or $k_{M,\text{field}}$, depending on the section being verified.

The maximum crack spacing was calculated as

$$s_{r,max} = k_3 c + k_1 k_2 k_4 \frac{\phi}{\rho_{p,ef}}, \tag{A.56}$$

where c is the concrete cover, ϕ is the bar diameter, and $\rho_{p,ef}$ is the effective reinforcement ratio.

For bars with good bond properties, the coefficient k_1 was taken as

$$k_1 = 0.8. \tag{A.57}$$

For bending, the coefficient k_2 was taken as

$$k_2 = 0.5. \tag{A.58}$$

The recommended values

$$k_3 = 3.4 \tag{A.59}$$

and

$$k_4 = 0.425 \tag{A.60}$$

were used. The concrete cover was taken as

$$c = c_{nom}. \tag{A.61}$$

The relative neutral axis depth ξ, the modular ratio α_e, and the effective modulus of elasticity $E_{c,ef}$ were calculated using the definitions given in Section A.6. The neutral axis depth was calculated as

$$x = \xi d. \tag{A.62}$$

The effective tension area depth was calculated as

$$h_{c,ef} = \min \begin{cases} 2.5(h-d) \\ h/2 \\ (h-x)/3 \end{cases}. \tag{A.63}$$

The effective tension area was then calculated as

$$A_{c,ef} = bh_{c,ef}. \tag{A.64}$$

The effective reinforcement ratio was calculated as

$$\rho_{p,ef} = \frac{A_s}{A_{c,ef}}. \tag{A.65}$$

The cracked second moment of area was calculated as

$$I_{II} = A_s d^2 (1-\xi)\left(1 - \frac{\xi}{3}\right). \tag{A.66}$$

The internal lever arm was taken as

$$z = d - x. \tag{A.67}$$

The steel stress was then calculated as

$$\sigma_s = \frac{M_{Ed,SLS}}{I_{II}} z. \tag{A.68}$$

The strain difference between reinforcement and concrete was calculated as

$$\varepsilon_{sm} - \varepsilon_{cm} = \frac{\sigma_s - k_t \frac{f_{ct,ef}}{\rho_{p,ef}}(1 + \alpha_e \rho_{p,ef})}{E_s} \geq 0.6 \frac{\sigma_s}{E_s}, \tag{A.69}$$

where $k_t = 0.4$ was used for long-term loading.

The crack width was then calculated as

$$w_k = s_{r,max}(\varepsilon_{sm} - \varepsilon_{cm}). \tag{A.70}$$

The limiting crack width was taken as

$$w_k \leq w_{max}, \tag{A.71}$$

with

$$w_{max} = 0.4 \text{ mm}. \tag{A.72}$$

A.9 Vibration verification

The vibration verification was carried out as a simplified serviceability check based on the estimated fundamental frequency of the slab strip. The method follows the relationship presented by MacGregor, where the natural frequency of a floor may be estimated from the immediate static deflection if this deflection can be calculated [9].

The immediate static deflection was calculated using the same structural coefficients as defined in Table A.2. This means that the support condition was included through the deflection coefficient k_v. The slab was assumed to remain uncracked in the vibration calculation.

The second moment of area was calculated for the gross concrete section as

$$I = \frac{bh^3}{12}. \tag{A.73}$$

The flexural stiffness used in the vibration check was calculated as

$$EI = E_{cm}I. \tag{A.74}$$

The immediate static deflection Δ_{is} was taken as the maximum instantaneous deflection for the considered support condition. For the single-span model and the fixed ended model, the maximum deflection occurs at midspan. For the model with one fixed end and one simply supported end, the maximum deflection occurs at approximately $0.42L$ from the simply supported end. The deflection was therefore calculated using the coefficient k_v from Table A.2,

$$\Delta_{is} = k_v \frac{q_v L^4}{E_{cm}I}, \tag{A.75}$$

where q_v is the load included in the vibration calculation.

The fundamental frequency was estimated as

$$f = 0.18\sqrt{\frac{g}{\Delta_{is}}}, \tag{A.76}$$

where g is the gravitational acceleration and Δ_{is} is the maximum immediate static deflection for the considered support condition. MacGregor states that Δ_{is} should be calculated from the loads expected to be present on the floor during vibration, including the dead load and the relevant part of the live load [9].

The frequency criterion was taken from Betongelementforeningen. For walking-induced vibrations, Betongelementforeningen states that a common rule of thumb is that the resonance frequency of the floor should be higher than twice the highest load frequency, corresponding to a minimum frequency of 5.2 Hz for walking traffic [10]. The adopted criterion was therefore

$$f \geq f_{min}, \tag{A.77}$$

with

$$f_{min} = 5.2 \text{ Hz}. \tag{A.78}$$

The allowable span was determined iteratively in Excel by varying L until the calculated fundamental frequency was equal to the limiting value,

$$f(L) = f_{min}. \tag{A.79}$$

Appendix B

Wall calculations

This appendix presents the detailed calculation procedure used for the wall model described in Section 2.5. The appendix includes the geometrical definitions, material properties, reinforcement area calculation, stiffness calculation, second-order moment amplification, cross-sectional equilibrium and the unreinforced wall comparison model.

B.1 General calculation assumptions

The following modelling assumptions were used as the basis for the reinforced wall calculation procedure presented in this appendix:

- The wall was analysed as a one metre wide wall strip.
- The wall was subjected to vertical axial compression.
- The wall was assumed to be pinned at the top and bottom. The effective buckling length was therefore taken as equal to the clear wall height, $l_0 = H$.
- The effect of unavoidable imperfections was represented by an initial eccentricity.
- second-order effects were included through a nominal stiffness approach.
- Plane sections were assumed to remain plane.
- Concrete in tension was neglected in the ultimate limit state.
- The vertical reinforcement was assumed to be symmetrically placed on the two wall faces.
- The reinforcement stress was limited by the design yield strength.
- The design axial resistance was obtained from simultaneous axial force and moment equilibrium.

The wall thickness is denoted by t, the clear wall height by H, the width of the analysed wall strip by b, and the effective buckling length by l_0. In this study, $b = 1000$ mm.

B.2 Geometry and material properties

The reinforcement ratio was calculated as

$$\rho = \frac{A_s}{A_c} \tag{B.1}$$

where A_s is the total vertical reinforcement area per metre wall length, including both wall faces.

The reinforcement was assumed to be placed symmetrically on the two faces of the wall. The distance from the compressed edge to the reinforcement on the compression side was taken as

$$d' = c_{nom} + \frac{\phi}{2} \tag{B.2}$$

and the distance from the compressed edge to the reinforcement on the opposite side was taken as

$$d = t - d' \tag{B.3}$$

where c_{nom} is the nominal concrete cover and ϕ is the bar diameter.

The design compressive strength of concrete was calculated as

$$f_{cd} = \frac{f_{ck}}{\gamma_c} \tag{B.4}$$

and the yield strain of the reinforcement was calculated as

$$\varepsilon_{sy} = \frac{f_{yd}}{E_s} \tag{B.5}$$

where f_{yd} is the design yield strength of the reinforcement and E_s is the elastic modulus of reinforcing steel.

B.3 Reinforcement area from welded mesh

The investigated reinforcement amounts were based on standard welded reinforcement meshes placed on both wall faces. For one mesh layer, the reinforcement area per metre wall length was calculated as

$$A_{s,mesh} = \frac{\pi\phi^2}{4}\frac{1000}{s} \tag{B.6}$$

where ϕ is the bar diameter and s is the bar spacing in millimetres.

Since one mesh layer was assumed on each wall face, the total reinforcement area was

$$A_s = 2A_{s,mesh} \tag{B.7}$$

This total reinforcement area was used in the axial force and moment resistance calculation.

B.4 Initial eccentricity and first-order moment

The initial eccentricity was taken as

$$e_0 = \frac{l_0}{400}$$

The cross-section equilibrium was formulated with moments taken about the reinforcement layer at $y = d$. The shift from the centroidal axis of the wall section to this reference level was therefore

$$e_{\text{shift}} = d - \frac{t}{2}$$

The first-order moment about the centroidal axis was

$$M_{0,c} = N_{Ed}e_0$$

and the moment contribution caused only by shifting the moment reference point to the reinforcement layer at $y = d$ was

$$M_{\text{shift}} = N_{Ed}e_{\text{shift}}$$

The total first-order external moment about the reinforcement layer at $y = d$ was therefore

$$M_{0,d} = M_{\text{shift}} + M_{0,c} = N_{Ed}\left(d - \frac{t}{2}\right) + N_{Ed}e_0$$

The term $N_{Ed}(d - t/2)$ is only a change of moment reference point and is therefore not amplified when second-order effects are included.

B.5 Slenderness and second-order effects

The slenderness ratio was calculated as

$$\lambda = \frac{l_0}{i} \tag{B.8}$$

second-order effects were included when the wall slenderness exceeded the limiting slenderness,

$$\lambda \geq \lambda_{lim} \tag{B.9}$$

The limiting slenderness was evaluated as

$$\lambda_{lim} = \frac{20ABC}{\sqrt{n}} \tag{B.10}$$

where

$$n = \frac{N_{Ed}}{A_c f_{cd}} \tag{B.11}$$

and

$$\omega = \frac{A_s f_{yd}}{A_c f_{cd}} \tag{B.12}$$

In the calculation model, the coefficients were taken as

$$A = 0.7 \tag{B.13}$$

$$B = \sqrt{1 + 2\omega} \tag{B.14}$$

$$C = 1.7 - r_m \tag{B.15}$$

where r_m is the moment ratio. For the studied wall strip, $r_m = 1.0$ was used.

B.6 Effective creep coefficient

Creep was included in the nominal stiffness used for the second-order calculation. The effective creep coefficient was calculated as

$$\varphi_{eff} = \varphi(t, t_0)\frac{N_{qp}}{N_{Ed}} \tag{B.16}$$

where $\varphi(t, t_0)$ is the creep coefficient calculated according to the same Eurocode 2 procedure as described in Appendix A.

The quasi-permanent axial force was calculated as

$$N_{qp} = G_k + \psi_2 Q_k \tag{B.17}$$

and the design axial force used for the load ratio was calculated as

$$N_{Ed} = 1.2G_k + 1.5Q_k \tag{B.18}$$

For residential imposed load, the quasi-permanent factor was taken as

$$\psi_2 = 0.3 \tag{B.19}$$

The load ratio used in the effective creep coefficient was therefore

$$\frac{N_{qp}}{N_{Ed}} = \frac{G_k + 0.3Q_k}{1.2G_k + 1.5Q_k} \tag{B.20}$$

The notional size of the wall section was calculated as

$$h_0 = \frac{2A_c}{u} \tag{B.21}$$

where u is the perimeter exposed to drying. In the wall calculation, the two large wall faces were assumed to be exposed, giving

$$u = 2b \tag{B.22}$$

B.7 Nominal stiffness and second-order moment

The second moment of area of the concrete section was calculated as

$$I_c = \frac{bt^3}{12} \tag{B.23}$$

The design value of the concrete elastic modulus was calculated as

$$E_{cd} = \frac{E_{cm}}{1.2} \tag{B.24}$$

The reinforcement contribution to the second moment of area was calculated using Steiner's theorem. Since the reinforcement was placed symmetrically on the two wall faces, the steel contribution was calculated as

$$I_s = A_s \left[z^2 + \frac{\phi^2}{16} \right] \tag{B.25}$$

where A_s is the total reinforcement area on both wall faces, z is the distance from the wall centreline to each reinforcement layer, and ϕ is the bar diameter.

$$z = \frac{t}{2} - c_{nom} - \frac{\phi}{2} \tag{B.26}$$

The nominal flexural stiffness was then calculated as

$$EI = K_c E_{cd} I_c + K_s E_s I_s \tag{B.27}$$

For walls with

$$0.002 \leq \rho < 0.01 \tag{B.28}$$

the stiffness coefficients were taken as

$$K_s = 1.0 \tag{B.29}$$

and

$$K_c = \frac{k_1 k_2}{1 + \varphi_{eff}} \tag{B.30}$$

where

$$k_1 = \sqrt{\frac{f_{ck}}{20}} \tag{B.31}$$

and

$$k_2 = \min\left(\frac{n\lambda}{170}, 0.2\right) \tag{B.32}$$

For walls with

$$\rho \geq 0.01 \tag{B.33}$$

the stiffness coefficients were taken as

$$K_s = 0 \tag{B.34}$$

and

$$K_c = \frac{0.3}{1 + 0.5\varphi_{eff}} \tag{B.35}$$

The Euler buckling load corresponding to the nominal stiffness was calculated as

$$N_B = \frac{\pi^2 EI}{l_0^2} \tag{B.36}$$

If second-order effects were required, only the real first-order bending moment about the centroidal axis was amplified. The amplification factor was calculated as

$$\alpha_M = 1 + \frac{\beta}{N_B/N_{Ed} - 1}$$

where

$$\beta = \frac{\pi^2}{8}$$

The amplified moment about the centroidal axis was then

$$M_{Ed,c} = M_{0,c}\alpha_M$$

The design moment used in the cross-section equilibrium was finally expressed about the reinforcement layer at $y = d$ as

$$M_{Ed,d} = N_{Ed}\left(d - \frac{t}{2}\right) + N_{Ed}e_0\left(1 + \frac{\beta}{N_B/N_{Ed} - 1}\right)$$

or equivalently

$$M_{Ed,d} = M_{\text{shift}} + M_{Ed,c}$$

If second-order effects were not required, the design moment was taken as

$$M_{Ed,d} = M_{0,d}$$

B.8 Strain distribution and reinforcement stresses

The cross-section resistance was calculated using strain compatibility. Plane sections were assumed to remain plane, and the coordinate y was measured from the compressed edge of the wall. The neutral axis depth was denoted by x.

In the calculation model, compression was taken as positive and tension as negative. The concrete strain at the compressed edge was taken as

$$\varepsilon_{cu} = 0.0035 \tag{B.37}$$

The strain in the reinforcement layer at $y = d$ was therefore calculated as

$$\varepsilon_s = \varepsilon_{cu}\frac{x - d}{x} \tag{B.38}$$

and the strain in the reinforcement layer at $y = d'$ was calculated as

$$\varepsilon'_s = \varepsilon_{cu}\frac{x - d'}{x} \tag{B.39}$$

With this sign convention, tensile strains become negative. This is equivalent to the common formulation where the tensile strain is written as $\varepsilon_{cu}(d - x)/x$, but with the opposite sign convention.

The reinforcement stresses were calculated using an elastic-perfectly plastic stress-strain relationship. The stresses were limited to the interval $-f_{yd} \leq \sigma_s \leq f_{yd}$:

$$\sigma_s = \max\left[-f_{yd}, \min(E_s\varepsilon_s, f_{yd})\right] \tag{B.40}$$

$$\sigma'_s = \max\left[-f_{yd}, \min(E_s\varepsilon'_s, f_{yd})\right] \tag{B.41}$$

The corresponding reinforcement resultants were calculated as signed internal forces,

$$F_s = \sigma_s \frac{A_s}{2} \tag{B.42}$$

and

$$F'_s = \sigma'_s \frac{A_s}{2} \tag{B.43}$$

where $A_s/2$ is the reinforcement area on each wall face. A positive reinforcement force represents compression, while a negative reinforcement force represents tension.

The same strain distribution, reinforcement stress model and sign convention were used in both concrete compression models described below. The difference between the two models is only how the concrete compression force and its moment contribution were calculated.

B.9 Concrete compression model for $d' \leq x \leq d$

When the neutral axis was located between the two reinforcement layers,

$$d' \leq x \leq d \tag{B.44}$$

a rectangular stress block was used for the concrete compression zone.

To avoid confusion with the slenderness ratio λ, the rectangular stress block factor is denoted here by λ_b. For the concrete strength classes used in this study, $f_{ck} \leq 50$ MPa, the stress block factors were

$$\lambda_b = 0.8 \tag{B.45}$$

The effective compression zone depth was calculated as

$$a = \lambda_b x \tag{B.46}$$

The concrete compression force was then calculated as

$$F_c = f_{cd} b a \tag{B.47}$$

and its point of application was taken as

$$y_c = \frac{a}{2} \tag{B.48}$$

The internal axial force resultant of the section was calculated as

$$N_R = F_c + F_s + F'_s \tag{B.49}$$

where compression was taken as positive. Therefore, F_c is positive, while reinforcement forces are positive in compression and negative in tension. This is equivalent to writing the tensile reinforcement force as a positive magnitude and subtracting it from the compression resultants.

The moment resistance in the reinforcement layer at $y = d$ was calculated as

$$M_R = F_c(d - y_c) + F'_s(d - d') \tag{B.50}$$

The force in the reinforcement layer at $y = d$ does not contribute to the moment about this same reference level.

B.10 General concrete compression model

For compression-dominated cases, the neutral axis may fall outside the range

$$d' \leq x \leq d \tag{B.51}$$

In these cases, the rectangular stress block was not used. Instead, the concrete compression force and moment contribution were calculated by dividing the wall thickness into a number of horizontal concrete layers. The same strain distribution and sign convention as described above were used.

For a concrete layer j, located at a distance y_j from the compressed edge, the concrete strain was calculated as

$$\varepsilon_c(y_j) = \varepsilon_{cu} \frac{x - y_j}{x} \tag{B.52}$$

Concrete tension was neglected. Therefore,

$$\sigma_c(y_j) = 0 \quad \text{for} \quad \varepsilon_c(y_j) \leq 0 \tag{B.53}$$

For concrete in compression, a parabolic-rectangular stress-strain relationship was used. For

$$0 < \varepsilon_c(y_j) \leq \varepsilon_{c2} \tag{B.54}$$

the concrete stress was calculated as

$$\sigma_c(y_j) = f_{cd}\left[1 - \left(1 - \frac{\varepsilon_c(y_j)}{\varepsilon_{c2}}\right)^2\right] \tag{B.55}$$

where ε_{c2} is the concrete strain at which the design compressive strength f_{cd} is reached.

For larger compressive strains,

$$\varepsilon_{c2} < \varepsilon_c(y_j) \leq \varepsilon_{cu} \tag{B.56}$$

the concrete stress was kept constant at

$$\sigma_c(y_j) = f_{cd} \tag{B.57}$$

where

$$\varepsilon_{c2} = 0.002 \tag{B.58}$$

The force contribution from one concrete layer was calculated as

$$\Delta F_{c,j} = \sigma_c(y_j) b \Delta y \tag{B.59}$$

and its moment contribution about the reinforcement layer at $y = d$ was calculated as

$$\Delta M_{c,j} = \Delta F_{c,j}(d - y_j) \tag{B.60}$$

The lever arm $d - y_j$ was treated as a signed distance. Layers located above the reference level $y = d$ give a positive moment contribution, while layers located below this level give a negative moment contribution.

The total concrete compression force and concrete moment contribution were then obtained by summing all concrete layers:

$$F_c = \sum_j \Delta F_{c,j} \tag{B.61}$$

$$M_c = \sum_j \Delta M_{c,j} \tag{B.62}$$

The total internal axial force resultant was calculated as

$$N_R = F_c + F_s + F'_s \tag{B.63}$$

where F_c is positive in compression and the reinforcement forces are signed according to the stress convention defined above.

The moment resistance about the reinforcement layer at $y = d$ was calculated as

$$M_R = M_c + F'_s(d - d') \tag{B.64}$$

The reinforcement force F_s does not contribute to this moment equation because it acts at the reference level $y = d$, giving it zero lever arm.

This general model was used when the simplified rectangular stress block was not applicable. It is based on the same equilibrium equations as the rectangular stress block model, but the concrete compression resultant is obtained by numerical integration instead of assuming a single concrete compression force from a rectangular stress block.

B.11 Equilibrium conditions

The reinforced wall model uses the same equilibrium principles as a conventional N-M interaction diagram. The difference is that the complete interaction curve is not generated explicitly. Instead, the calculation searches directly for the resistance point corresponding to the adopted load path $M_{Ed,d}(N_{Ed})$, including the initial eccentricity and second-order moment amplification.

The equilibrium equations were formulated using the same sign convention throughout the calculation. Compression was positive and tension was negative.

For a trial value of the design axial force N_{Ed}, the neutral axis depth x was determined from axial force equilibrium:

$$R_N = N_R - N_{Ed} = 0 \tag{B.65}$$

After the neutral axis depth had been found, moment equilibrium was checked as

$$R_M = M_R - M_{Ed,d} = 0 \tag{B.66}$$

Both the internal moment resistance M_R and the external design moment $M_{Ed,d}$ were evaluated about the same reference level, namely the reinforcement layer at $y = d$. This ensures that the moment residual is formed using consistent lever arms.

The wall axial resistance was defined as the largest axial force satisfying both equilibrium conditions:

$$N_{Rd} = \max \{N_{Ed} : R_N = 0 \quad \text{and} \quad R_M = 0\} \tag{B.67}$$

B.12 Numerical solution procedure

The axial resistance was obtained using an iterative numerical procedure:

1. A trial value of N_{Ed} was selected.
2. The first-order moment M_0 was calculated from the axial force and initial eccentricity.
3. The effective creep coefficient and nominal stiffness were calculated.
4. If required, the moment was amplified to include second-order effects.
5. For the selected N_{Ed}, the neutral axis depth x was determined from axial force equilibrium.
6. If $d' \leq x \leq d$, the rectangular stress block model was used.
7. If x was outside this range, the general layered concrete model was used.
8. The moment resistance M_R was compared with the design moment $M_{Ed,d}$.
9. The procedure was repeated for increasing values of N_{Ed}.
10. The largest axial force for which $R_N = 0$ and $M_R \geq M_{Ed,d}$ was taken as N_{Rd}.

The calculated output from the wall model was the design axial resistance per metre wall length, expressed as

$$N_{Rd} \text{ [kN/m]} \tag{B.68}$$

B.13 Unreinforced wall comparison model

An unreinforced wall model was included as a comparison case. The calculation was based on the simplified method for unreinforced concrete walls and columns in Eurocode 2, Section 12.6.5.2. The design axial resistance was calculated as

$$N_{Rd,plain} = btf_{cd,pl}\Phi \tag{B.69}$$

where b is the width of the wall strip, t is the wall thickness, $f_{cd,pl}$ is the design compressive strength used for the unreinforced concrete model, and Φ is a reduction factor accounting for eccentricity, second-order effects and normal creep effects.

In this study, the wall thickness is denoted by t. The wall strip width was taken as

$$b = 1000 \text{ mm} \tag{B.70}$$

The total eccentricity was taken as

$$e_{tot} = \frac{l_0}{400} \tag{B.71}$$

in order to use the same eccentricity assumption as in the reinforced wall comparison.

The reduction factor was calculated as

$$\Phi_i = 1.14\left(1 - \frac{2e_{tot}}{t}\right) - 0.02\frac{l_0}{t} \tag{B.72}$$

and was limited by

$$\Phi_{max} = 1 - \frac{2e_{tot}}{t} \tag{B.73}$$

The value used in the resistance calculation was

$$\Phi = \min(\Phi_i, \Phi_{max}) \tag{B.74}$$

Cases where $\Phi \leq 0$ were excluded from the comparison, since this indicates that the simplified unreinforced model does not provide a valid positive axial resistance for the considered geometry and eccentricity.

The slenderness was calculated as

$$\lambda = \frac{l_0}{i} \tag{B.75}$$

with

$$i = \frac{t}{\sqrt{12}} \tag{B.76}$$

Combinations exceeding the adopted slenderness limit were also excluded from the unreinforced wall comparison.

cases with

$$\lambda \leq 86$$

were included as valid unreinforced wall comparison cases.

B.14 Minimum reinforcement and detailing check

For reinforced concrete walls, the minimum vertical reinforcement was checked as

$$A_{s,v,min} = 0.002 A_c \tag{B.77}$$

and the maximum vertical reinforcement outside lap zones was taken as

$$A_{s,v,max} = 0.04 A_c \tag{B.78}$$

When the minimum reinforcement requirement governed, the vertical reinforcement was assumed to be distributed equally between the two wall faces.

The minimum horizontal reinforcement was checked as

$$A_{s,h,min} = \max\left(0.25 A_{s,v}, 0.001 A_c\right) \tag{B.79}$$

where $A_{s,v}$ is the vertical reinforcement area.

Combinations that did not satisfy the adopted minimum reinforcement requirement were not included as valid reinforced wall alternatives in the comparison.

Appendix C

Tables and Diagrams

C.1 Slab result tables

The complete slab parameter study is presented in this appendix. The table and diagram for the case with C20/25 concrete, $\phi 9$ reinforcement and the three-span slab model are presented in Section 4.1 as Table C.5 and Figure C.6. They are therefore not repeated here.

C.1.1 Three-span slab model

The three span slab model used in the parameter study is shown schematically in Figure C.1. The model represents a one metre wide slab strip with restraint at both ends. Top reinforcement was considered in the support regions, while bottom reinforcement was considered in the span region. The figure is schematic and is only intended to clarify the support condition and the reinforcement side used in the sectional checks.

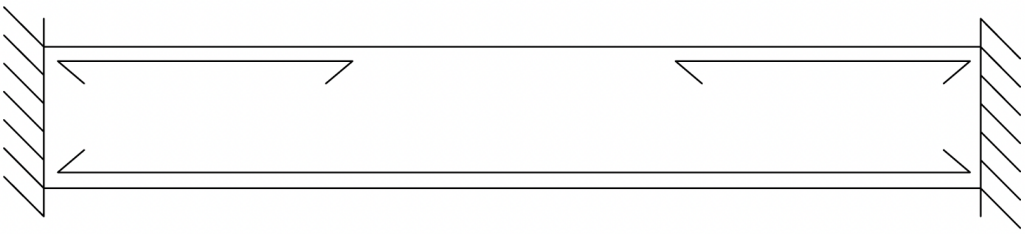

Figure C.1: Schematic illustration of the three span slab model used in the slab parameter study, showing the assumed support condition and the reinforcement considered in the support and field sections.

C12/15 concrete

Table C.1: Maximum allowable span for the slab using C12/15, $\phi 6$ and the three-span support model. The columns marked "min" include the minimum reinforcement required for the corresponding slab thickness. Orange cells are governed by bending resistance, while green cells are governed by deflection.

A_s [mm^2/m]	min 120	s150	min 140	s125	min 160	s100	min 180	min 200	min 220	s75	min 240	min 260	min 280	min 300	s50	s40
t [mm]	175	188	211	226	248	283	284	320	357	377	393	430	466	502	565	707
120	3.44	3.56	3.75	3.88	4.05	4.30	4.31	4.55	4.78	4.89	4.98	5.18	5.36	5.53	5.81	6.25
140			3.98	4.12	4.30	4.57	4.58	4.84	5.09	5.22	5.32	5.53	5.73	5.92	6.23	6.84
160					4.50	4.79	4.80	5.08	5.34	5.48	5.58	5.82	6.03	6.24	6.57	7.23
180							4.99	5.28	5.55	5.70	5.81	6.05	6.28	6.50	6.85	7.56
200								5.44	5.73	5.88	6.00	6.25	6.49	6.72	7.09	7.83
220									5.89	6.04	6.16	6.43	6.67	6.91	7.29	8.07
240											6.30	6.57	6.83	7.07	7.47	8.27
260												6.70	6.96	7.21	7.62	8.45
280													7.08	7.34	7.76	8.61
300														7.45	7.88	8.75

Note. Empty cells indicate reinforcement amounts below the minimum reinforcement requirement for the corresponding slab thickness.

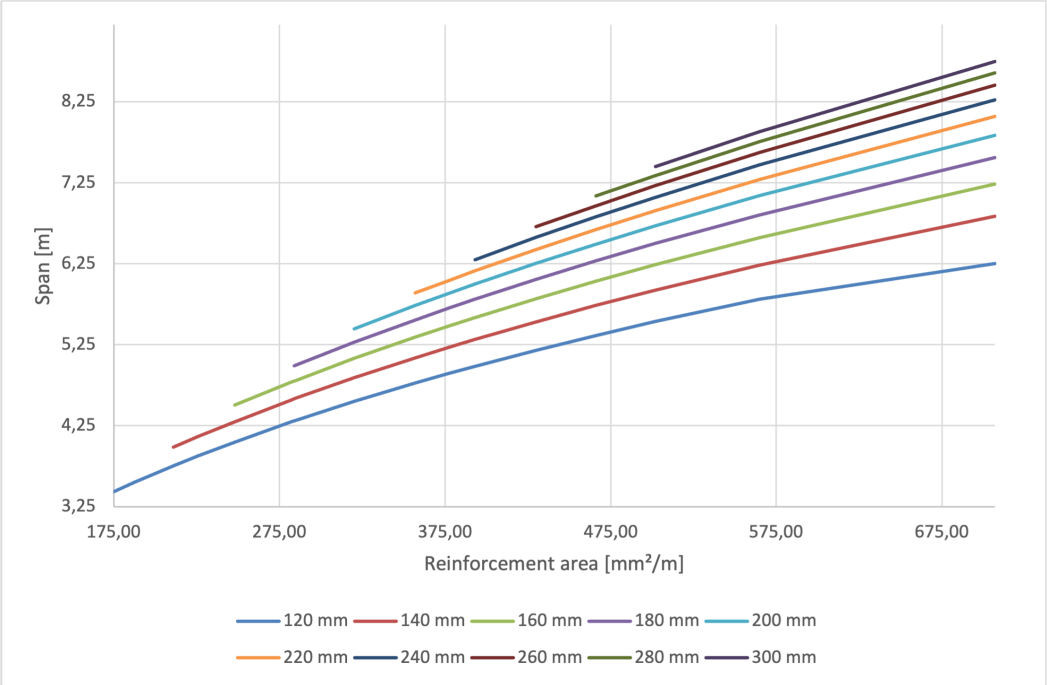

Figure C.2: Maximum allowable span as a function of reinforcement area for slabs with C12/15 concrete, $\phi 6$ reinforcement and the three-span support model. Each line represents a slab thickness between 120 mm and 300 mm.

Table C.2: Maximum allowable span for the slab using C12/15, $\phi 9$ and the three span support model. The columns marked "min" include the minimum reinforcement required for the corresponding slab thickness. The columns marked "max" indicate the largest reinforcement level before over reinforced behaviour for the corresponding slab thickness. Orange cells are governed by bending resistance, while green cells are governed by deflection.

A_s [mm^2/m]	min 120	min 140	min 160	s250	s225	min 180	s200	min 200	min 220	s175	min 240	s150	min 260	min 280	min 300	s125	s100	s75	max 120	max 140	max 160	s50
t [mm]	175	211	248	254	283	284	318	320	357	364	393	424	430	466	502	509	636	848	866	1048	1229	1272
120	3.41	3.72	4.01	4.06	4.26	4.27	4.50	4.51	4.73	4.78	4.94	5.10	5.14	5.32	5.48	5.52	6.03	6.38	6.40			
140		3.96	4.27	4.32	4.54	4.55	4.79	4.81	5.05	5.10	5.28	5.46	5.49	5.69	5.88	5.92	6.50	7.16	7.19	7.44		
160			4.48	4.53	4.77	4.77	5.03	5.05	5.31	5.36	5.55	5.75	5.78	6.00	6.20	6.24	6.87	7.74	7.80	8.19	8.42	
180						4.96	5.23	5.25	5.53	5.58	5.78	5.98	6.02	6.25	6.46	6.50	7.18	8.12	8.19	8.84	9.14	9.20
200								5.42	5.71	5.76	5.97	6.19	6.23	6.46	6.69	6.73	7.44	8.43	8.51	9.21	9.80	9.87
220									5.86	5.92	6.13	6.36	6.40	6.64	6.88	6.92	7.66	8.70	8.78	9.52	10.16	10.30
240											6.28	6.51	6.55	6.80	7.04	7.09	7.86	8.94	9.02	9.79	10.47	10.61
260													6.68	6.94	7.19	7.23	8.02	9.14	9.23	10.03	10.73	10.89
280														7.06	7.32	7.36	8.17	9.32	9.41	10.24	10.97	11.13
300															7.43	7.48	8.30	9.48	9.57	10.43	11.18	11.34

Note. Empty cells indicate reinforcement amounts below the minimum reinforcement requirement or over reinforced cross sections excluded from the results.

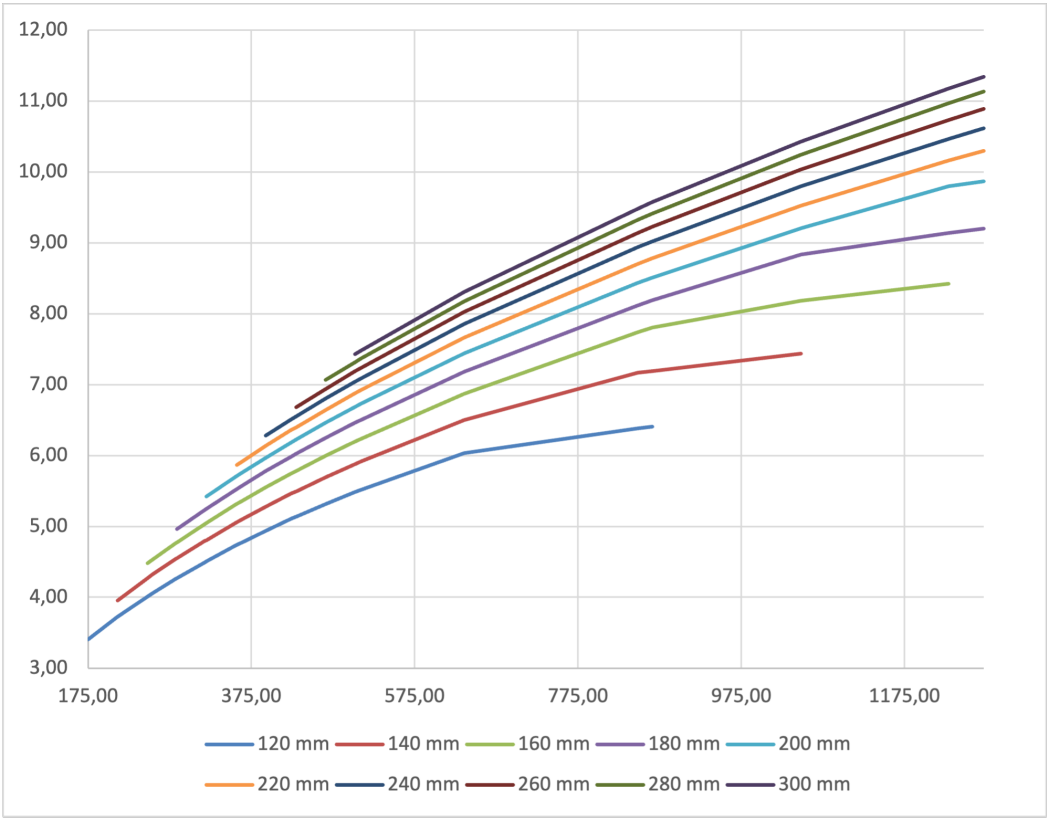

Figure C.3: Maximum allowable span as a function of reinforcement area for slabs with C12/15 concrete, $\phi 9$ reinforcement and the three-span support model. Each line represents a slab thickness between 120 mm and 300 mm.

Table C.3: Maximum allowable span for the slab using C12/15, $\phi 12$ and the three span support model. The columns marked "min" include the minimum reinforcement required for the corresponding slab thickness. The columns marked "max" indicate the largest reinforcement level before over reinforced behaviour for the corresponding slab thickness. Orange cells are governed by bending resistance, while green cells are governed by deflection.

A_s [mm^2/m]	min 120	min 140	min 160	min 180	min 200	min 220	min 240	min 260	$s250$	min 280	min 300	$s225$	$s200$	$s175$	$s150$	max 120	$s125$	max 140	$s100$	max 160	max 180	$s75$
t [mm]	175	211	248	284	320	357	393	430	452	466	502	503	565	646	754	852	905	1034	1131	1215	1397	1508
120	3.38	3.69	3.98	4.23	4.47	4.69	4.90	5.09	5.20	5.27	5.43	5.44	5.70	6.01	6.19	6.32						
140		3.93	4.24	4.52	4.77	5.02	5.24	5.45	5.58	5.65	5.84	5.84	6.14	6.49	6.90	7.11	7.18	7.35				
160			4.45	4.75	5.02	5.28	5.52	5.75	5.88	5.96	6.16	6.17	6.49	6.87	7.33	7.70	7.89	8.10	8.24	8.34		
180				4.94	5.22	5.50	5.75	5.99	6.13	6.22	6.43	6.44	6.78	7.19	7.68	8.09	8.29	8.74	8.94	9.06	9.29	
200					5.40	5.68	5.94	6.20	6.34	6.43	6.66	6.66	7.02	7.46	7.98	8.41	8.63	9.11	9.44	9.71	9.98	10.13
220						5.84	6.11	6.37	6.52	6.62	6.85	6.86	7.23	7.68	8.23	8.68	8.91	9.43	9.78	10.07	10.63	10.78
240							6.25	6.53	6.68	6.78	7.02	7.02	7.41	7.88	8.45	8.92	9.16	9.70	10.07	10.37	10.97	11.30
260								6.66	6.82	6.92	7.16	7.17	7.57	8.05	8.64	9.13	9.38	9.94	10.33	10.64	11.27	11.62
280										7.04	7.29	7.30	7.71	8.21	8.81	9.31	9.57	10.15	10.55	10.88	11.53	11.90
300											7.41	7.42	7.83	8.34	8.96	9.47	9.74	10.33	10.75	11.09	11.77	12.15

Note. Empty cells indicate reinforcement amounts below the minimum reinforcement requirement or over reinforced cross sections excluded from the results.

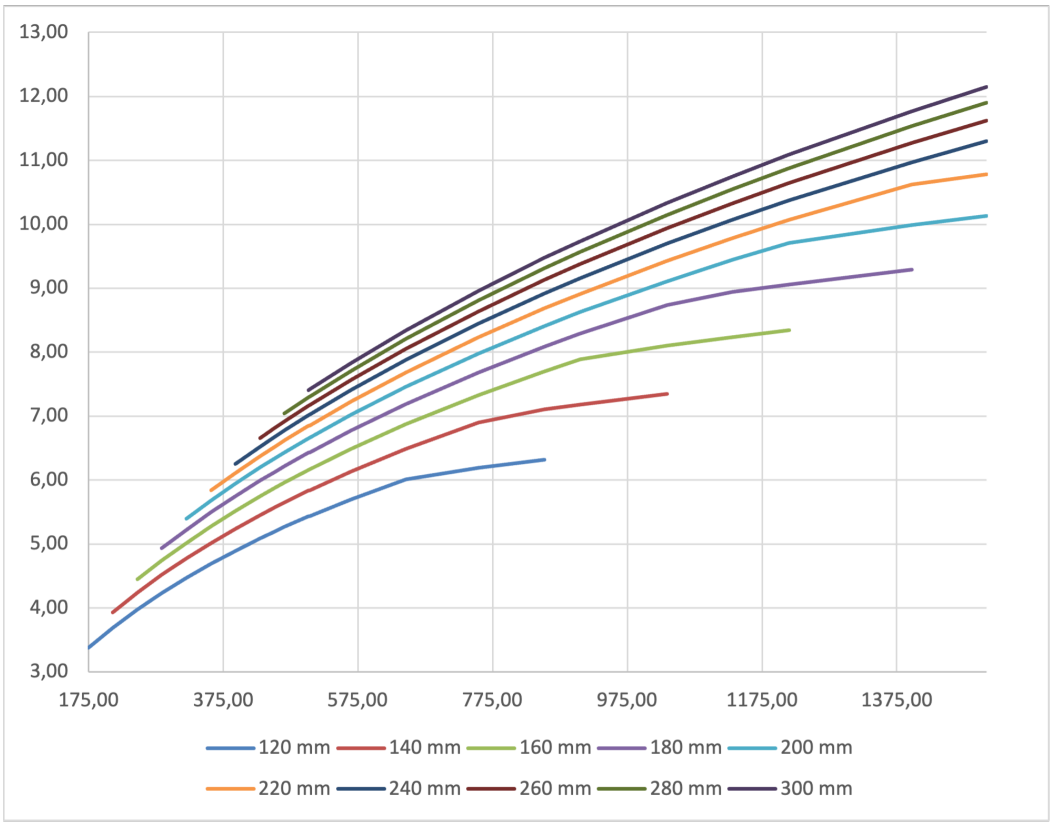

Figure C.4: Maximum allowable span as a function of reinforcement area for slabs with C12/15 concrete, $\phi 12$ reinforcement and the three-span support model. Each line represents a slab thickness between 120 mm and 300 mm.

C20/25 concrete

Table C.4: Maximum allowable span for the slab using C20/25, $\phi 6$ and the three-span support model. The columns marked "min" include the minimum reinforcement required for the corresponding slab thickness. Orange cells are governed by bending resistance, while green cells are governed by deflection.

A_s [mm^2/m]	min 120	s150	min 140	s125	min 160	s100	min 180	min 200	min 220	s75	min 240	min 260	min 280	min 300	s50	s40
t [mm]	175	188	211	226	248	283	284	320	357	377	393	430	466	502	565	707
120	3.47	3.60	3.80	3.93	4.11	4.37	4.38	4.64	4.88	5.01	5.10	5.32	5.52	5.71	6.03	6.57
140			4.03	4.16	4.35	4.64	4.65	4.92	5.18	5.32	5.42	5.65	5.87	6.08	6.42	7.10
160					4.55	4.85	4.86	5.15	5.42	5.57	5.68	5.93	6.15	6.37	6.73	7.47
180							5.04	5.34	5.63	5.78	5.89	6.15	6.39	6.62	7.00	7.77
200								5.50	5.80	5.95	6.07	6.34	6.59	6.83	7.22	8.02
220									5.95	6.11	6.23	6.51	6.76	7.01	7.41	8.24
240											6.37	6.65	6.91	7.16	7.58	8.43
260												6.77	7.04	7.30	7.73	8.60
280													7.16	7.42	7.86	8.75
300														7.53	7.97	8.88

Note. Empty cells indicate reinforcement amounts below the minimum reinforcement requirement for the corresponding slab thickness.

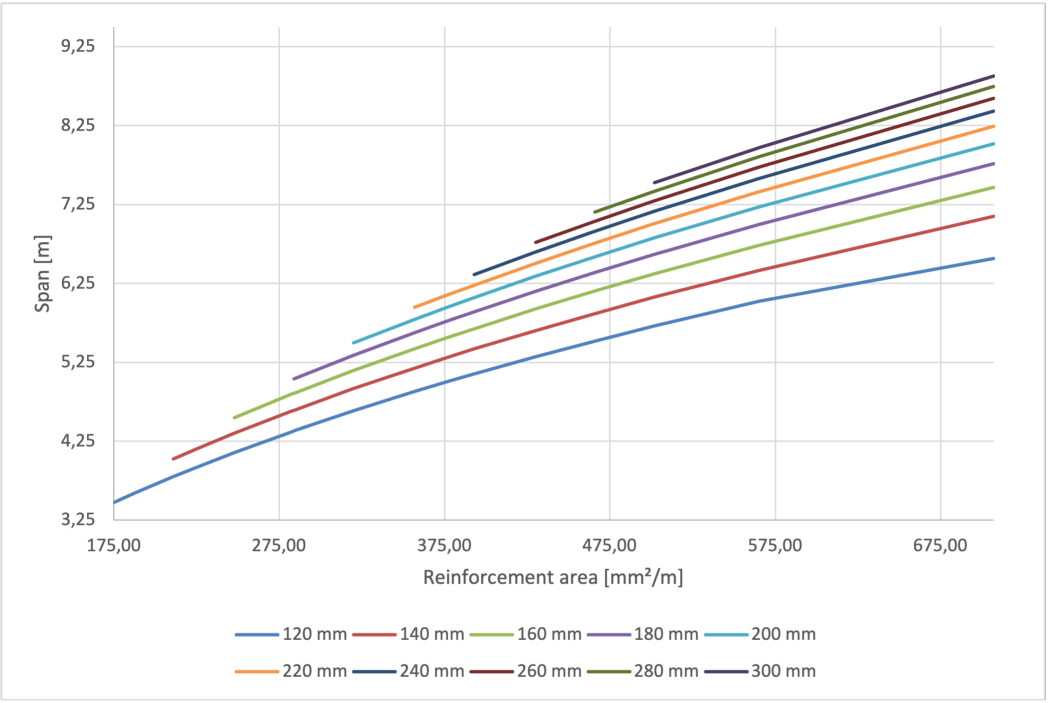

Figure C.5: Maximum allowable span as a function of reinforcement area for slabs with C20/25 concrete, $\phi 6$ reinforcement and the three-span support model. Each line represents a slab thickness between 120 mm and 300 mm.

The corresponding table and diagram for $\phi 9$ are presented in Section 4.1 and are not repeated here.

Table C.5: Maximum allowable span for the slab using C20/25, $\phi 9$ and the three-span support model. The columns marked "min" include the minimum reinforcement required for the corresponding slab thickness. Orange cells are governed by bending resistance, while green cells are governed by deflection.

A_s [mm^2/m]	min 120	min 140	min 160	$s250$	$s225$	min 180	$s200$	min 200	min 220	$s175$	min 240	$s150$	min 260	min 280	min 300	$s125$	$s100$	$s75$	$s50$
t [mm]	175	211	248	254	283	284	318	320	357	364	393	424	430	466	502	509	636	848	1272
120	3.44	3.77	4.07	4.12	4.34	4.35	4.58	4.60	4.84	4.88	5.06	5.24	5.28	5.48	5.66	5.70	6.30	6.70	7.13
140		4.00	4.32	4.37	4.61	4.61	4.87	4.88	5.15	5.19	5.38	5.58	5.62	5.83	6.04	6.07	6.72	7.49	8.01
160			4.53	4.58	4.82	4.83	5.10	5.12	5.39	5.44	5.65	5.85	5.89	6.12	6.34	6.38	7.07	8.05	8.82
180						5.01	5.30	5.31	5.60	5.65	5.86	6.08	6.12	6.36	6.59	6.63	7.36	8.40	9.55
200								5.48	5.77	5.83	6.05	6.27	6.31	6.56	6.80	6.84	7.60	8.69	10.23
220									5.92	5.98	6.21	6.44	6.48	6.74	6.98	7.03	7.81	8.93	10.73
240											6.34	6.58	6.62	6.89	7.14	7.19	7.99	9.15	11.01
260													6.75	7.02	7.28	7.32	8.15	9.34	11.26
280														7.14	7.40	7.45	8.29	9.51	11.47
300															7.51	7.56	8.42	9.65	11.67

Note. Empty cells indicate reinforcement amounts below the minimum reinforcement requirement for the corresponding slab thickness.

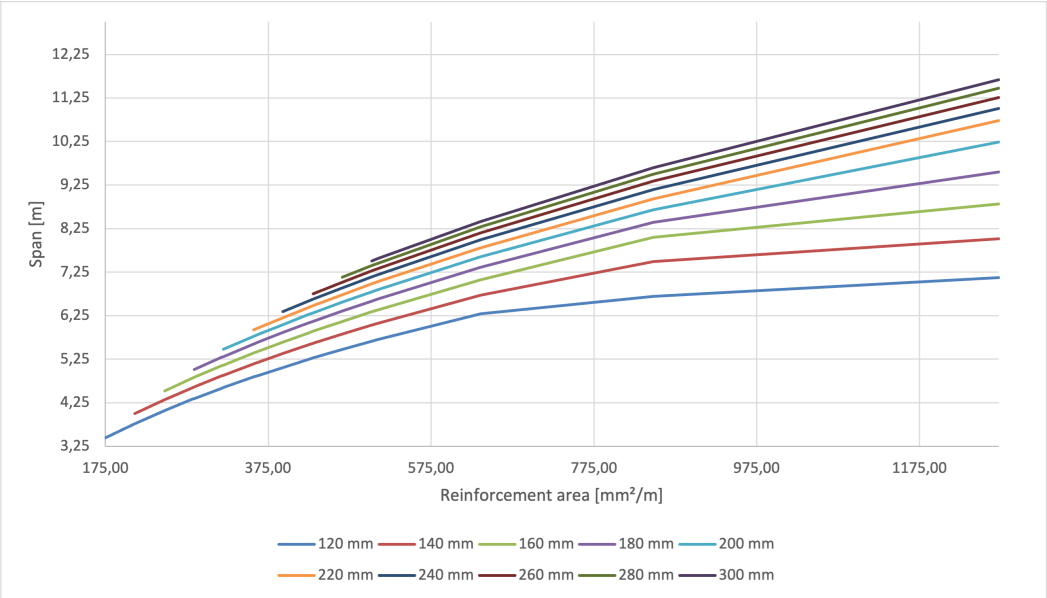

Figure C.6: Maximum allowable span as a function of reinforcement area for slabs with C20/25 concrete, $\phi 9$ reinforcement and the three-span support model. Each line represents a slab thickness between 120 mm and 300 mm.

Table C.6: Maximum allowable span for the slab using C20/25, ϕ12 and the three span support model. The columns marked "min" include the minimum reinforcement required for the corresponding slab thickness. The column marked "max" indicates the largest reinforcement level before over reinforced behaviour for the corresponding slab thickness. Orange cells are governed by bending resistance, while green cells are governed by deflection.

A_s [mm^2/m]	min 120	min 140	min 160	min 180	min 200	min 220	min 240	min 260	$s250$	min 280	min 300	$s225$	$s200$	$s175$	$s150$	$s125$	$s100$	max 120	$s75$
t [mm]	175	211	248	284	320	357	393	430	452	466	502	503	565	646	754	905	1131	1421	1508
120	3.42	3.74	4.04	4.31	4.56	4.80	5.02	5.23	5.35	5.43	5.62	5.62	5.92	6.28	6.52	6.70	6.93	7.17	
140		3.97	4.29	4.58	4.85	5.11	5.35	5.58	5.71	5.79	5.99	6.00	6.33	6.72	7.20	7.52	7.80	8.09	8.17
160			4.50	4.80	5.09	5.36	5.61	5.86	6.00	6.08	6.30	6.30	6.66	7.08	7.59	8.23	8.58	8.92	9.01
180				4.99	5.29	5.57	5.83	6.09	6.24	6.33	6.55	6.56	6.93	7.37	7.92	8.60	9.30	9.68	9.79
200					5.45	5.75	6.02	6.29	6.44	6.53	6.77	6.77	7.16	7.62	8.19	8.91	9.84	10.39	10.50
220						5.90	6.18	6.45	6.61	6.71	6.95	6.96	7.35	7.84	8.43	9.17	10.14	11.04	11.17
240							6.32	6.60	6.76	6.86	7.11	7.12	7.53	8.02	8.63	9.40	10.41	11.52	11.79
260								6.73	6.89	7.00	7.25	7.26	7.68	8.18	8.81	9.59	10.63	11.79	12.10
280										7.11	7.38	7.38	7.81	8.33	8.96	9.77	10.84	12.03	12.35
300											7.49	7.49	7.93	8.45	9.10	9.93	11.02	12.23	12.57

Note. Empty cells indicate reinforcement amounts below the minimum reinforcement requirement or over reinforced cross sections excluded from the results.

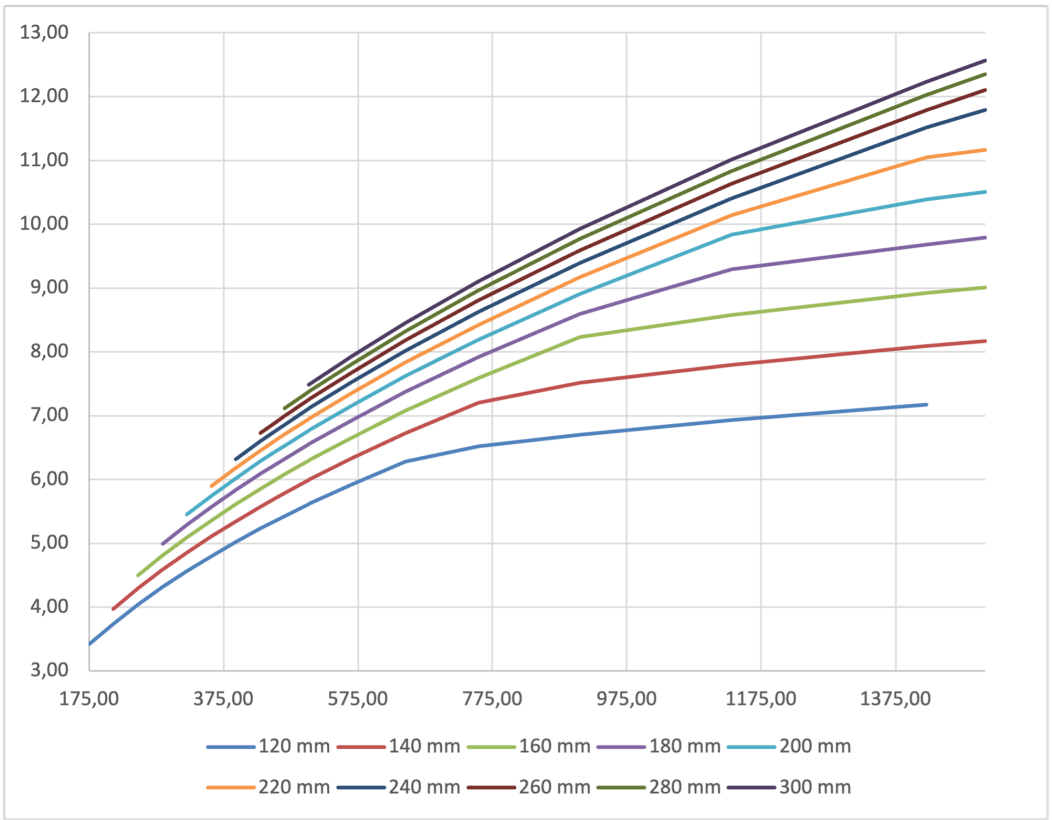

Figure C.7: Maximum allowable span as a function of reinforcement area for slabs with C20/25 concrete, ϕ12 reinforcement and the three-span support model. Each line represents a slab thickness between 120 mm and 300 mm.

C40/50 concrete

Table C.7: Maximum allowable span for the slab using C40/50, $\phi 6$ and the three-span support model. The columns marked "min" include the minimum reinforcement required for the corresponding slab thickness. Orange cells are governed by bending resistance.

A_s [mm^2/m]	min 120	s150	min 140	s125	min 160	s100	min 180	min 200	min 220	s75	min 240	min 260	min 280	min 300	s50	s40
t [mm]	175	188	211	226	248	283	284	320	357	377	393	430	466	502	565	707
120	3.50	3.62	3.84	3.97	4.15	4.43	4.44	4.70	4.96	5.09	5.19	5.42	5.64	5.84	6.18	6.87
140			4.06	4.19	4.39	4.68	4.69	4.97	5.25	5.39	5.50	5.74	5.97	6.19	6.55	7.29
160					4.59	4.89	4.90	5.20	5.48	5.63	5.75	6.01	6.24	6.47	6.86	7.63
180							5.08	5.38	5.68	5.83	5.95	6.22	6.47	6.71	7.11	7.92
200								5.54	5.85	6.01	6.13	6.41	6.66	6.91	7.32	8.16
220									5.99	6.15	6.28	6.57	6.83	7.08	7.50	8.37
240											6.41	6.70	6.97	7.23	7.66	8.55
260												6.82	7.10	7.36	7.80	8.71
280													7.21	7.48	7.93	8.85
300														7.59	8.04	8.97

Note. Empty cells indicate reinforcement amounts below the minimum reinforcement requirement for the corresponding slab thickness.

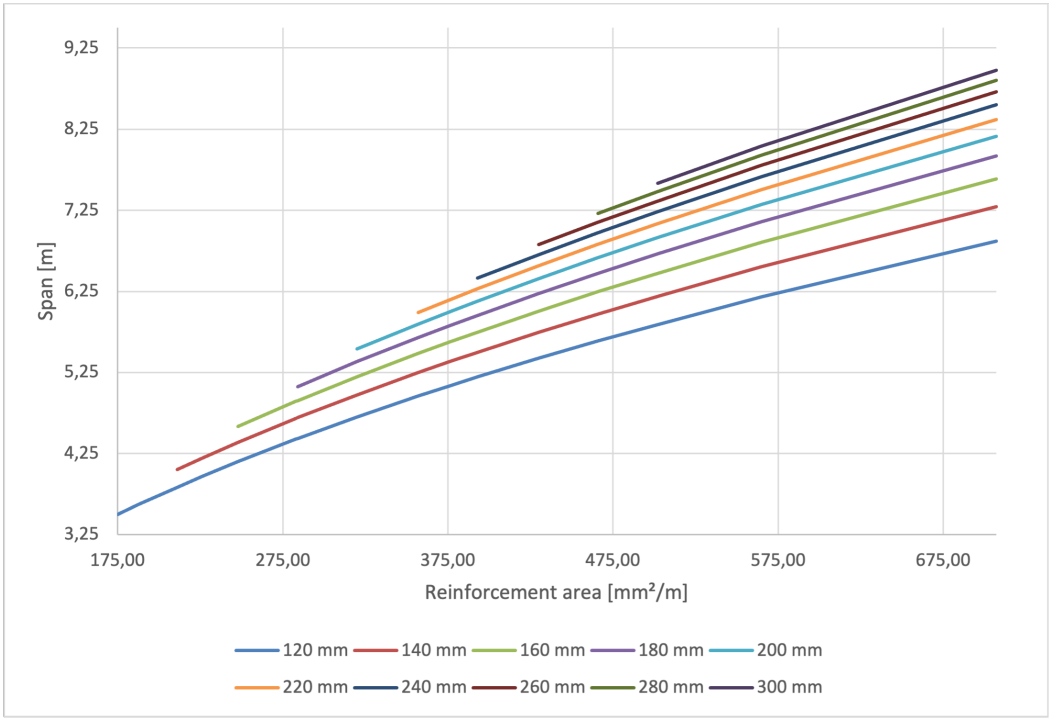

Figure C.8: Maximum allowable span as a function of reinforcement area for slabs with C40/50 concrete, $\phi 6$ reinforcement and the three-span support model. Each line represents a slab thickness between 120 mm and 300 mm.

Table C.8: Maximum allowable span for the slab using C40/50, $\phi 9$ and the three-span support model. The columns marked "min" include the minimum reinforcement required for the corresponding slab thickness. Orange cells are governed by bending resistance, while green cells are governed by deflection.

A_s [mm^2/m]	min 120	min 140	min 160	$s250$	$s225$	min 180	$s200$	min 200	min 220	$s175$	min 240	$s150$	min 260	min 280	min 300	$s125$	$s100$	$s75$	$s50$
t [mm]	175	211	248	254	283	284	318	320	357	364	393	424	430	466	502	509	636	848	1272
120	3.47	3.81	4.12	4.17	4.39	4.40	4.65	4.66	4.92	4.97	5.15	5.34	5.38	5.59	5.80	5.83	6.48	7.41	7.82
140		4.03	4.36	4.41	4.65	4.66	4.93	4.94	5.21	5.26	5.46	5.67	5.71	5.93	6.15	6.19	6.89	7.89	8.74
160			4.56	4.61	4.87	4.87	5.15	5.17	5.45	5.51	5.72	5.93	5.97	6.21	6.44	6.48	7.22	8.28	9.58
180						5.05	5.34	5.36	5.65	5.71	5.93	6.15	6.19	6.44	6.68	6.72	7.49	8.60	10.35
200								5.52	5.82	5.88	6.10	6.34	6.38	6.64	6.88	6.93	7.72	8.87	10.75
220									5.97	6.03	6.26	6.50	6.54	6.80	7.06	7.10	7.92	9.10	11.05
240											6.39	6.63	6.68	6.95	7.21	7.26	8.09	9.31	11.30
260													6.80	7.08	7.34	7.39	8.24	9.48	11.53
280														7.19	7.46	7.51	8.38	9.64	11.72
300															7.56	7.62	8.50	9.78	11.90

Note. Empty cells indicate reinforcement amounts below the minimum reinforcement requirement for the corresponding slab thickness.

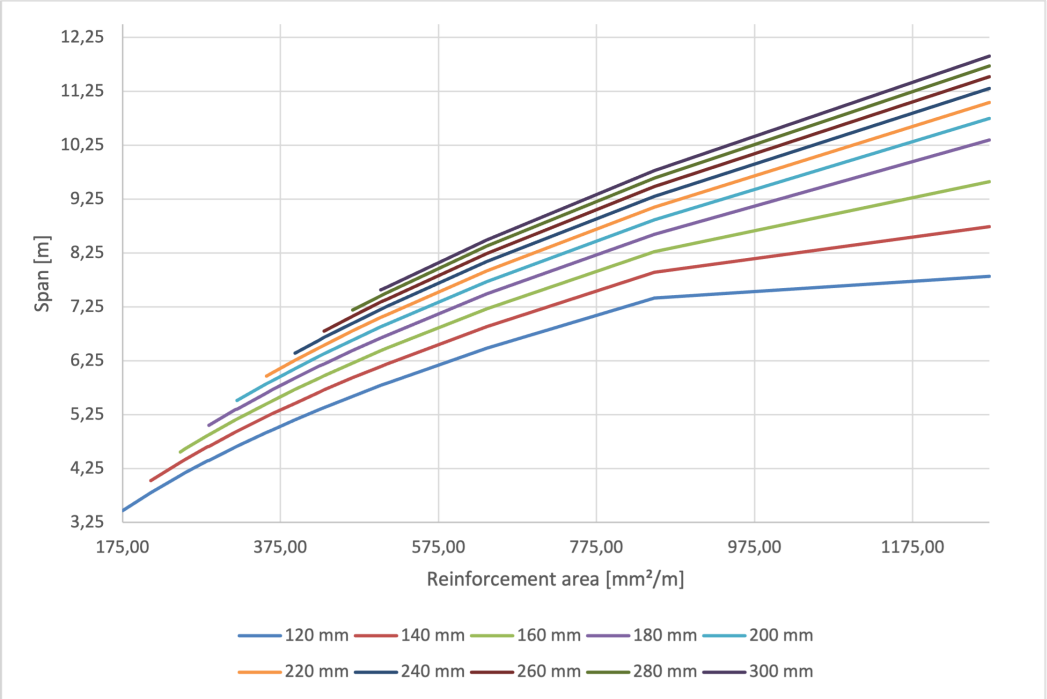

Figure C.9: Maximum allowable span as a function of reinforcement area for slabs with C40/50 concrete, $\phi 9$ reinforcement and the three-span support model. Each line represents a slab thickness between 120 mm and 300 mm.

Table C.9: Maximum allowable span for the slab using C40/50, ϕ12 and the three-span support model. The columns marked "min" include the minimum reinforcement required for the corresponding slab thickness. Orange cells are governed by bending resistance, while green cells are governed by deflection.

A_s [mm^2/m]	min 120	min 140	min 160	min 180	min 200	min 220	min 240	min 260	$s250$	min 280	min 300	$s225$	$s200$	$s175$	$s150$	$s125$	$s100$	$s75$
t [mm]	175	211	248	284	320	357	393	430	452	466	502	503	565	646	754	905	1131	1508
120	3.44	3.78	4.09	4.37	4.63	4.88	5.11	5.34	5.47	5.55	5.75	5.75	6.08	6.48	6.96	7.42	7.64	7.93
140		4.00	4.33	4.63	4.91	5.18	5.43	5.67	5.81	5.89	6.11	6.11	6.46	6.89	7.42	8.08	8.54	8.90
160			4.53	4.85	5.14	5.42	5.68	5.94	6.08	6.17	6.40	6.41	6.78	7.23	7.78	8.48	9.36	9.77
180				5.03	5.33	5.63	5.90	6.16	6.31	6.41	6.64	6.65	7.04	7.51	8.09	8.82	9.80	10.58
200					5.49	5.80	6.08	6.35	6.51	6.61	6.85	6.86	7.26	7.74	8.35	9.11	10.13	11.32
220						5.95	6.23	6.51	6.68	6.78	7.03	7.04	7.45	7.95	8.57	9.35	10.41	11.92
240							6.37	6.66	6.82	6.92	7.18	7.19	7.61	8.12	8.76	9.57	10.65	12.20
260								6.78	6.95	7.05	7.32	7.32	7.75	8.28	8.93	9.75	10.86	12.45
280										7.17	7.44	7.44	7.88	8.42	9.08	9.92	11.05	12.68
300											7.54	7.55	8.00	8.54	9.21	10.07	11.21	12.87

Note. Empty cells indicate reinforcement amounts below the minimum reinforcement requirement for the corresponding slab thickness.

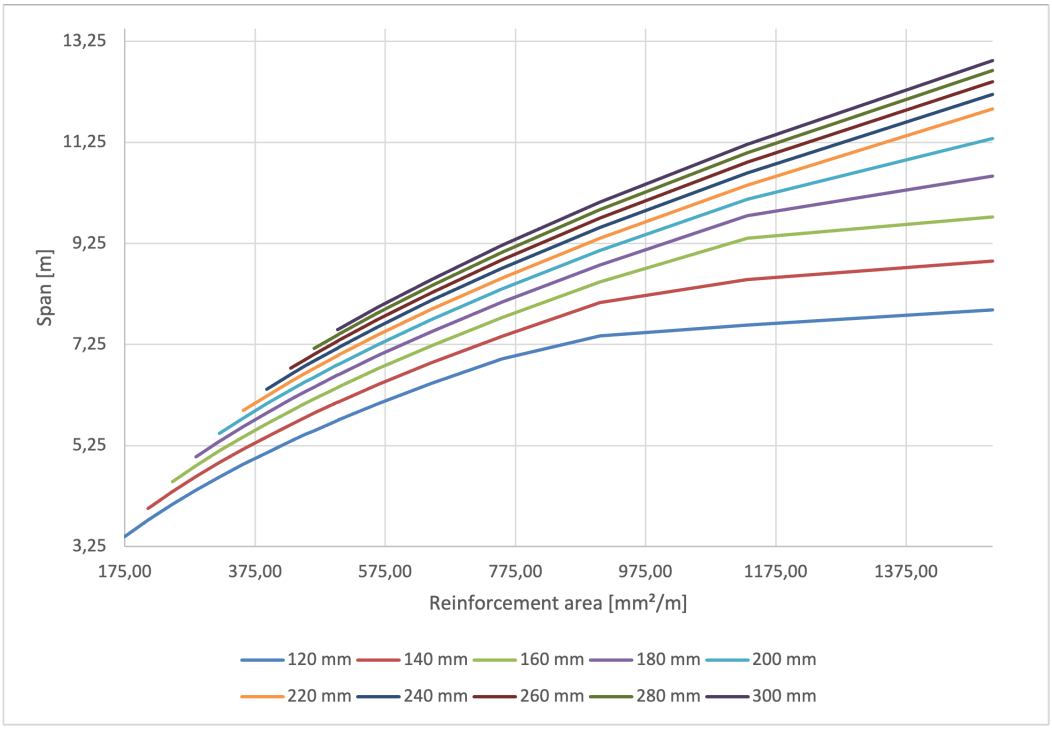

Figure C.10: Maximum allowable span as a function of reinforcement area for slabs with C40/50 concrete, ϕ12 reinforcement and the three-span support model. Each line represents a slab thickness between 120 mm and 300 mm.

C.1.2 Two-span slab model

The two span slab model used in the parameter study is shown schematically in Figure C.11. The model represents a one metre wide slab strip with one simply supported end and one restrained end. Top reinforcement was considered at the restrained support, while bottom reinforcement was considered in the span region. The figure is schematic and is only intended to clarify the support condition and the reinforcement side used in the sectional checks.

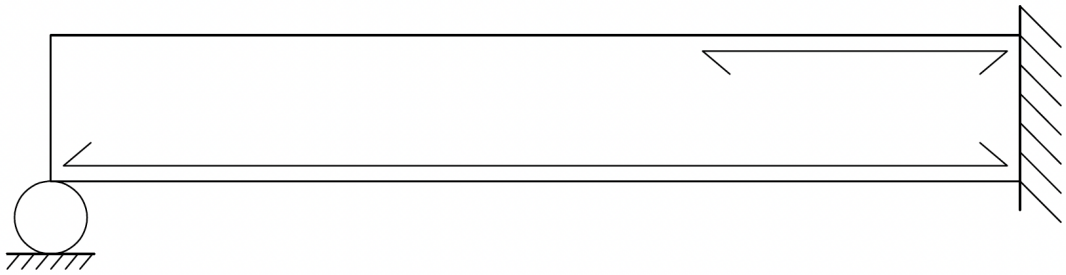

Figure C.11: Schematic illustration of the two span slab model used in the slab parameter study, showing the assumed support condition and the reinforcement considered in the support and field sections.

C12/15 concrete

Table C.10: Maximum allowable span for the slab using C12/15, $\phi 6$ and the two-span support model. The columns marked "min" include the minimum reinforcement required for the corresponding slab thickness. Orange cells are governed by bending resistance, while green cells are governed by deflection.

A_s [mm^2/m]	min 120	s150	min 140	s125	min 160	s100	min 180	min 200	min 220	s75	min 240	min 260	min 280	min 300	s50	s40
t [mm]	175	188	211	226	248	283	284	320	357	377	393	430	466	502	565	707
120	2.81	2.90	3.07	3.17	3.30	3.51	3.52	3.71	3.90	3.99	4.07	4.23	4.38	4.52	4.71	4.90
140			3.25	3.36	3.51	3.73	3.74	3.95	4.16	4.26	4.34	4.52	4.68	4.84	5.09	5.48
160					3.68	3.91	3.92	4.15	4.36	4.47	4.56	4.75	4.93	5.09	5.37	5.91
180							4.07	4.31	4.54	4.65	4.74	4.94	5.13	5.31	5.59	6.17
200								4.44	4.68	4.80	4.90	5.11	5.30	5.48	5.79	6.40
220									4.81	4.93	5.03	5.25	5.45	5.64	5.95	6.59
240											5.14	5.37	5.57	5.77	6.10	6.76
260												5.47	5.69	5.89	6.22	6.90
280													5.78	5.99	6.33	7.03
300														6.08	6.43	7.14

Note. Empty cells indicate reinforcement amounts below the minimum reinforcement requirement for the corresponding slab thickness.

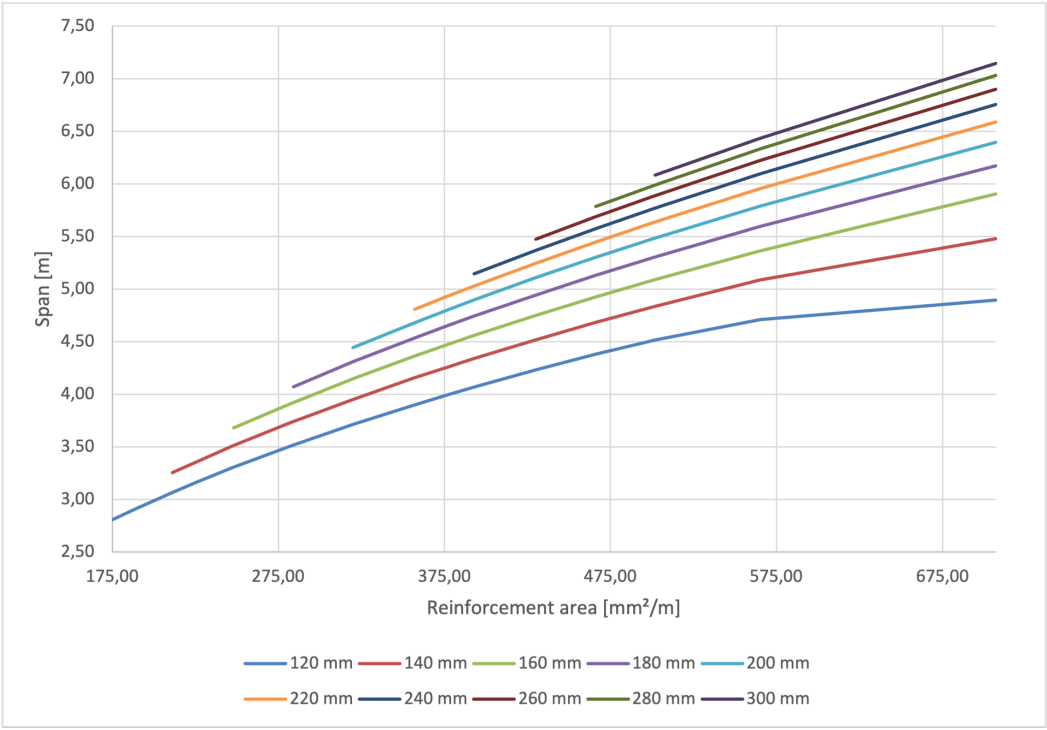

Figure C.12: Maximum allowable span as a function of reinforcement area for slabs with C12/15 concrete, $\phi 6$ reinforcement and the two-span support model. Each line represents a slab thickness between 120 mm and 300 mm.

Table C.11: Maximum allowable span for the slab using C12/15, $\phi 9$ and the two span support model. The columns marked "min" include the minimum reinforcement required for the corresponding slab thickness. The columns marked "max" indicate the largest reinforcement level before over reinforced behaviour for the corresponding slab thickness. Orange cells are governed by bending resistance, while green cells are governed by deflection.

A_s [mm^2/m]	min 120	min 140	min 160	s250	s225	min 180	s200	min 200	min 220	s175	min 240	s150	min 260	min 280	min 300	s125	s100	s75	max 120	max 140	max 160	s50
t [mm]	175	211	248	254	283	284	318	320	357	364	393	424	430	466	502	509	636	848	866	1048	1229	1272
120	2.78	3.04	3.28	3.31	3.48	3.49	3.67	3.68	3.87	3.90	4.03	4.17	4.19	4.34	4.48	4.50	4.76	5.00	5.02			
140		3.23	3.49	3.53	3.71	3.71	3.91	3.92	4.13	4.16	4.31	4.46	4.49	4.65	4.80	4.83	5.31	5.61	5.63	5.83		
160			3.66	3.70	3.89	3.90	4.11	4.12	4.34	4.38	4.53	4.69	4.72	4.90	5.06	5.09	5.61	6.17	6.19	6.41	6.60	
180						4.05	4.27	4.29	4.51	4.55	4.72	4.89	4.92	5.10	5.28	5.31	5.86	6.63	6.69	6.95	7.16	7.21
200								4.43	4.66	4.70	4.87	5.05	5.08	5.28	5.46	5.49	6.08	6.89	6.95	7.44	7.68	7.73
220									4.79	4.83	5.01	5.19	5.23	5.42	5.62	5.65	6.26	7.11	7.17	7.78	8.16	8.22
240											5.13	5.31	5.35	5.55	5.75	5.79	6.41	7.30	7.37	8.00	8.55	8.67
260													5.46	5.67	5.87	5.91	6.55	7.46	7.53	8.19	8.76	8.89
280														5.77	5.97	6.01	6.67	7.61	7.68	8.36	8.96	9.09
300															6.07	6.11	6.78	7.74	7.82	8.51	9.13	9.26

Note. Empty cells indicate reinforcement amounts below the minimum reinforcement requirement or over reinforced cross sections excluded from the results.

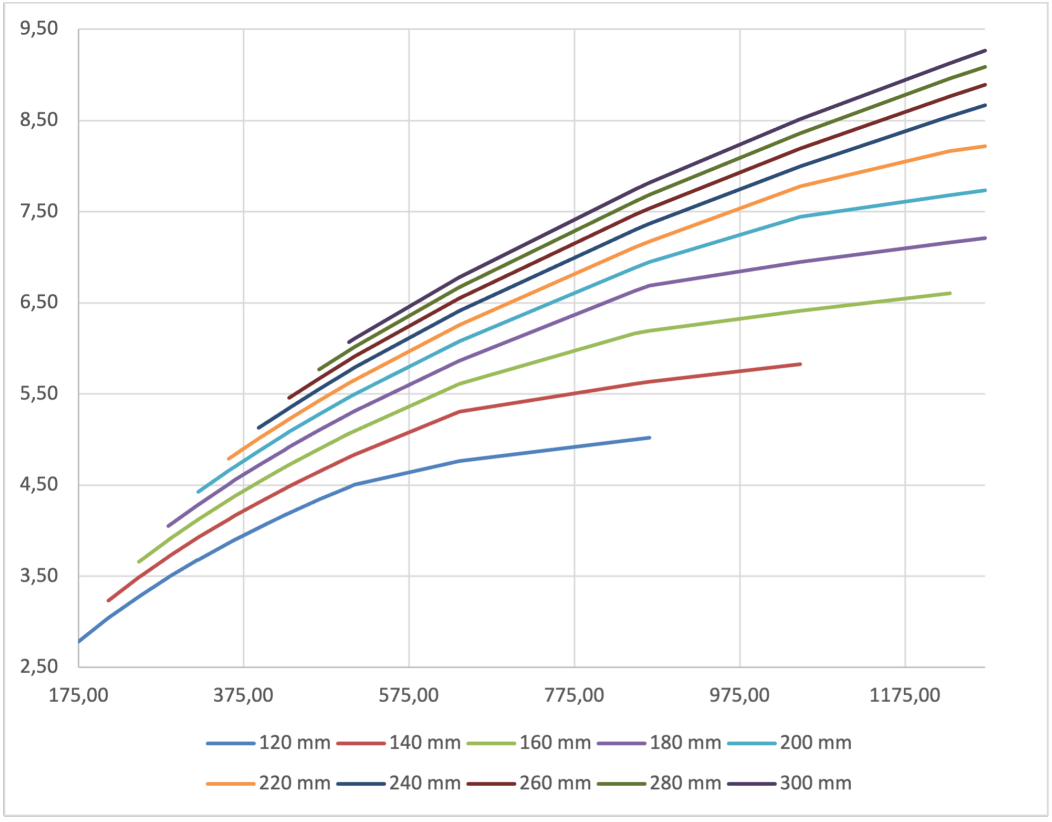

Figure C.13: Maximum allowable span as a function of reinforcement area for slabs with C12/15 concrete, $\phi 9$ reinforcement and the two-span support model. Each line represents a slab thickness between 120 mm and 300 mm.

Table C.12: Maximum allowable span for the slab using C12/15, $\phi 12$ and the two span support model. The columns marked "min" include the minimum reinforcement required for the corresponding slab thickness. The columns marked "max" indicate the largest reinforcement level before over reinforced behaviour for the corresponding slab thickness. Orange cells are governed by bending resistance, while green cells are governed by deflection.

A_s [mm^2/m]	min 120	min 140	min 160	min 180	min 200	min 220	min 240	min 260	$s250$	min 280	min 300	$s225$	$s200$	$s175$	$s150$	max 120	$s125$	max 140	$s100$	max 160	max 180	$s75$
t [mm]	175	211	248	284	320	357	393	430	452	466	502	503	565	646	754	852	905	1034	1131	1215	1397	1508
120	2.76	3.01	3.25	3.46	3.65	3.83	4.00	4.16	4.25	4.30	4.44	4.44	4.62	4.73	4.85	4.95						
140		3.21	3.46	3.69	3.90	4.10	4.28	4.45	4.55	4.61	4.77	4.77	5.01	5.30	5.45	5.57	5.63	5.76				
160			3.64	3.88	4.10	4.31	4.51	4.69	4.80	4.87	5.03	5.03	5.30	5.61	5.99	6.13	6.19	6.35	6.45	6.54		
180				4.03	4.26	4.49	4.69	4.89	5.01	5.08	5.25	5.25	5.54	5.87	6.27	6.60	6.71	6.89	7.00	7.10	7.28	
200					4.41	4.64	4.85	5.06	5.18	5.25	5.43	5.44	5.73	6.09	6.52	6.87	7.04	7.38	7.51	7.62	7.82	7.94
220						4.77	4.99	5.20	5.33	5.40	5.59	5.60	5.90	6.27	6.72	7.09	7.28	7.70	7.98	8.10	8.33	8.45
240							5.11	5.33	5.45	5.53	5.73	5.73	6.05	6.44	6.90	7.28	7.48	7.92	8.22	8.47	8.80	8.93
260								5.44	5.57	5.65	5.85	5.85	6.18	6.58	7.06	7.45	7.66	8.11	8.43	8.69	9.20	9.38
280										5.75	5.96	5.96	6.30	6.70	7.19	7.60	7.81	8.29	8.61	8.88	9.42	9.72
300											6.05	6.05	6.40	6.81	7.32	7.74	7.95	8.44	8.78	9.05	9.61	9.92

Note. Empty cells indicate reinforcement amounts below the minimum reinforcement requirement or over reinforced cross sections excluded from the results.

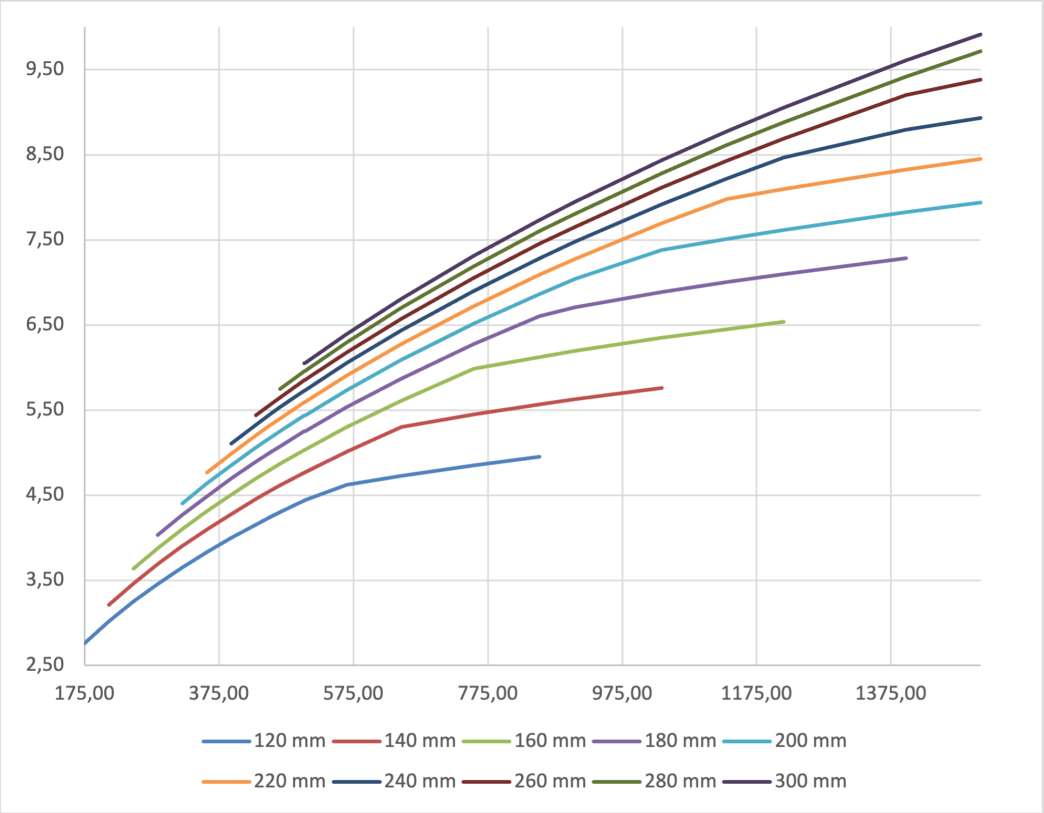

Figure C.14: Maximum allowable span as a function of reinforcement area for slabs with C12/15 concrete, $\phi 12$ reinforcement and the two-span support model. Each line represents a slab thickness between 120 mm and 300 mm.

C20/25 concrete

Table C.13: Maximum allowable span for the slab using C20/25, $\phi 6$ and the two-span support model. The columns marked "min" include the minimum reinforcement required for the corresponding slab thickness. Orange cells are governed by bending resistance, while green cells are governed by deflection.

A_s [mm^2/m]	min 120	$s150$	min 140	$s125$	min 160	$s100$	min 180	min 200	min 220	$s75$	min 240	min 260	min 280	min 300	$s50$	$s40$
t [mm]	175	188	211	226	248	283	284	320	357	377	393	430	466	502	565	707
120	2.84	2.94	3.10	3.21	3.35	3.57	3.58	3.79	3.99	4.09	4.17	4.35	4.51	4.66	4.92	5.14
140			3.29	3.40	3.55	3.79	3.79	4.02	4.23	4.34	4.43	4.62	4.79	4.96	5.24	5.73
160					3.72	3.96	3.97	4.20	4.43	4.55	4.64	4.84	5.03	5.20	5.50	6.10
180							4.11	4.36	4.59	4.72	4.81	5.02	5.22	5.41	5.71	6.34
200								4.49	4.73	4.86	4.96	5.18	5.38	5.58	5.90	6.55
220									4.86	4.99	5.09	5.31	5.52	5.72	6.05	6.73
240											5.20	5.43	5.64	5.85	6.19	6.89
260												5.53	5.75	5.96	6.31	7.02
280													5.84	6.06	6.41	7.14
300														6.15	6.51	7.25

Note. Empty cells indicate reinforcement amounts below the minimum reinforcement requirement for the corresponding slab thickness.

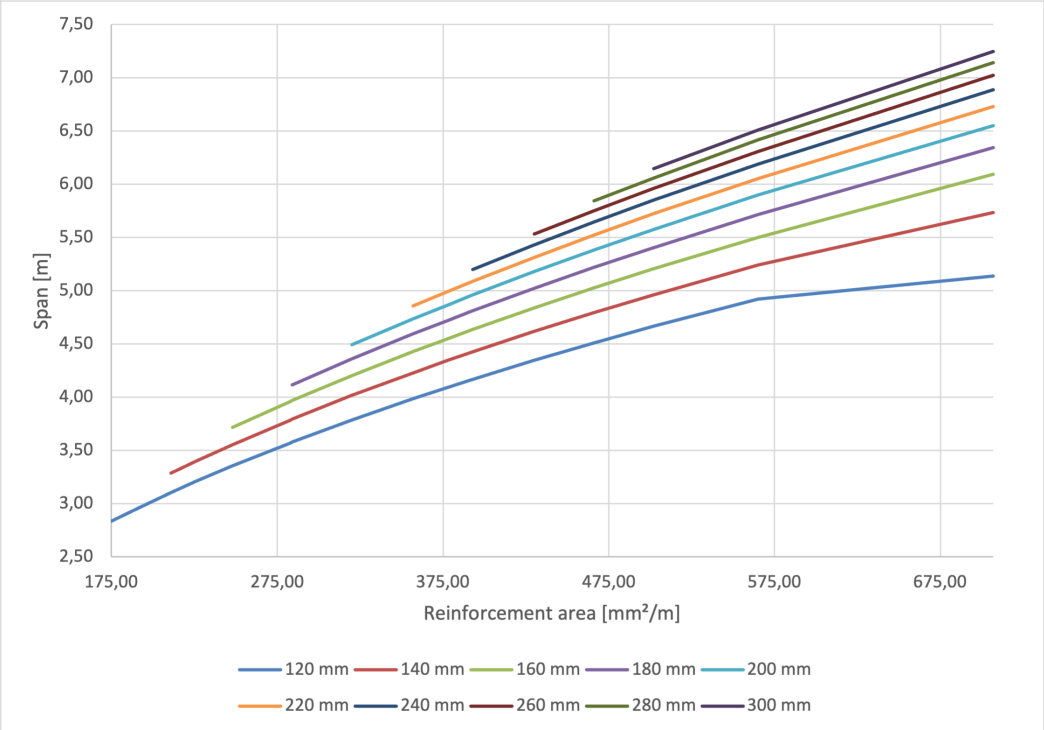

Figure C.15: Maximum allowable span as a function of reinforcement area for slabs with C20/25 concrete, $\phi 6$ reinforcement and the two-span support model. Each line represents a slab thickness between 120 mm and 300 mm.

Table C.14: Maximum allowable span for the slab using C20/25, $\phi 9$ and the two-span support model. The columns marked "min" include the minimum reinforcement required for the corresponding slab thickness. Orange cells are governed by bending resistance, while green cells are governed by deflection.

A_s [mm^2/m]	min 120	min 140	min 160	$s250$	$s225$	min 180	$s200$	min 200	min 220	$s175$	min 240	$s150$	min 260	min 280	min 300	$s125$	$s100$	$s75$	$s50$
t [mm]	175	211	248	254	283	284	318	320	357	364	393	424	430	466	502	509	636	848	1272
120	2.81	3.08	3.33	3.36	3.54	3.55	3.74	3.75	3.95	3.99	4.13	4.28	4.31	4.47	4.62	4.65	5.01	5.24	5.58
140		3.26	3.53	3.57	3.76	3.77	3.98	3.99	4.20	4.24	4.40	4.56	4.59	4.76	4.93	4.96	5.49	5.87	6.28
160			3.70	3.74	3.94	3.95	4.17	4.18	4.40	4.44	4.61	4.78	4.81	5.00	5.17	5.21	5.77	6.43	6.91
180						4.09	4.32	4.34	4.57	4.61	4.79	4.96	5.00	5.19	5.38	5.41	6.01	6.85	7.48
200								4.47	4.71	4.76	4.94	5.12	5.16	5.36	5.55	5.59	6.21	7.09	8.02
220									4.84	4.88	5.07	5.26	5.29	5.50	5.70	5.74	6.38	7.29	8.51
240											5.18	5.37	5.41	5.62	5.83	5.87	6.53	7.47	8.98
260													5.51	5.73	5.94	5.98	6.65	7.62	9.19
280														5.83	6.04	6.08	6.77	7.76	9.37
300															6.13	6.17	6.87	7.88	9.53

Note. Empty cells indicate reinforcement amounts below the minimum reinforcement requirement for the corresponding slab thickness.

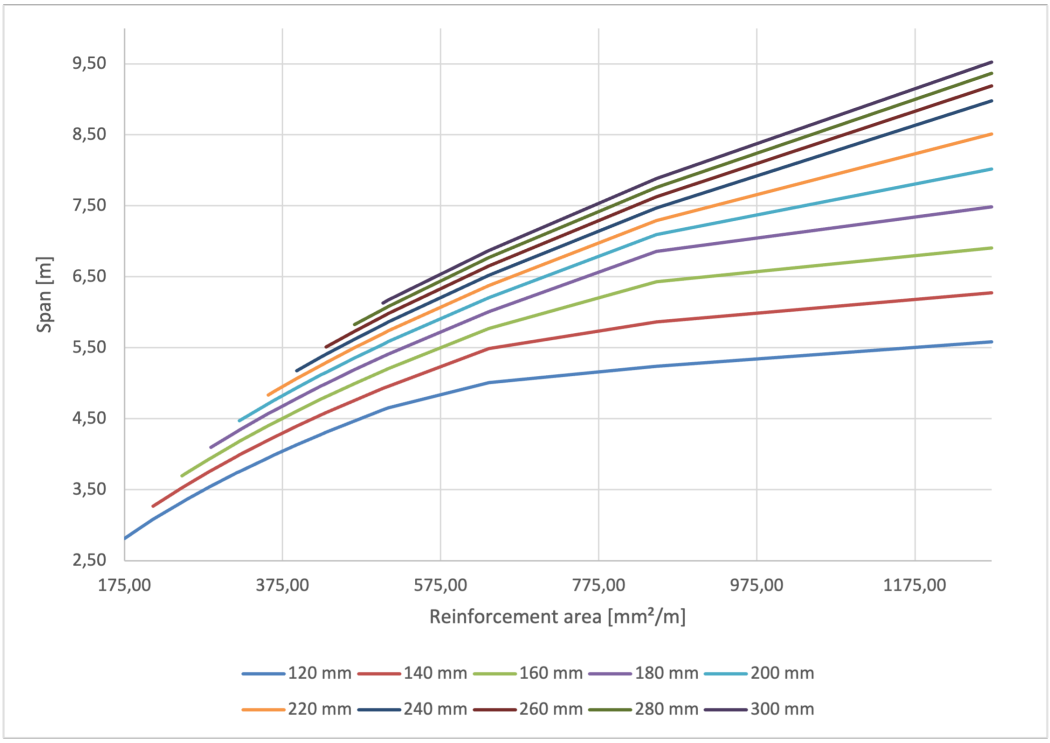

Figure C.16: Maximum allowable span as a function of reinforcement area for slabs with C20/25 concrete, $\phi 9$ reinforcement and the two-span support model. Each line represents a slab thickness between 120 mm and 300 mm.

Table C.15: Maximum allowable span for the slab using C20/25, ϕ12 and the two span support model. The columns marked "min" include the minimum reinforcement required for the corresponding slab thickness. The column marked "max" indicates the largest reinforcement level before over reinforced behaviour for the corresponding slab thickness. Orange cells are governed by bending resistance, while green cells are governed by deflection.

A_s [mm^2/m]	min 120	min 140	min 160	min 180	min 200	min 220	min 240	min 260	$s250$	min 280	min 300	$s225$	$s200$	$s175$	$s150$	$s125$	$s100$	max 120	$s75$
t [mm]	175	211	248	284	320	357	393	430	452	466	502	503	565	646	754	905	1131	1421	1508
120	2.79	3.05	3.30	3.52	3.72	3.92	4.10	4.27	4.37	4.43	4.58	4.59	4.83	4.98	5.10	5.25	5.43	5.62	
140		3.24	3.51	3.74	3.96	4.17	4.37	4.55	4.66	4.73	4.89	4.90	5.17	5.49	5.71	5.88	6.11	6.34	6.40
160			3.67	3.92	4.15	4.38	4.58	4.78	4.90	4.97	5.14	5.15	5.43	5.78	6.20	6.46	6.72	6.99	7.06
180				4.07	4.32	4.55	4.76	4.97	5.09	5.17	5.35	5.36	5.66	6.02	6.46	6.99	7.28	7.59	7.67
200					4.45	4.69	4.92	5.13	5.26	5.33	5.53	5.53	5.84	6.22	6.69	7.27	7.80	8.14	8.23
220						4.82	5.05	5.27	5.40	5.48	5.68	5.68	6.01	6.40	6.88	7.49	8.28	8.65	8.75
240							5.16	5.39	5.52	5.60	5.81	5.81	6.14	6.55	7.05	7.67	8.50	9.13	9.24
260								5.49	5.63	5.71	5.92	5.93	6.27	6.68	7.19	7.83	8.68	9.58	9.70
280										5.81	6.02	6.03	6.38	6.80	7.32	7.98	8.85	9.82	10.08
300											6.11	6.12	6.47	6.90	7.43	8.10	9.00	9.99	10.26

Note. Empty cells indicate reinforcement amounts below the minimum reinforcement requirement or over reinforced cross sections excluded from the results.

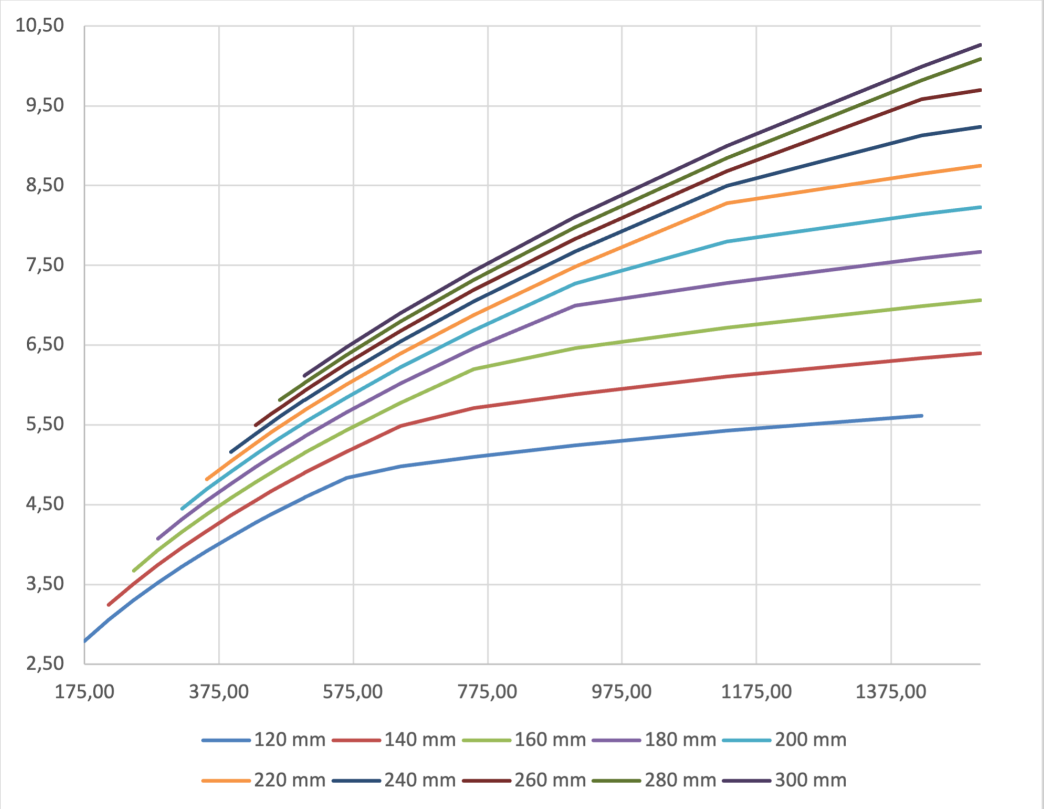

Figure C.17: Maximum allowable span as a function of reinforcement area for slabs with C20/25 concrete, ϕ12 reinforcement and the two-span support model. Each line represents a slab thickness between 120 mm and 300 mm.

C40/50 concrete

Table C.16: Maximum allowable span for the slab using C40/50, $\phi 6$ and the two-span support model. The columns marked "min" include the minimum reinforcement required for the corresponding slab thickness. Orange cells are governed by bending resistance.

A_s [mm^2/m]	min 120	s150	min 140	s125	min 160	s100	min 180	min 200	min 220	s75	min 240	min 260	min 280	min 300	s50	s40
t [mm]	175	188	211	226	248	283	284	320	357	377	393	430	466	502	565	707
120	2.86	2.96	3.13	3.24	3.39	3.62	3.62	3.84	4.05	4.16	4.24	4.43	4.60	4.77	5.05	5.61
140			3.31	3.43	3.59	3.83	3.83	4.06	4.28	4.40	4.49	4.69	4.88	5.05	5.35	5.95
160					3.74	4.00	4.00	4.24	4.48	4.60	4.69	4.90	5.10	5.29	5.60	6.23
180							4.15	4.40	4.64	4.76	4.86	5.08	5.28	5.48	5.80	6.47
200								4.52	4.77	4.90	5.01	5.23	5.44	5.64	5.98	6.66
220									4.89	5.03	5.13	5.36	5.58	5.78	6.13	6.83
240											5.24	5.47	5.69	5.91	6.26	6.98
260												5.57	5.80	6.01	6.37	7.11
280													5.89	6.11	6.47	7.23
300														6.19	6.56	7.33

Note. Empty cells indicate reinforcement amounts below the minimum reinforcement requirement for the corresponding slab thickness.

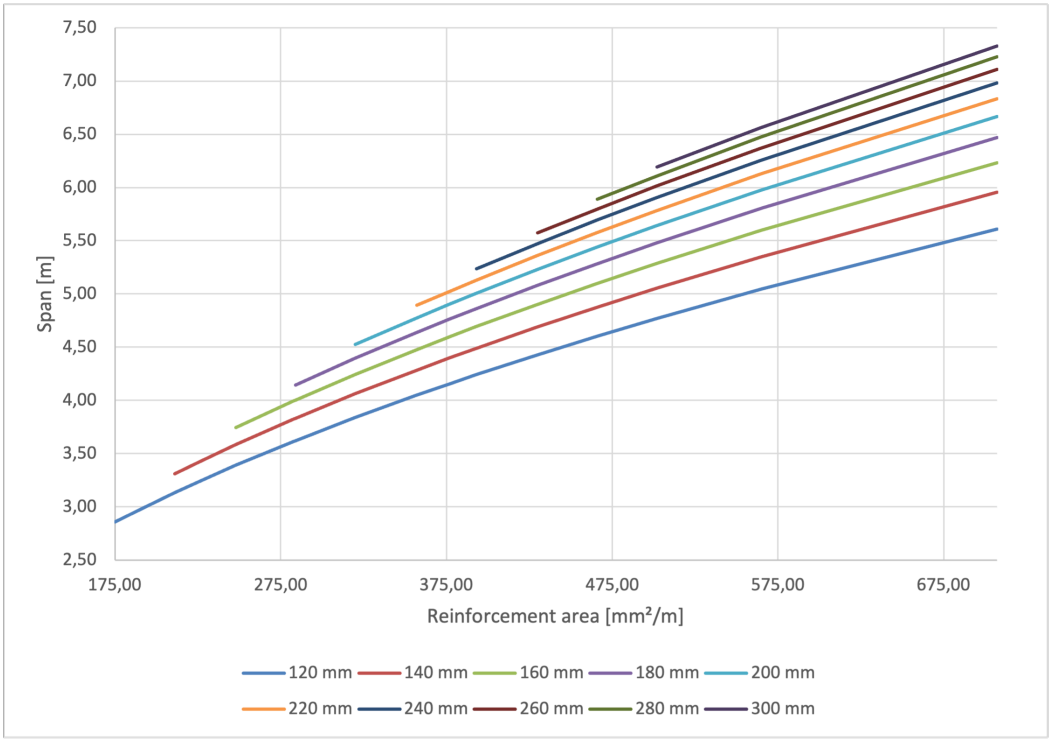

Figure C.18: Maximum allowable span as a function of reinforcement area for slabs with C40/50 concrete, $\phi 6$ reinforcement and the two-span support model. Each line represents a slab thickness between 120 mm and 300 mm.

Table C.17: Maximum allowable span for the slab using C40/50, $\phi 9$ and the two-span support model. The columns marked "min" include the minimum reinforcement required for the corresponding slab thickness. Orange cells are governed by bending resistance, while green cells are governed by deflection.

A_s [mm^2/m]	min 120	min 140	min 160	$s250$	$s225$	min 180	$s200$	min 200	min 220	$s175$	min 240	$s150$	min 260	min 280	min 300	$s125$	$s100$	$s75$	$s50$
t [mm]	175	211	248	254	283	284	318	320	357	364	393	424	430	466	502	509	636	848	1272
120	2.83	3.11	3.36	3.40	3.59	3.59	3.80	3.81	4.02	4.05	4.21	4.36	4.39	4.57	4.73	4.76	5.29	5.79	6.12
140		3.29	3.56	3.60	3.80	3.81	4.02	4.04	4.26	4.30	4.46	4.63	4.66	4.84	5.02	5.05	5.62	6.44	6.84
160			3.72	3.77	3.97	3.98	4.21	4.22	4.45	4.50	4.67	4.84	4.88	5.07	5.26	5.29	5.89	6.76	7.49
180						4.12	4.36	4.37	4.62	4.66	4.84	5.02	5.06	5.26	5.45	5.49	6.11	7.02	8.09
200								4.51	4.75	4.80	4.98	5.17	5.21	5.42	5.62	5.66	6.30	7.24	8.65
220									4.87	4.92	5.11	5.30	5.34	5.55	5.76	5.80	6.47	7.43	9.02
240											5.22	5.42	5.45	5.67	5.89	5.93	6.61	7.60	9.23
260													5.55	5.78	5.99	6.03	6.73	7.74	9.41
280														5.87	6.09	6.13	6.84	7.87	9.57
300															6.18	6.22	6.94	7.99	9.72

Note. Empty cells indicate reinforcement amounts below the minimum reinforcement requirement for the corresponding slab thickness.

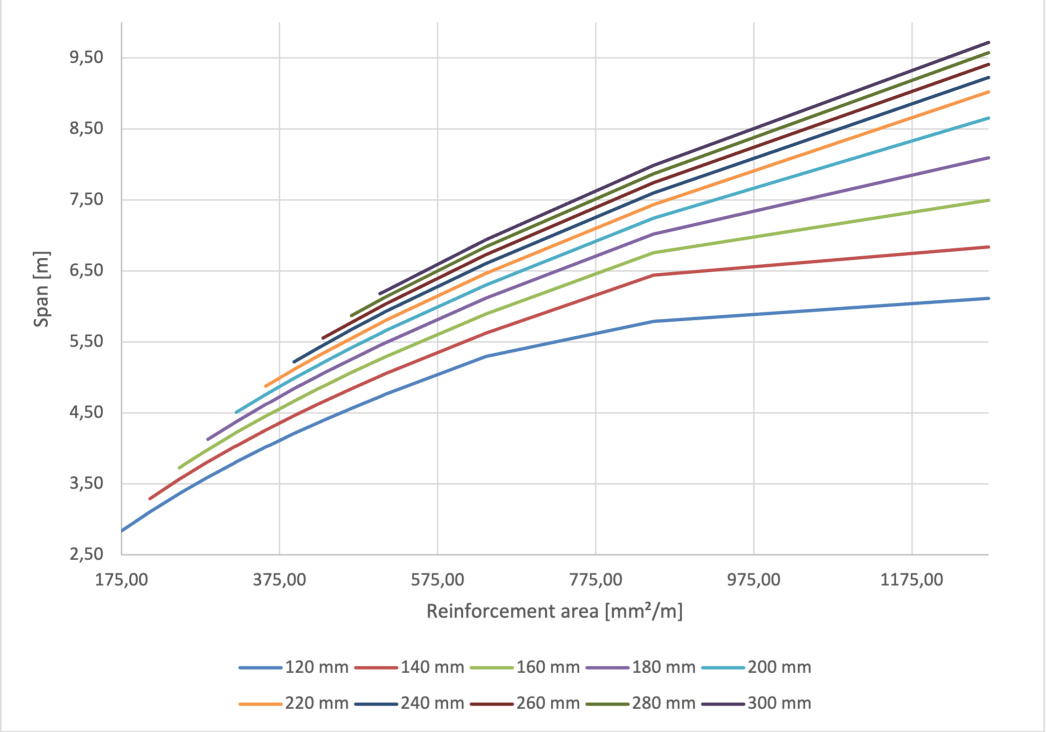

Figure C.19: Maximum allowable span as a function of reinforcement area for slabs with C40/50 concrete, $\phi 9$ reinforcement and the two-span support model. Each line represents a slab thickness between 120 mm and 300 mm.

Table C.18: Maximum allowable span for the slab using C40/50, ϕ12 and the two-span support model. The columns marked "min" include the minimum reinforcement required for the corresponding slab thickness. Orange cells are governed by bending resistance, while green cells are governed by deflection.

A_s [mm^2/m]	min 120	min 140	min 160	min 180	min 200	min 220	min 240	min 260	$s250$	min 280	min 300	$s225$	$s200$	$s175$	$s150$	$s125$	$s100$	$s75$
t [mm]	175	211	248	284	320	357	393	430	452	466	502	503	565	646	754	905	1131	1508
120	2.81	3.08	3.34	3.56	3.78	3.98	4.17	4.36	4.46	4.53	4.69	4.70	4.96	5.29	5.67	5.80	5.97	6.21
140		3.27	3.54	3.78	4.01	4.23	4.43	4.63	4.74	4.81	4.99	4.99	5.28	5.63	6.05	6.47	6.68	6.96
160			3.70	3.96	4.20	4.43	4.64	4.85	4.97	5.04	5.23	5.23	5.53	5.90	6.35	6.93	7.32	7.65
180				4.10	4.35	4.59	4.81	5.03	5.15	5.23	5.43	5.43	5.75	6.13	6.60	7.20	7.90	8.28
200					4.49	4.73	4.96	5.19	5.31	5.39	5.59	5.60	5.93	6.32	6.81	7.44	8.27	8.86
220						4.85	5.09	5.32	5.45	5.53	5.74	5.74	6.08	6.49	6.99	7.64	8.50	9.40
240							5.20	5.43	5.57	5.65	5.86	5.87	6.21	6.63	7.15	7.81	8.69	9.91
260								5.54	5.67	5.76	5.97	5.98	6.33	6.76	7.29	7.96	8.87	10.17
280										5.85	6.07	6.08	6.44	6.87	7.41	8.10	9.02	10.35
300											6.16	6.17	6.53	6.97	7.52	8.22	9.16	10.51

Note. Empty cells indicate reinforcement amounts below the minimum reinforcement requirement for the corresponding slab thickness.

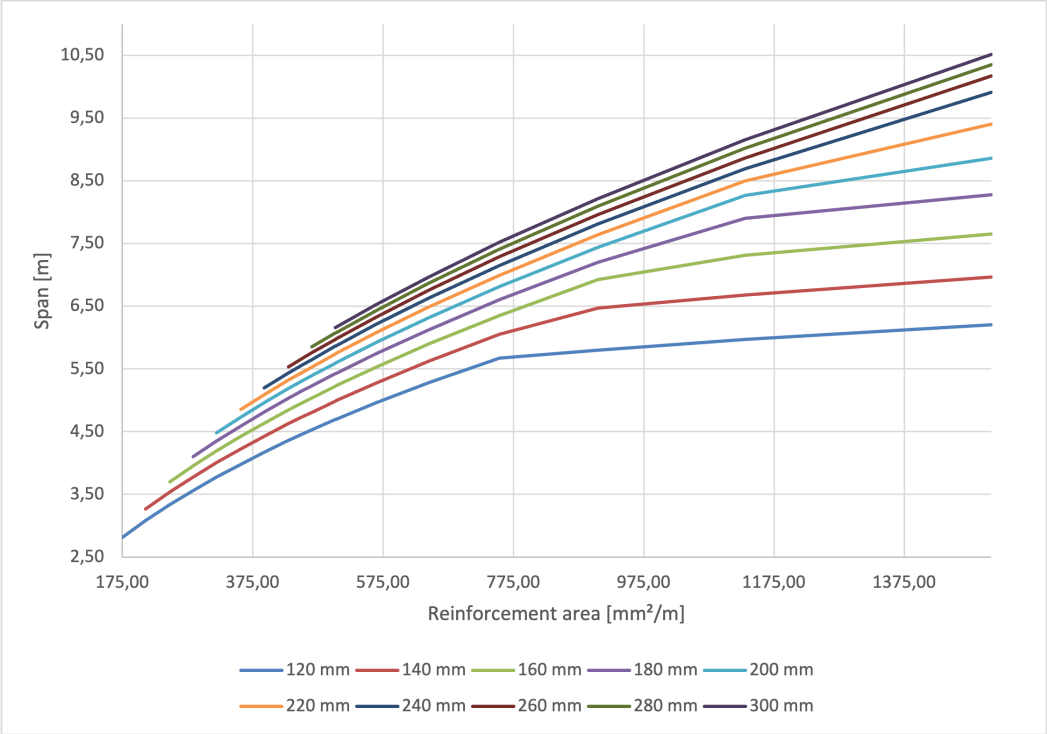

Figure C.20: Maximum allowable span as a function of reinforcement area for slabs with C40/50 concrete, ϕ12 reinforcement and the two-span support model. Each line represents a slab thickness between 120 mm and 300 mm.

C.1.3 Single-span slab model

The single span slab model used in the parameter study is shown schematically in Figure C.21. The model represents a one metre wide slab strip with simple supports at both ends. Bottom reinforcement was considered in the span region, where the governing bending moment occurs. The figure is schematic and is only intended to clarify the support condition and the reinforcement side used in the sectional checks.

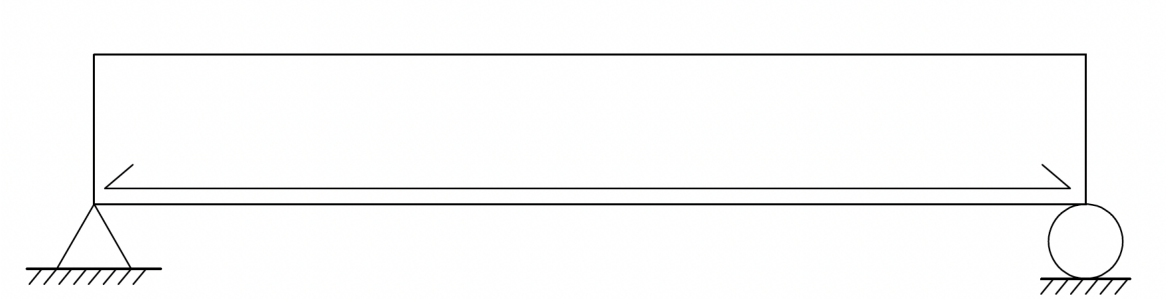

Figure C.21: Schematic illustration of the single span slab model used in the slab parameter study, showing the assumed simple support condition and the reinforcement considered in the field section.

C12/15 concrete

Table C.19: Maximum allowable span for the slab using C12/15, $\phi 6$ and the single-span support model. The columns marked "min" include the minimum reinforcement required for the corresponding slab thickness. Orange cells are governed by bending resistance, while green cells are governed by deflection.

A_s [mm^2/m]	min 120	s150	min 140	s125	min 160	s100	min 180	min 200	min 220	s75	min 240	min 260	min 280	min 300	s50	s40
t [mm]	175	188	211	226	248	283	284	320	357	377	393	430	466	502	565	707
120	2.81	2.90	2.98	3.01	3.06	3.12	3.12	3.19	3.25	3.28	3.30	3.35	3.40	3.44	3.51	3.65
140			3.25	3.34	3.39	3.46	3.47	3.54	3.61	3.64	3.67	3.73	3.78	3.84	3.92	4.09
160					3.68	3.77	3.77	3.86	3.93	3.97	4.00	4.07	4.13	4.19	4.29	4.48
180							4.06	4.15	4.23	4.27	4.31	4.38	4.45	4.52	4.62	4.83
200								4.41	4.51	4.55	4.59	4.67	4.75	4.82	4.93	5.16
220									4.76	4.81	4.85	4.94	5.02	5.09	5.22	5.46
240											5.10	5.19	5.27	5.36	5.49	5.75
260												5.43	5.52	5.60	5.74	6.02
280													5.74	5.83	5.98	6.27
300														6.05	6.21	6.51

Note. Empty cells indicate reinforcement amounts below the minimum reinforcement requirement for the corresponding slab thickness.

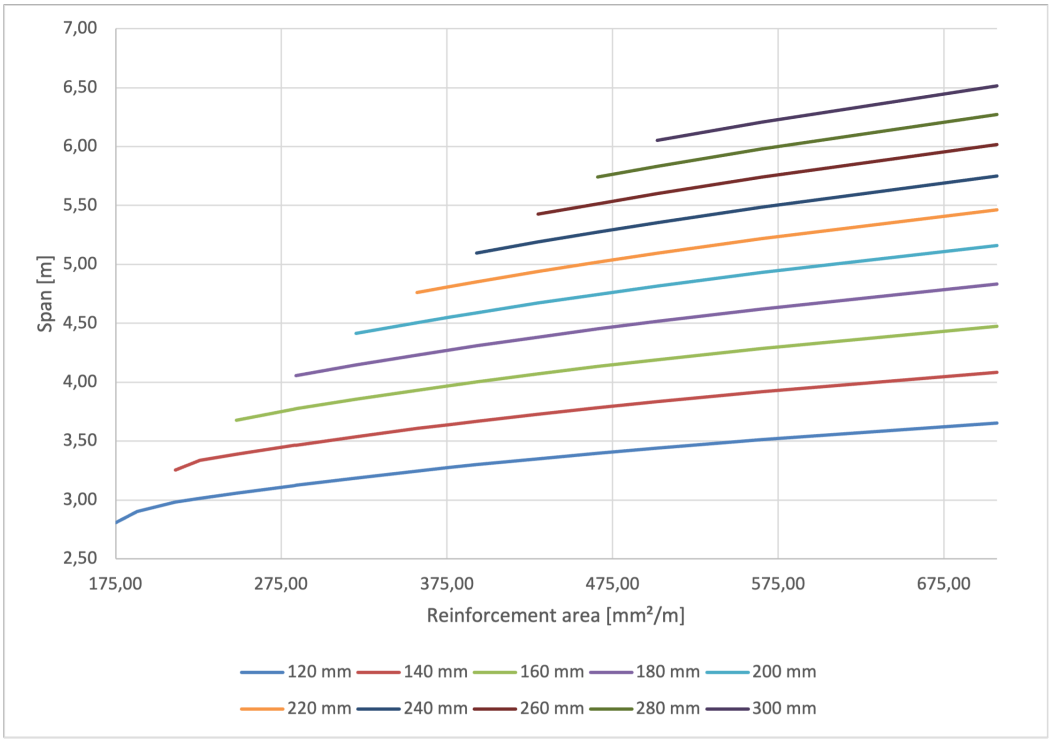

Figure C.22: Maximum allowable span as a function of reinforcement area for slabs with C12/15 concrete, $\phi 6$ reinforcement and the single-span support model. Each line represents a slab thickness between 120 mm and 300 mm.

Table C.20: Maximum allowable span for the slab using C12/15, $\phi 9$ and the single-span support model. The columns marked "min" include the minimum reinforcement required for the corresponding slab thickness. The columns marked "max" indicate the largest reinforcement level before over reinforced behaviour for the corresponding slab thickness. Orange cells are governed by bending resistance, while green cells are governed by deflection.

A_s [mm^2/m]	min 120	min 140	min 160	s250	s225	min 180	s200	min 200	min 220	s175	min 240	s150	min 260	min 280	min 300	s125	s100	s75	max 120	max 140	max 160	s50
t [mm]	175	211	248	254	283	284	318	320	357	364	393	424	430	466	502	509	636	848	866	1048	1229	1272
120	2.78	2.96	3.04	3.05	3.10	3.10	3.16	3.16	3.22	3.23	3.27	3.31	3.32	3.37	3.41	3.42	3.55	3.73	3.74			
140		3.23	3.37	3.38	3.44	3.44	3.51	3.51	3.58	3.59	3.64	3.69	3.70	3.76	3.81	3.82	3.97	4.19	4.20	4.35		
160			3.66	3.68	3.75	3.75	3.83	3.83	3.91	3.92	3.98	4.04	4.05	4.11	4.16	4.18	4.36	4.60	4.62	4.78	4.92	
180						4.04	4.12	4.13	4.21	4.22	4.29	4.35	4.36	4.43	4.49	4.50	4.70	4.98	5.00	5.18	5.34	5.38
200								4.40	4.49	4.50	4.57	4.64	4.65	4.72	4.79	4.81	5.02	5.32	5.35	5.55	5.73	5.77
220									4.74	4.76	4.83	4.90	4.92	5.00	5.07	5.09	5.32	5.65	5.67	5.90	6.09	6.13
240											5.08	5.16	5.17	5.25	5.33	5.35	5.60	5.95	5.97	6.22	6.42	6.47
260													5.41	5.50	5.58	5.60	5.86	6.23	6.26	6.52	6.74	6.79
280														5.72	5.81	5.83	6.11	6.50	6.53	6.80	7.04	7.09
300															6.03	6.05	6.35	6.75	6.78	7.07	7.32	7.38

Note. Empty cells indicate reinforcement amounts below the minimum reinforcement requirement or over reinforced cross sections excluded from the results.

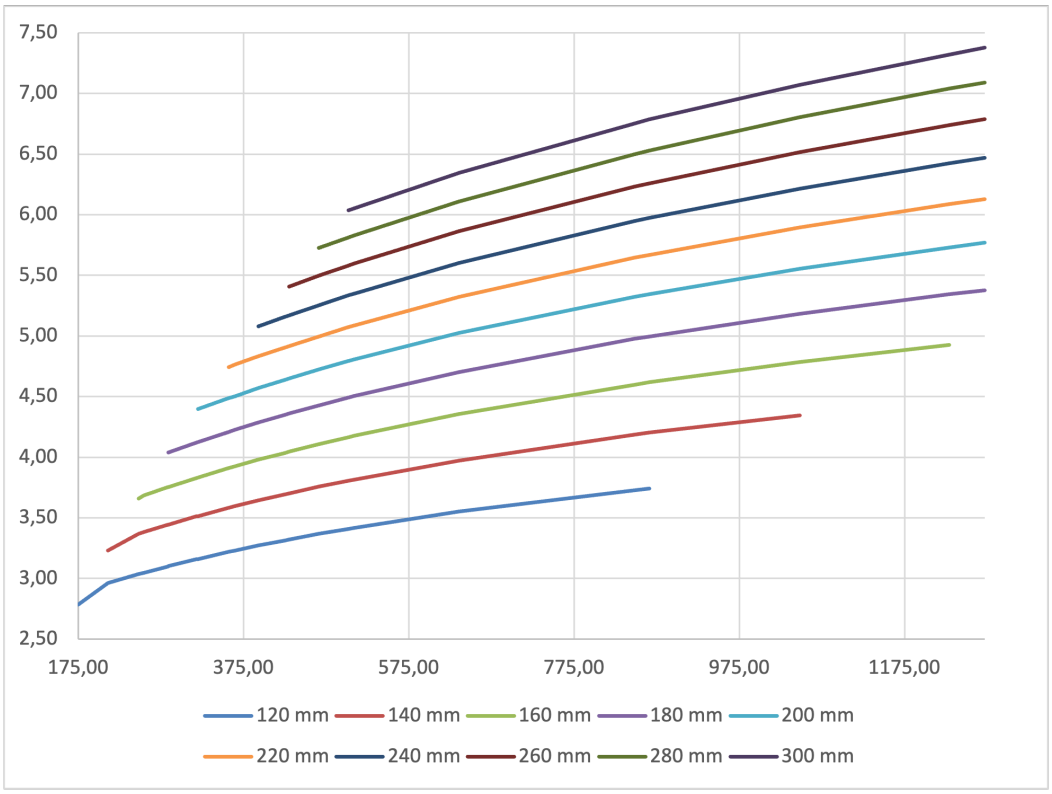

Figure C.23: Maximum allowable span as a function of reinforcement area for slabs with C12/15 concrete, $\phi 9$ reinforcement and the single-span support model. Each line represents a slab thickness between 120 mm and 300 mm.

Table C.21: Maximum allowable span for the slab using C12/15, $\phi 12$ and the single-span support model. The columns marked "min" include the minimum reinforcement required for the corresponding slab thickness. The columns marked "max" indicate the largest reinforcement level before over reinforced behaviour for the corresponding slab thickness. Orange cells are governed by bending resistance, while green cells are governed by deflection.

A_s [mm^2/m]	min 120	min 140	min 160	min 180	min 200	min 220	min 240	min 260	$s250$	min 280	min 300	$s225$	$s200$	$s175$	$s150$	max 120	$s125$	max 140	$s100$	max 160	max 180	$s75$
t [mm]	175	211	248	284	320	357	393	430	452	466	502	503	565	646	754	852	905	1034	1131	1215	1397	1508
120	2.76	2.94	3.01	3.08	3.14	3.19	3.24	3.29	3.32	3.34	3.38	3.38	3.45	3.53	3.62	3.69						
140		3.21	3.35	3.42	3.49	3.56	3.62	3.68	3.71	3.73	3.78	3.78	3.86	3.95	4.06	4.15	4.20	4.30				
160			3.64	3.73	3.81	3.89	3.96	4.02	4.06	4.08	4.14	4.14	4.23	4.34	4.47	4.57	4.62	4.74	4.81	4.88		
180				4.02	4.11	4.19	4.26	4.34	4.38	4.40	4.47	4.47	4.57	4.69	4.83	4.95	5.01	5.14	5.22	5.30	5.43	
200					4.38	4.47	4.55	4.63	4.67	4.70	4.77	4.77	4.88	5.01	5.17	5.30	5.36	5.51	5.60	5.68	5.84	5.92
220						4.72	4.81	4.90	4.95	4.98	5.05	5.05	5.17	5.31	5.48	5.62	5.69	5.85	5.96	6.04	6.21	6.30
240							5.06	5.15	5.20	5.23	5.31	5.31	5.44	5.59	5.78	5.93	6.00	6.17	6.28	6.38	6.56	6.66
260								5.39	5.44	5.48	5.56	5.56	5.70	5.86	6.05	6.21	6.29	6.47	6.59	6.69	6.89	7.00
280										5.71	5.79	5.80	5.94	6.11	6.31	6.48	6.57	6.76	6.89	6.99	7.20	7.32
300											6.02	6.02	6.17	6.35	6.56	6.74	6.83	7.03	7.16	7.28	7.50	7.62

Note. Empty cells indicate reinforcement amounts below the minimum reinforcement requirement or over reinforced cross sections excluded from the results.

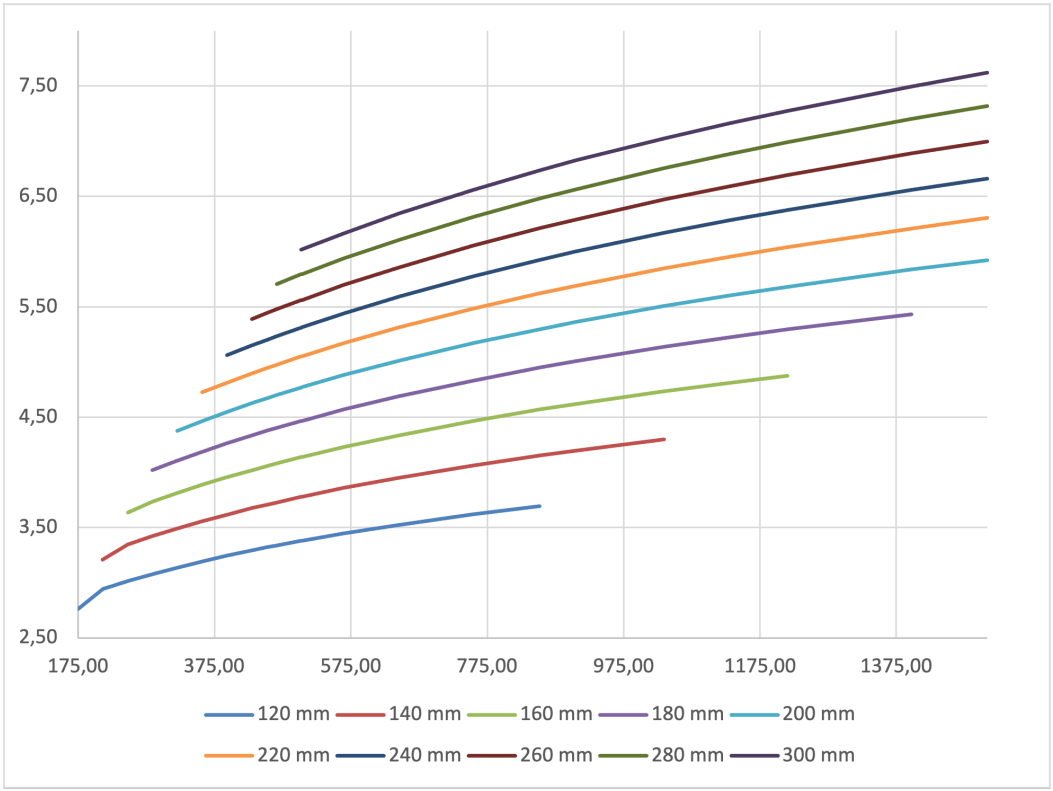

Figure C.24: Maximum allowable span as a function of reinforcement area for slabs with C12/15 concrete, $\phi 12$ reinforcement and the single-span support model. Each line represents a slab thickness between 120 mm and 300 mm.

C20/25 concrete

Table C.22: Maximum allowable span for the slab using C20/25, $\phi 6$ and the single-span support model. The columns marked "min" include the minimum reinforcement required for the corresponding slab thickness. Orange cells are governed by bending resistance, while green cells are governed by deflection.

A_s [mm^2/m]	min 120	$s150$	min 140	$s125$	min 160	$s100$	min 180	min 200	min 220	$s75$	min 240	min 260	min 280	min 300	$s50$	$s40$
t [mm]	175	188	211	226	248	283	284	320	357	377	393	430	466	502	565	707
120	2.84	2.94	3.10	3.21	3.29	3.35	3.35	3.40	3.45	3.48	3.50	3.55	3.59	3.63	3.70	3.83
140			3.29	3.40	3.55	3.71	3.71	3.77	3.83	3.86	3.89	3.94	3.99	4.04	4.12	4.27
160					3.72	3.96	3.97	4.11	4.17	4.21	4.24	4.30	4.35	4.41	4.50	4.68
180							4.11	4.36	4.49	4.53	4.56	4.62	4.69	4.75	4.84	5.04
200								4.49	4.73	4.82	4.85	4.93	4.99	5.06	5.17	5.38
220									4.86	4.99	5.09	5.21	5.28	5.35	5.47	5.70
240											5.20	5.43	5.55	5.62	5.75	5.99
260												5.53	5.75	5.88	6.01	6.27
280													5.84	6.06	6.26	6.54
300														6.15	6.50	6.79

Note. Empty cells indicate reinforcement amounts below the minimum reinforcement requirement for the corresponding slab thickness.

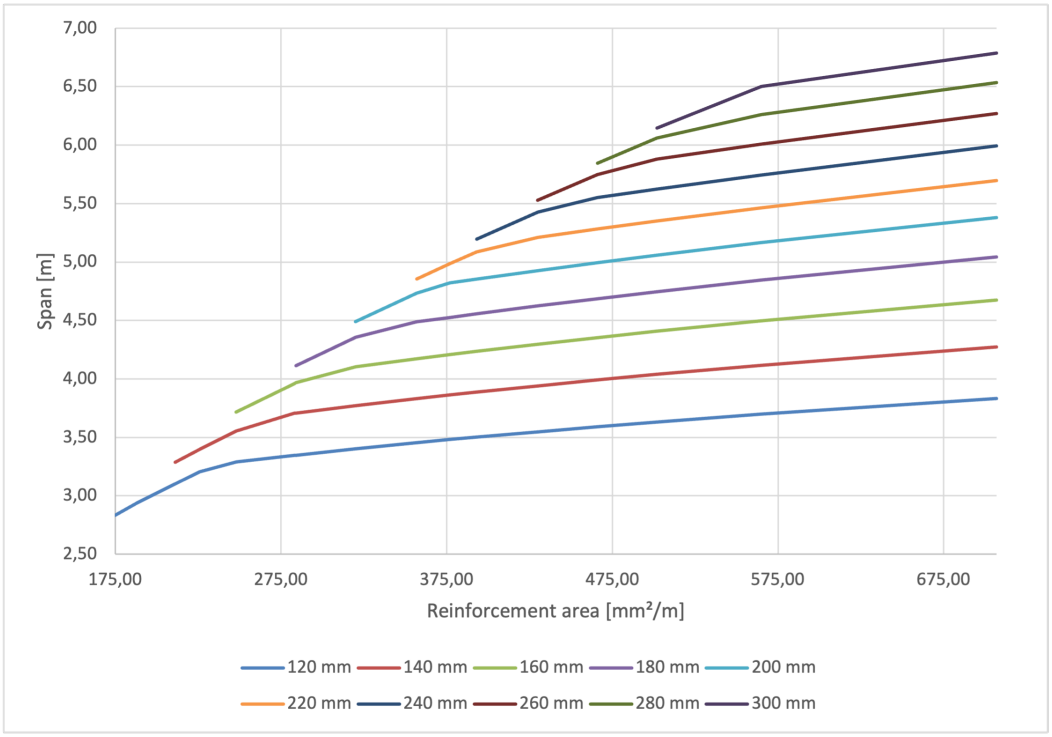

Figure C.25: Maximum allowable span as a function of reinforcement area for slabs with C20/25 concrete, $\phi 6$ reinforcement and the single-span support model. Each line represents a slab thickness between 120 mm and 300 mm.

Table C.23: Maximum allowable span for the slab using C20/25, $\phi 9$ and the single-span support model. The columns marked "min" include the minimum reinforcement required for the corresponding slab thickness. Orange cells are governed by bending resistance, while green cells are governed by deflection.

A_s [mm^2/m]	min 120	min 140	min 160	$s250$	$s225$	min 180	$s200$	min 200	min 220	$s175$	min 240	$s150$	min 260	min 280	min 300	$s125$	$s100$	$s75$	$s50$
t [mm]	175	211	248	254	283	284	318	320	357	364	393	424	430	466	502	509	636	848	1272
120	2.81	3.08	3.27	3.28	3.33	3.33	3.38	3.38	3.43	3.44	3.48	3.52	3.52	3.57	3.60	3.61	3.74	3.91	4.16
140		3.26	3.53	3.57	3.69	3.69	3.75	3.75	3.81	3.82	3.86	3.91	3.92	3.97	4.01	4.02	4.17	4.38	4.68
160			3.70	3.74	3.94	3.95	4.08	4.09	4.15	4.17	4.22	4.27	4.28	4.33	4.38	4.39	4.56	4.80	5.15
180						4.09	4.32	4.34	4.47	4.48	4.54	4.59	4.60	4.67	4.72	4.74	4.92	5.18	5.58
200								4.47	4.71	4.76	4.84	4.90	4.91	4.97	5.04	5.05	5.25	5.54	5.98
220									4.84	4.88	5.07	5.18	5.19	5.26	5.33	5.34	5.56	5.87	6.35
240											5.18	5.37	5.41	5.53	5.61	5.62	5.85	6.18	6.69
260													5.51	5.73	5.86	5.88	6.13	6.47	7.02
280														5.83	6.04	6.08	6.38	6.75	7.33
300															6.13	6.17	6.63	7.01	7.62

Note. Empty cells indicate reinforcement amounts below the minimum reinforcement requirement for the corresponding slab thickness.

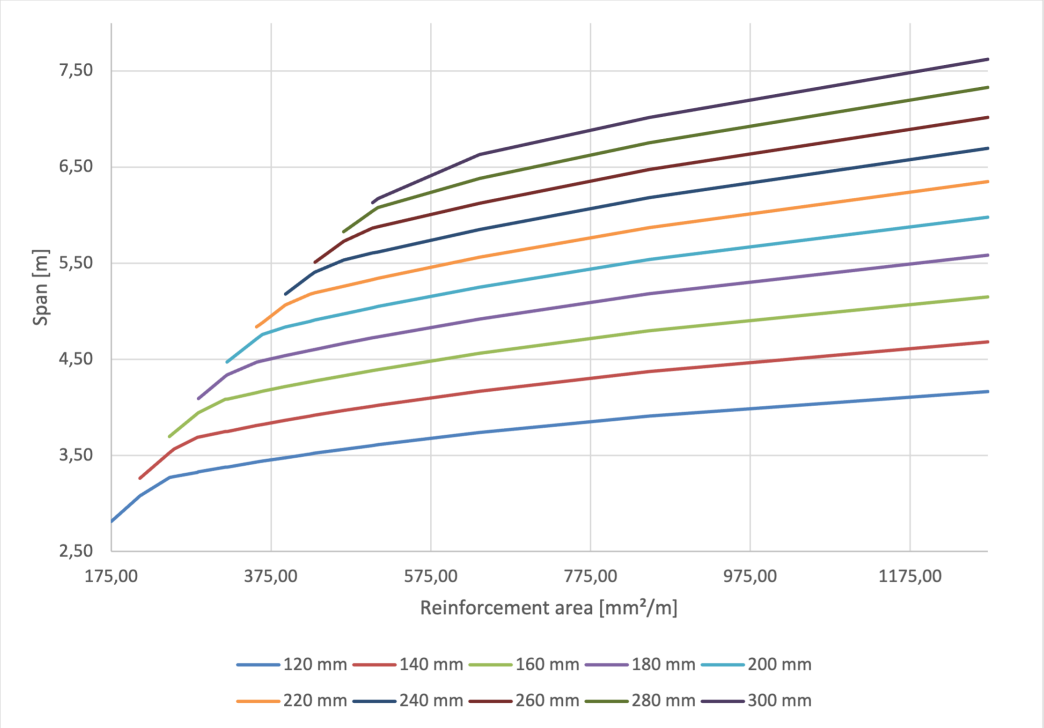

Figure C.26: Maximum allowable span as a function of reinforcement area for slabs with C20/25 concrete, $\phi 9$ reinforcement and the single-span support model. Each line represents a slab thickness between 120 mm and 300 mm.

Table C.24: Maximum allowable span for the slab using C20/25, ϕ12 and the single-span support model. The columns marked "min" include the minimum reinforcement required for the corresponding slab thickness. The column marked "max" indicates the largest reinforcement level before over reinforced behaviour for the corresponding slab thickness. Orange cells are governed by bending resistance, while green cells are governed by deflection.

A_s [mm^2/m]	min 120	min 140	min 160	min 180	min 200	min 220	min 240	min 260	s250	min 280	min 300	s225	s200	s175	s150	s125	s100	max 120	s75
t [mm]	175	211	248	284	320	357	393	430	452	466	502	503	565	646	754	905	1131	1421	1508
120	2.79	3.05	3.25	3.31	3.36	3.41	3.45	3.50	3.52	3.54	3.58	3.58	3.64	3.71	3.80	3.91	4.05	4.19	
140		3.24	3.51	3.67	3.73	3.79	3.84	3.89	3.92	3.94	3.99	3.99	4.06	4.15	4.26	4.39	4.55	4.73	4.77
160			3.67	3.92	4.07	4.13	4.20	4.25	4.29	4.31	4.36	4.36	4.45	4.55	4.67	4.82	5.01	5.21	5.27
180				4.07	4.32	4.45	4.52	4.58	4.62	4.64	4.70	4.70	4.80	4.91	5.05	5.21	5.43	5.66	5.72
200					4.45	4.69	4.82	4.89	4.93	4.95	5.02	5.02	5.12	5.24	5.39	5.58	5.82	6.07	6.14
220						4.82	5.05	5.17	5.22	5.24	5.31	5.31	5.42	5.56	5.72	5.92	6.18	6.45	6.53
240							5.16	5.39	5.49	5.51	5.59	5.59	5.71	5.85	6.02	6.23	6.51	6.81	6.89
260								5.49	5.63	5.71	5.85	5.85	5.97	6.12	6.31	6.53	6.83	7.15	7.23
280										5.81	6.02	6.03	6.23	6.38	6.58	6.82	7.13	7.47	7.56
300											6.11	6.12	6.47	6.63	6.83	7.08	7.41	7.77	7.87

Note. Empty cells indicate reinforcement amounts below the minimum reinforcement requirement or over reinforced cross sections excluded from the results.

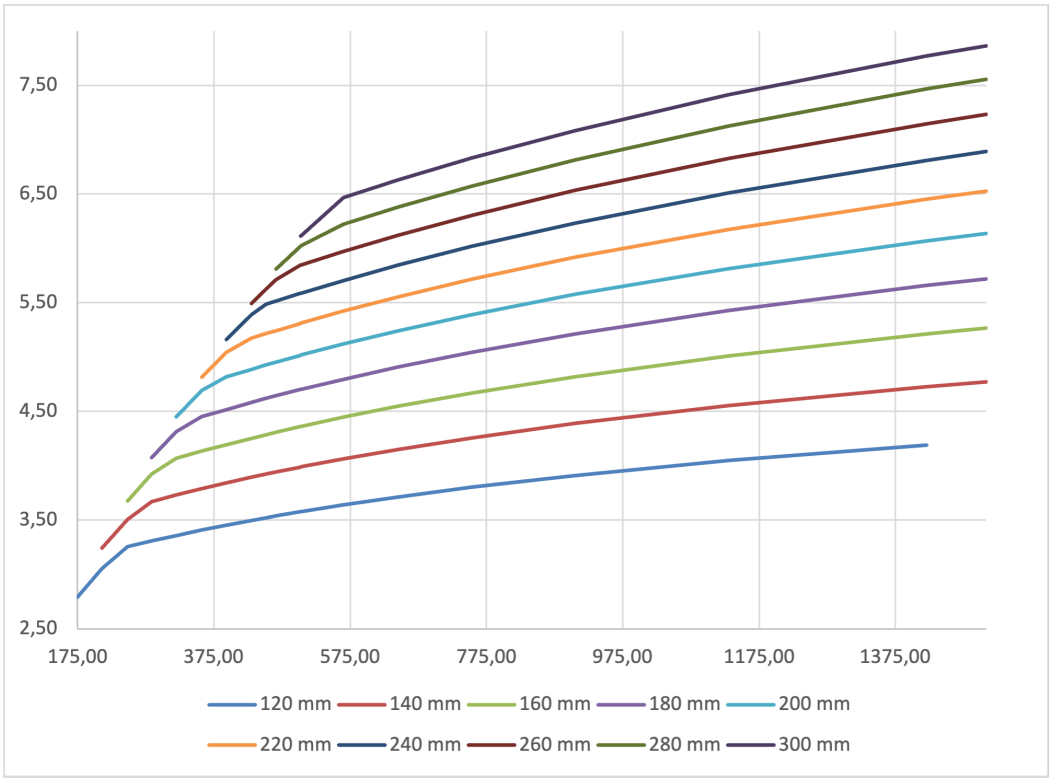

Figure C.27: Maximum allowable span as a function of reinforcement area for slabs with C20/25 concrete, ϕ12 reinforcement and the single-span support model. Each line represents a slab thickness between 120 mm and 300 mm.

C40/50 concrete

Table C.25: Maximum allowable span for the slab using C40/50, ϕ6 and the single-span support model. The columns marked "min" include the minimum reinforcement required for the corresponding slab thickness. Orange cells are governed by bending resistance, while green cells are governed by deflection.

A_s [mm^2/m]	min 120	s150	min 140	s125	min 160	s100	min 180	min 200	min 220	s75	min 240	min 260	min 280	min 300	s50	s40
t [mm]	175	188	211	226	248	283	284	320	357	377	393	430	466	502	565	707
120	2.86	2.96	3.13	3.24	3.39	3.62	3.62	3.84	4.05	4.08	4.08	4.08	4.08	4.08	4.13	4.25
140			3.31	3.43	3.59	3.83	3.83	4.06	4.28	4.40	4.49	4.49	4.49	4.52	4.58	4.72
160					3.74	4.00	4.00	4.24	4.48	4.60	4.69	4.88	4.88	4.92	4.99	5.14
180							4.15	4.40	4.64	4.76	4.86	5.08	5.24	5.29	5.37	5.54
200								4.52	4.77	4.90	5.01	5.23	5.44	5.63	5.72	5.90
220									4.89	5.03	5.13	5.36	5.58	5.78	6.05	6.25
240											5.24	5.47	5.69	5.91	6.26	6.57
260												5.57	5.80	6.01	6.37	6.87
280													5.89	6.11	6.47	7.16
300														6.19	6.56	7.33

Note. Empty cells indicate reinforcement amounts below the minimum reinforcement requirement for the corresponding slab thickness.

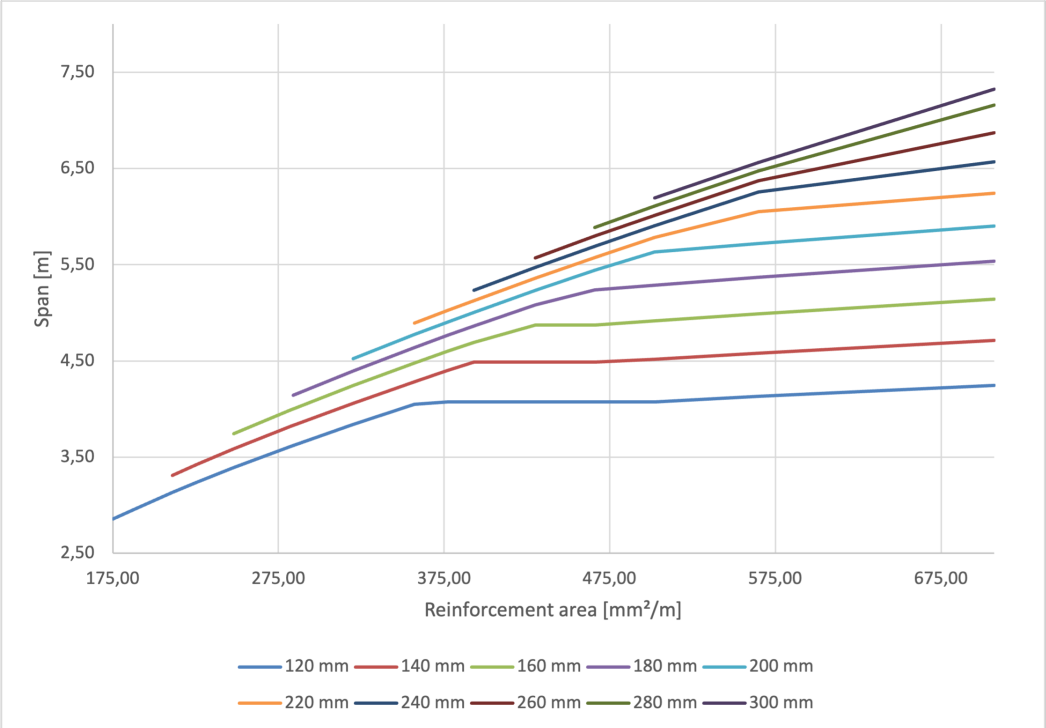

Figure C.28: Maximum allowable span as a function of reinforcement area for slabs with C40/50 concrete, ϕ6 reinforcement and the single-span support model. Each line represents a slab thickness between 120 mm and 300 mm.

Table C.26: Maximum allowable span for the slab using C40/50, $\phi 9$ and the single-span support model. The columns marked "min" include the minimum reinforcement required for the corresponding slab thickness. Orange cells are governed by bending resistance, while green cells are governed by deflection.

A_s [mm^2/m]	min 120	min 140	min 160	$s250$	$s225$	min 180	$s200$	min 200	min 220	$s175$	min 240	$s150$	min 260	min 280	min 300	$s125$	$s100$	$s75$	$s50$
t [mm]	175	211	248	254	283	284	318	320	357	364	393	424	430	466	502	509	636	848	1272
120	2.83	3.11	3.36	3.40	3.59	3.59	3.80	3.81	4.02	4.05	4.08	4.08	4.08	4.08	4.08	4.08	4.17	4.32	4.56
140		3.29	3.56	3.60	3.80	3.81	4.02	4.04	4.26	4.30	4.46	4.49	4.49	4.49	4.50	4.50	4.63	4.81	5.10
160			3.72	3.77	3.97	3.98	4.21	4.22	4.45	4.50	4.67	4.84	4.88	4.88	4.90	4.91	5.05	5.25	5.59
180						4.12	4.36	4.37	4.62	4.66	4.84	5.02	5.06	5.24	5.27	5.28	5.44	5.66	6.04
200								4.51	4.75	4.80	4.98	5.17	5.21	5.42	5.62	5.63	5.80	6.04	6.45
220									4.87	4.92	5.11	5.30	5.34	5.55	5.76	5.80	6.13	6.40	6.84
240											5.22	5.42	5.45	5.67	5.89	5.93	6.45	6.73	7.20
260													5.55	5.78	5.99	6.03	6.73	7.05	7.55
280														5.87	6.09	6.13	6.84	7.35	7.87
300															6.18	6.22	6.94	7.63	8.18

Note. Empty cells indicate reinforcement amounts below the minimum reinforcement requirement for the corresponding slab thickness.

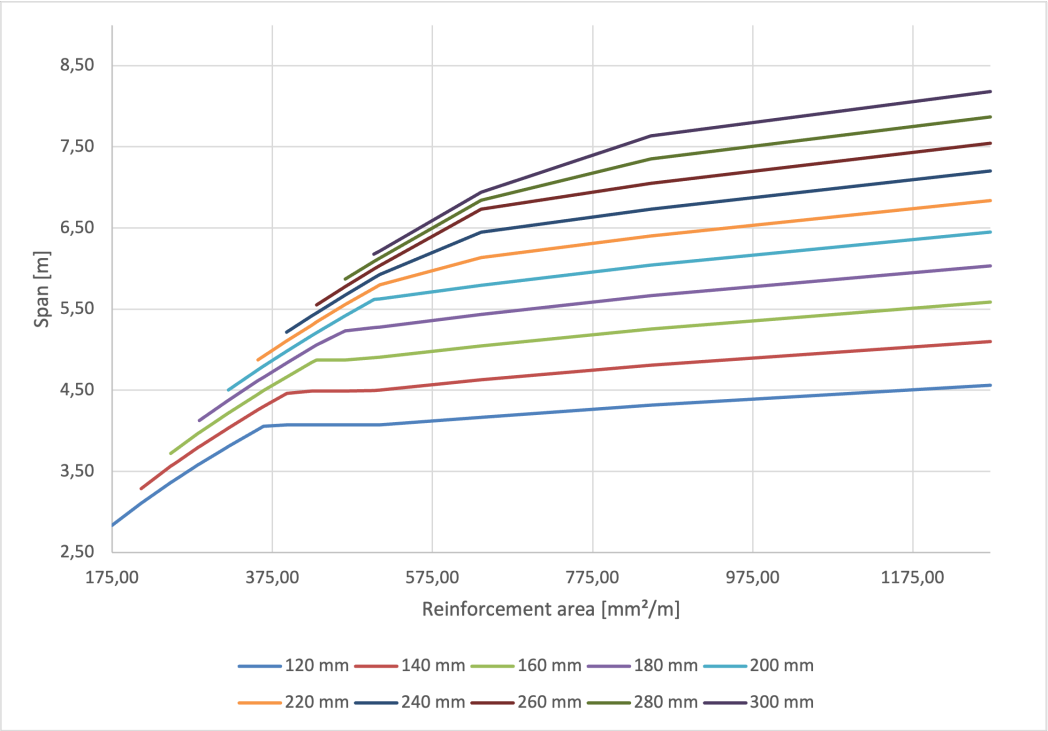

Figure C.29: Maximum allowable span as a function of reinforcement area for slabs with C40/50 concrete, $\phi 9$ reinforcement and the single-span support model. Each line represents a slab thickness between 120 mm and 300 mm.

Table C.27: Maximum allowable span for the slab using C40/50, ϕ12 and the single-span support model. The columns marked "min" include the minimum reinforcement required for the corresponding slab thickness. Orange cells are governed by bending resistance, while green cells are governed by deflection.

A_s [mm^2/m]	min 120	min 140	min 160	min 180	min 200	min 220	min 240	min 260	$s250$	min 280	min 300	$s225$	$s200$	$s175$	$s150$	$s125$	$s100$	$s75$
t [mm]	175	211	248	284	320	357	393	430	452	466	502	503	565	646	754	905	1131	1508
120	2.81	3.08	3.34	3.56	3.78	3.98	4.08	4.08	4.08	4.08	4.08	4.08	4.09	4.15	4.23	4.33	4.45	4.63
140		3.27	3.54	3.78	4.01	4.23	4.43	4.49	4.49	4.49	4.49	4.49	4.54	4.61	4.71	4.82	4.98	5.19
160			3.70	3.96	4.20	4.43	4.64	4.85	4.88	4.88	4.88	4.88	4.95	5.04	5.14	5.28	5.46	5.70
180				4.10	4.35	4.59	4.81	5.03	5.15	5.23	5.25	5.26	5.33	5.43	5.55	5.70	5.89	6.17
200					4.49	4.73	4.96	5.19	5.31	5.39	5.59	5.60	5.69	5.79	5.92	6.08	6.30	6.61
220						4.85	5.09	5.32	5.45	5.53	5.74	5.74	6.02	6.13	6.27	6.44	6.68	7.01
240							5.20	5.43	5.57	5.65	5.86	5.87	6.21	6.45	6.59	6.78	7.03	7.39
260								5.54	5.67	5.76	5.97	5.98	6.33	6.75	6.90	7.10	7.37	7.75
280										5.85	6.07	6.08	6.44	6.87	7.20	7.41	7.69	8.09
300											6.16	6.17	6.53	6.97	7.48	7.70	7.99	8.41

Note. Empty cells indicate reinforcement amounts below the minimum reinforcement requirement for the corresponding slab thickness.

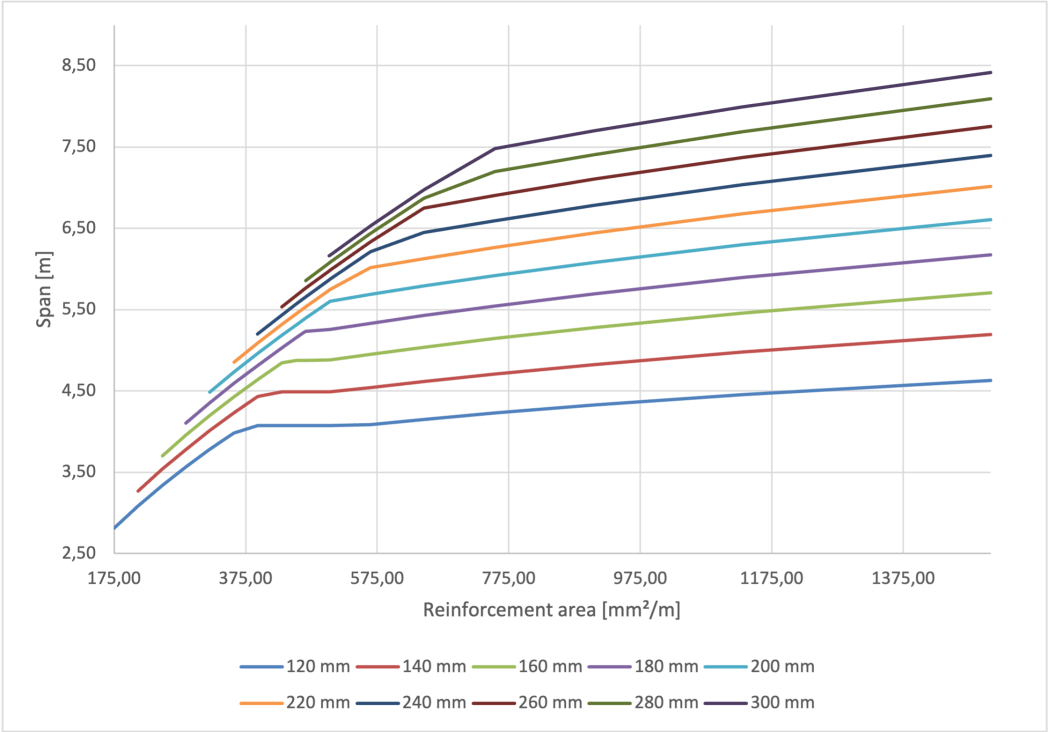

Figure C.30: Maximum allowable span as a function of reinforcement area for slabs with C40/50 concrete, ϕ12 reinforcement and the single-span support model. Each line represents a slab thickness between 120 mm and 300 mm.

C.1.4 Influence of concrete strength class

The influence of concrete strength class was also evaluated for the one-span and two-span slab models. The comparison was carried out for $\phi 9$ reinforcement and slab thicknesses of 120 mm, 200 mm and 300 mm. The concrete strength classes C12/15, C20/25 and C40/50 were compared using the same reinforcement range as in the main slab parameter study.

Figure C.31 shows the result for the one-span support model. Figure C.32 shows the corresponding result for the two-span support model. The results show the same general tendency as the three-span comparison in Section 4.1.3. At low reinforcement levels, the influence of concrete strength class is limited. At higher reinforcement levels, the difference between the concrete strength classes becomes more visible, especially for thinner slabs where deflection becomes more important.

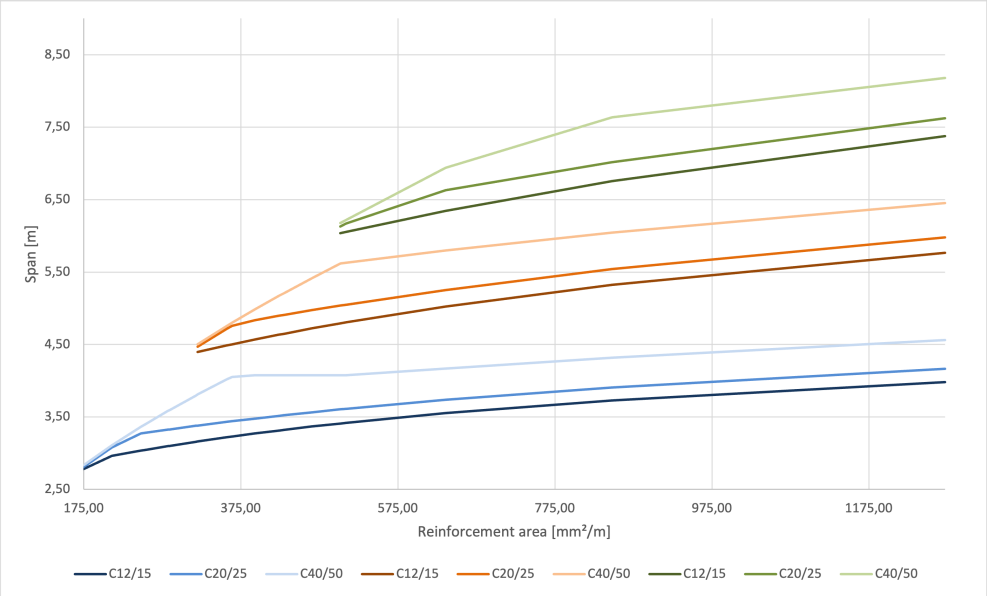

Figure C.31: Influence of concrete strength class on the maximum allowable span for slabs with $\phi 9$ reinforcement and the one-span support model. The results are shown for slab thicknesses of 120 mm, 200 mm and 300 mm. The blue, orange and green line groups represent 120 mm, 200 mm and 300 mm slabs, respectively. Within each group, the lines represent C12/15, C20/25 and C40/50.

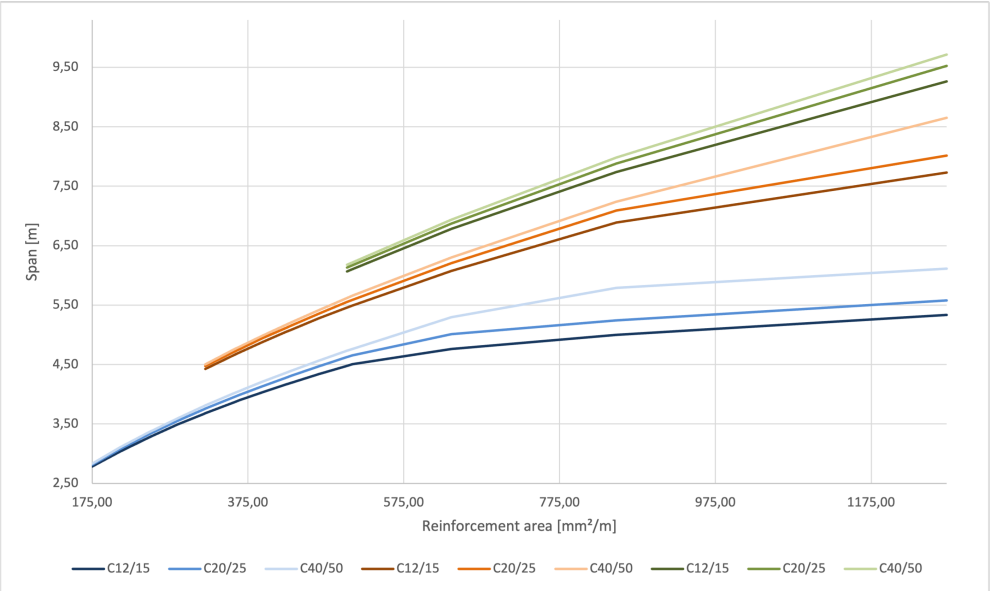

Figure C.32: Influence of concrete strength class on the maximum allowable span for slabs with $\phi 9$ reinforcement and the two-span support model. The results are shown for slab thicknesses of 120 mm, 200 mm and 300 mm. The blue, orange and green line groups represent 120 mm, 200 mm and 300 mm slabs, respectively. Within each group, the lines represent C12/15, C20/25 and C40/50.

The comparison shows that the influence of concrete strength class depends on the governing verification. For the one-span model, shown in Figure C.31, the difference between the concrete classes becomes visible for several of the thinner slab cases, since deflection governs for a larger part of the studied reinforcement range. A higher concrete strength class gives a higher modulus of elasticity and a higher cracking moment, which increases the calculated stiffness and therefore allows a longer span when deflection is governing.

For the two-span model, shown in Figure C.32, the same tendency can be seen, but the curves are closer for a larger part of the reinforcement range. This indicates that the influence of concrete strength class is smaller when bending resistance governs and becomes more relevant when the governing verification shifts towards deflection.

C.2 Reinforced Wall Capacity Results

C.2.1 Minimum Mesh Selected for Each Wall Thickness

C20/25

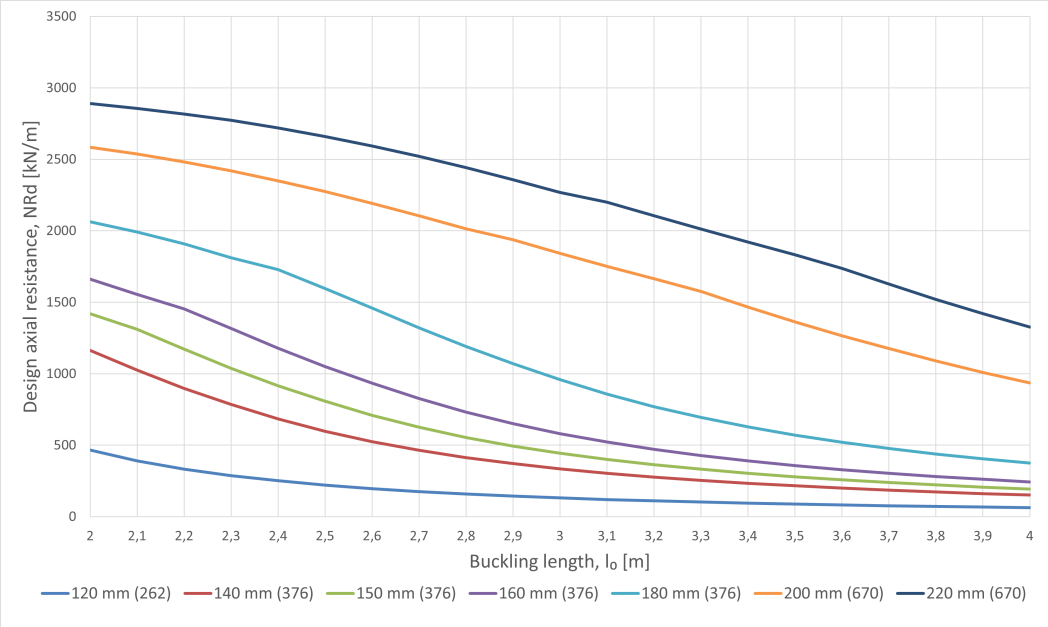

Figure C.33: Design axial resistance N_{Rd} as a function of effective buckling length for reinforced wall strips with concrete class C20/25 and the selected minimum vertical reinforcement mesh for each wall thickness. The eccentricity is taken as $e_0 = l_0/400$.

Table C.28: Design axial resistance N_{Rd} for reinforced wall strips with concrete class C20/25 and the selected minimum vertical reinforcement mesh for each wall thickness. Values are given in kN/m.

t [mm]	$A_{s,\mathrm{tot}}$ [mm^2/m]	2.0	2.1	2.2	2.3	2.4	2.5	2.6	2.7	2.8	2.9	3.0	3.1	3.2	3.3	3.4	3.5	3.6	3.7	3.8	3.9	4.0
120	262	464.9	390.8	333.1	287.5	250.9	221.2	196.5	175.9	158.5	143.7	130.9	119.9	110.2	101.7	94.1	87.4	81.4	76.1	71.2	66.8	62.8
140	376	1162.5	1024.4	897.0	785.4	683.7	596.9	524.4	464.2	413.7	371.1	334.9	303.8	277.0	253.8	233.4	215.4	199.6	185.4	172.8	161.4	151.2
150	376	1420.5	1310.5	1171.5	1037.5	915.8	807.3	708.6	624.9	554.0	494.2	443.6	400.5	363.4	331.4	303.6	279.2	257.7	238.7	221.8	206.7	193.2
160	376	1662.1	1554.6	1453.8	1316.3	1178.8	1049.4	933.1	825.7	730.9	650.1	580.8	521.7	471.2	427.7	390.1	357.4	328.7	303.4	281.0	261.1	243.3
180	376	2062.8	1992.2	1908.8	1811.0	1727.9	1597.0	1458.9	1320.9	1189.9	1070.2	958.1	857.1	769.3	693.3	627.5	570.1	520.3	476.8	438.5	404.9	375.0
200	670	2583.9	2536.9	2481.0	2418.5	2349.6	2274.2	2191.8	2104.0	2013.0	1937.5	1843.1	1751.5	1663.8	1575.0	1465.5	1362.0	1265.6	1176.7	1089.7	1009.0	935.9
220	670	2890.5	2855.6	2817.4	2773.4	2718.9	2658.5	2592.2	2520.2	2441.8	2357.6	2269.2	2199.9	2104.7	2011.0	1919.9	1832.1	1737.6	1626.2	1520.0	1420.1	1327.1

Note. The eccentricity is taken as $e_0 = l_0/400$. The selected minimum vertical reinforcement area is $A_{s,\mathrm{tot}} = 262$ mm^2/m for $t = 120$ mm, 376 mm^2/m for $t = 140$–180 mm, and 670 mm^2/m for $t = 200$–220 mm.

C.2.2 Constant Reinforcement Amounts

The following figures and tables show the design axial resistance for reinforced wall strips with a constant total vertical reinforcement amount of $A_{s,\text{tot}} = 262$ mm^2/m, corresponding to mesh #5150 placed on both wall faces.

C12/15

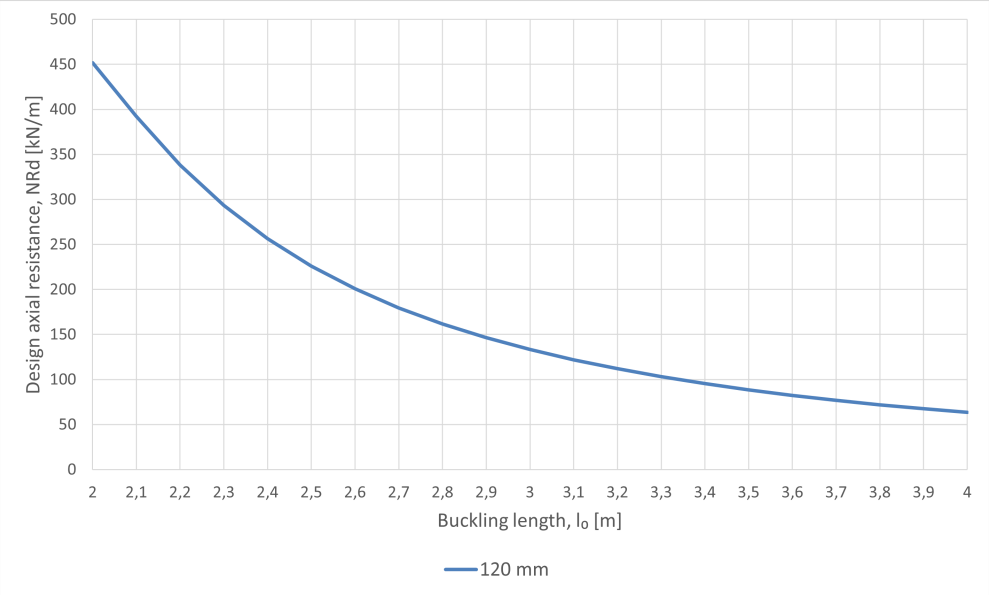

Figure C.34: Design axial resistance N_{Rd} for reinforced wall strips with concrete class C12/15 and $A_{s,\text{tot}} = 262$ mm^2/m, corresponding to mesh #5150 on both wall faces. The eccentricity is taken as $e_0 = l_0/400$.

Table C.29: Design axial resistance N_{Rd} for reinforced wall strips with concrete class C12/15 and $A_{s,\text{tot}} = 262$ mm^2/m, corresponding to mesh #5150 on both wall faces. Values are given in kN/m.

t [mm] / l_0 [m]	2.0	2.1	2.2	2.3	2.4	2.5	2.6	2.7	2.8	2.9	3.0	3.1	3.2	3.3	3.4	3.5	3.6	3.7	3.8	3.9	4.0
120	451.7	392.2	338.2	293.2	256.3	225.9	200.7	179.6	161.7	146.4	133.2	121.8	111.9	103.1	95.4	88.5	82.4	76.9	71.9	67.4	63.4

Note. The eccentricity is taken as $e_0 = l_0/400$.

C20/25

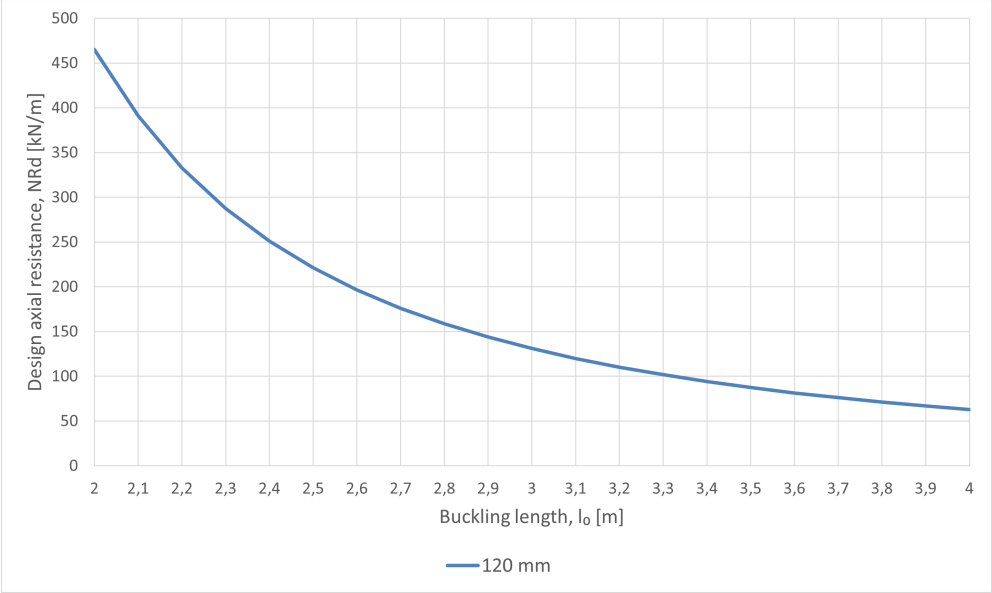

Figure C.35: Design axial resistance N_{Rd} for reinforced wall strips with concrete class C20/25 and $A_{s,\text{tot}} = 262$ mm^2/m, corresponding to mesh #5150 on both wall faces. The eccentricity is taken as $e_0 = l_0/400$.

Table C.30: Design axial resistance N_{Rd} for reinforced wall strips with concrete class C20/25 and $A_{s,\text{tot}} = 262$ mm^2/m, corresponding to mesh #5150 on both wall faces. Values are given in kN/m.

t [mm] / l_0 [m]	2.0	2.1	2.2	2.3	2.4	2.5	2.6	2.7	2.8	2.9	3.0	3.1	3.2	3.3	3.4	3.5	3.6	3.7	3.8	3.9	4.0
120	464.9	390.8	333.1	287.5	250.9	221.2	196.5	175.9	158.5	143.7	130.9	119.9	110.2	101.7	94.1	87.4	81.4	76.1	71.2	66.8	62.8

Note. The eccentricity is taken as $e_0 = l_0/400$.

C30/37

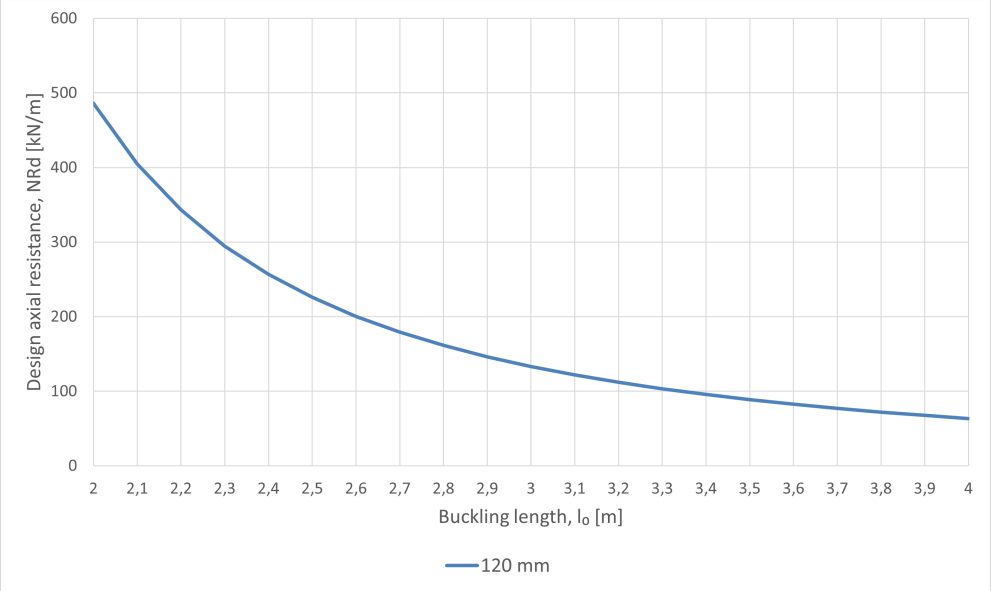

Figure C.36: Design axial resistance N_{Rd} for reinforced wall strips with concrete class C30/37 and $A_{s,\text{tot}} = 262$ mm^2/m, corresponding to mesh #5150 on both wall faces. The eccentricity is taken as $e_0 = l_0/400$.

Table C.31: Design axial resistance N_{Rd} for reinforced wall strips with concrete class C30/37 and $A_{s,\text{tot}} = 262$ mm^2/m, corresponding to mesh #5150 on both wall faces. Values are given in kN/m.

t [mm] / l_0 [m]	2.0	2.1	2.2	2.3	2.4	2.5	2.6	2.7	2.8	2.9	3.0	3.1	3.2	3.3	3.4	3.5	3.6	3.7	3.8	3.9	4.0
120	486.2	404.9	343.1	294.7	256.6	225.7	200.3	179.2	161.4	146.2	133.1	121.8	111.9	103.2	95.4	88.6	82.4	76.9	72.0	67.5	63.4

Note. The eccentricity is taken as $e_0 = l_0/400$.

The following figures and tables show the design axial resistance for reinforced wall strips with a constant total vertical reinforcement amount of $A_{s,\text{tot}} = 376$ mm^2/m, corresponding to mesh #6150 placed on both wall faces.

C12/15

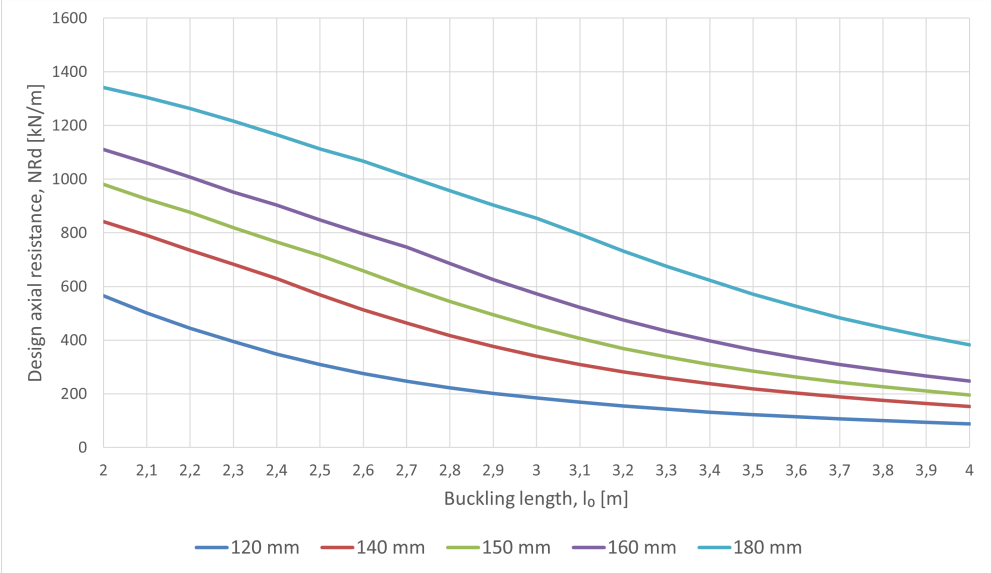

Figure C.37: Design axial resistance N_{Rd} for reinforced wall strips with concrete class C12/15 and $A_{s,\text{tot}} = 376$ mm^2/m, corresponding to mesh #6150 on both wall faces. The eccentricity is taken as $e_0 = l_0/400$.

Table C.32: Design axial resistance N_{Rd} for reinforced wall strips with concrete class C12/15 and $A_{s,\text{tot}} = 376$ mm^2/m, corresponding to mesh #6150 on both wall faces. Values are given in kN/m.

t [mm] / l_0 [m]	2.0	2.1	2.2	2.3	2.4	2.5	2.6	2.7	2.8	2.9	3.0	3.1	3.2	3.3	3.4	3.5	3.6	3.7	3.8	3.9	4.0
120	565.8	501.4	444.2	394.7	348.8	309.1	275.6	247.2	223.0	202.2	184.3	168.7	155.0	143.0	132.3	122.8	114.4	106.8	99.9	93.7	88.1
140	842.3	791.4	735.7	683.7	630.5	568.9	513.5	464.5	417.6	376.4	340.4	309.2	282.1	258.4	237.6	219.2	203.0	188.5	175.5	163.9	153.4
150	981.2	925.9	876.8	820.0	766.1	715.7	658.9	598.6	544.1	494.8	447.7	406.2	369.7	337.6	309.4	284.6	262.7	243.3	225.9	210.4	196.5
160	1111.1	1061.2	1007.6	952.2	903.6	848.3	795.9	746.9	685.3	626.1	572.4	522.6	475.5	433.9	397.1	364.3	335.3	309.6	286.8	266.4	248.2
180	1341.9	1304.4	1262.7	1216.5	1166.1	1112.8	1067.8	1011.3	956.4	903.9	854.3	794.7	732.9	675.8	623.5	572.1	525.6	483.9	446.6	413.2	383.3

Note. The eccentricity is taken as $e_0 = l_0/400$.

C20/25

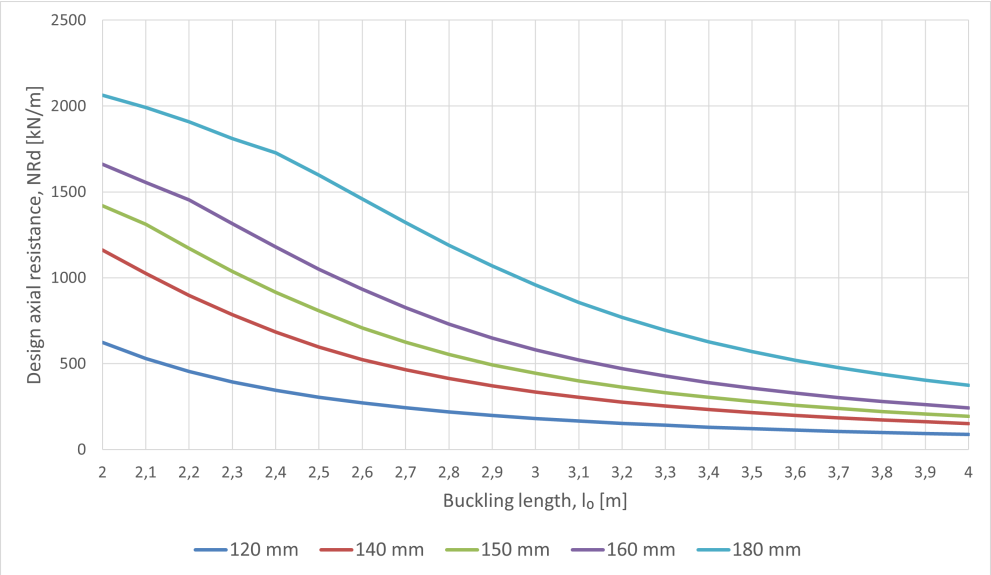

Figure C.38: Design axial resistance N_{Rd} for reinforced wall strips with concrete class C20/25 and $A_{s,\text{tot}} = 376$ mm^2/m, corresponding to mesh #6150 on both wall faces. The eccentricity is taken as $e_0 = l_0/400$.

Table C.33: Design axial resistance N_{Rd} for reinforced wall strips with concrete class C20/25 and $A_{s,\text{tot}} = 376$ mm^2/m, corresponding to mesh #6150 on both wall faces. Values are given in kN/m.

t [mm] / l_0 [m]	2.0	2.1	2.2	2.3	2.4	2.5	2.6	2.7	2.8	2.9	3.0	3.1	3.2	3.3	3.4	3.5	3.6	3.7	3.8	3.9	4.0
120	623.3	529.9	454.9	394.5	345.4	305.0	271.5	243.4	219.6	199.2	181.6	166.3	152.8	141.1	130.6	121.4	113.1	105.6	98.9	92.8	87.3
140	1162.5	1024.4	897.0	785.4	683.7	596.9	524.4	464.2	413.7	371.1	334.9	303.8	277.0	253.8	233.4	215.4	199.6	185.4	172.8	161.4	151.2
150	1420.5	1310.5	1171.5	1037.5	915.8	807.3	708.6	624.9	554.0	494.2	443.6	400.5	363.4	331.4	303.6	279.2	257.7	238.7	221.8	206.7	193.2
160	1662.1	1554.6	1453.8	1316.3	1178.8	1049.4	933.1	825.7	730.9	650.1	580.8	521.7	471.2	427.7	390.1	357.4	328.7	303.4	281.0	261.1	243.3
180	2062.8	1992.2	1908.8	1811.0	1727.9	1597.0	1458.9	1320.9	1189.9	1070.2	958.1	857.1	769.3	693.3	627.5	570.1	520.3	476.8	438.5	404.9	375.0

Note. The eccentricity is taken as $e_0 = l_0/400$.

C30/37

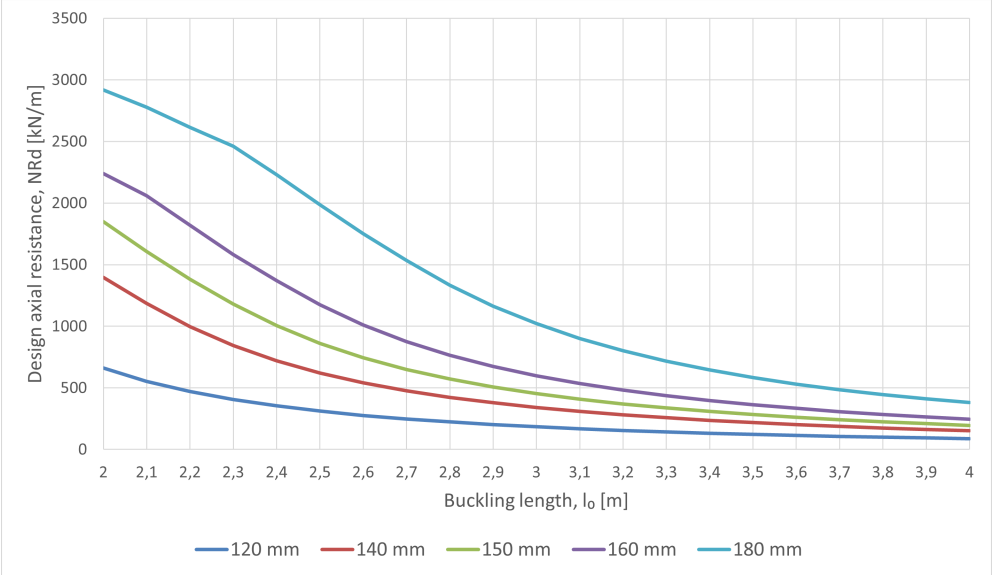

Figure C.39: Design axial resistance N_{Rd} for reinforced wall strips with concrete class C30/37 and $A_{s,\text{tot}} = 376$ mm^2/m, corresponding to mesh #6150 on both wall faces. The eccentricity is taken as $e_0 = l_0/400$.

Table C.34: Design axial resistance N_{Rd} for reinforced wall strips with concrete class C30/37 and $A_{s,\text{tot}} = 376$ mm^2/m, corresponding to mesh #6150 on both wall faces. Values are given in kN/m.

t [mm] / l_0 [m]	2.0	2.1	2.2	2.3	2.4	2.5	2.6	2.7	2.8	2.9	3.0	3.1	3.2	3.3	3.4	3.5	3.6	3.7	3.8	3.9	4.0
120	660.9	554.2	471.6	406.6	354.5	312.2	277.1	248.1	223.5	202.6	184.5	168.9	155.2	143.2	132.6	123.1	114.6	107.1	100.2	94.0	88.4
140	1397.0	1185.1	997.3	842.9	719.7	621.4	542.1	477.3	423.8	379.2	341.5	309.3	281.5	257.6	236.8	218.4	202.2	187.8	175.0	163.5	153.1
150	1850.0	1608.5	1381.8	1180.1	1004.2	860.2	743.8	649.2	571.8	507.7	454.1	408.9	370.3	337.2	308.5	283.2	261.3	241.9	224.7	209.3	195.5
160	2239.8	2059.2	1818.7	1582.4	1368.9	1173.9	1010.4	875.6	765.0	674.0	598.6	535.3	481.9	436.4	397.2	363.3	333.8	307.8	284.7	264.4	246.3
180	2917.5	2779.6	2613.5	2461.1	2229.9	1987.2	1751.1	1535.2	1334.7	1164.3	1021.4	901.5	801.1	716.6	645.0	583.8	531.2	485.7	446.0	411.1	380.3

Note. The eccentricity is taken as $e_0 = l_0/400$.

The following figures and tables show the design axial resistance for reinforced wall strips with a constant total vertical reinforcement amount of $A_{s,\text{tot}} = 670$ mm^2/m, corresponding to mesh #8150 placed on both wall faces.

C12/15

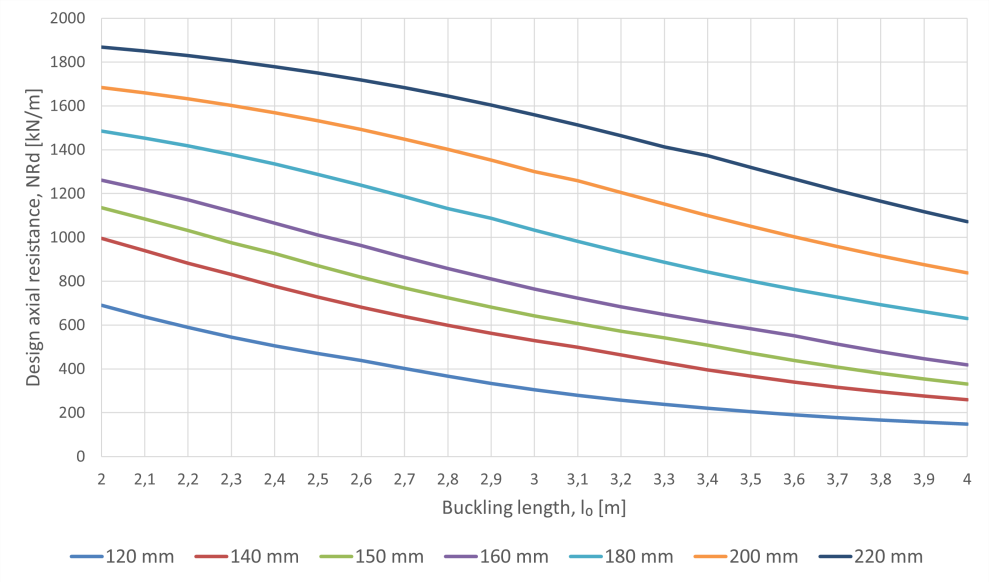

Figure C.40: Design axial resistance N_{Rd} for reinforced wall strips with concrete class C12/15 and $A_{s,\text{tot}} = 670$ mm^2/m, corresponding to mesh #8150 on both wall faces. The eccentricity is taken as $e_0 = l_0/400$.

Table C.35: Design axial resistance N_{Rd} for reinforced wall strips with concrete class C12/15 and $A_{s,\text{tot}} = 670$ mm^2/m, corresponding to mesh #8150 on both wall faces. Values are given in kN/m.

t [mm] / l_0 [m]	2.0	2.1	2.2	2.3	2.4	2.5	2.6	2.7	2.8	2.9	3.0	3.1	3.2	3.3	3.4	3.5	3.6	3.7	3.8	3.9	4.0
120	689.9	636.9	588.7	545.0	505.7	470.1	438.0	401.5	366.6	333.8	305.1	279.9	257.7	238.1	220.6	205.0	191.1	178.5	167.2	156.9	147.6
140	995.1	938.8	882.2	831.6	777.8	727.6	681.1	638.3	598.9	562.8	529.7	499.2	464.4	428.8	396.1	366.7	340.3	316.6	295.4	276.2	258.8
150	1135.0	1084.6	1030.7	975.3	926.2	871.1	818.7	769.6	723.9	681.5	642.3	606.2	572.7	541.9	508.8	472.4	438.4	407.8	379.8	354.5	331.7
160	1261.1	1218.0	1170.6	1119.2	1065.4	1010.7	962.9	909.1	858.0	809.9	764.9	723.0	684.0	647.9	614.3	583.1	551.0	513.8	478.7	446.8	417.8
180	1485.2	1453.1	1417.3	1377.7	1334.7	1287.9	1237.8	1185.4	1132.1	1086.7	1033.2	981.7	932.7	886.4	842.7	801.7	763.2	727.2	693.4	661.8	629.5
200	1684.5	1660.2	1633.0	1602.7	1569.0	1532.0	1491.8	1448.5	1401.8	1352.3	1300.8	1259.3	1205.1	1151.8	1100.3	1050.7	1003.5	958.5	916.0	875.8	837.8
220	1869.0	1850.6	1829.2	1805.5	1779.1	1749.9	1717.8	1682.6	1644.5	1603.6	1559.9	1513.0	1463.7	1412.8	1373.1	1319.3	1266.3	1214.8	1164.9	1117.0	1071.1

Note. The eccentricity is taken as $e_0 = l_0/400$.

C20/25

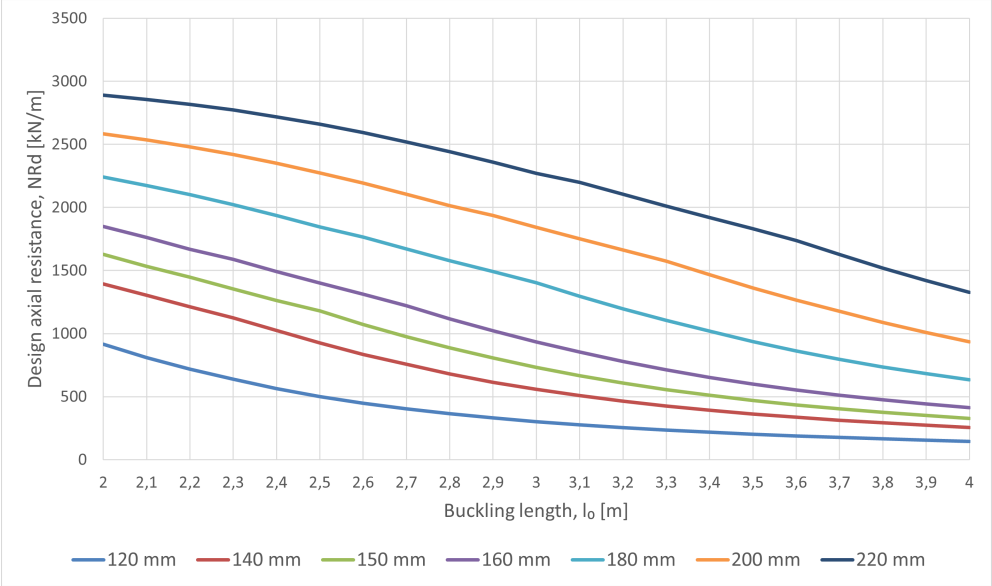

Figure C.41: Design axial resistance N_{Rd} for reinforced wall strips with concrete class C20/25 and $A_{s,\text{tot}} = 670$ mm^2/m, corresponding to mesh #8150 on both wall faces. The eccentricity is taken as $e_0 = l_0/400$.

Table C.36: Design axial resistance N_{Rd} for reinforced wall strips with concrete class C20/25 and $A_{s,\text{tot}} = 670$ mm^2/m, corresponding to mesh #8150 on both wall faces. Values are given in kN/m.

t [mm] / l_0 [m]	2.0	2.1	2.2	2.3	2.4	2.5	2.6	2.7	2.8	2.9	3.0	3.1	3.2	3.3	3.4	3.5	3.6	3.7	3.8	3.9	4.0
120	914.3	809.2	717.3	637.1	563.7	501.0	447.9	402.8	364.2	331.0	302.2	277.1	255.1	235.6	218.3	203.0	189.2	176.8	165.6	155.5	146.3
140	1391.9	1304.9	1211.6	1125.0	1024.1	924.3	835.2	755.9	680.7	614.6	557.3	507.5	464.0	425.9	392.4	362.7	336.4	312.9	291.8	272.8	255.7
150	1627.2	1532.4	1447.9	1352.4	1262.3	1178.4	1072.1	974.5	886.8	806.9	731.6	665.3	606.7	555.3	510.1	470.2	434.9	403.4	375.3	350.1	327.4
160	1848.5	1761.9	1669.6	1588.5	1491.8	1399.2	1311.8	1220.9	1116.5	1020.9	934.5	853.7	778.5	712.0	652.9	600.3	553.8	512.4	475.5	442.5	412.9
180	2240.4	2175.0	2102.6	2022.3	1935.2	1843.8	1765.8	1670.5	1578.5	1490.8	1403.5	1296.2	1196.0	1104.0	1019.6	936.9	862.6	796.0	736.3	682.7	634.3
200	2583.9	2536.9	2481.0	2418.5	2349.6	2274.2	2191.8	2104.0	2013.0	1937.5	1843.1	1751.5	1663.8	1575.0	1465.5	1362.0	1265.6	1176.7	1089.7	1009.0	935.9
220	2890.5	2855.6	2817.4	2773.4	2718.9	2658.5	2592.2	2520.2	2441.8	2357.6	2269.2	2199.9	2104.7	2011.0	1919.9	1832.1	1737.6	1626.2	1520.0	1420.1	1327.1

Note. The eccentricity is taken as $e_0 = l_0/400$.

C30/37

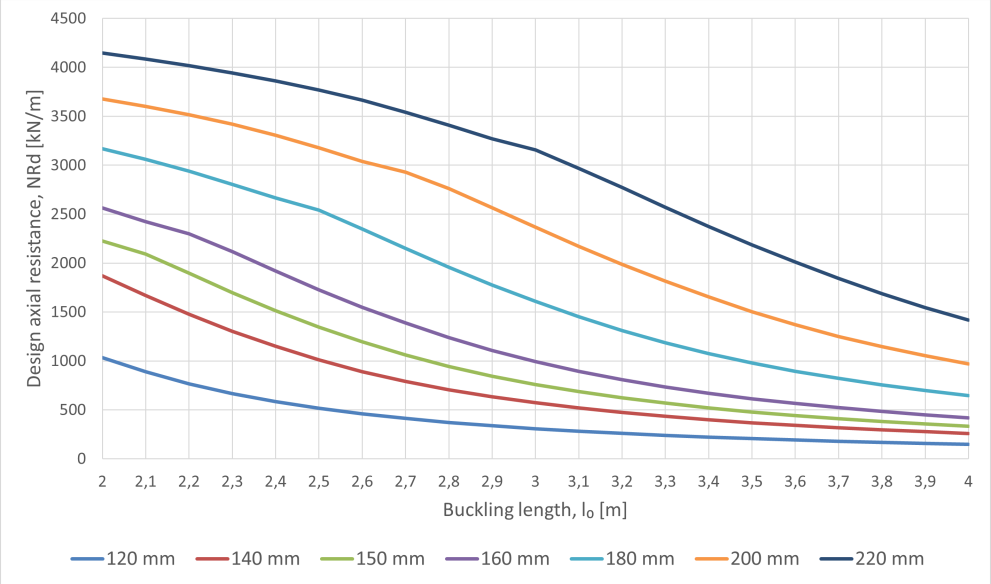

Figure C.42: Design axial resistance N_{Rd} for reinforced wall strips with concrete class C30/37 and $A_{s,\text{tot}} = 670$ mm^2/m, corresponding to mesh #8150 on both wall faces. The eccentricity is taken as $e_0 = l_0/400$.

Table C.37: Design axial resistance N_{Rd} for reinforced wall strips with concrete class C30/37 and $A_{s,\text{tot}} = 670$ mm^2/m, corresponding to mesh #8150 on both wall faces. Values are given in kN/m.

t [mm] / l_0 [m]	2.0	2.1	2.2	2.3	2.4	2.5	2.6	2.7	2.8	2.9	3.0	3.1	3.2	3.3	3.4	3.5	3.6	3.7	3.8	3.9	4.0
120	1033.8	890.5	766.9	666.3	584.1	516.3	459.8	412.3	372.1	337.6	307.8	281.9	259.2	239.3	221.5	205.8	191.7	179.1	167.7	157.4	148.0
140	1868.2	1667.5	1475.6	1302.3	1151.2	1011.2	891.2	790.4	705.4	633.4	572.1	519.3	473.7	434.0	399.3	368.7	341.6	317.4	295.8	276.5	259.0
150	2227.0	2093.2	1895.5	1698.3	1513.2	1346.9	1197.7	1061.3	944.1	844.0	758.7	685.6	622.7	568.2	520.7	479.1	442.4	409.9	380.9	355.1	331.8
160	2563.2	2422.6	2298.1	2117.0	1918.7	1726.0	1547.5	1387.6	1238.9	1106.5	992.0	893.0	807.7	734.0	670.1	614.2	565.2	522.0	483.7	449.5	419.0
180	3167.7	3060.7	2938.2	2804.4	2663.6	2541.1	2348.2	2150.2	1956.4	1774.2	1608.0	1452.5	1309.9	1184.8	1075.3	979.4	895.0	821.1	756.0	698.4	647.3
200	3675.7	3600.3	3516.0	3420.3	3304.2	3176.5	3040.3	2928.6	2760.4	2565.4	2366.4	2171.1	1985.9	1814.8	1653.4	1502.9	1369.0	1250.5	1145.7	1053.0	970.5
220	4147.5	4086.1	4018.4	3943.5	3860.6	3769.0	3663.9	3541.5	3409.9	3269.4	3157.1	2968.8	2771.0	2570.3	2373.1	2185.2	2010.2	1843.1	1686.3	1545.3	1419.2

Note. The eccentricity is taken as $e_0 = l_0/400$.

The following figures and tables show the design axial resistance for reinforced wall strips with a constant total vertical reinforcement amount of $A_{s,\text{tot}} = 848$ mm^2/m, corresponding to mesh #9150 placed on both wall faces.

C12/15

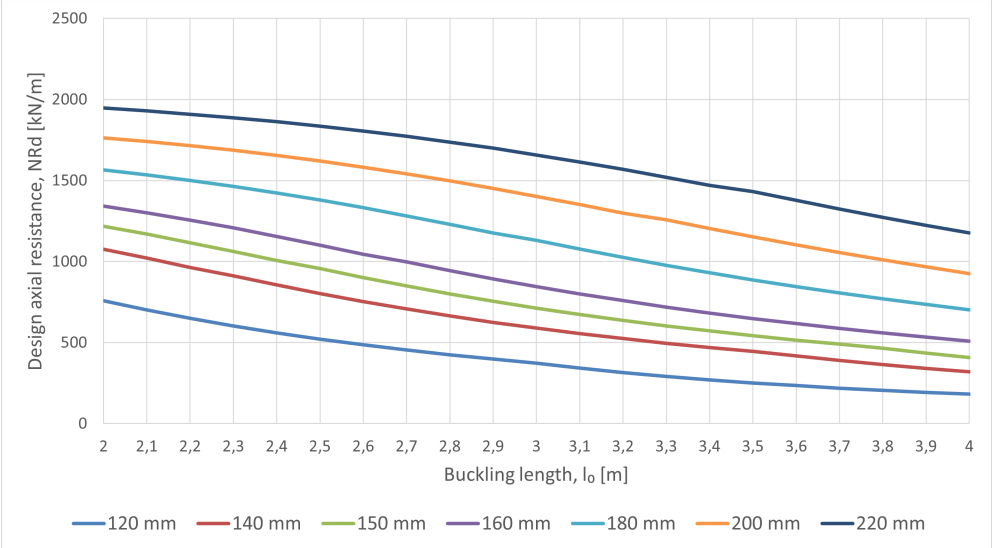

Figure C.43: Design axial resistance N_{Rd} for reinforced wall strips with concrete class C12/15 and $A_{s,\text{tot}} = 848$ mm^2/m, corresponding to mesh #9150 on both wall faces. The eccentricity is taken as $e_0 = l_0/400$.

Table C.38: Design axial resistance N_{Rd} for reinforced wall strips with concrete class C12/15 and $A_{s,\text{tot}} = 848$ mm^2/m, corresponding to mesh #9150 on both wall faces. Values are given in kN/m.

t [mm] / l_0 [m]	2.0	2.1	2.2	2.3	2.4	2.5	2.6	2.7	2.8	2.9	3.0	3.1	3.2	3.3	3.4	3.5	3.6	3.7	3.8	3.9	4.0
120	758.0	701.5	649.7	602.5	559.7	520.9	485.8	453.9	424.5	397.9	371.7	341.9	315.2	291.4	270.2	251.3	234.3	219.0	205.1	192.6	181.2
140	1076.5	1020.8	963.5	912.3	855.9	802.6	752.8	706.6	664.0	624.7	588.5	555.2	524.4	496.0	469.8	445.0	417.6	389.1	363.3	340.0	318.8
150	1216.5	1168.5	1116.2	1061.2	1005.3	955.8	901.0	849.0	800.1	754.6	712.2	672.8	636.4	602.6	571.3	542.2	515.2	489.9	465.3	435.7	408.4
160	1342.5	1301.2	1256.2	1207.2	1154.7	1100.4	1045.7	997.7	944.2	893.3	845.3	800.3	758.2	718.9	682.3	648.3	616.5	586.9	559.3	533.4	508.1
180	1565.0	1534.8	1501.1	1463.8	1423.0	1379.0	1331.6	1281.1	1228.8	1175.7	1130.4	1077.2	1025.9	976.9	930.4	886.4	844.9	806.0	769.3	734.9	702.6
200	1763.0	1740.1	1714.5	1686.2	1654.7	1620.2	1582.4	1541.7	1498.2	1451.5	1402.3	1351.2	1299.3	1256.4	1203.5	1152.1	1102.6	1055.1	1009.9	966.9	926.1
220	1947.6	1929.3	1909.1	1886.8	1862.2	1835.0	1805.2	1772.6	1737.1	1698.8	1657.9	1614.4	1568.1	1519.5	1469.3	1430.6	1377.4	1324.9	1273.5	1223.6	1175.6

Note. The eccentricity is taken as $e_0 = l_0/400$.

C20/25

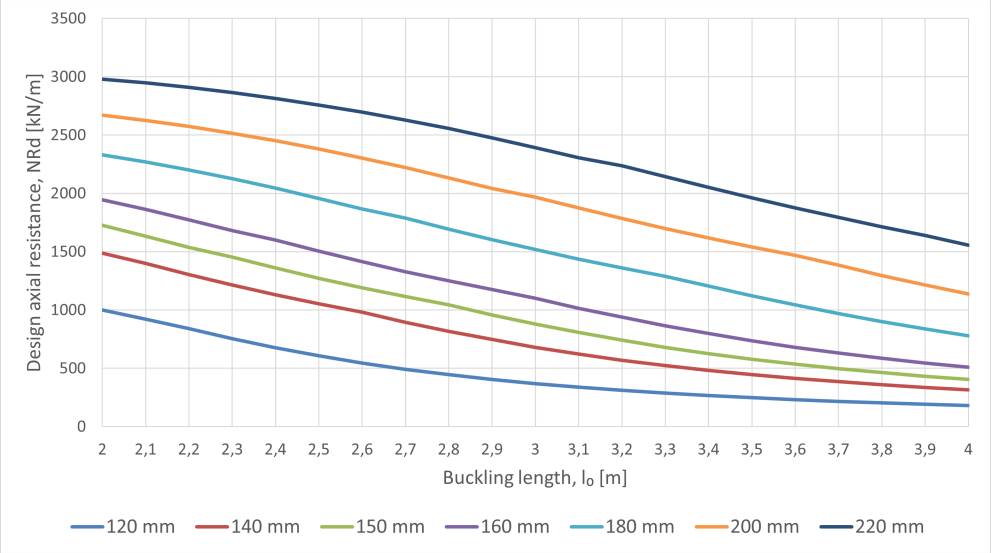

Figure C.44: Design axial resistance N_{Rd} for reinforced wall strips with concrete class C20/25 and $A_{s,\text{tot}} = 848$ mm^2/m, corresponding to mesh #9150 on both wall faces. The eccentricity is taken as $e_0 = l_0/400$.

Table C.39: Design axial resistance N_{Rd} for reinforced wall strips with concrete class C20/25 and $A_{s,\text{tot}} = 848$ mm^2/m, corresponding to mesh #9150 on both wall faces. Values are given in kN/m.

t [mm] / l_0 [m]	2.0	2.1	2.2	2.3	2.4	2.5	2.6	2.7	2.8	2.9	3.0	3.1	3.2	3.3	3.4	3.5	3.6	3.7	3.8	3.9	4.0
120	1000.8	920.2	840.5	753.2	675.9	607.9	545.0	491.2	444.8	404.7	369.8	339.3	312.5	288.8	267.8	249.0	232.1	217.0	203.3	190.9	179.6
140	1486.9	1400.3	1304.2	1213.9	1130.3	1053.6	980.9	894.5	817.2	747.3	680.5	621.2	569.0	523.0	482.4	446.3	414.2	385.4	359.6	336.4	315.4
150	1724.9	1632.3	1537.3	1452.8	1359.8	1272.3	1190.9	1115.8	1042.7	957.1	879.7	808.8	741.0	680.5	626.3	578.2	535.4	497.1	462.8	432.0	404.2
160	1944.0	1862.2	1773.2	1680.3	1598.8	1504.1	1413.8	1328.7	1249.4	1175.7	1100.1	1015.2	938.0	866.0	797.4	735.9	680.7	630.8	586.1	546.0	509.9
180	2330.8	2269.4	2201.1	2126.2	2044.0	1956.1	1865.0	1787.2	1693.7	1603.6	1517.8	1436.9	1360.9	1289.9	1203.9	1120.5	1043.9	969.4	900.0	837.0	779.9
200	2672.4	2626.1	2573.9	2515.5	2451.0	2380.5	2303.8	2220.8	2133.3	2043.2	1968.4	1875.7	1785.9	1699.8	1617.8	1540.2	1467.0	1383.9	1295.7	1213.9	1136.7
220	2979.7	2947.5	2910.3	2864.9	2814.1	2757.9	2696.0	2628.6	2556.0	2477.3	2393.4	2305.9	2237.5	2144.0	2051.9	1962.4	1876.0	1793.3	1714.5	1639.8	1556.1

Note. The eccentricity is taken as $e_0 = l_0/400$.

C30/37

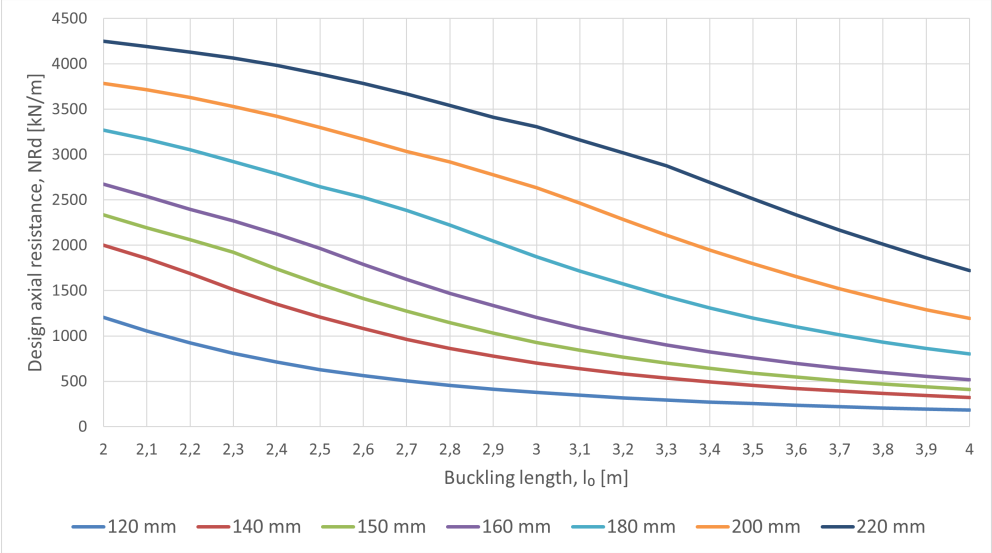

Figure C.45: Design axial resistance N_{Rd} for reinforced wall strips with concrete class C30/37 and $A_{s,\text{tot}} = 848$ mm^2/m, corresponding to mesh #9150 on both wall faces. The eccentricity is taken as $e_0 = l_0/400$.

Table C.40: Design axial resistance N_{Rd} for reinforced wall strips with concrete class C30/37 and $A_{s,\text{tot}} = 848$ mm^2/m, corresponding to mesh #9150 on both wall faces. Values are given in kN/m.

t [mm] / l_0 [m]	2.0	2.1	2.2	2.3	2.4	2.5	2.6	2.7	2.8	2.9	3.0	3.1	3.2	3.3	3.4	3.5	3.6	3.7	3.8	3.9	4.0
120	1204.4	1054.2	924.7	807.4	710.1	629.2	561.3	504.0	455.1	413.2	377.0	345.5	317.8	293.4	271.8	252.6	235.4	219.9	205.8	193.2	181.7
140	2000.1	1854.2	1687.2	1510.2	1349.6	1207.7	1079.1	962.0	861.5	775.5	701.6	637.8	582.4	534.1	491.7	454.2	421.0	391.4	364.9	341.1	319.6
150	2336.0	2191.2	2062.2	1921.3	1739.6	1568.0	1412.3	1273.9	1144.5	1029.1	928.1	840.7	765.0	699.0	641.3	590.6	545.7	505.9	470.4	438.6	410.0
160	2671.6	2535.7	2393.5	2267.9	2124.1	1966.4	1787.7	1621.1	1469.7	1334.4	1204.1	1089.9	989.5	901.4	824.3	756.7	697.1	644.4	597.5	555.7	518.2
180	3269.6	3166.0	3050.9	2923.5	2787.2	2646.5	2525.2	2383.0	2223.8	2043.9	1873.2	1715.3	1571.7	1434.4	1308.8	1197.3	1098.4	1010.5	932.0	862.3	800.1
200	3782.8	3714.2	3628.1	3528.9	3419.8	3299.4	3169.2	3032.5	2919.6	2774.8	2633.8	2464.7	2283.4	2109.6	1946.8	1796.7	1653.6	1519.1	1398.2	1289.7	1192.6
220	4248.0	4191.6	4129.7	4061.7	3982.9	3886.8	3781.8	3667.0	3542.3	3409.9	3307.2	3162.0	3018.3	2877.6	2692.5	2509.5	2333.0	2166.2	2010.9	1862.7	1720.9

Note. The eccentricity is taken as $e_0 = l_0/400$.

The following figures and tables show the design axial resistance for reinforced wall strips with a constant total vertical reinforcement amount of $A_{s,\text{tot}} = 1048$ mm^2/m, corresponding to mesh #10150 placed on both wall faces.

C12/15

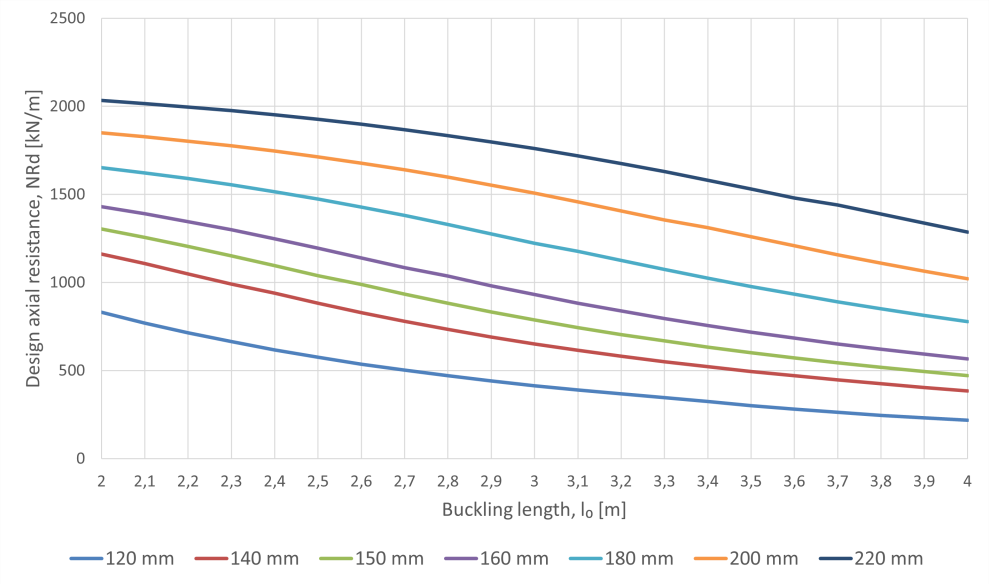

Figure C.46: Design axial resistance N_{Rd} for reinforced wall strips with concrete class C12/15 and $A_{s,\text{tot}} = 1048$ mm^2/m, corresponding to mesh #10150 on both wall faces. The eccentricity is taken as $e_0 = l_0/400$.

Table C.41: Design axial resistance N_{Rd} for reinforced wall strips with concrete class C12/15 and $A_{s,\text{tot}} = 1048$ mm^2/m, corresponding to mesh #10150 on both wall faces. Values are given in kN/m.

t [mm] / l_0 [m]	2.0	2.1	2.2	2.3	2.4	2.5	2.6	2.7	2.8	2.9	3.0	3.1	3.2	3.3	3.4	3.5	3.6	3.7	3.8	3.9	4.0
120	829.9	770.0	714.4	663.6	617.2	575.0	536.7	501.8	469.8	440.5	413.8	389.4	367.1	346.2	323.2	300.8	280.6	262.3	245.8	230.9	217.2
140	1161.7	1106.5	1048.8	990.5	938.3	882.0	829.0	779.5	733.5	690.9	651.5	615.1	581.5	550.4	521.6	494.9	470.1	446.8	424.4	403.4	383.5
150	1302.8	1256.1	1205.2	1150.9	1094.6	1038.0	987.9	933.1	881.2	832.4	786.8	744.2	704.6	667.8	633.6	601.8	572.2	544.6	518.8	494.8	471.4
160	1429.2	1389.3	1345.7	1298.5	1247.5	1193.8	1138.8	1083.6	1035.2	981.7	930.8	882.7	837.5	795.1	755.4	718.3	683.7	651.3	621.0	592.7	566.2
180	1651.2	1622.4	1590.2	1554.7	1515.7	1473.5	1428.3	1379.9	1328.8	1276.2	1222.9	1177.4	1124.2	1072.8	1023.6	976.8	932.4	890.5	850.9	813.5	778.4
200	1848.7	1826.8	1802.5	1775.6	1745.9	1713.2	1677.5	1638.9	1597.4	1553.3	1506.4	1457.1	1406.1	1354.3	1311.6	1258.8	1207.4	1157.7	1109.9	1064.2	1020.6
220	2033.0	2015.4	1996.2	1975.0	1951.7	1926.1	1898.1	1867.4	1834.1	1798.0	1759.4	1718.2	1674.7	1628.7	1580.4	1530.6	1479.9	1439.8	1387.4	1336.1	1286.1

Note. The eccentricity is taken as $e_0 = l_0/400$.

C20/25

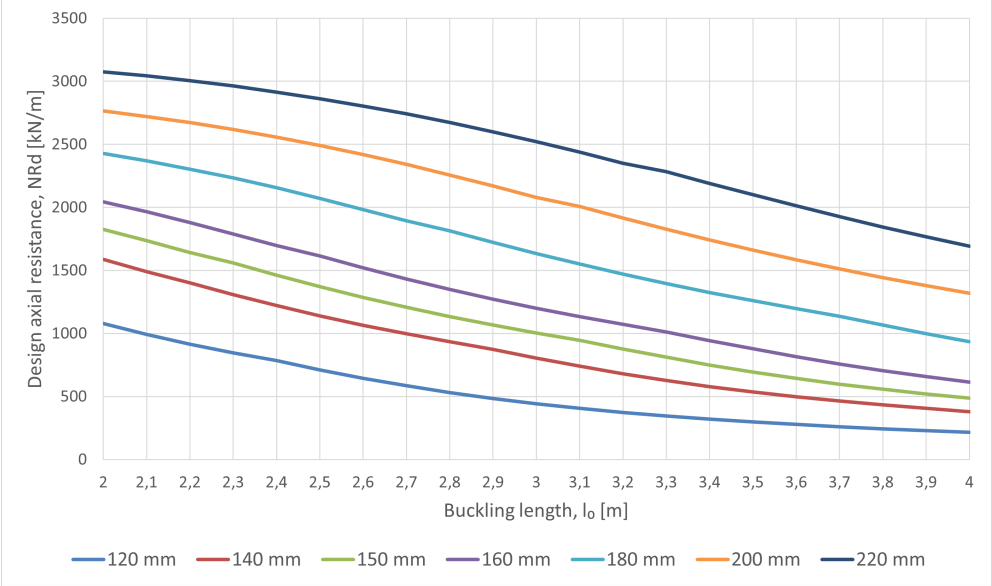

Figure C.47: Design axial resistance N_{Rd} for reinforced wall strips with concrete class C20/25 and $A_{s,\text{tot}} = 1048$ mm^2/m, corresponding to mesh #10150 on both wall faces. The eccentricity is taken as $e_0 = l_0/400$.

Table C.42: Design axial resistance N_{Rd} for reinforced wall strips with concrete class C20/25 and $A_{s,\text{tot}} = 1048$ mm^2/m, corresponding to mesh #10150 on both wall faces. Values are given in kN/m.

t [mm] / l_0 [m]	2.0	2.1	2.2	2.3	2.4	2.5	2.6	2.7	2.8	2.9	3.0	3.1	3.2	3.3	3.4	3.5	3.6	3.7	3.8	3.9	4.0
120	1078.1	992.9	916.1	847.0	784.8	709.8	643.9	584.5	530.2	483.1	441.9	405.7	373.9	345.7	320.7	298.3	278.2	260.1	243.7	228.9	215.4
140	1585.9	1488.8	1401.8	1308.1	1220.5	1139.5	1065.0	996.9	934.5	872.3	803.9	741.0	680.8	626.8	578.8	536.1	497.9	463.7	432.9	405.1	379.9
150	1825.9	1736.0	1641.8	1558.2	1462.7	1371.8	1286.5	1207.3	1134.0	1066.4	1004.2	944.8	875.3	811.5	749.6	693.8	643.3	598.0	557.2	520.5	487.3
160	2043.2	1965.6	1880.3	1789.5	1696.3	1614.4	1521.5	1433.1	1349.9	1272.2	1200.1	1133.1	1071.1	1012.7	942.5	877.7	814.3	756.9	705.0	657.5	614.6
180	2426.5	2368.6	2304.0	2233.1	2155.7	2071.7	1983.2	1892.3	1814.6	1722.6	1634.1	1549.8	1470.1	1395.3	1325.1	1259.4	1198.1	1136.9	1066.1	999.0	933.5
200	2764.9	2721.3	2672.3	2617.5	2556.8	2490.3	2418.3	2340.3	2256.8	2169.5	2080.1	2005.9	1914.6	1826.2	1741.3	1660.4	1583.6	1511.1	1442.7	1378.3	1317.7
220	3074.6	3043.3	3005.0	2962.3	2914.8	2862.2	2804.3	2741.0	2672.7	2599.4	2520.5	2436.9	2350.2	2282.4	2190.3	2099.7	2011.4	1926.1	1844.4	1766.3	1692.0

Note. The eccentricity is taken as $e_0 = l_0/400$.

C30/37

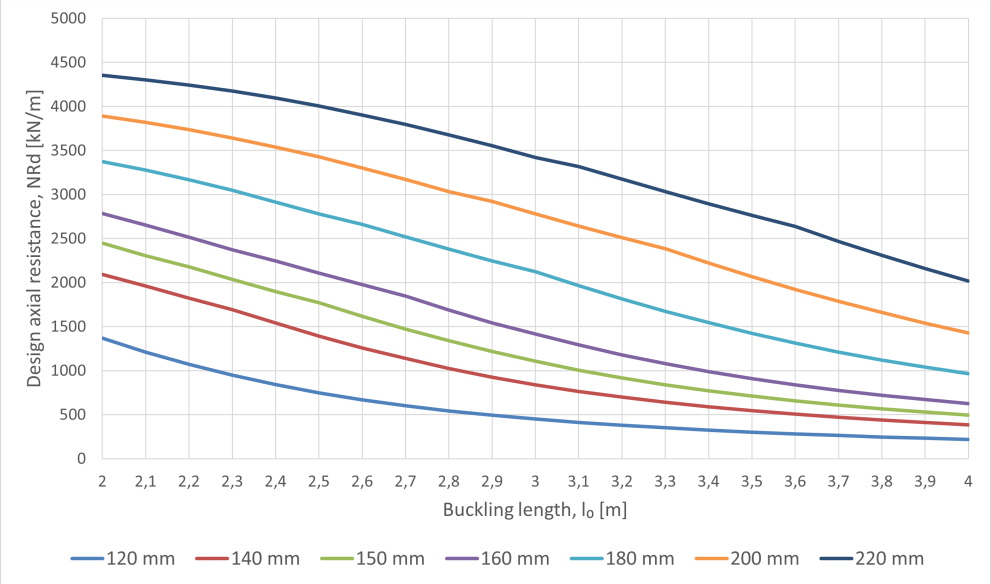

Figure C.48: Design axial resistance N_{Rd} for reinforced wall strips with concrete class C30/37 and $A_{s,\text{tot}} = 1048$ mm^2/m, corresponding to mesh #10150 on both wall faces. The eccentricity is taken as $e_0 = l_0/400$.

Table C.43: Design axial resistance N_{Rd} for reinforced wall strips with concrete class C30/37 and $A_{s,\text{tot}} = 1048$ mm^2/m, corresponding to mesh #10150 on both wall faces. Values are given in kN/m.

t [mm] / l_0 [m]	2.0	2.1	2.2	2.3	2.4	2.5	2.6	2.7	2.8	2.9	3.0	3.1	3.2	3.3	3.4	3.5	3.6	3.7	3.8	3.9	4.0
120	1369.5	1211.0	1071.7	951.0	842.2	748.2	668.8	601.3	543.6	494.0	451.0	413.4	380.5	351.4	325.7	302.7	282.1	263.6	246.9	231.8	218.0
140	2093.5	1962.1	1821.7	1691.3	1542.7	1392.3	1258.0	1139.4	1025.9	926.1	839.7	764.5	699.0	641.6	591.1	546.4	506.7	471.2	439.5	410.9	385.1
150	2449.6	2306.5	2179.0	2035.2	1899.5	1773.3	1618.4	1471.2	1338.9	1219.9	1106.1	1005.5	916.9	839.2	770.9	710.6	657.2	609.7	567.2	529.1	494.8
160	2784.0	2653.3	2514.2	2371.8	2246.4	2106.9	1975.5	1845.4	1688.2	1544.0	1413.7	1293.5	1179.8	1079.1	989.2	909.6	839.1	776.4	720.6	670.6	625.7
180	3374.8	3276.3	3167.4	3046.6	2915.6	2778.1	2660.9	2517.4	2379.0	2247.1	2122.8	1964.0	1813.2	1674.3	1547.8	1424.3	1311.7	1210.6	1120.0	1038.5	964.9
200	3892.7	3820.7	3736.7	3642.8	3539.3	3426.2	3302.5	3170.7	3034.0	2920.6	2778.7	2641.1	2509.1	2383.7	2223.2	2067.6	1922.3	1788.2	1659.7	1537.5	1426.5
220	4353.0	4300.7	4243.6	4176.2	4094.4	4003.7	3904.3	3796.4	3678.9	3552.6	3420.0	3316.2	3173.3	3032.5	2895.5	2763.5	2635.7	2468.8	2309.3	2159.0	2018.9

Note. The eccentricity is taken as $e_0 = l_0/400$.

C.2.3 Unreinforced Wall Capacity Results

C12/15

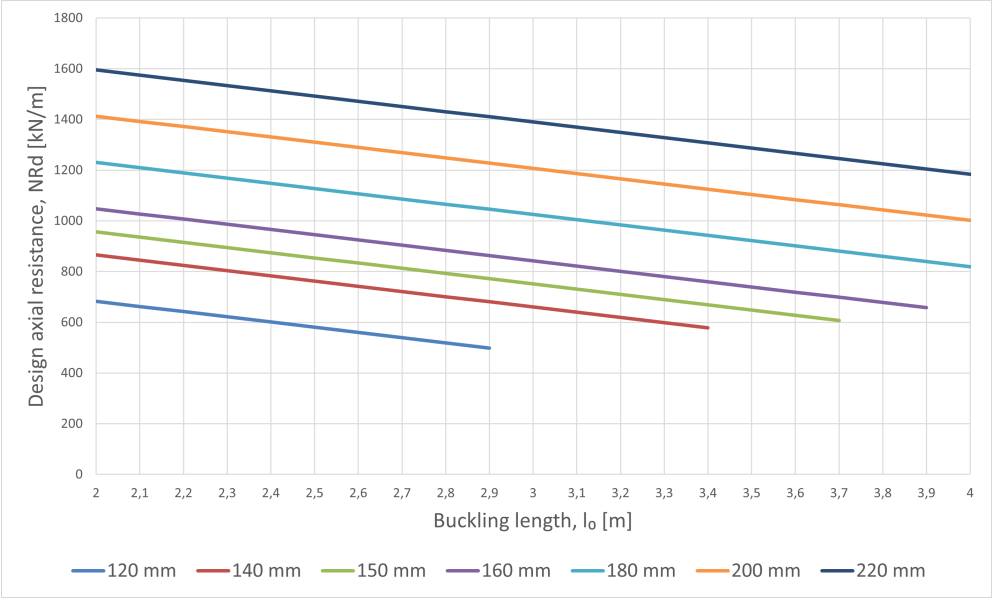

Figure C.49: Design axial resistance N_{Rd} for unreinforced wall strips with concrete class C12/15. The eccentricity is taken as $e_0 = l_0/400$.

Table C.44: Design axial resistance N_{Rd} for unreinforced wall strips with concrete class C12/15. Values are given in kN/m.

t [mm] / l_0 [m]	2.0	2.1	2.2	2.3	2.4	2.5	2.6	2.7	2.8	2.9	3.0	3.1	3.2	3.3	3.4	3.5	3.6	3.7	3.8	3.9	4.0
120	683.2	662.6	642.1	621.5	601.0	580.4	559.8	539.3	518.7	498.2											
140	865.6	845.0	824.5	803.9	783.4	762.8	742.2	721.7	701.1	680.6	660.0	639.4	618.9	598.3	577.8						
150	956.8	936.2	915.7	895.1	874.6	854.0	833.4	812.9	792.3	771.8	751.2	730.6	710.1	689.5	669.0	648.4	627.8	607.3			
160	1048.0	1027.4	1006.9	986.3	965.8	945.2	924.6	904.1	883.5	863.0	842.4	821.8	801.3	780.7	760.2	739.6	719.0	698.5	677.9	657.4	
180	1230.4	1209.8	1189.3	1168.7	1148.2	1127.6	1107.0	1086.5	1065.9	1045.4	1024.8	1004.2	983.7	963.1	942.6	922.0	901.4	880.9	860.3	839.8	819.2
200	1412.8	1392.2	1371.7	1351.1	1330.6	1310.0	1289.4	1268.9	1248.3	1227.8	1207.2	1186.6	1166.1	1145.5	1125.0	1104.4	1083.8	1063.3	1042.7	1022.2	1001.6
220	1595.2	1574.6	1554.1	1533.5	1513.0	1492.4	1471.8	1451.3	1430.7	1410.2	1389.6	1369.0	1348.5	1327.9	1307.4	1286.8	1266.2	1245.7	1225.1	1204.6	1184.0

Note. Empty cells indicate combinations outside the adopted validity range for the unreinforced wall model.

C20/25

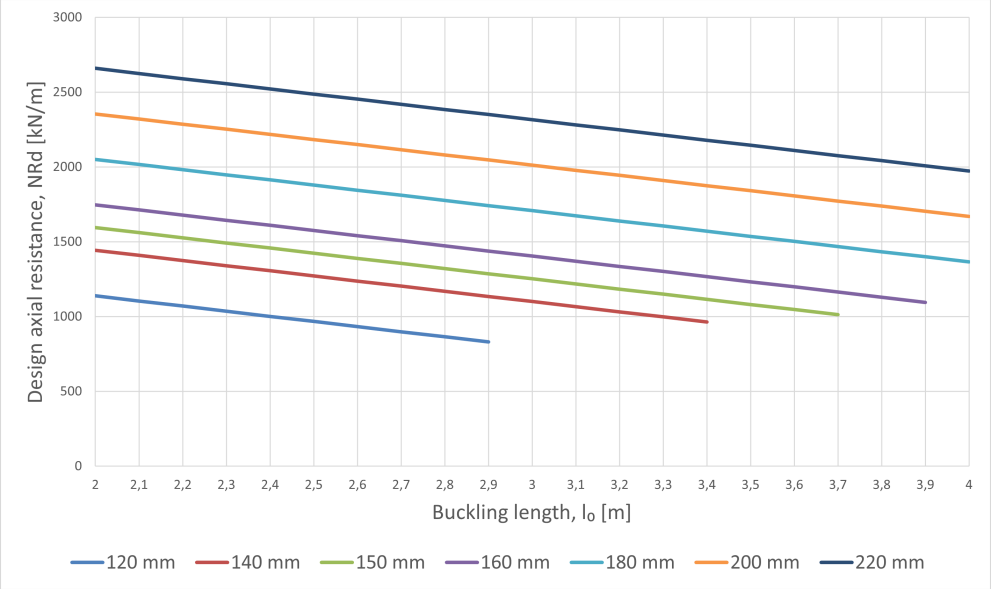

Figure C.50: Design axial resistance N_{Rd} for unreinforced wall strips with concrete class C20/25. The eccentricity is taken as $e_0 = l_0/400$.

Table C.45: Design axial resistance N_{Rd} for unreinforced wall strips with concrete class C20/25. Values are given in kN/m.

t [mm] / l_0 [m]	2.0	2.1	2.2	2.3	2.4	2.5	2.6	2.7	2.8	2.9	3.0	3.1	3.2	3.3	3.4	3.5	3.6	3.7	3.8	3.9	4.0
120	1138.7	1104.4	1070.1	1035.9	1001.6	967.3	933.1	898.8	864.5	830.3											
140	1442.7	1408.4	1374.1	1339.9	1305.6	1271.3	1237.1	1202.8	1168.5	1134.3	1100.0	1065.7	1031.5	997.2	962.9						
150	1594.7	1560.4	1526.1	1491.9	1457.6	1423.3	1389.1	1354.8	1320.5	1286.3	1252.0	1217.7	1183.5	1149.2	1114.9	1080.7	1046.4	1012.1			
160	1746.7	1712.4	1678.1	1643.9	1609.6	1575.3	1541.1	1506.8	1472.5	1438.3	1404.0	1369.7	1335.5	1301.2	1266.9	1232.7	1198.4	1164.1	1129.9	1095.6	
180	2050.7	2016.4	1982.1	1947.9	1913.6	1879.3	1845.1	1810.8	1776.5	1742.3	1708.0	1673.7	1639.5	1605.2	1570.9	1536.7	1502.4	1468.1	1433.9	1399.6	1365.3
200	2354.7	2320.4	2286.1	2251.9	2217.6	2183.3	2149.1	2114.8	2080.5	2046.3	2012.0	1977.7	1943.5	1909.2	1874.9	1840.7	1806.4	1772.1	1737.9	1703.6	1669.3
220	2658.7	2624.4	2590.1	2555.9	2521.6	2487.3	2453.1	2418.8	2384.5	2350.3	2316.0	2281.7	2247.5	2213.2	2178.9	2144.7	2110.4	2076.1	2041.9	2007.6	1973.3

Note. Empty cells indicate combinations outside the adopted validity range for the unreinforced wall model.

C30/37

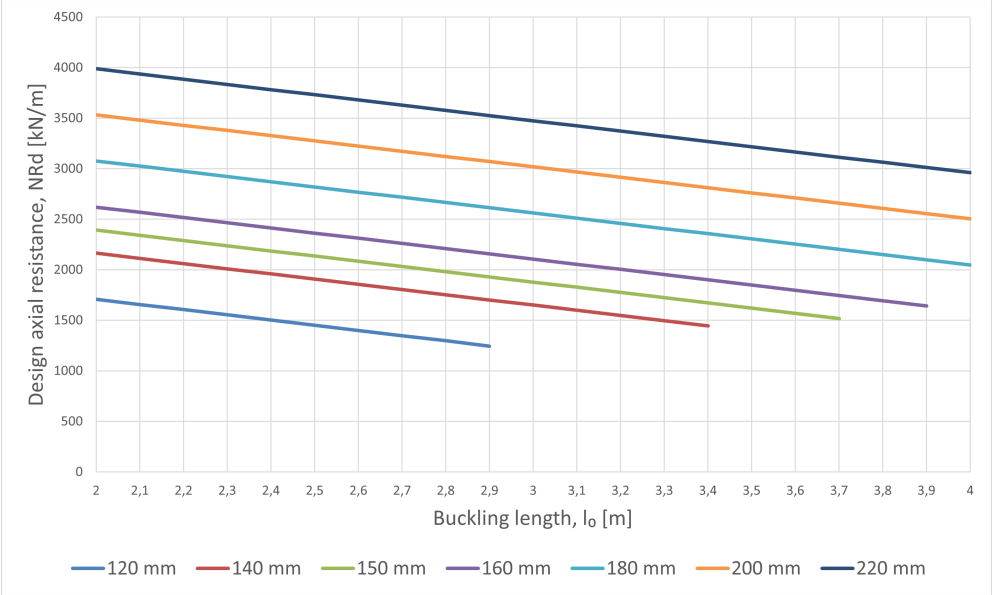

Figure C.51: Design axial resistance N_{Rd} for unreinforced wall strips with concrete class C30/37. The eccentricity is taken as $e_0 = l_0/400$.

Table C.46: Design axial resistance N_{Rd} for unreinforced wall strips with concrete class C30/37. Values are given in kN/m.

t [mm] / l_0 [m]	2.0	2.1	2.2	2.3	2.4	2.5	2.6	2.7	2.8	2.9	3.0	3.1	3.2	3.3	3.4	3.5	3.6	3.7	3.8	3.9	4.0
120	1708.0	1656.6	1605.2	1553.8	1502.4	1451.0	1399.6	1348.2	1296.8	1245.4											
140	2164.0	2112.6	2061.2	2009.8	1958.4	1907.0	1855.6	1804.2	1752.8	1701.4	1650.0	1598.6	1547.2	1495.8	1444.4						
150	2392.0	2340.6	2289.2	2237.8	2186.4	2135.0	2083.6	2032.2	1980.8	1929.4	1878.0	1826.6	1775.2	1723.8	1672.4	1621.0	1569.6	1518.2			
160	2620.0	2568.6	2517.2	2465.8	2414.4	2363.0	2311.6	2260.2	2208.8	2157.4	2106.0	2054.6	2003.2	1951.8	1900.4	1849.0	1797.6	1746.2	1694.8	1643.4	
180	3076.0	3024.6	2973.2	2921.8	2870.4	2819.0	2767.6	2716.2	2664.8	2613.4	2562.0	2510.6	2459.2	2407.8	2356.4	2305.0	2253.6	2202.2	2150.8	2099.4	2048.0
200	3532.0	3480.6	3429.2	3377.8	3326.4	3275.0	3223.6	3172.2	3120.8	3069.4	3018.0	2966.6	2915.2	2863.8	2812.4	2761.0	2709.6	2658.2	2606.8	2555.4	2504.0
220	3988.0	3936.6	3885.2	3833.8	3782.4	3731.0	3679.6	3628.2	3576.8	3525.4	3474.0	3422.6	3371.2	3319.8	3268.4	3217.0	3165.6	3114.2	3062.8	3011.4	2960.0

Note. Empty cells indicate combinations outside the adopted validity range for the unreinforced wall model.

Appendix D

Drawings

D.1 Cykelskrapan Drawings

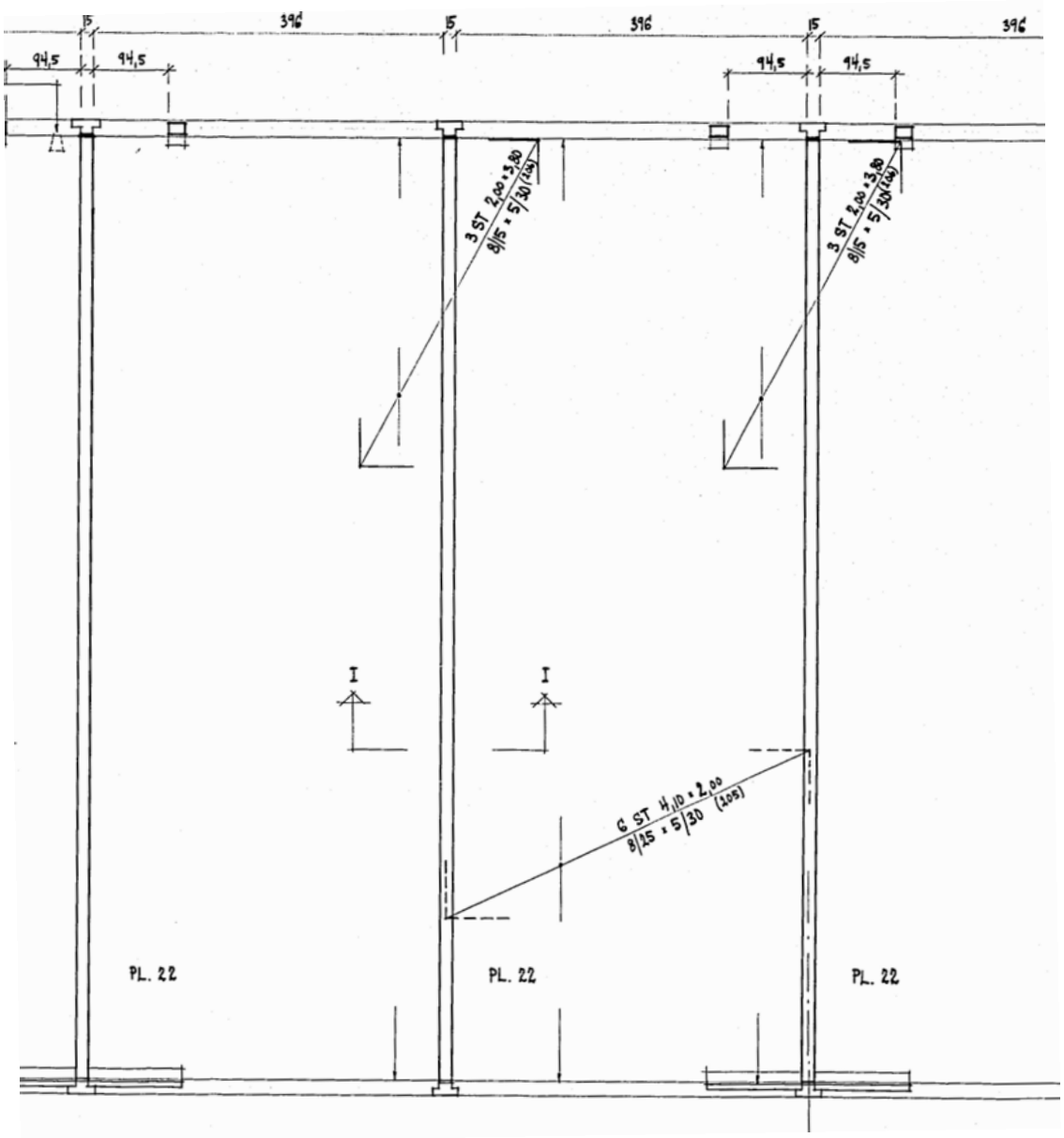

Figure D.1: Picture from the original Cykelskrapan structural drawing showing the location of section I–I. Source: Lund City Archives.

D.2 Troja Drawings

The structural drawings included in this appendix were provided through email correspondence by NIMAB Entreprenad AB and DANEWIDS INGENJÖRSBYRÅ AB. The drawings are used as project documentation for the Troja reference case. Since several original drawings are larger than A4, selected enlarged extracts are included to improve readability.

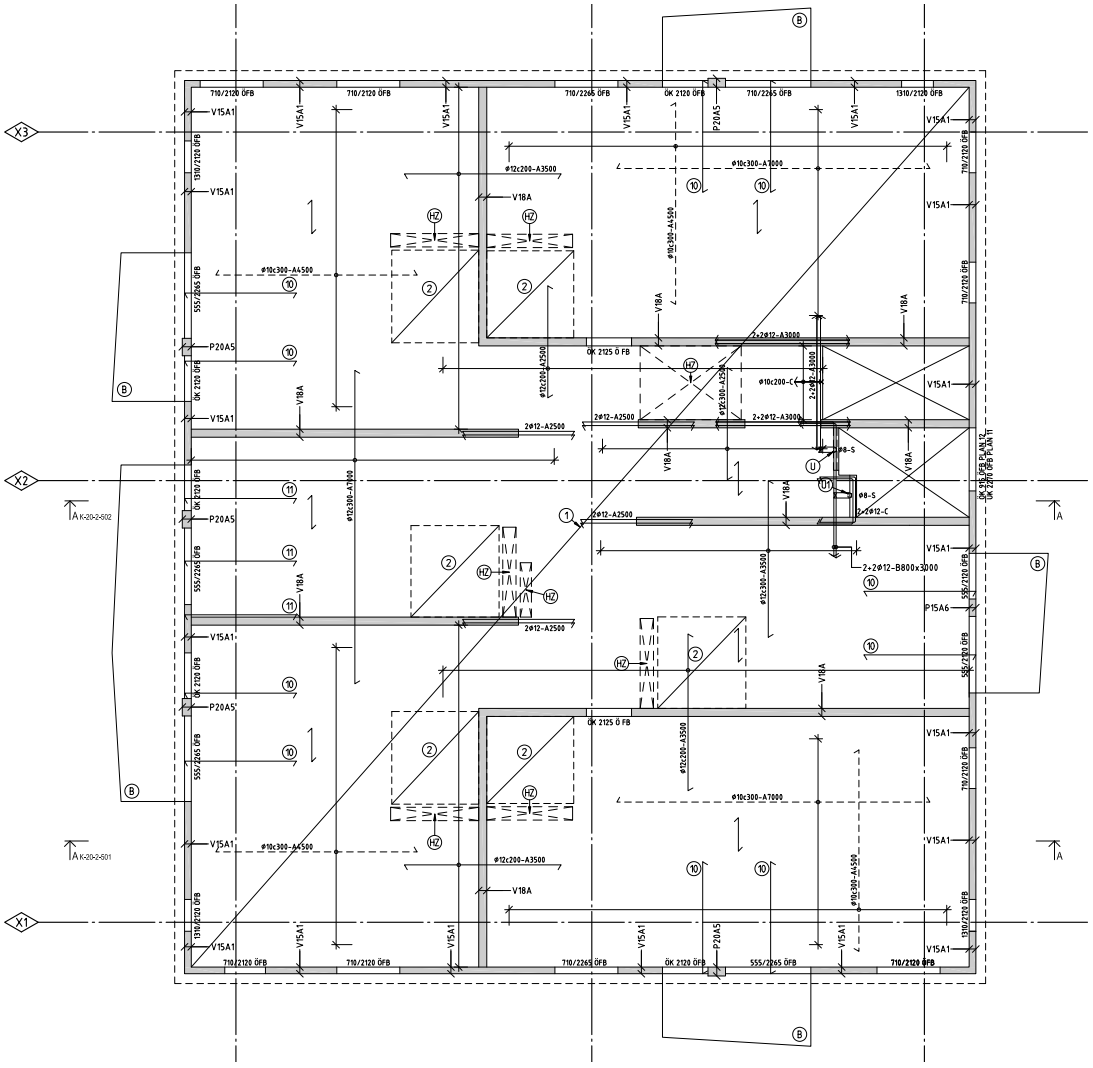

Figure D.2: Structural drawing K-22-1-5110 used as project documentation for the Troja reference case. Drawing provided by NIMAB Entreprenad AB through email correspondence.

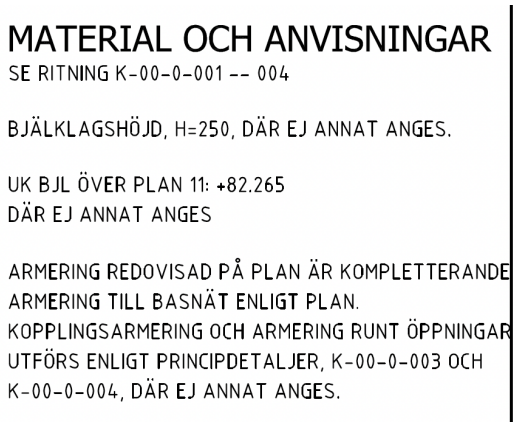

Figure D.3: Enlarged extract from drawing K-22-1-5110 showing material notes and general references. Drawing provided by NIMAB Entreprenad AB through email correspondence.

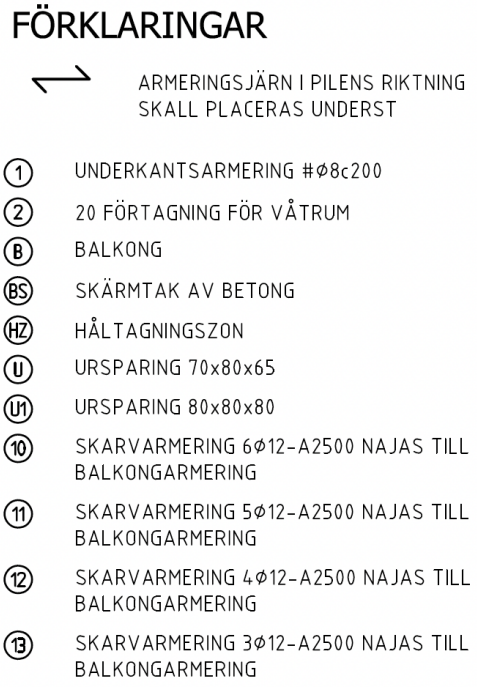

Figure D.4: Enlarged extract from drawing K-22-1-5110 showing symbols and drawing explanations. Drawing provided by NIMAB Entreprenad AB through email correspondence.

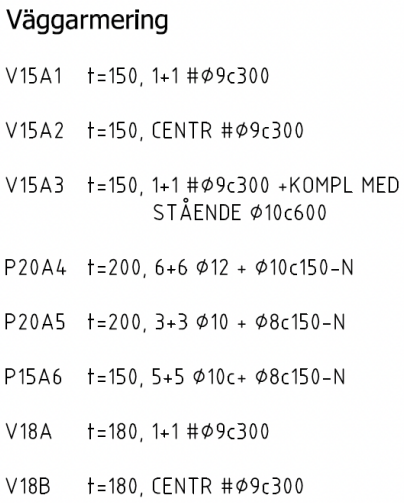

Figure D.5: Enlarged extract from drawing K-22-1-5110 showing the wall reinforcement schedule. Drawing provided by NIMAB Entreprenad AB through email correspondence.

6.1.4 Betongkvalitet

BYGGNADSDEL	BETONG-KVALITET	vct	EXPONERINGS-KLASS	TÄCKANDE BETONGSKIKT min ø+10	LIVSLÄNGDS-KATEGORI	KLIMATFÖR-BÄTTRAD NIVÅ	KLIMATPÅ-VERKAN CO2/m3
KÄLLARGOLV OCH KÄLLARYTTERVÄGG	C30/37 VT C35/45	0,55 0,50	XC4	35	L100	2	186,4 177,8
GRUNDPLATTOR (SULOR) HISS-, PUMP- OCH ELGROPAR	C30/37 C35/45	0,55	XC4	50 MOT MARK 35 MOT ISOLERING	L100	3	157,5 155,5
SULSKAFT	C45/55	0,38	XC3 XC4	35	L100	3	207,9 187,6
120-GOLV MARKPLAN	C30/37	0,50	XC1	20	L50	3	155,4 143,1
INNER- OCH YTTERVÄGGAR	C30/37	0,55	XC1	20	L50	3	157,5
BJÄLKLAG	C40/50	0,45	XC1	20	L50	2	220,8 193,4
BALKONGPLATTOR	C30/37	0,55	XC4+XF3	35	L50	2	197,4
LOFTGÅNGSPLATTOR, UTOMHUSPELARE, PLINTSKAFT UTOMHUS, SOCKLAR, BRUNNAR	C35/45	0,40	XD3+XF4	45	L50	2	276,5 271

Figure D.6: Extract from project documentation showing concrete quality, exposure class, water cement ratio, concrete cover, service life category and climate impact for different structural components. The yellow highlighted values indicate revisions made by DANEWIDS INGENJÖRSBYRÅ AB. Document provided by DANEWIDS INGENJÖRSBYRÅ AB through email correspondence.

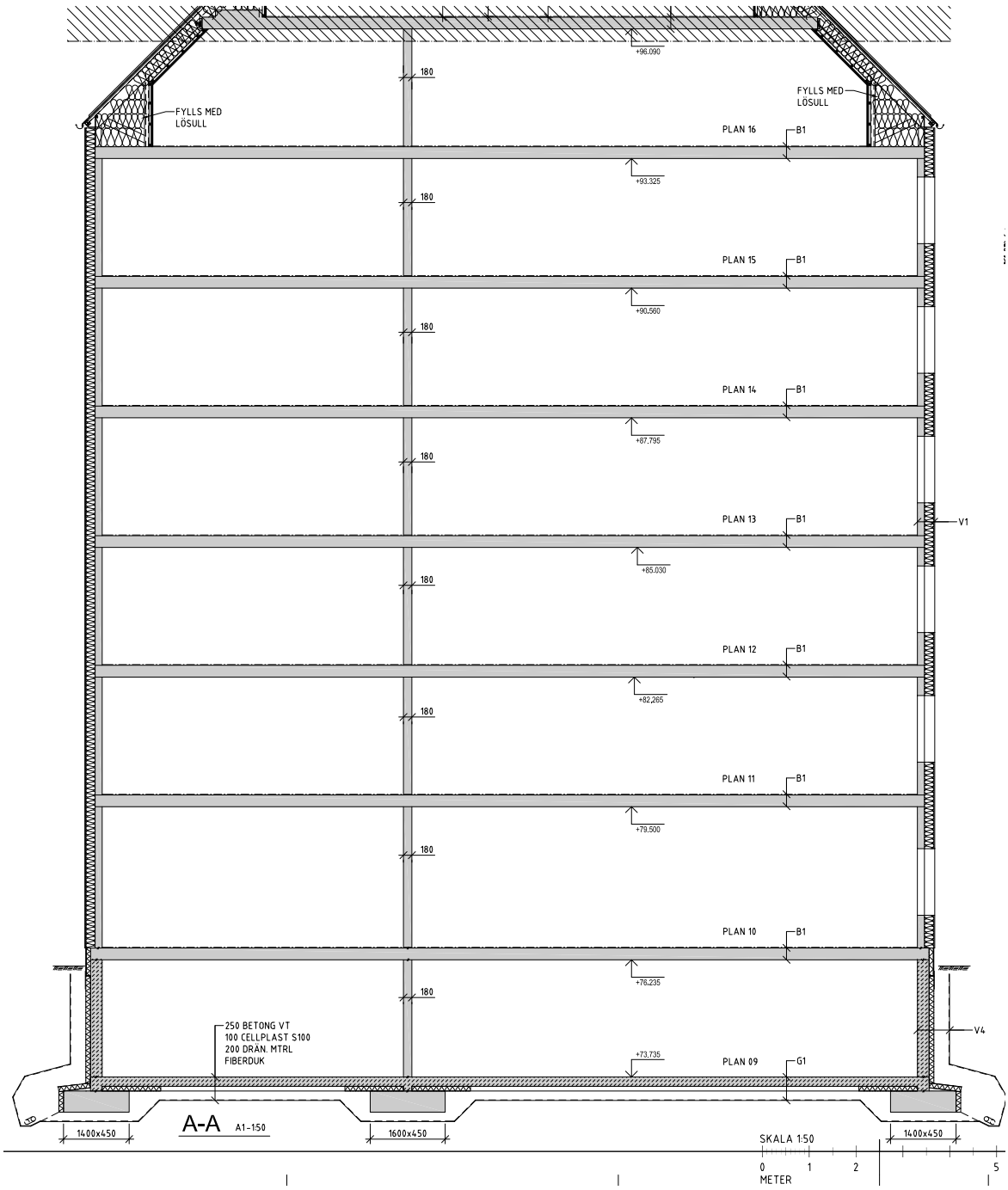

Figure D.7: Structural drawing K-20-2-501 used as project documentation for the Troja reference case. Drawing provided by DANEWIDS INGENJÖRSBYRÅ AB through email correspondence.